University of Alberta

5' UTR RNA Secondary Structure of a Cold-Induced RNA Helicase Functions as a Thermosensor

by

Jessica Marie Brown 

A thesis submitted to the Faculty of Graduate Studies and Research in partial fulfillment of the requirements for the degree of Master of Science

in

Microbiology and Biotechnology

Department of Biological Sciences

Edmonton, Alberta
Fall 2005

Your file Votre référence
ISBN: 978-0-494-22426-7
Our file Notre référence
ISBN: 978-0-494-22426-7

ABSTRACT

Expression of the cyanobacterial RNA helicase ,CrhC, is temperature-regulated as both transcript and protein accumulate at growth temperatures below 30°C (cold stress) however, the regulatory mechanism(s) providing temperature-dependent expression are not known.

At the transcriptional level, a putative repressor was identified that bound to the *crhC* promoter in a phosphorylation-dependent manner. Repressor binding encompasses an AT-rich regulatory element shown to be important for transcription however was not required for temperature-regulated expression.

At the post-transcriptional level, temperature-regulated expression is conveyed solely by the 5' UTR when *crhC* is expressed from a constitutive promoter in a heterologous system. Analysis of the 5' UTR secondary structure using MFOLD and transcriptional reporter fusions identified two stem-loop structures required for temperature-dependent *crhC* expression. Following transfer from 30°C to 20°C, MFOLD predicted a thermodynamic increase in the secondary structure of the 5' loop, suggesting that the 5' UTR RNA secondary structure functions as a thermosensor. The results and proposed mechanisms by which the 5' UTR of *crhC* stabilizes and destabilizes the *crhC* mRNA at 20°C and 30°C respectively, are discussed.

ACKNOWLEDGEMENTS

I would like to express my deepest appreciation to the following people who have made the completion of this study possible:

Dr. George W.Owttrim for guidance, patience, advice, and a great sense of humor. Thanks for being such a fantastic supervisor.

My supervisory committee, Dr. L. Frost and Dr. B. Leskiw, for their valuable suggestions and support.

Dr. Dana Chamot for her advice, support, and for teaching me RNA techniques.

Laura Patterson-Fortin and the other members of the Owttrim lab, for their suggestions, companionship, and for proofreading my thesis.

Dr. Mike Surette and Carla Davidson from the University of Calgary for their insight on luciferase assays, cloning, and for providing the pSC26, pSIG11, and pSIG16 vectors

Dr. Tracy Raivio and Nancy Price for the pNLP10 vector and for the use of their luminometer.

Members of the Page lab for their helpful suggestions and valuable insight.

University of Alberta, Institute for Biomolecular Design and Dr. Liang Lee (Chemistry) for their continuous efforts in attempting to sequence my protein.

Claire Spink for proofreading my thesis and for providing me with moral support.

Finally, I want to thank my family and my boyfriend Brian, for helping me print my thesis and for their continuous love and moral support.

TABLE OF CONTENTS

LIST OF TABLES

LIST OF FIGURES

LIST OF ABBREVIATIONS

APS	ammonium persulfate
bp	basepair(s)
BSA	bovine serum albumin
b/w	between
°C	degrees centigrade
CIP	calf intestinal alkaline phosphatase
cpm	counts per minute
cm^2	centimeter(s) square
CS	cold shock
CSP	cold shock proteins
DB	downstream box
DMSO	dimethyl sufoxide
DNA	deoxyribonucleic acid
dNTP	any deoxynucleoside triphosphate
ddNTP	any dideoxynucleoside triphosphate
ds	double strand(ed)
DTT	dithiothreitol
EDTA	ethylene diamine tetra acetic acid
fmoles	femta moles
g	gram(s)
HEPES	N-[2-hydroxyethyl]piperazine-N'-[2-ethanesulfonic acid]
HK	histidine kinase
IPTG	isopropyl-β-D-thiogalactoside
kb	kilobase(s)/kilobasepair(s)
kDa	kiloDalton(s)
L	liter(s)
M	molar
m^2	meter(s) square
mA	milliamps
MCS	multiple cloning site

mg	milligram(s)
min	minute(s)
mL	milliliter(s)
mM	millimolar
mQ	milliQ
mRNA	messenger RNA
msec	millisecond(s)
NEB	New England Biolabs
nm	nanometer(s)
ng	nanogram(s)
nt	nucleotide
OD	optimal density
%	percent
pBS	pBluescript KS+
PEG	polyethylene glycol
pmol	picomole(s)
RNA	ribonucleic acid
RNase	ribonuclease
rpm	rotations per minute
RR	response regulator
sarkosyl	N-laurylsarcosine
SD	Shine-Dalgarno
SDS	sodium dodecyl sulfate
sec	second(s)
ss	single strand(ed)
TAE	Tris/acetate/EDTA
TBE	Tris/borate/EDTA
TBS	Tris buffered saline
TEMED	N,N,N',N'-tetramethylethylenediamine
Tris	Tris (hydroxymethyl) aminomethane
U	units

UB	upstream box
μg	microgram(s)
μL	microliter(s)
μM	micromolar
UTR	untranslated region
UV	ultraviolet
V	volt(s)
v/v	volume per volume
W	watts
w/v	weight per volume
X-gal	5-bromo-4chloro-3indolyl-β-D-galactopyranoside

CHAPTER ONE
INTRODUCTION

1.1 CELLULAR ROLE OF RNA

Ribonucleic acids (RNA) are important cellular intermediates having informational, structural, and even catalytic functions, which are required for all aspects of cell growth and development (de la Cruz *et al.*, 1999). Depending on its structure and size, RNA can have either a coding function (e.g. mRNA) or a structural and/or regulatory function (e.g. all other RNA), acting as an intermediate template for downstream events on which all cellular processes are dependent (de la Cruz *et al.*, 1999). RNA species are found in several varieties including messenger RNA, ribosomal RNA, transfer RNA, transfer-messenger RNA, interference RNA, and antisense RNA. Messenger RNA (mRNA) plays a crucial role in the transfer of genetic information and contains the complementary DNA message that is translated into proteins. Ribosomal RNA (rRNA) forms an integral and functional part of the ribosome, which is the cellular machinery for protein synthesis. Transfer RNA (tRNA) serves as an adaptor molecule by escorting the correct amino acids to the ribosome during protein elongation. Transfer-messenger RNAs (tmRNA) aid in the removal of stalled ribosomes, and remove incorrectly translated peptides by tagging them with a proteolytic signal (Shpanchenko *et al.*, 2005; Withey and Friedman, 2003).

As demonstrated above, a large number of RNA species are regulatory and/or structural and do not result in a protein product. Interference RNA (RNAi) and antisense RNA are small, non-coding RNA involved in gene silencing. The formation of double-stranded (ds) RNA through complementary base pairing between specific RNAs modifies mRNA stability, processing, and translation thereby causing a suppressive effect on gene expression (Szymanski and Barciszewski, 2003). Variation in RNA functionality and metabolism therefore provides the cell with multiple regulatory options to creatively regulate gene expression at both the transcriptional and translation level.

The majority of RNA is synthesized as a single-stranded, long-chain macromolecule of ribonucleotides capable of forming inter- and intra-molecular hydrogen bonds via Watson-Crick complementary base pairing. Under various

conditions, RNA will form stable secondary (2°) and/or tertiary (3°) structures, such as a double-stranded (ds) stem hairpin loop or even pseudoknots, by base pairing within a single-strand (ss). Similar to proteins, the secondary structure of the RNA is often more important in determining the function of the RNA, than the primary sequence. For example, changes in duplex or folded RNA secondary structure vary transcript functionality by altering protein/RNA accessibility to the RNA (Rauhut and Klug, 1999). The stability of the mRNA, as determined by its secondary structure, provides the cell with a sufficient way to control the expression of a specific gene.

Structural inhibitions due to RNA folding are removed through the interaction of RNA binding proteins, which bind to specific RNA sequences and stabilize or modify single-stranded RNA (ssRNA) (Gorbalenya *et al.*, 1988). RNA binding proteins are involved in such processes as, protection of the RNA from degradation by ribonucleases (RNases), and altering mRNA secondary structure to effect translation initiation and transcription elongation (Stulke, 2002). For example, RNA binding protein-induced conformational changes allow ssRNA molecules to interact with other essential RNAs or proteins (e.g. ribosome), thereby permitting the RNA to perform its intended physiological role (de la Cruz *et al.*, 1999; Herschlag, 1995). One important family of RNA binding proteins involved in RNA metabolism and the modulation of RNA 2° and 3° structures is RNA helicases. Without the kinetic and thermodynamic modifications of RNA secondary structures, normal cellular processes such as protein synthesis could not occur. Thus, RNA binding proteins such as RNA helicases are essential for cellular differentiation and development.

1.2 GENERAL ROLE OF RNA HELICASES

For fundamental cellular processes to take place, a modulation of the RNA secondary and tertiary structure must occur to allow for dynamic protein-RNA and RNA-RNA interactions. Using an energy-dependent system, alterations of RNA structure allow cellular processes such as translation, mRNA splicing, and ribosome biogenesis to take place (Fuller-Pace, 1994). In the late 1980s, a class of RNA binding proteins called the RNA helicases was identified as proteins that could interact and modify RNA structure (Linder *et al.*, 1989; Rozen *et al*, 1989; Ray *et al.*, 1985). RNA helicases

function by unwinding double-stranded RNA or duplex regions of single-stranded RNA, in combination with the hydrolysis of nucleoside triphosphates (NTPs) (de la Cruz *et al.*, 1999; Cho *et al.*, 1998; Fuller-Pace, 1994; Linder *et al.*, 1989). To date, the majority of RNA helicases unwind RNA unidirectionally in the 3' to 5' direction in a semi-processive manner, however a few have been shown to have bi-directional unwinding capabilities (Lee and Hurwitz, 1992; Rozen *et al.*, 1990).

The prototypical RNA helicase, eIF-4A (eukaryotic translation initiation factor 4A), is required for translation initiation of all eukaryotic mRNAs. eIF-4A unwinds secondary and tertiary structures within the 5′ UTR of mRNA, allowing the ribosome to bind and initiate translation (Zakowicz *et al.*, 2005; Rogers *et al.*, 2002; Rozen *et al.*, 1989). eIF-4A is a DEAD-box RNA helicase (Section 1.2.1) used as a model for comparing amino acid sequence and biochemical similarities in the identification of putative RNA helicases. The definitive assignment of proteins as RNA helicases based on biochemical activity alone is inaccurate due to the fact that not all RNA helicases exhibit unwinding activity. For example, the PRP proteins from *S. cerevisiae* possess ATPase activity but lack unwinding capabilities, and the *E. coli* DbpA protein possesses RNA destabilizing activity (Boddeker *et al.*, 1997; Kim *et al.*, 1992). Thus, sequence homology of the RNA helicase conserved motifs (Section 1.2.1) is used to identify proteins as putative RNA helicases, followed by extensive biochemical and genetic analysis to elucidate the helicase's biochemical and functional role within the cell.

1.2.1 The RNA Helicase Family

Helicases (DNA and RNA) are grouped into five superfamilies (SF) based on sequence homology (Gorbalenya and Koonin, 1993). RNA helicases are ubiquitous enzymes belonging to the large helicase superfamilies I and II (SF-I and SF-II), playing an essential role in all aspects of RNA metabolism (Singleton and Wigley, 2002; Rauhut and Klug, 1999). RNA helicase classification is broken down into smaller families based on the spatial and sequence conservation of several amino acid motifs. RNA helicases were originally classified as "DEAD-box" proteins based on the conserved Asp-Glu-Ala-Asp (DEAD for single-letter amino acid code) motif, and are a subset of helicase SF-II. As show in Figure 1.1, two additional families, DEAH and DExH, have variations in

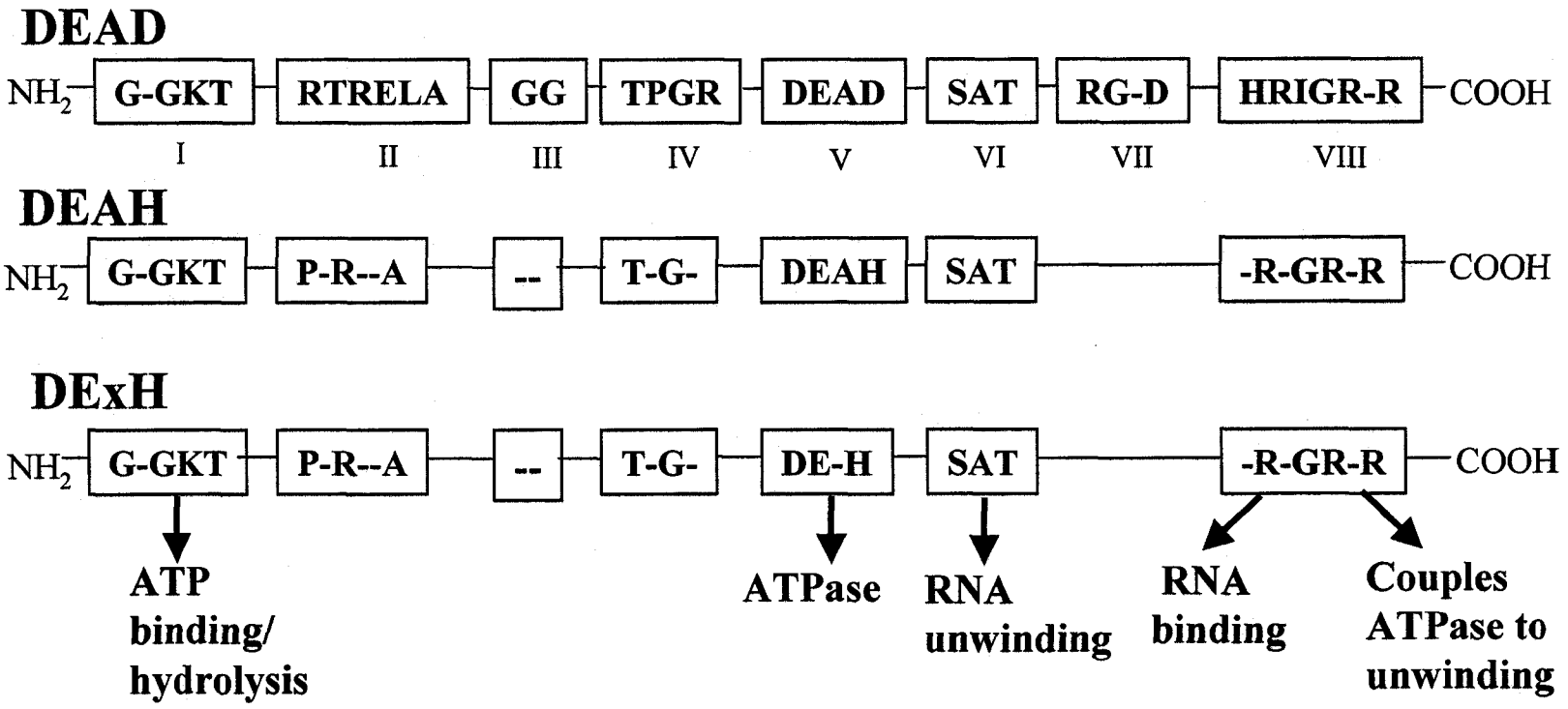

Figure 1.1. Schematic representations of the DEAD, DEAH, DExH box RNA helicase families. Boxed regions indicate conserved amino acid motifs and are numbered I - VIII. Diagrams are not drawn to scale (adapted from Fuller-Pace, 1994).

their conserved amino acid motifs but the functional role of the motif remains the same (Rocak and Linder, 2004; Fuller-Pace and Lane, 1994; Linder *et al.,* 1989).

RNA helicases are characterized by having a core domain comprised of 300 - 350 amino acids (Schmid and Linder, 1992). As shown in Figure 1.1, contained within this core domain are six to eight conserved motifs that are responsible for specific biochemical activities (Fuller-Pace, 1994; Linder *et al.,* 1989). The conserved motifs are also flanked by unconserved regions that vary in amino acid sequence but are similar in length (Rocak and Linder, 2004; Fuller-Pace, 1994; Linder *et al.*, 1989). The conserved motifs and the conserved spacing between them are proposed to provide the structural framework and biochemical activities (Section 1.2.2) characteristic of RNA helicases (Hodgman, 1988).

The amino (N) and carboxy (C)-terminal sequences flanking the conserved core domain are highly variable, and proposed to provide RNA or protein interaction. Individual family members also have distinct N- and C-terminal regions that vary in length and sequence (Fuller-Pace, 1994). These regions of variation provide each RNA helicase with specificity elements for substrate targeting and are believed to influence the biological function of the helicase (Rocak and Linder, 2004; Aubourg *et al.,* 1999; Koonin, 1991).

Biochemical and genetic characterization of several of the conserved motifs has provided a better understanding of the functional importance of the RNA helicase core domain. Mutational analysis, *in vitro* enzymatic assays, and *in vivo* viability tests on human, mouse, and yeast eIF-4A homologs, have assigned specific biochemical properties to several of the motifs (Fuller-Pace, 1994; Liang *et al.,* 1994; Pause and Sonenberg, 1992; Schmid and Linder, 1991 and 1992). As defined by Walker *et al.* (1982), motif I (GxGKT/S) is a typical Walker box A with an ATP-binding motif present mostly in ATP and GTP binding proteins (Figure 1.1). Motif I is conserved throughout all RNA helicase families whereas motifs II - VIII are conserved within a particular family but vary considerably between families (Linder *et al.*, 2001). Base-pair mutations of the conserved alanine and lysine residues within motif I (GxGKT/S) inhibited cell viability and abolished ATP binding activity respectively (Pause and Sonenberg, 1992 and 1993). These results along with the presence of several catalytic sites found in many

enzymes that use nucleoside triphosphates, suggest that the Walker A box motif is involved in ATP-binding and hydrolysis (Magee, 1997; Pause and Sonenberg, 1993 and 1992; Linder *et al.*, 1989; Rozen *et al.*, 1989; Gorbalenya *et al.*, 1988).

The DEAD box motif (V) is a unique version of the Walker box B found in NTP-binding proteins. Site-specific mutagenesis and enzyme assays demonstrated that the DEAD box motif was necessary for ATP hydrolysis and was important for coupling of ATPase activity and RNA unwinding (Pause and Sonenberg, 1992). Structure-based mutational analysis and X-ray crystallography indicates that the DEAD box motif ATPase activity is dependent on the aspartic acid residue binding Mg^{2+} via a water molecule, allowing Mg^{2+} to complex with the β and δ phosphates of the nucleotides (Tai *et al.*, 2001).

The third motif studied for enzymatic activity was the SAT motif (VI). Site-specific mutagenesis abolished RNA unwinding capabilities within eIF-4A and PRP2 (pre-RNA processing) mutants but had no effect on ATP-binding or hydrolysis properties (Plumpton *et al.*, 1994; Pause and Sonenberg, 1992). This suggests that the SAT motif is essential for RNA unwinding. Amino acid variations within the SAT motif are extremely rare. For example, several viral RNA helicases have the SAT motif replaced by the functionally and structurally related TAT motif (Gross and Shuman, 1998). CrhC, the cold –inducible RNA helicase (Section 1.5) isolated from *Anabaena* sp. strain PCC 7120 and the major focus of this thesis, has a FAT motif replacing the SAT motif (Chamot *et al.*, 1999). The exact importance of the FAT motif variation is not known but it may play a role in RNA helicase kinetics as suggested by X-ray crystallography. X-ray crystallography results of the yeast eIF-4A showed that the core domain including the SAT motif, are built around a core scaffold of alpha-beta strands (Johnson and McKay, 1999). The crystallographic structure shows that the eIF-4A protein structure permits specific interactions between motifs I, V, and VI. CrhC's conversion of the SAT motif to a FAT motif may therefore inhibit specific interactions between the Walker A motif (I), the DEAD box motif (V), and the FAT motif (VI) creating a unique coupling between the ATPase cycle and RNA unwinding activity, specific for CrhC function.

The final motif characterized to date is motif VIII, which contains the conserved amino acid sequence HRIGRxxR. Mutational analysis in both eIF-4A and Vasa, a

Drosophila RNA helicase, indicated that motif VIII is involved in ATP-dependent RNA binding and unwinding and is also involved in coupling ATPase activity to RNA unwinding (Liang *et al.,* 1994; Pause *et al.,* 1993). Pause and Sonenberg (1993) demonstrated that site-specific mutagenesis of the arginine residues completely abolished RNA helicase activity while limiting RNA binding. To date, the remainder of the RNA helicase motifs have not been characterized but based on their high conservation between families, they are likely involved in normal RNA helicase cellular processes including, ATP binding and hydrolysis, and RNA binding and unwinding.

Based on the conserved domains within the amino acid sequence, and the motif properties shared amongst helicase families, Pause *et al.* (1993) proposed a series of putative biochemical events to describe the cellular involvement of the prototypical eIF-4A, which may be applicable for all DEAD-box proteins. ATP is first thought to bind to motif I (GxGKT/S) and motif V (VLDEAD) inducing a conformational change in the protein, which then enables the RNA to interact with motif VIII (HRIGR). The protein-RNA interaction induces hydrolysis of ATP and provides the necessary energy to unwind duplex regions of RNA. This proposed model for the motifs' involvement in RNA helicase activity provides a model for RNA helicase interactions with RNA and ATP substrates.

The crystal structures of DNA and RNA helicases are shown to be structurally similar within the core region, providing suggestions into the functional roles of the helicase motifs (Linder et *al.*, 2001). Crystallographic structures are available for several SF-II helicases such as the UvrB DNA helicase, hepatitis C virus (HCV) RNA helicase, and the yeast eIF-4A RNA helicase (Tuteja and Tuteja, 2004; Caruthers *et al.*, 2001). Although there is distinct structural difference between helicases, two common domains with similar topology and tertiary structure are consistently found within all helicase structures (Caruthers *et al.*, 2001). Contained within these two common domains are the conserved catalytic helicase motifs, sharing structural similarities with the RecA protein and the F1-ATPase (Egelman, 1998). Structural conservation of the core domain therefore suggests that the sequence along with the spatial position appears to play an important role in determining helicase function and specificity, providing a mechanism for coupling ATP hydrolysis with RNA binding and unwinding.

1.2.2 RNA Helicase Enzymatic Activities

Generally, RNA helicases are characterized as enzymes possessing RNA-dependent ATPase activity and ATP-dependent RNA unwinding activity. This definition is loosely used due to the fact that the majority of RNA helicases analyzed do not possess both enzymatic activities. eIF-4A is one of the few well-characterized DEAD-box RNA helicases that possesses both ATPase activity and RNA unwinding capabilities (Rozen *et al.,* 1989). Other proteins with both enzymatic capabilities include hepatitis C virus NS3 (Gallinari *et al.,* 1998), RNA helicase II/GU (Florez-Rozas and Hurwitz, 1993), human p68 protein (Hirling *et al.,* 1989), yeast DedIp (Iost *et al,*. 1999), *Xenopus* An3 (Gururajan and Weeks, 1997) and Xp54 (Ladomery *et al.*, 1997), vaccinia virus DEXH protein NPH-II (Shuman, 1992), *Arabidopsis thaliana* AtDRH1 (Okanami *et al.*, 1998), PRP 16, PRP 22 (Wang *et al.,* 1998), Dbp5 (Tseng *et al.,* 1998), and CrhC (Yu and Owttrim, 2000).

Several RNA helicases only possess RNA-dependent ATPase activity. For example, several PRP (pre-RNA processing) proteins from *S. cerevisiae* possess only RNA-dependent ATPase activity involved in pre-mRNA splicing (Schwer and Cuthrie, 1991). Other RNA helicases, like *E. coli* DpbA (Section 1.2.4), destabilize the RNA helix in the absence of ATP hydrolysis (Boddeker *et al.,* 1997; Kim *et al.,* 1992).

Recent evidence has also indicated that a limited number of RNA helicases have a broader ranger of enzymatic activities. CrhR, a redox regulated RNA helicase from *Synechocystis* sp. strain PCC 6803, possess both RNA unwinding and annealing activities (Chamot *et al.*, 2005). In an ATP-dependent reaction, CrhR catalyzes the restructuring of RNA secondary structure by combining RNA unwinding and annealing activity to generate RNA strand exchange via a branch migration mechanism (Chamot *et al.*, 2005). Yeast nuclear DEAD-box RNA helicases p68 and p72 (Rössler *et al.*, 2001), and DexD-box RNA helicase II/Gu (Valdez *et al.*, 1997) have also been shown to catalyze RNA annealing, but in an ATP-independent manner. Modulation of RNA secondary structure by coupling helicase and annealing activities provides a mechanism for RNA helicases to regulate both RNA-RNA and RNA-protein interactions (i.e. RNA restructuring).

Recent questions have also arisen about the possibility that RNA helicases possess functional roles beyond RNA unwinding activity, contributing to a much larger

cellular role than originally suggested. RNA helicases have been shown to be involved with protein-RNA interactions, suggesting a specific role for RNA helicases in the active disruption of RNA-protein complexes (Linder *et al.,* 2001). Jankowsky *et al.* (2001) suggested that the DEAD and DexH (collectively known as DexD/H families) proteins might function as RNPases, that is, enzymes that disrupt RNA-protein interactions, either by modulating ribonucleoprotein (RNP) composition and/or RNA structure. To support this hypothesis, Jankowsky and colleagues (2001) produced a U1A-specific dsRNA substrate and demonstrated that the RNA helicase NPH-II dissociated the U1A protein from the dsRNA substrate in an energy-dependent manner (Linder *et al.,* 2001; Schwer, 2001). Kinetic studies also demonstrated continuous dsRNA unwinding activity by NPH-II upon displacement of the U1A protein from the substrate. It was concluded that NPH-II loads onto the dsRNA substrate, displaces the UA1 protein and unwinds the duplex RNA (Jankowsky *et al.,* 2001). It is interesting to note that NPH-II unwinding activity is not required for UA1 protein removal.

Helicase-catalyzed protein displacement is also accomplished by Prp28p, a RNA helicase involved in spliceosome assembly (Section 1.2.3). Pre-mRNA splicing studies showed that Prp28p is required for both dsRNA unwinding activity and the disruption of a ribonucleoprotein complex from its RNA substrate (Chen *et al.,* 2001). These results, along with those published by Jankowsky *et al.* (2001), illustrate the potential for a much broader cellular role for RNA helicases than originally envisioned. Thus, along with contributing to translation initiation, mRNA stability, and pre-mRNA splicing, RNA helicases could also contribute to the efficiency, maintenance, accuracy, and fidelity of cellular processes such as RNA maturation (e.g. tRNA and rRNA), and transcription and/or translation attenuation (Linder *et al.,* 2001). Further research is needed to classify DexH/D proteins as definitive RNPases and to determine their ribonucleoprotein targets.

Not only are there variations in enzymatic activity amongst RNA helicases but their activities can also vary depending on their interaction with various RNA and protein complexes. Due to the existence of very few RNA helicases possessing both biochemical properties *in vitro*, the potential of accessory proteins or specific RNA secondary structures interacting with RNA helicases to provide functionality and substrate specificity is highly possible. In fact, many RNA helicases are assumed to not exhibit

activity *in vitro* because they are not part of a complex and/or do not have specific RNA substrates. For example, biochemical analysis has identified several DEAD-box RNA helicases that are inactive in their free form but are active in the presence of a multi-subunit complex. RhlB, a DEAD-box protein from *E. coli* (Section 1.2.3) can bind RNA but does not exhibit ATPase activity unless found in the multi-complex degradosome (Py *et al.,* 1996). The degradosome is composed of four major proteins; enolase, PNPase, RNase E, and RhlB, which are only capable of mRNA turn-over as a functional unit.

eIF-4A is also found as part of a complex, necessary for efficient translation initiation and protein synthesis. As mentioned previously, eIF-4A possesses both RNA-dependent ATPase activity and ATP-dependent RNA binding and unwinding activity, but the degree of activity varies depending on the protein's form. Complexed with eIF-4B, eIF-4A exhibits increased unwinding activity compared to its free form (Pause and Sonenberg, 1993; Abramson *et al.,* 1987). Through the interaction of various accessory proteins, RhlB and eIF-4A are capable of acquiring enzymatic activities that they lack in their free form.

RNA helicase enzyme activity also depends on the interaction with specific RNA targets. *In vitro*, most RNA helicase are capable of acting on a wide array of RNA substrates however, a limited number of RNA helicases require specific RNA substrates for enzyme activity. The *E. coli* RNA helicase DbpA, is the only DEAD-box RNA helicase known to require a specific RNA substrate for activity (Nicol and Fuller-Pace, 1995; Fuller-Pace *et al.,* 1993; Iggo *et al.,* 1990). DbpA's ATPase activity is maximized in the presence of a specific region of the 23S rRNA (Pugh *et al.*, 1999). More specifically, DpbA helicase activity is dependent on the sequence and structure of hairpin 92 of the 23S rRNA (Diges and Uhlenbeck, 2001). These results support that some RNA helicases require specific substrate structures for unwinding activity.

Although the majority of RNA helicases are presumed to have specific roles within the cell (i.e. RNA helicases involved in eukaryotic mRNA splicing (Section 1.2.4) and/or rRNA maturation) some perform more general roles (i.e. eIF4A). Differences in helicase function are attributed to variation in helicase activity, which arise due to the interaction with different accessory proteins, complexes, and RNA substrates.

1.2.3 Cellular Roles of RNA Helicases

To date, RNA helicases have been found in almost every organism analyzed including bacteria, mammals, plants, and viruses, suggesting a fundamental role in normal cellular processes. As already mentioned, RNA helicases have been shown to be involved in cellular functions ranging from RNA splicing, editing, maturation, mRNA export, degradation, translation initiation, ribosome biogenesis, cell growth, oncogenesis and oogenesis (Rocak and Linder, 2004; Fuller-Pace, 1994; Grifo *et al.,* 1984; Kim *et al.,* 1996; Kressler *et al.,* 1997). The cellular importance of RNA helicases is evident due to the presence of all three RNA helicases families (DEAD, DEAH, DexH) within the nucleus, cytoplasm, mitochondria, and chloroplasts of the cell. However, the general inability of RNA helicases to complement each other suggests that each RNA helicase has a specific and unique function.

In *S. cerevisiae,* over 30 RNA helicases have been identified comprising all three families (DEAD, DEAH, DexH), performing different cellular roles. A group of PRP (pre-RNA processing) proteins were identified that participated in specific and distinct steps during pre-mRNA splicing and disassembly in yeast cells. Among them, PRP2, PRP16, PRP22 and PRP43 belong to the DEAH-box protein family, whereas PRP5 and PRP28 are DEAD-box proteins (Kim *et al.,* 1996). PRP2 participates in pre-mRNA splicing by binding to a precatalytic spliceosome prior to the first step of splicing, and hydrolyzes ATP, altering the spliceosome. PRP28 participates in the first step of splicing by unwinding the duplex between U4 and U6 small nuclear RNAs (*sn*RNA) to produce an active spliceosome (Kim *et al.,* 1996). PRP16 briefly interacts with the spliceosome during step two of the splicing reactions and upon ATP-hydrolysis is released from the complex to allow for the second cleavage-ligation step to take place (Schwer *et al.,* 1991). PRP22 catalyzes two functional roles during pre-mRNA splicing; in the presence of ATP hydrolysis PRP22 will release mRNA from the spliceosome, whereas in the absence of energy, PRP will act upon a stagnant pre-assembled spliceosome from step one (Schneider and Schwer, 2001). Finally, PRP43 is involved in the late steps of pre-mRNA splicing, participating in spliceosome disassembly and recycling (Arenas and Abelson, 1997). As demonstrated, a wide array of RNA helicases are required for the

pre-mRNA splicing process, with each RNA helicase having a transient interaction and specific function at each step.

In several organisms, RNA helicases have been shown to be required for a more generalized role, such as the translation initiation of all mRNAs (e.g. eIF-4A). RNA helicases related to eIF-4A are found in all eukaryotic organisms. eIF-4A unwinds secondary structure within the 5' 'UTR to allow the 40S ribosomal subunit to bind and initiate translation (Pause and Sonenberg, 1993). The DEAD-box RNA helicase, DedI, has also been shown to be required for translation initiation in *S. cerevisiae* (Iost *et al.*, 1999).

The majority of prokaryotic RNA helicase research has been performed in *E. coli*, where 26 RNA helicases have been identified based on sequence homology. Although all RNA helicase families are present in *E. coli*, five RNA helicases from the DEAD-box family have been studied the most. The first DEAD-box protein identified, SrmB, is involved in ribosome biogenesis. This conclusion was drawn due to the capability of overexpressed SrmB to suppress a mutation in ribosomal protein L24 (Nishi *et al.*, 1988). The L24 mutation inhibited rRNA maturation by preventing interaction of the L24 ribosomal protein with the 23S rRNA, making the protein defective in the formation of the large ribosomal subunit and inhibiting downstream protein synthesis. By overexpressing SrmB, it is believed to stabilize the 23S rRNA by binding to a specific site on the 23S rRNA. Alternatively, SrmB binding may protect an unstable assembly precursor from degradation (Nishe *et al.*, 1988). A second *E. coli* DEAD-box RNA helicase, DbpA, is also involved in ribosome biogenesis. DbpA is the first and only DEAD-box protein for which a specific RNA substrate, bacterial 23S rRNA, has been identified *in vitro* (Nicol and Fuller-Pace, 1995; Fuller-Pace *et al.*, 1993; Iggo *et al.*, 1990). DbpA functions in either the assembly of the 50S ribosomal subunit, which is necessary for translation, or is involved in the rearrangement of the 23S rRNA secondary structure in the vicinity of the peptidyltransferase center (Boddeker *et al.*, 1997; Nicol and Fuller-Pace, 1995).

A third *E. coli* DEAD-box RNA helicase, RhlB, is an active component of the RNA degradosome and thus is important for mRNA turnover (Miczak *et al.*, 1996; Py *et al.*, 1996). The proposed role performed by RhlB in the degradosome is to unwind RNA

structures that impede the processive 3' to 5' exoribonuclease activity of PNPase (Py *et al.,* 1996). The fourth *E. coli* DEAD-box RNA helicase, CsdA, is a cold-induced RNA helicase capable of suppressing mutations in ribosomal protein S2 (Toone *et al.,* 1991) and, mutations causing cold-sensitive growth (Yamanaka *et al.,* 1994). At reduced growth temperatures, CsdA is ribosome-associated, required for either biogenesis of the 50S subunit or helix destabilizing of mRNA structures, to increase translation efficiency (Charollais *et al.*, 2004; Jones *et al.,* 1996). The fifth *E. coli* DEAD-box RNA helicase studied is RhlE. In an effort to determine the cellular function of RhlE, Ohmori (1994) created a null mutant and found no phenotypic changes in the growth rate compared to the wild-type. RhlE may therefore not be essential for growth however future work must be done to determine its exact function.

The location of the RNA helicase within the cell also appears to play a role in determining helicase activity and function. Protein localization studies within the bacterial cytoplasm have shown that the cytoplasm is not a homogeneous, undifferentiated medium in which proteins are free to diffuse, rather several proteins are compartmentalized into specific subcellular regions based on their functions (Lewis *et al.,* 2000). For example, proteins involved in cell division, DNA replication, and chromosome segregation appear to have specific subcellular locations, spatially orientated based on their cellular functions (Jacobs and Shapiro, 1999; Losick and Shapiro, 1999). This concept also applies to RNA helicases. In eukaryotes, several RNA helicases have been shown to localize to specific regions within the cell, particularly to the nucleus (Valgardsdottir and Prydz, 2003; Styhler *et al.* 2002; Valderez *et al.,* 2002; Valgardsdottir *et al.* 2001).

Subcellular localization of RNA helicases has only recently been reported in prokaryotes. El-Fahmawi and Owttrim (2003) identified that CrhC, a cold-inducible RNA helicase in *Anabaena* (Section 1.5), localizes to the plasma membrane (PM). Immunogold labeling illustrated that CrhC localized to the cytoplasmic face of the plasma membrane primarily at the septa separating adjacent cells, indicating that CrhC is membrane associated. A hypothesized reason for CrhC localization to the membrane involves facilitating the removal of membrane constraints induced by low temperatures (Section 1.4.1.1). Upon a temperature downshift, CrhC could facilitate translation of

cold shock mRNAs whose protein products adjust membrane fluidity (El-Fahmawi and Owttrim, 2003). From both the eukaryotic and prokaryotic studies, it appears that spatial arrangement of proteins such as RNA helicases, allows for efficient subcellular functional processing.

1.3 CYANOBACTERIA AS A MODEL ORGANISM

1.3.1 General Characteristics of Cyanobacteria

Cyanobacteria are one of the largest, most diverse subgroups of Gram-negative, photosynthetic prokaryotes and represent some of the most ancient life forms on earth (Fay, 1983; Schopf *et al.,* 1965). Cyanobacteria are a heterogeneous group of eubacterial photoautotrophs that harvest light energy using chlorophyll *a* and perform oxygenic photosynthesis, making cyanobacteria a very attractive model for studying oxygen-evolving photosynthesis (Whitton and Potts, 1982).

Cyanobacteria were traditionally classified as algae based on the Botanical Code, and were commonly referred to as blue-green algae (Stafleu *et al.,* 1971). Further analysis on their structure and development provided a generic description of cyanobacteria under the Bacteriological Code. Based on comparative studies, over 178 strains of cyanobacteria have been identified comprising 22 genera placed into five categories (Rippka *et al.,* 1979). As shown in Table 1.1, Section 1 and II are unicellular cyanobacteria that differ in their reproductive cycles whereas Sections III-V are filamentous cyanobacteria that differ in their vegetative cell states and plane of division.

Cyanobacteria are morphologically and physiologically diverse, which is evident in their varied cell development and differentiation. Four different specialized cells are present in cyanobacteria, each with specific developmental roles. Baeocyte cells are small, spherical reproductive cells (Rippka *et al.,* 1979; Waterbury and Stanier, 1978), hormogonium cells are motile trichome (filament of cells) fragments, akinetes are resting cells developed during stationary growth, and heterocysts are metabolically active cells that have the capacity for fixing dinitrogen under aerobic conditions (Stanier and Cohen-Bazire, 1977; Rippka *et al.,* 1979).

Heterogeneity is also evident in cyanobacterial colonization and adaptive survival mechanisms. Cyanobacteria can colonize terrestrial, marine, and fresh water

Table 1.1: Cyanobacterial Classification

Section #	Cellular Arrangement	Reproduction or Vegetative State	Strain Total	Strain Example (Rippka *et al*., 1979)
Section 1	Unicellular	binary fission or budding	57	*Synechococcus, Synechocystis, Gloeobacter*
Section 2	Unicellular	mutliple fission or in combination with binary fission (i.e. baeocytes)	32	*Dermocarpa, Xenococcus*
Section 3	Filamentous	non-heterocystous, divide in one plane	44	*Spirulina, Pseudanabaena*
Section 4	Filamentous	non-branching, heterocystous, divide in one plane	36	*Anabaena, Nostoc, Calothrix*
Section 5	Filamentous	branching, heterocystous, divide in more than one plane	9	*Fischerella, Chlorogloeopsis*

environments and are found all over the world (Fay, 1983). They are found in the Antarctic (Psenner and Sattler, 1998), in hot springs (Ward *et al.,* 1998), along shorelines, in tropical soils, and in salt marshes (Whitton and Potts, 1982) and thus are comprised of psychrophilic, psychrotrophic, mesophilic, and thermophilic species (Dmitry and Murata, 1999). Their ability to grow in a wide array of environments suggests highly advanced adaptive mechanisms. Several strains of cyanobacteria have adapted gliding motility, pigmentation mechanisms (chromatic adaptation), and gas vacuoles to allow them to maximize light harvesting (Stanier and Cohen-Bazire, 1977). The induction of cold shock proteins has also been identified to allow for survival at reduced temperatures (Chamot and Owttrim, 2000; Phadtare *et al.,* 2000; Chamot *et al.,* 1999; Thieringer *et al.,* 1998).

Unlike most Gram-negative organisms, cyanobacteria have an expanded membrane structure. Cyanobacteria have three different membranes, the characteristic outer and plasma (inner) membranes and a third, intracytoplasmic thylakoid membrane, where photosynthesis takes place (Whitton and Potts, 1982). The outer and inner membranes are consistent with characteristics of Gram-negative structure and function however, the peptidoglycan thickness and composition is more similar to that of the Gram-positive membrane. The plasma and thylakoid lipid composition and protein assembly are similar to that of higher plant chloroplasts, implying that cyanobacteria are the endosymbiotic progenitors of chloroplasts (Murata and Wada, 1995).

Although cyanobacteria are morphologically and physiologically diverse, they provide a useful and powerful model for studying molecular processes. The lifespan and photosynthetic capabilities have caused cyanobacteria to be labeled as the "ancestor of modern chloroplasts," providing insight into phototrophic metabolism for organisms such as higher plants (Gray and Doolittle, 1982). Several strains of cyanobacteria are also easily cultured, growing on semi-solid and liquid media, making them ideal for laboratory use. Advances in gene transfer techniques (Cai and Wolk, 1990; Elhai and Wolk, 1988; Thiel and Poo, 1989), overexpression systems, reporter fusion constructs (Bauer and Haselkorn, 1995), and gene inactivation (Golden, 1988; Haselkorn, 1991) have also made cyanobacteria an ideal model system for molecular studies. In addition, a large number (10) of cyanobacterial genomes have been sequenced, including *Anabaena*

sp. strain PCC 7120 (herein *Anabaena*), the model organism used in this thesis (http://www.kazusa.or.jp/cyano/cyano.html). For all of the above reasons, cyanobacteria are being used for molecular studies including nitrogen fixation, oxygenic photosynthesis, cellular differentiation and morphology, pattern formation and, for the purpose of this thesis, environmental regulation of gene expression.

1.3.2 *Anabaena* sp. strain PCC 7120

The genus *Anabaena* is a heterocystous, non-branching, filamentous cyanobacterium belonging to Section IV as described by Rippka *et al* (1978) (Table 1.1). *Anabaena* is an obligate photoautotroph capable of nitrogen fixation in specialized, terminally differentiated, heterocyst cells (Rippka *et al.,* 1978). *Anabaena* is found in fresh water and several strains are responsible for eutrophication or massive blooms known as "red tides" that produce harmful toxins (Rapala *et al.,* 1993). The occurrence of *Anabaena* blooms has a wide range of economic and environmental impacts. Of particular importance are the bioactive metabolites that are passively leaked by *Anabaena* during cell death and senescence. The toxic metabolites produced by *Anabaena* include hepatoxic alkaloids, neurotoxins, and microcystins (Kankaanpaa *et al.*, 2005; Carmichael *et al.*, 2001; Patocka, 2001). *Anabaena* neurotoxins include anatoxin-*a*, saxitoxin, and neosaxitoxin, which appear to have lesser toxic potency whereas microcystins have been shown to cause the greatest amount of physical harm to wildlife and aquatic animals (Falconer, 1996). A puzzling attribute of *Anabaena* and other toxic cyanobacteria is the presence of different toxins at diverse geographical locations within a single genus, suggesting a putative survival role for cyanobacterial toxins (http://ntp-server.niehs.nih.gov/).

The *Anabaena* genome contains a single 6.41 megabase chromosome and six plasmids (Kaneko *et al.,* 2001; http://www.kazusa.or.jp/cyano/Anabaena/index.html). The *Anabaena* chromosome contains 5368 putative protein-encoding genes, four copies of rRNA genes, and 48 tRNA encoding genes (Kaneko *et al.*, 2001). Interestingly, only 37% of the genes identified in *Anabaena* showed significant sequence similarity to the well-studied cyanobacterium, *Synechocystis* sp. strain PC 6803. These results suggest a vast divergence of genetic information between the two species. The current

advancements in molecular techniques (Section 1.3.1) plus the availability of the full genome sequence (http://www.kazusa.or.jp/cyano/Anabaena), established *Anabaena* as a model system for studying environmental stress gene regulation.

1.4 THE COLD SHOCK RESPONSE

Microorganisms encounter various levels of stress every day including osmotic, alkaline, acid, nutrient, and thermal stress. The organisms' survival depends on the cells' ability to adapt rapidly and specifically to external stimuli, permitting growth under stressful conditions. One of the major stresses encountered by microorganisms is a downshift in temperature, well below the optimal growth temperature. This is referred to as cold shock and/or cold stress (herein cold stress) and is characterized by specific changes in the cell physiology and gene expression in response to reduced temperature. Cold stress is species-specific; what is cold to one species may be optimal for another. For example, a drop in temperature greater than 13°C from *E. coli's* optimal growth temperature (37°C) is considered cold shock (Jones and Inouye, 1994) whereas in *Anabaena*, a drop of greater than 5°C from its optimal laboratory growth temperature (30°C) is sufficient to elicit the cold shock response (Chamot *et al.,* 1999; Yu and Owttrim, 2000).

During the cold shock response each cell goes through two growth phases, an initial lag phase called the acclimation phase, and the recovery phase where normal growth resumes after adaptation. During the acclimation phase, many physiological changes occur within the cell including a decrease in membrane lipid saturation, an increase in mRNA stability, hindered and/or altered ribosomal function, misfolding of proteins, increase in DNA superhelicity, and inhibition of DNA, RNA and protein synthesis (Phadtare, 2004; Mizushima *et al.*, 1997; Jones and Inouye, 1994). In response to the cold-induced cellular and physiological constraints, the cell reprograms gene expression, activating specific cold shock (CS) genes that encode cold shock proteins (CSPs). Thus, the cold shock response governs the expression of CSPs whose function allows adaptation to low temperatures (Wick and Egli, 2004).

CSPs are a diverse group of proteins involved in cellular cold acclimation processes involving transcription, translation, and mRNA function (Phadtare *et al*, 2003;

Thieringer *et al.,* 1998). Most CSPs bind nucleic acids and can alter nucleic acid secondary structure, antitermination of transcription, ribosome assembly and association, and mRNA degradation (Gualerzi *et al.,* 2003). Some exemplary CSPs include RNA chaperones, RNA helicases, proteases, and proteins involved in the transcriptional and translational machinery (Chamot and Owttrim, 2000; Thieringer *et al.,* 1998). The most extensively studied CSP is the major cold shock protein in *E. coli*, CspA. CspA comprises a large gene family (CspA-I) of small (~7.5 kD) proteins of which, four are cold-inducible (CspA, CspB, CspG, and CspI). The Csp protein family has a high degree of homology with CSPs from several other species including, *Bacillus subtilis* (Graumann *et al.,* 1997 and 1996), *Bacillus cereus* (Mayr *et al.,* 1996), and the eukaryotic Y-box proteins (Matsumoto, 2005). The identification of homologous CSPs throughout various prokaryotic and eukaryotic systems leads to the assumption that the Csp protein family members play a crucial role in acclimating to reduced growth temperature (Graumann and Marahiel, 1996).

Two different classes of CSPs have been identified: Class I, whose expression is dramatically increased upon a temperature downshift, and Class II, whose expression is constitutively low at optimal growth temperatures with a marginal increase in expression in the cold (Bae *et al.,* 1997). Class I CSPs include proteins such as, DesB and DesD from *Synechocystis*, and CrhC from *Anabaena.* Class II CSPs include DesC and CrhR from *Synechocystis* and CrhB from *Anabaena* (Suzuki *et al.,* 2000; Chamot *et al.,* 1999). Thus, the levels of cold shock gene expression vary depending on gene regulation and the protein's cellular role in adapting to low temperatures.

Unlike the heat shock response, which is organized as a regulon, the induction of CSPs in *E. coli* is organized as a complex stimulon and does not require a specific cold shock sigma (σ) factor (Section 1.7.1.1) (Weber and Marahiel, 2003; Ramos *et al.,* 2001; Etchegaray and Inouye, 1999; Jones and Inouye, 1994). For fast and efficient cold adaptation, the cell uses existing resources present at the time of the temperature downshift. Contradictory, Gualerzi *et al.* (2003) have also shown that CspA (Section 1.4.2) protein synthesis is inhibited in the presence of chloramphenicol and kanamycin suggesting that the induction of some CSPs may require *de novo* protein synthesis.

As shown in Figure 1.2, several conserved *cis*-acting elements have been identified within the majority of cold shock genes including CspA, involved in the regulation of cold shock gene transcription and translation. Located downstream of the Shine-Dalgarno (SD) sequence, the conserved downstream box (DB) enhances CSP synthesis by facilitating initiation of translation. The downstream box is complementary to the 3' end of the 16S rRNA (anti-downstream box) and is therefore proposed to enhance 16S rRNA interactions with the cold shock mRNAs during translation initiation. Cold shock genes also possess long, 5' untranslated regions (UTR), which leads to enhanced transcript accumulation by increasing mRNA stability in the cold (Ramos *et al.*, 2001). Cold shock genes also contain an evolutionarily conserved cold shock box, located within the 5' UTR that confers sequence-specific binding to ssDNA and RNA and is involved in transcription attenuation (Phadtare *et al.*, 1999; Graumann and Marahiel, 1996). Finally, an AT-rich element found within the promoter region functions as a transcriptional enhancer during the cold shock response.

Although the cold shock response is a fairly new area of study, related CSPs have been identified in a number of prokaryotic and eukaryotic organisms. The majority of cold shock research has been performed in *E. coli* (Section 1.4.2) but cold shock proteins have also been identified in several other species including *B. subtilis* (Willimsky *et al.*, 1992), psychrophilic bacteria (Araki, 1991), *Caulobacter crescentus* (Lang and Marques, 2004), *Chlorella vulgaris* (Salerno and Pontis, 1988), *Lactobacillus* (Serror *et al.*, 2003) *Anabaena* (Chamot and Owttrim, 2000; Chamot *et al.*, 1999), *Synechocystis* (Suzuki *et al.*, 2000), *Dictyostelium discoideum* (Maniak and Nellen, 1988), *Saccharomyces cerevisiae* (Clouter *et al.*, 1992), and *Triticum aestivum* (Danyluk *et al.*, 1991). The abundant presence of CSPs throughout a variety of different species supports that CSPs play an essential role in the cell's survival during cold stress.

1.4.1 Cellular Constraints Imposed by Cold Stress

1.4.1.1 Changes in Membrane Fluidity

Alterations to membrane fluidity are one of the major cellular changes that occur due to a reduction in growth temperature. Upon a temperature downshift, the bacterial membrane structure changes from a liquid crystalline phase to a gel phase. Cold-induced

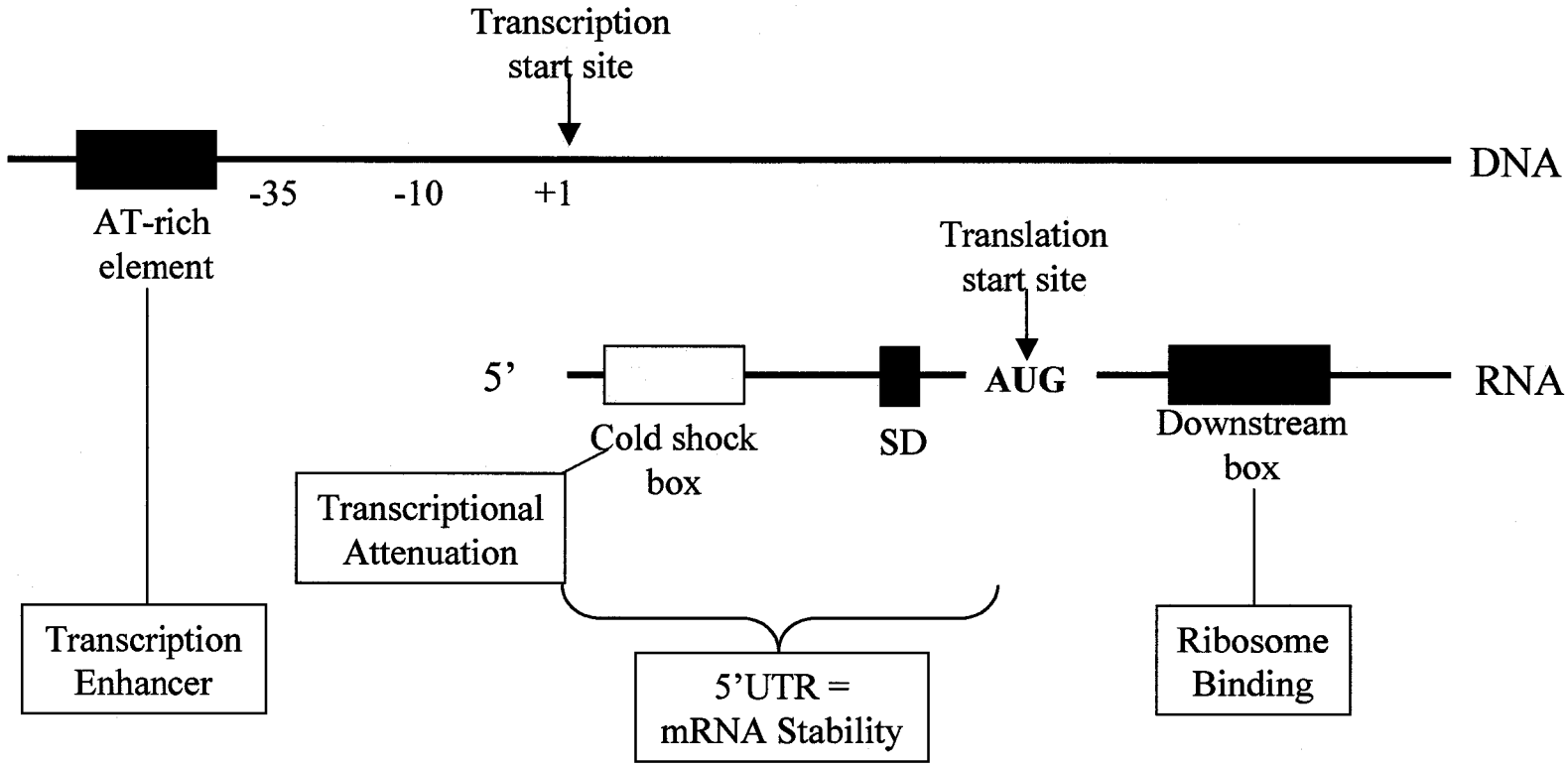

Figure 1.2. ***Cis*–acting regulatory elements implicated in the cold-induced regulation of CspA, the major cold shock protein in *E. coli*** (Thieringer *et al*, 1998). Abbreviations: UTR = untranslated region, SD = Shine-Dalgarno

membrane rigidification inhibits membrane functions such as gas exchange, enzyme activity, nutrient uptake, and nutrient transport, which are all necessary for cell survival (Graumann and Marahiel, 1996). To compensate for stress-induced cellular disturbances the cell undergoes homeoviscous adaptation, where physiological and biochemical mechanisms adjust the membrane lipid composition (Vigh *et al.,* 1998). The membrane remodeling system common in most bacteria involves the activation or induction of lipid desaturases. Lipid desaturases, such as the *Synechocystis* DesA, B, C, and D, alter the dynamic properties of the membrane by increasing the proportion of unsaturated fatty acids (UFA) present within the phospholipid bilayer. Commonly, desaturases increase membrane fluidity by inserting double bonds into specific positions within previously synthesized fatty acyl chains, thereby increasing the proportion of *cis*-unsaturated fatty-acyl groups (Mansilla and de Mendoza, 2005; Aguilar *et al.*, 2001; Suzuki *et al.*, 2000). The cold-induced unsaturated fatty acids have a lower melting point and a higher degree of flexibility, returning the membrane to its liquid state.

A significant amount of research has focused on the gene expression patterns of the cold-induced lipid desaturases. Temperature-dependent desaturase expression was first identified in *E. coli* with the cold-activation of the synthase II enzyme to produce *cis*-vaccenate (UFA) (Carty *et al.,* 1999). *B. subtilis* possesses only one cold-inducible membrane-bound desaturase (Des) that inserts double bonds into the acyl chain of membrane glycerolipids (Aguilar *et al.*, 1998; Thieringer *et al.,* 1998). The cyanobacterium *Synechocystis* sp. strain PC 6803 has four desaturase genes, induced to various degrees by cold stress (Los *et al.*, 1997). DesA, DesB, and DesD are cold-induced with DesB having the greatest magnitude of induction. DesC is constitutively expressed, regardless of temperature (Suzuki *et al.,* 2000). All four *Synechocystis* desaturases have a similar mode of action as the *B. subtilis* desaturase, and are localized in the thylakoid and cytoplasmic membranes whereas, eukaryotic desaturases are localized to the endoplasmic reticulum (Mustardy *et al.,* 1996).

By altering membrane fluidity, desaturase enzymes play an essential and specific role during cold acclimation. Mutational analysis on the desaturase (*des*) gene(s) in *B. subtilis* and *Synechocystis* produced different phenotypic results dependent on the role of the gene(s) in cold adaptation. In *B. subtilis*, the *des* mutation had a lethal effect whereas

in *Synechocystis* the *desA* mutation produced cold-sensitivity, suggesting that each cold-induced desaturase provides a specific and essential function during cold shock (Murata and Wada, 1995).

1.4.1.2 Inhibition of Translation Initiation

The second major constraint imposed on the cell due to a downshift in temperature is a block in general protein synthesis. Reduced growth temperature is proposed to inhibit translation initiation of non-cold shock genes by; altering the nucleic acid secondary structure causing a reduction in mRNA translation efficiency and/or inhibiting normal ribosomal functions (Phadtare, 2004; Jones and Inouye, 1994). Evidence of cold-induced blockage of translation initiation was observed in *E. coli*, where following a decrease in growth temperature, a decrease in polysomes was observed accompanied by an increase in the 50S and 30S ribosomal subunits (Jones and Inouye, 1996).

Translation initiation restrictions caused by cold stress appear to play an important role in inducing the cold shock response. *In vivo*, antibiotics inhibiting translation were capable of inducing the cold shock response in *E. coli*. These results proposed that a functional blockage of the ribosome by the antibiotics mimicked the physiological signal for cold shock protein (CSP) induction (Thieringer *et al.*, 1998; Jiang *et al.*, 1993; VanBogelen and Neidhard, 1990). The transient blockage of translation initiation appears to be the rate-limiting step during cold stress, halting cell growth and possibly being a signal for inducing the cold shock response (Etchegaray and Inouye, 1999; Theiringer *et al.*, 1998).

If bulk translation of new proteins is inhibited, then how are proteins synthesized during cold adaptation? The ribosome adaptation model states that genes translated during the acclimation phase of the cold shock response encode a set of ribosome-associated proteins required for the formation of translation-initiation complexes at low temperature. In *E. coli*, in response to cold stress, the cold-adapted translation-initiation complex requires three CSPs for formation, ribosomal binding factor A (RbfA), initiation factor 2 (IF-2), and CsdA, a cold-induced RNA helicase (Ramos *et al.*, 2001). The cold-adapted initiation complex can then interact with the ribosome to convert the cold-

sensitive, non-translating ribosome into a cold-resistant, translating state, capable of overcoming mRNA secondary structure restraints to synthesize non-cold shock proteins essential to restore normal growth (Jones and Inouye, 1996; Thieringer *et al.,* 1998).

Based on the ribosome adaptation model, preferential synthesis of CSPs during the acclimation phase must occur to allow non-cold shock proteins to be synthesized. This indicates that cold shock mRNAs, unlike most other cellular mRNAs, possess a mechanism to assemble the translation-initiation complex in the absence of the cold shock ribosome-associated proteins (Thieringer *et al.,* 1998). Unlike most mRNAs, cold shock mRNAs are equipped with *cis*-elements that are proposed to make them more prone to being translated in the cold. For example, contradictory evidence suggests that the downstream box present within the coding region (Figure 1.2) may (Etchegaray and Inouye, 1999; Thieringer *et al.,* 1998) or may not (La Teana *et al.*, 2000; Rocha *et al.*, 2000; O'Conner *et al.*, 1999) provide an extra 30S ribosome-binding site via Watson-Crick complementarity with the 16S rRNA (Gualerzi *et al*, 2003).

Translational bias of cold shock genes may also be caused by a transient induction of *trans*-acting elements. In *E. coli*, it is proposed that cold-induced increases in CspA and the translation initiation factors IF1, IF2, and IF3 result in a transient imbalance in the initiation factors/ribosome ratio, selectively stimulating the translation of cold shock mRNA (Giuliodori *et al.*, 2004; Gualerzi *et al.*, 2003). More specifically, IF3 levels alone appear to be the essential component for the selective translation of cold shock mRNA (Giuliodori *et al.*, 2004; Gualerzi *et al.*, 2003; Howe and Hershey, 1983). Multiple control elements are therefore potentially involved in the modification of the translational apparatus during cold shock, allowing the formation of the translation initiation complex and the preferential translation of cold shock mRNAs.

1.4.2 mRNA Stability

Alteration in mRNA stability is an intrinsic property that permits timely changes in gene expression by changing the half-life of a transcript. Recent cold shock research has identified that post-transcriptional mechanisms appear to play an important role in determining cold shock transcript stability and translation efficiency. Cold-induced thermodynamic changes within the secondary structure of cold shock mRNAs stabilizes

the transcript by, inhibiting accessibility of the mRNA degradation machinery to the transcript, or by providing accessibility of the transcript to accessory protein and/or the translation apparatus.

Goldenberg *et al.* (1996) observed several variations in *cspA* mRNA levels when *E. coli* was grown at different growth temperatures. At 37°C the *cspA* mRNA was destabilized with a half-life ($t_{1/2}$) of 0.66 minutes, indicating that the mRNA degradation machinery was functional at 37°C and could access the *cspA* mRNA. However, following a downshift in temperature to 15°C for 30 minutes, the *cspA* mRNA was stabilized with a transcript half-life greater than 70 minutes. Interestingly, following 120 minutes of exposure to cold shock conditions the transcript half-life decreased to 12 minutes suggesting that transcript stability is transient. These results suggest that there are structural and/or functional changes that occur during the acclimation phase to alter *cspA* mRNA stability (Gualerzi *et al*, 2003; Goldenberg *et al.*, 1996). It was proposed that cold-induced alterations in the RNA degradation machinery block its ability to interact and degrade the *cspA* transcript, thereby stabilizing the transcript at low temperature (Gualerzi *et al*, 2003; Goldenberg *et al.*, 1996).

Although the above explanation is plausible, the most likely cause for an increase in cold shock transcript half-life is due to an increase in thermodynamic stability of the RNA secondary structure during cold stress. An increase in RNA secondary structure can prevent ribonuclease accessibility and/or allow access of the ribosome to ribosome-binding sites, thereby stabilizing the transcript and increasing translation efficiency. In support, Sato and Nakamura (1998) determined the mRNA half-life of the cold-induced RNA binding protein, *rbpA1,* to be 4-fold higher in cold-shocked cells compared to optimally grown cells, supporting the idea that mRNA stability increases upon a temperature downshift. Similar results were observed by Chamot and Owttrim (2000), where the cold-induced RNA helicase gene, *crhC*, was shown to have a six-fold longer transcript half-life at 20°C than at 30°C.

The unusually long 5' UTR regions of cold shock mRNAs have been proposed as putative mRNA stabilizing elements during cold stress (Jager *et al.*, 2004; Afonyushkin *et al*, 2003; Yamanaka *et al.*, 1999). Under different temperature conditions, the 5' UTR is capable of forming altered secondary structures, which may be active at one

temperature and inactive at another. Similar post-transcriptional mechanisms have been observed regulating translation of several rhizobial heat shock genes and *Listeria* virulence genes (Johansson *et al.*, 2002; Nocker *et al.*, 2001). At high temperature, the mRNA secondary structure melts providing access to the ribosome-binding site, which is inaccessible at low temperatures due to complementary base pairing. A similar mechanism may also be used to explain cold shock mRNA stabilization at reduced temperature. Rather than melting of 5' UTR secondary structures, exposure to reduced temperature alters the structure of the 5' UTR in such as way that it stabilizes it. For example, cold-induced altered formation of specific stem loop or hairpin structures within the CSP 5' UTR may protect the transcript from degradation by blocking an endoribonuclease (RNase E or RNase P) cleavage site or by allowing specific stem-loop binding factors to interact (Gualerzi *et al.*, 2003; Yamanaka *et al.*, 1999; Goldenberg *et al.*, 1996). Thermodynamically altered stem-loop structures may also be involved in the antitermination of transcription by protecting or providing access to RNase III degradation (Goldenberg *et al.*, 1996).

Cold-induced altered RNA secondary structures may also be used to explain why non-cold shock proteins are not selectively translated during cold stress. Thermodynamic changes within non-cold shock mRNAs (lack long 5' UTR) may mask ribosomal binding sites thereby inhibiting translation initiation by preventing ribosomal interactions. Cold stress-induced changes of the RNA degradosome, increased or altered 5' UTR secondary structure, and alterations in the protein synthesis apparatus may all aid in the induction of cold shock protein synthesis at reduced growth temperatures.

Although transcriptional regulation has been shown to be important for the expression of some (*hns* and *gyrA*) cold shock genes (La Teana *et al.*, 1991), the majority of cold shock activation mechanisms are now focusing on post-transcriptional regulatory events. Overexpression studies using an expression vector containing the *cspA* gene under the transcriptional control of constitutive λpL or *lpp* promoters demonstrated that the *cspA* promoter was not required for *cspA* cold-induction (Gualerzi *et al.*, 2003; Brandi *et al.*, 1996). These results support the involvement of post-transcriptional regulatory events in the temperature-dependent expression of *cspA*, suggesting a regulatory complexity beyond transcriptional activation. Post-transcriptional regulation of cold

shock gene expression not only allows the cell to rapidly respond to environmental signals but also provides mechanisms to "fine-tune" cold shock gene regulation for efficient cold adaptation.

1.4.3 Cold Shock Response in *E. coli*

The cold shock response was first identified in *E. coli,* making it the model organism for cold shock studies. In *E. coli*, growth occurs between 10°C to 45°C, with normal protein expression occurring between 25°C to 37°C (Stanier *et al.,* 1976). Below 25°C, *E. coli* exhibits cold-induced patterns of gene expression including the induction of CSPs, synthesis of proteins involved in transcription and translation, flagella, sugar transport, metabolism (Phadtare and Inouye, 2004), and repression of heat shock proteins (Jones and Inouye, 1994). *E. coli* contains 26 proteins that are cold-inducible, 12 of which have been identified that are transiently expressed during cold acclimation (Gualerzi *et al.*, 2003). For example, some *E. coli* Class I CSPs (Section 1.4) include, CspA, CspB, CspG and CspI (proposed RNA chaperones), CsdA (RNA helicase), RbfA (ribosome-binding factor), NusA (transcription termination and antitermination factor), and PNPase (exoribonuclease) (Phadtare *et al.,* 2000). Class I CSP mRNAs share the common feature of having long 5' UTRs. For example, CspA's 5' UTR is 159 bp, CspB's is 161 bp, CspG's is 155 bp, and CsdA's is 226 bp (Mitta *et al.*, 1997). Class II proteins have short 5' UTRs and include, RecA (recombination factor), IF-2 (initiation factor), H-NS (DNA-binding protein), GyrA (α subunit of DNA gyrase involved in DNA supercoiling), Hsc66 (Hsp70 homologue), HscB (proposed molecular chaperone), dihyrolipoamide transferase, and pyruvate dehydrogenase (energy generators) (Phadtare *et al.,* 2000; Etchegaray and Inouye, 1999; Wang *et al.*, 1999; Jones *et al.*, 1987; Herendeen *et al.*, 1979).

The large cold shock protein (Csp) family of *E. coli* consists of nine genes (*cspA - cspI*) with over 50 homologues in an array of different prokaryotes (Thieringer *et al.,* 1998; Yamanaka *et al.*, 1998). CspA, CspB, CspC, and CspI all have very long 5' UTRs (a conserved feature for Class I CSPs). CspA is the major cold shock protein in *E. coli*, comprising over 10% of the total cellular protein synthesis (Goldstein *et al.*, 1990). CspA is a 70 amino-acid β-barrel protein (7.4 kDa) with two RNA-binding motifs

involved in RNA chaperoning and destabilization of nucleic acid secondary structure to increase translation efficiency (Phadtare *et al.*, 2004; Yamanaka *et al.*, 1998). CspA also mediates the downstream expression of cold shock genes, *nusA, infB, pnp,* and *rbfA* through transcriptional anti-termination of Rho-independent terminators (Ramos *et al.*, 2001, Bae *et al.*, 2000).

As shown in Figure 1.3, regulation of *cspA* expression involves an intertwined network of regulatory mechanisms at the transcriptional, mRNA stability, protein stability, and translational levels. For example, *cspA* is positively regulated at the transcriptional level by an upstream AT-rich element, which interacts with the α–subunit of the RNA polymerase (Mitta *et al.*, 1997; Ross *et al.*, 1993). CspA is also negatively autoregulated by its own cold shock box and is proposed to bind a putative repressor which blocks transcription and/or destabilizes the mRNA (Fang *et al.*, 1998; Jiang *et al.*, 1996). Transcription of *cspA* is controlled by a transcriptional attenuation mechanism through CspC and CspE, both non-cold shock proteins (Thieringer *et al.*, 1998). *cspA* is also regulated post-transcriptionally by its unusually long (159 bp) 5' UTR and downstream box, both necessary for efficient translation initiation (Ramos *et al.*, 2001; Phadtare *et al.*, 2000; Thieringer *et al.*, 1998; Yamanaka *et al.*, 1998). The *cspA* 5' UTR conveys mRNA stability by adopting a different RNA secondary structure which favors translation initiation at reduced temperatures (Yamanaka *et al.*, 1999). The downstream box enhances translation by permitting ribosomal binding without the synthesis of new ribosomal factors, at low temperatures. Transcription of the 5' non-coding region of *cspA* is also involved in the depression of CspA expression at the end of the acclimation phase (Yamanaka *et al.*, 1998; Jones and Inouye, 1994). Under non-stressful conditions, the expression of *cspA* is also transcriptionally regulated by the activator Fis and the repressor H-NS (Ramos *et al.*, 2001).

It is interesting to note that, although CspA is the major cold shock protein present during cold acclimation, its presence is not necessary for survival of *E. coli* at low temperatures. A *cspA*-deletion mutant showed no phenotypic effect during cold shock due to functional complementation by the CspA homologs, CspB, CspG and CspE (Phadtare and Inouye, 2004; Yamanaka *et al.*, 1998). A quadruple deletion strain (Δ*cspA* Δ*cspB* Δ*cspE* Δ*cspG*) does exhibit cold sensitivity at 15°C but the mutation can be

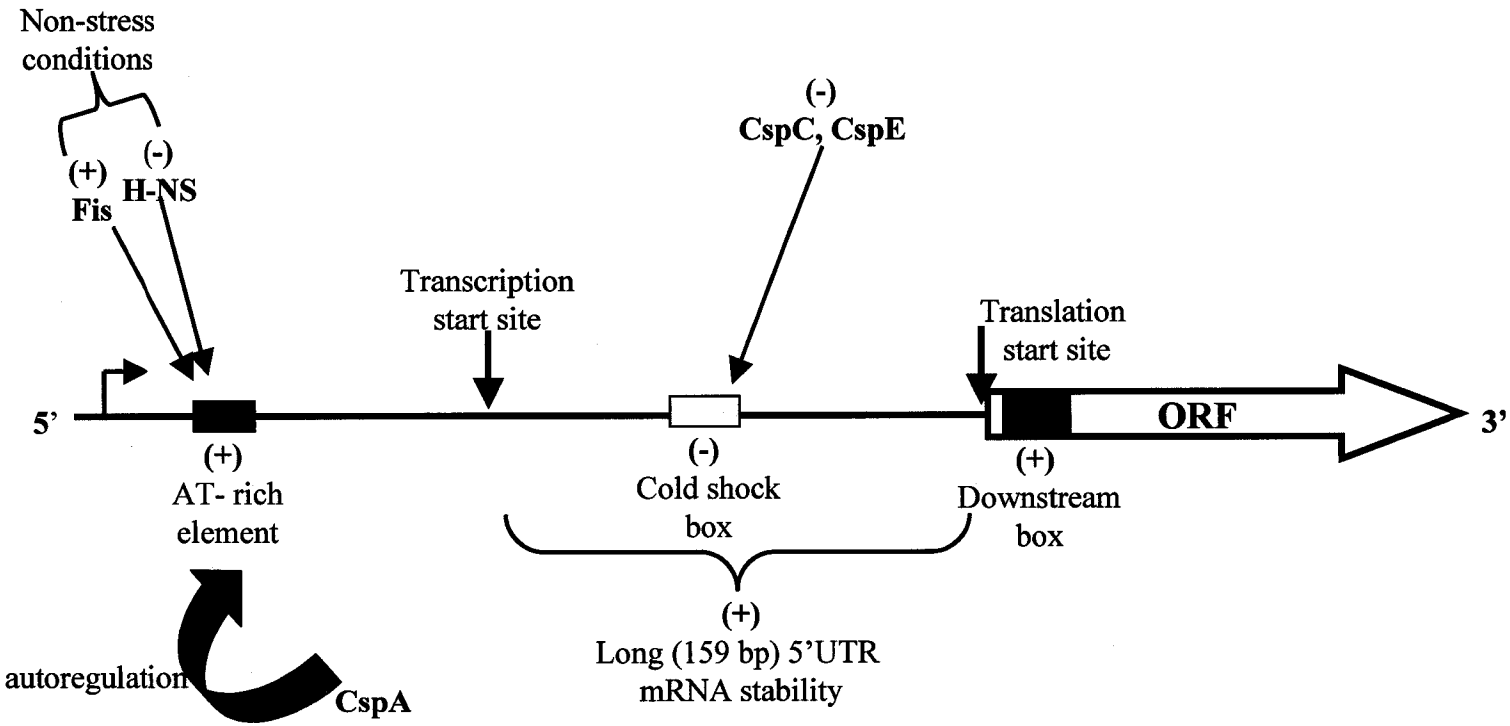

Figure 1.3. Multiple levels of *cspA* regulation during cold shock. The *cis*-acting regulatory elements are indicated by the colored boxes. The (+) indicates a positive regulatory effect, activating or enhancing transcription or translation of CspA during cold stress (15°C). The (-) indicates a negative regulatory effect, repressing transcription or translation of CspA at optimal growth temperature (37°C).

suppressed by almost all members of the Csp family (except CspD) (Phadtare and Inouye, 2004, Xia *et al.*, 2001). The presence of at least four functionally complementing CspA homologues provides evidence that *E. coli* is well protected against cold stress and suggests that the Csp family is very important for cold acclimation (Phadtare and Inouye, 2004, Xia *et al.*, 2001).

1.4.4 Cold Shock Response in Cyanobacteria

In contrast to *E. coli* and other bacteria in which the Csp family of CSPs constitutes the major cold shock protein, cyanobacteria do not possess homologues of the *csp* genes. It has been proposed that a family of RNA chaperones encoding RNA-binding proteins (Rbps) replaces the Csp family in cyanobacteria. RNA-binding proteins bind to RNA with high affinity for polyU and polyG sequences (Graumann and Marahiel, 1996) and are involved in various aspects of RNA metabolism such as splicing, modification, maintenance of stability, and translation (Nagai *et al.,* 1995; Kenan *et al.,* 1991). Although the cold shock domain (CSD) and the ribosome-binding (RBD) domain of the Rbps differ in topology and sequence from Csps, research suggests that they may have a converged function with respect to the cold shock response and that the Rbps may be the cyanobacterial counterpart of *E. coli* CSPs (Sato, 1995; Murata, 1989).

In the cyanobacterial strain *Anabaena variabilis* M3, five cold-regulated *rbp* genes (*rbpA1*, *A2*, *B*, *C,* and *D*) have been identified with similarities to UIA snRNP, the well-characterized RNA-binding protein family in eukaryotes (Sato, 1995). *Anabaena* M3 Rpbs are also similar in sequence to the plant chloroplast RBD proteins, but differ structurally from CspA (Graumann and Marahiel, 1996; Sato, 1995). Several additional cold-inducible proteins have been identified in cyanobacteria including a family of fatty acid desaturases (Murata and Wada, 1995), RNA helicases (Chamot *et al.,* 1999), caseinolytic proteases (Clps) (Dmitry and Murata, 1999; Porankiewicz and Clarke, 1997), the ribosomal small subunit protein S21 (Sato *et al.*, 1997), and Lti2, an α-amylase and glucanotransferase homolog (Sato, 1992).

The majority of cyanobacterial cold shock studies have focused on the cell membrane and the cellular processes involved in adapting membrane fluidity via lipid desaturases. Cyanobacterial acyl-lipid desaturases are bound to the thylakoid and plasma

membrane and introduce double bonds into specific regions of fatty acids that have been esterified (Murata and Wada, 1995; Phadtare *et al.*, 2000). Four (*desA - D*) (Section 1.4.1.1), and three desaturase genes (*desA – C*) have been identified in *Synechocystis* sp. strain PCC 6803 and *Synechococcus* respectively, which are differentially regulated during the cold shock response (Dimtry *et al.* 1997; Sakamoto *et al.*, 1997). A redox-regulated RNA helicase, CrhR, has also been shown to be differentially regulated by temperature in *Synechocystis* (Kujat and Owtrrim, unpublished). Two RNA helicases, CrhB and CrhC, have also been identified in *Anabaena* sp. strain PCC 7120 (Chamot *et al.*, 1999). CrhC was shown to be strictly cold-inducible upon a temperature shift from 30°C to 20°C (Section 1.5), whereas CrhB is expressed under a broad range of conditions, with enhanced expression in the cold (Chamot *et al.*, 1999). The abundance of CSP throughout the different cyanobacterial species suggests that Rbps, like the *E. coli* Csp family, play a major role in cyanobacterial adaptation to reduced temperature.

1.5 COLD-INDUCIBLE RNA HELICASES IN *ANABAENA*

RNA helicases can be involved in any cellular process that involves modulation of RNA secondary structure. RNA helicases are encoded in almost all species (except for a few bacteroids) and aid in essential cellular functions by unwinding double-stranded or duplexed RNA into a single-stranded, functional form. Using PCR cloning and degenerate primers modeled after conserved sequences in the tobacco eIF-4A gene family, Chamot *et al.* (1999) identified two putative cyanobacterial RNA helicases (Crh), CrhB and CrhC, which are differentially expressed in *Anabaena*. CrhB and CrhC were the first RNA helicases to be identified and characterized in cyanobacteria. Based on spatial and sequence similarities to eIF-4A, both cyanobacterial RNA helicases belong to the DEAD-box family with CrhB showing 51% similarity to CrhC. CrhC showed sequence similarity to a large majority of known RNA helicases, particularly to the *E. coli* RNA helicase RhlE, with 74% similarity (Chamot *et al.*, 1999).

CrhC is a 47 kDa protein containing seven of the eight conserved helicase motifs (Figure 1.2) with a novel FAT box (Phe-Ala-Thr) replacing the conserved SAT motif (Ser-Ala-Thr) (Chamot *et al.*, 1999). The SAT motif is required for helicase unwinding activity (Section 1.2.1) therefore an amino acid modification (S to F) may imply changes

to CrhC activity and substrate specificity. The modified SAT to FAT motif introduces a hydrophobic, aromatic phenylalanine residue, which is not capable of normal serine hydrogen bond formation, producing a more rigid protein. This unique property of CrhC may limit RNA substrate interactions, specify accessory protein interactions, or may allow for CrhC to unwind RNA in a unidirectional fashion (Section 1.5.2) (Chamot *et al.*, 1999; Yu and Owttrim, 2000).

Transcript analysis determined that the *crhB* transcript is expressed under a variety of stress conditions, implying that it plays a role in the general stress response. c*rhC* is solely temperature-regulated, with transcript accumulation occurring only during cold stress (Chamot *et al.*, 1999). The *crhC* transcript is not detectable at 30°C, but following a downshift in temperature to less than 25°C (cold stress) there is a rapid accumulation of *crhC* transcript. *crhC* transcript levels remain elevated during cold stress but return to basal levels upon a return to 30°C (Chamot and Owttrim, 2000; Chamot *et al.*, 1999). The CrhC protein expression profile follows a similar pattern as the *crhC* transcript profile, with CrhC present only in cold-shocked cells.

Due to the expression patterns of CrhB and CrhC, both RNA helicases are believed to play a unique and specific role in cold acclimation. Proposed mechanisms include unwinding RNA secondary structure in the 5' UTR of cold-induced mRNAs thereby removing the block in translation initiation (Section 1.4.1.2). CrhC could therefore initiate the translation of specific CSP mRNAs, whose protein products alleviate the physiological constraints imposed by a temperature downshift.

1.5.1 *Cis*-Acting Regulatory Factors of CrhC

DNA is referred to as the genetic blueprint of life, providing vital information about gene function and regulation. Comparative CSP sequence analysis has identified several conserved *cis*-acting sequences (Figure 1.2) shown to be involved in cold shock functions such as transcription, and translation. Sequence analysis of the *crhC* promoter region, along with the upstream and downstream sequences, identified sequences similar or related to those known to be required for cold-induced gene expression.

Based on sequence analysis, the cold-induced expression of *crhC* may be transcriptionally regulated by a number of elements within the promoter and 5' UTR.

Primer extension analysis (Yu and Owttrim, 1999) identified two putative transcriptional start sites at -115 and -120 base pairs upstream of the translation start site (AUG). It is not uncommon for cyanobacteria to have multiple transcription start sites but their exact functions are not known. Promoter analysis to identify transcriptional regulatory elements found a σ^{70}-dependent, -10-like sequence but a -35-like region was not observed. This was to be expected since differentially expressed genes do not usually possess a –35 region (Chamot *et al.,* 1999). An AT-rich element was also found 53 to 65 base pairs upstream of the transcriptional start site (+1), resembling an enhancer element. A similarly localized AT-rich element is a positive transcriptional regulator of the *E. coli* cold shock gene, *cspA* (Jiang *et al.,* 1996). Finally, transcriptional regulation may also be achieved by a cold shock box found downstream (+87 to +97) of the *crhC* transcription start site (Chamot *et al.,* 1999). This sequence shows 64% sequence similarity to the *E. coli cspA* cold shock box, involved in transcription attenuation (Chamot *et al.,* 1999).

Temperature-dependent expression of CrhC may also be regulated by conserved elements found within the translation initiation region. A putative downstream box (DB) (+137 to + 151) was identified within the *crhC* open reading frame (ORF) having sequence complementation to the *Anabaena* 16S rRNA (putative anti-downstream box). The *E. coli* DB is predicted to be involved in the formation of extended complementary base pairing around the Shine-Dalgarno (SD) sequence thereby enhancing translation initiation (Figure 1.2). Like all Class I CSPs in *E. coli*, *crhC* also has a long (115 bp) 5' UTR that is predicted to fold into a stable secondary structure. The translation start site (AUG) is found in a loop whereas the SD sequence and the DB are proposed to form a partial, base pairing stem (Chamot *et al.*, 1999). Finally, downstream of the translation stop codon is a putative 22 bp stem loop followed by a stretch of four U residues, a structure characteristic of a Rho-independent transcriptional terminator. This 3'UTR structure could provide *crhC* with not only a mechanism for terminating transcription, but may also be involved in mRNA stability.

Comparably, the *crhC* sequence harbors conserved *cis*-acting elements identified in *cspA* as contributing to temperature-regulated expression. The reoccurrence of cold-regulating *cis*-acting elements throughout different species may suggest similar or even global regulatory mechanisms involved in regulating cold shock gene expression.

1.5.2 Biochemical Properties of CrhC

Deduced amino acid sequence analysis identified CrhC as a DEAD-box RNA helicase. Biochemical assays identified CrhC as having RNA-dependent ATPase activity, ATP-independent RNA binding and (d)ATP-dependent RNA unwinding activity (Yu and Owttrim, 2000).

Yu and Owttrim (2000) purified CrhC using a His-tag overexpression and purification system. His-tagged CrhC exhibited low levels of ATPase activity in the absence of RNA but upon the addition of exogenous RNA, ATPase activity levels increased 7 to 10-fold (Yu and Owttrim, 2000). Upon examination of RNA substrate specificity, it was determined that CrhC did not show specificity *in vitro* but increased ATPase activity was detected when assayed with exogenous rRNA from *E. coli,* and crude polysome preparations from cold-shocked *Anabaena* cells (Yu and Owttrim, 2000). Small variations in RNA substrate specificity suggest that CrhC may be ribosome-associated. RNA-dependent ATPase activity was also shown to be dependent on the presence of Mg^{2+} and Mn^{2+}. CrhC's ability to unwinding dsRNA non-specifically *in vitro* is not unexpected, as the majority of RNA helicases analyzed to date do not unwind a specific RNA substrate (i.e. NPH-II, CsdA, SrmB, p69, etc.). The only RNA helicase known to require a specific RNA substrate for activity is DbpA, which unwinds only the 23S rRNA (Section1.2.2) (Diges and Uhlenbeck, 2001; Pugh *et al.*, 1999)

In contrast to eIF-4A, the majority of RNA helicases analyzed have ATP-independent RNA binding activity (Pause *et al.,* 1993). Electrophoretic mobility shift assays (EMSA) performed with purified CrhC in the presence of partial dsRNA showed retarded gel migration, irrespective of ATP addition (Yu and Owttrim, 2000). This demonstrates that, like the majority of RNA helicases, CrhC binds RNA substrates in the absence of ATP, most likely via motif VIII (HRIGRxxR) (Figure 1.1). Although the *in vitro* results suggest that CrhC binding is not dependent on ATP or RNA substrate specificity, this may not be the case *in vivo* in the presence of native RNA substrates and accessory proteins.

Yu and Owttrim (2000) also demonstrated that *in vitro*, CrhC was capable of unwinding artificially duplexed RNA with unwinding activity being 5' specific and

adenosine nucleotide-dependent. Artificial partially duplexed RNA substrates containing only 5' single-stranded ends or both 5' and 3' single-stranded ends were readily unwound by CrhC whereas single-stranded RNA duplexes containing only 3' ends were not (Yu and Owttrim, 2000). These results suggest that CrhC unwinds in a unidirectional 5'to 3' fashion, or that co-factors are required for CrhC to unwind in the 3'to 5' direction. Unidirectional 5' to 3' unwinding is a rare characteristic of RNA helicases as the majority of helicases unwind bidirectionally or unidirectionally in the 3'to 5' direction. One of the few other helicases shown to possess 5' to 3' unidirectional unwinding activity was RNA helicase II, a DEAD-box RNA helicase found in HeLa cells (Flores-Rozas and Hurwitz, 1993).

Several RNA helicases have shown to be biochemically active only in multisubunit complexes (Section 1.2.3). Far-Western analysis identified that CrhC forms a complex with a constitutively expressed 37 kDa protein (Yu and Owttrim, 2000). Recent research also supports that an active CrhC complex localized to the cell poles in *Anabaena*, may function in the transertion of proteins into or across the plasma membrane (El-Fahmawi and Owttrim, 2003). Together, this data suggests that CrhC interacts *in vivo* with accessory proteins either to provide substrate specificity or to optimize functionality during cold stress.

Structurally and biochemically, CrhC is classified as a DEAD-box RNA helicase but it also possesses unique properties that may provide CrhC with a specific function during cold adaptation. The novelty of CrhC is first evident with its modified SAT to FAT motif (motif VI). Several viral RNA helicases have been identified carrying a SAT to TAT modification, which upon mutational analysis has shown to be essential for coupling ATP hydrolysis and RNA unwinding (Plumpton *et al.*, 1994). The replacement of the serine residue with phenylalanine suggests that the FAT motif may be responsible for the 5' to 3' unidirectional RNA unwinding properties of CrhC. Besides CrhC, the only other prokaryotic DEAD-box RNA helicases that have been analyzed biochemically are the *E. coli* proteins DbpA and CsdA. CrhC is therefore, the first prokaryotic RNA helicase that has been shown to catalyze RNA unwinding *in vitro*, implying that CrhC does not require accessory proteins for the unwinding of artificial dsRNA substrates (Yu and Owttrim, 2000).

1.5.3 Regulation of CrhC Expression

CrhC is differentially expressed in responses to cold stress, therefore coordinated regulation is necessary for activation and inactivation of CrhC expression at low and optimal growth temperatures, respectively. CrhC expression is strictly dependent on a temperature downshift, with transcript and protein accumulation occurring constitutively at 20°C (cold stress) but not at 30°C (optimal growth) (Chamot and Owttrim, 2000; Chamot *et al.,* 1999). Chamot and Owttrim (2000) established that *crhC* transcript accumulation was temperature-dependent, with regulation occurring at the transcriptional, post-transcriptional, mRNA stability, and translational levels.

Anabaena is an obligate photoautotroph (Section 1.3.2) therefore it requires the presence of light for glucose metabolism and cell growth. To understand if light was required for cold-induced *crhC* expression, Northern analysis of *crhC* was performed in the absence and presence of light. Chamot and Owttrim (2000) observed that low temperature-induced *crhC* transcript accumulation was dependent on light-derived metabolic activity indicating that, for *crhC* to be induced and synthesized during cold stress, the cell requires energy derived from light harvesting.

Transcriptional regulation can be seen immediately upon a downshift in temperature with *crhC* transcript accumulation occurring within 15 minutes of cold stress. The *crhC* transcript is absent at 30°C and rapidly accumulates at temperatures below 25°C, with maximum transcript levels observed between 15°C to 20°C (Chamot and Owttrim, 2000). During extended exposures to cold stress, variations in *crhC* transcript levels are evident. After 24 hours of cold stress, *crhC* levels decrease 4-fold but recover to the initial induced levels (i.e. 15 minutes) after 48 hours (Chamot and Owttrim, 2000). This observation suggests that *crhC* may be transcriptionally regulated at two levels, with a rapid initial response at 30 minutes and a circadian response at 24 hours (Chamot and Owttrim, 2000). Cold-induced *crhC* accumulation is also completely reversible upon a temperature upshift to 30°C due to temperature altered mRNA stability. *crhC* transcript abundance is therefore tightly regulated by small changes in growth temperature and the duration of cold stress.

It is well known that the mRNA stability of cold shock genes is enhanced in the cold, which involves the long 5' UTRs characteristic of cold shock mRNAs (Section 1.4.1.2) (Yamanaka et al., 1999; Sato and Nakamura, 1998; Los *et al.,* 1997; Sakamoto and Bryant, 1997). Increased mRNA stability in the cold was shown to play a role in *crhC* transcript accumulation as demonstrated by Chamot and Owttrim (2000). In the presence of the transcriptional inhibitor rifampin the transcript half-life of *crhC* was shown to be 6 times longer at 20°C, than 30°C. Cold-induced stabilization of other bacterial cold shock mRNAs has also been observed including the four desaturase genes (*desA - D*) from *Synechocystis*, two desaturase genes (*desA* and *desB*) from *Synechococcus*, *rbpA1* from *Anabaena variabilis* M3, *cspA* from *E. coli* and *Rhodobacter capsulatus, rnr* from *E. coli*, and the *B. subtilis bkd* operon (Jager *et al.*, 2004; Nickel *et al.*, 2004; Cairrao *et al.*, 2003; Sato and Nakamura, 1998; Los *et al.*, 1997; Sakamoto and Bryant, 1997). Stabilization of the *crhC* transcript at 20°C appears to play an important role in providing temperature-regulated CrhC expression, although the exact mechanism(s) conveying stability is not known.

Temperature-induced changes in the rate of transcription may also play a role in *crhC* transcript accumulation at low temperature. By quantifying the *crhC* transcript in both the absence and presence of rifampin, Chamot and Owttrim (2000) demonstrated that transcription of *crhC* continued following a temperature upshift from 20°C to 30°C. Temperature-induced changes in transcription activity are also observed in several other bacterial cold shock genes including *desA* and *desB* from *Synechococcus* sp. strain PCC 7002 (Sakamoto and Bryant, 1997), *cspA* from *E. coli* (Goldenberg *et al.*, 1996) and *rbpA1* from *Anabaena variabilis* M3 (Sato and Nakamura, 1998). These results suggest that *crhC* temperature-regulated expression may be very complex, involving mechanisms at both the transcriptional and post-transcriptional level.

A downshift in temperature inhibits translation initiation (Section 1.4.1.2), suggesting that inhibition of protein synthesis could act as an induction signal for cold shock gene expression. When *in vivo* protein synthesis in *Anabaena* was inhibited by the addition of chloramphenicol or tetracycline at 30°C, the resulting *crhC* transcript accumulation only marginally mimicked cold-induced *crhC* transcript accumulation.

Inhibition of protein synthesis is therefore only one component of the signal for *crhC* accumulation during cyanobacterial cold stress (Chamot and Owttrim, 2000).

crhC transcript accumulation varied *in vivo* depending on the mode of inhibition by the various antibiotics tested, providing insight into the exact mode(s) of *crhC* regulation (Chamot and Owttrim, 2000). Differences in *crhC* transcript accumulation may suggest that derepressors or activator proteins may be involved in the regulation of *crhC* transcription. DNA-binding proteins have also been shown to regulate expression of other cold shock genes including *rbpA1* in *Anabaena variabilis* and *hns* and *gyrA* in *E. coli* (Sato and Nakamura, 1998; La Teena et al., 1991).

Finally, posttranscriptional regulation of *crhC* may also occur at the translational level. Induction of the CrhC polypeptide levels correspond to *crhC* transcript levels during the initial stages of cold shock, but with prolonged cold exposure the levels no longer correlate (Chamot and Owttrim, 2000). It is possible that CrhC may autoregulate its expression by unwinding its own 5' UTR region for efficient translation initiation, particularly during the acclimation phase.

Based on the sequence, regulation, and biochemical properties of CrhC, putative roles can be assigned for its involvement in cold acclimation. During the acclimation phase, CrhC may unwind specific RNA secondary structures of cold shock mRNAs (including itself), alleviating the blockage in translation initiation and allowing protein synthesis of these select genes. Upon adaptation, CrhC may unwind non-cold shock genes essential for the return to normal growth. Subcellular localization studies showing that CrhC associates with the cytoplasmic face of the inner membrane (El-Fahmawi and Owttrim, 2003) also suggests that CrhC may aid in the translation of mRNAs whose protein products are translocated into or across the cell membrane. The localization of CrhC to the plasma membrane has also proposed new roles for CrhC in RNA turnover. In *E. coli*, the RNA degradosome is plasma membrane associated (Liou *et al.*, 2001) and complexes with the DEAD-box RNA helicase, RhlB, for mRNA degradation (Py *et al.*, 1996). The ability of RhlB to be complemented by CsdA (and RhlE) (Khemici *et al.*, 2004) implies an involvement of CsdA in the cold-adapted *E. coli* RNA degradosome (Beran and Simons, 2001). In *Anabaena*, CrhC may also be incorporated into the cold-adapted RNA degradosome providing ssRNA to PNPase, for degradation (El-Fahmawi

and Owttrim, 2003; Py *et al.*, 1996). It has also been proposed the CrhC may play a role in mRNA maturation as two DEAD-box RNA helicases (HrpA and SrmB) have been shown to be required for mRNA processing and maturation in *E. coli* (Koo *et al.*, 2004; Charollais *et al.*, 2003). Although the exact role of CrhC is unknown, the inability to obtain CrhC mutants (Magee, 1997) suggests that its role is specific and essential for cell survival at a low temperature.

1.6 COLD SHOCK PERCEPTION AND TRANSDUCTION

1.6.1 Two-Component Signal Transduction Pathways

For a microorganism to maintain cellular equilibrium it must be able to sense, communicate, and respond to environmental stimuli. Bacteria, plants, yeast, and fungi commonly perceive and transduce environmental stresses using two-component signal transduction pathways. Specific external stimuli signal a communication cascade via phosphotransfer, regulating expression of a specific subset of genes whose protein products are required for adaptation to the changing conditions. A two-component signal transduction pathway is comprised of a membrane bound histidine kinase (HK) sensor and a cytoplasmic response regulator (RR). Through a series of phosphotransfers from the HK to the RR, a specific output response is elicited. In several cases, the two-component signaling transduction pathway contains multiple phosphotransfer steps between two or more proteins including auxiliary proteins, hybrid kinases, phosphatases, and proteins that enhance RR autophosphatase activity (Perraud *et al.*, 1999). Signal transduction pathways therefore form a potential cross-talk system for gene regulation (West and Stock, 2001).

The majority of HKs are membrane bound homodimeric proteins that are activated upon external stimulus and dimerization. There are 350 members of the HK superfamily, each containing several conserved domains (Grebe and Stock, 1999). As shown in Figure 1.4, each HK monomer has an amino-terminus periplasmic sensing domain coupled to a carboxy-terminus cytoplasmic, ATP-dependent, kinase signaling domain. The sensing domain varies in sequence depending on the external stimuli that it perceives whereas the ATP-binding kinase domain is highly conserved containing a

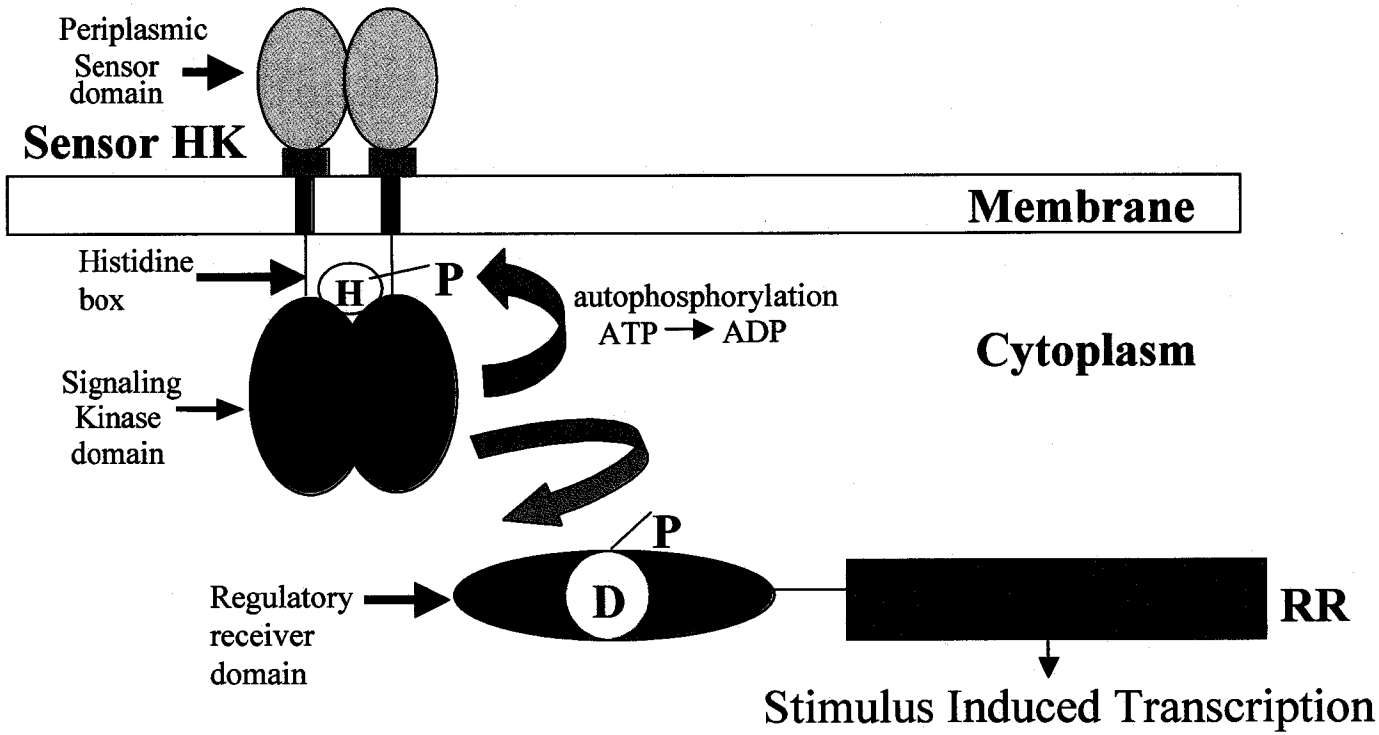

Figure 1.4. Conserved domains of the two-component signal transduction pathway involved in perceiving and transducing environmental stress signals (Perraud *et al.*, 1999). Abbreviations: HK= histidine kinase, RR= response regulator.

conserved histidine box that serves as both a dimerization domain and a substrate for autophosphorylation (Appleby *et al.,* 1996).

The RR acts at the end of the phosphotransfer pathway and functions as a phosphorylation-activated switch that regulates a specific gene output response (West and Stock, 2001). The RR is located in the cytoplasm and contains two conserved domains, an amino-terminus regulatory receiver domain and a carboxy-terminus effector domain. The receiver domain performs three functions; it catalyzes the transfer of a phosphoryl group from the HK to its own conserved aspartate residue, it catalyzes autodephosphorylation, and it regulates activities of its associate effector domain in a phosphorylation-dependent manner (Perraud *et al.,* 1999). The effector domain interacts with DNA and functions as a transcriptional regulator, activating or repressing specific genes according to the stimulus.

A proposed mechanism for the induction of the cold shock response (and other stress responses) begins with the extracellular, periplasmic sensor domain of the HK receiving an external stimulus, possibly indirectly via stressed-induced physiological restraints (Section 1.6.2). The stimulated sensor domain signals the HK to dimerize followed by ATP-dependent autophosphorlyation of the histidine residue within the histidine box of the cytoplasmic kinase signaling domain (Figure 1.4). The regulatory receiver domain of the RR then catalyzes dephosphorylation of the HK and phosphorylation of its own conserved aspartate residue, inducing a conformational change. This activates the effector domain, which will elicit a specific output response such as, the activation of cold shock genes and/or the repression of heat shock genes. The two-component signal transduction pathway allows for the incorporation of a wide array of proteins having different domain arrangements, therefore creating a large assortment of putative signaling pathways for environmental stress gene regulation.

Two-component signal transduction pathways have been identified in both prokaryotes and eukaryotes including *E. coli* (Mizuno, 1997), *Streptomyces coelicolor* (Sheeler *et al.*, 2005) *S. cerevisiae* (Li *et al.,* 1998), *Pyricularia oryzae* (Motoyama *et al.*, 2005), *Candida albicans* (Kruppa *et al.*, 2004), and *Arabidopsis thaliana* (Makino *et al.,* 2000). The use of a two-component signal transduction pathway for perceiving and transducing cold stress has been found in both *B. subtilis* and *Synechocystis* sp. strain

PCC 6803. In *B. subtilis*, Aguilar *et al.* (2001) identified the histidine kinase DesK, and the response regulator DesR, involved in the cold induction of the sole *des* gene, coding for the Δ5-lipid desaturase for maintenance of membrane fluidity. Also, using *des* gene reporter fusions Suzuki *et al.* (2000 and 2001) identified a membrane bound histidine kinase, Hik33, a downstream hybrid kinase, Hik19, and response regulator, Rer1, which are all involved in low-temperature-induced transcriptional regulation of the *desB* gene in *Synechocystis*.

The overall importance of these two-component signal transduction pathways in low-temperature sensing and regulation remains to be clarified. For example, Hik33, Hik19, and Rer1 were not shown to be involved in the temperature regulation of *desA* or *desD*, which are known cold-inducible desaturase genes in *Synechocystis* (Section 1.4.1.1). These results suggest that Hik33, Hik19, and Rer1 are not the only components responsible for cold shock gene regulation, and that several pathways may be involved in regulating the genes (such as *desA* and *desD*) required to elucidate the cold shock response. Therefore, little is known about the signaling events involved in low-temperature regulation of cold shock gene expression, and whether or not a global "cold-thermostat" exists.

One-component signal pathways are also widely distributed among bacteria and archaea and provide a more simplistic mechanism for bacteria to sense and respond to stressful environments. In this scenario, a single protein molecule containing both an input sensor domain and output effector domain regulates gene expression (Ulrich *et al.*, 2005). The two domains have high sequence homology to sensor and effector domains found within two-component signaling systems but lack the phosphotransfer kinase domain and the receiver domain. Unlike two-component systems, which primarily detect external stimuli, one-component systems detect signals inside the cell (i.e. block in translation initiation). By analyzing the information encoded by 145 different prokaryotic genomes, Ulrich (2005) found that one-component systems were abundant within all of the bacterial species studied including cyanobacteria, *B. subtilis* (RocR), *Bordetella pertussis*, and *Agrobacterium tumefaciens* (TraR). With the option of both one and two-component signaling systems found throughout all bacteria, it creates a large array of combinatorial diversity for gene regulation at the transcriptional level.

1.6.2 Thermosensors

Before the advent of the molecular tools required to identify the two-component cold-sensing signaling pathways described above, a number of possible bacterial thermosensors or thermosignals were proposed. Although these proposals do not fit as the sole "cold sensor", the observations leading to the proposals must be incorporated into the overall cold sensing model.

Bacteria cope with cold stress by using cellular thermosensors to sense changes in the temperature. Putative cellular thermosensors/thermosignals for cold shock include the membrane(s), nucleic acids, and proteins (Phadtare *et al.,* 1999). The first three examples of thermosensor listed below, are involved in sensing and eliciting the overall cold shock response, affecting a wide array of cold shock genes. A change in membrane lipid fluidity is the first physiological event that signals a change in temperature. This was demonstrated *in vivo* in *Synechococcus* sp. strain PCC 6803 where palladium-catalyzed hydrogenation of membrane lipids activated the transcription of *desA* without a temperature downshift (Vigh *et al.,* 1993). Inaba *et al.*, (2003) also demonstrated using DNA microarray analysis that they could enhance cold-responsive gene expression in *Synechocystis* by disrupting both *desA* and *desD* desaturase genes, which in turn increased the rigidity of the cell membranes. These results demonstrated that changes in membrane fluidity could act as a cold signal, communicating to the cell to induce the expression of desaturase genes and increase the ratio of unsaturated fatty acids within the membrane. The idea of membrane fluidity being a cold thermosensor suggests both a direct and indirect (i.e. HK perceives changes in membrane fluidity) mechanism to alter membrane fluidity, which in turn induces the cold shock response.

VanBogelen and Neidhardt (1990) also suggested that ribosomes could be the "cold sensor" in bacteria. They observed that the cold shock response was induced in the presence of certain antibiotics that target the ribosome. Antibiotics such as chloramphenicol, erythromycin, and tetracycline block the A-site of the tRNA, which alters the state of the ribosome and signals the induction of the cold shock response. During cold shock, the translation efficiency of non-cold shock mRNAs (Section 1.4.1.2) is reduced causing charged tRNAs to accumulate in the cell, blocking the tRNA A-sites,

and in turn decreasing the levels of (p)ppGpp within the cell due to blocked protein synthesis. In support, Jones *et al.* (1992a) demonstrated that low levels of (p)ppGpp could increase the levels CSP synthesis. Thus, the pleiotrophic nature of (p)ppGpp within the cell could stimulate the magnitude of the cold shock response (Wick and Egli, 2004; Graumann and Marahiel, 1996; Jones and Inouye, 1994). Furthermore, the ability of the cold shock ribosome to translate *cspA* more efficiently than ribosomes isolated from cells grown at 37°C (optimal) (Brandi *et al.*, 1999) suggests that the state of the ribosome and/or the factors associated with it, may act as a thermosignal for CSP induction (Graumann and Marahiel, 1996).

Supercoiling of DNA has also been suggested as a transcriptional thermosensor during cold shock (Wang and Syvanen, 1992). When cells are exposed to low temperatures, the synthesis of gyrase and negative supercoiling of the DNA transiently increases thereby changing the linking number and superhelical density, which in turn influences transcription (Phadtare *et al.,* 1999 and 2000). Grau *et al* (1994) proposed that DNA supercoiling might regulate unsaturated fatty acid synthesis in *B. subtilis*, as the desaturation of fatty acids induced by a temperature downshift is inhibited by novobiocin, an inhibitor of DNA gyrase. Similar results were observed in *Synechocystis* when monitoring the expression of the desaturase genes in the presence of novobiocin (Los, 2004). Novobiocin completely inhibited transcription of *desB* and thus blocked the formation of the corresponding omega3 unsaturated fatty acids. These results suggest that an increase in negative supercoiling at low temperatures may signal the induction of the cold shock response by the DNA gyrase altering the structure of the cold shock gene to permit access of the RNA polymerase to initiate transcription.

RNA secondary structures can also function as RNA thermosensors, however unlike the examples given above RNA thermosensors only regulate an individual gene. Recent data supports that the most likely thermosensor regulating cold shock gene expression is RNA secondary structure. Alterations within the RNA secondary structure can either stabilize or destabilize the transcript or affect translation initiation, depending on the thermodynamics. RNA thermosensors have been identified in *Listeria monocytogenes*, regulating expression of virulence genes at 37°C. Secondary structure within the 5' UTR of the virulence gene *prfA* partially melts at high temperature,

allowing ribosome entry and increasing the translation efficiency upon host infection (Johansson *et al.*, 2002). Similar RNA melting mechanisms are reported to provide post-transcriptional thermoregulation of virulence genes in *Yersinia pestis* (*lcrf*), and several heat shock genes in *E. coli* (*rpoH*) and rhizobia (Chowdhury *et al.*, 2003; Nocker *et al.*, 2001; Morita *et al.*, 1999; Hoe and Goguen, 1993). A similar but unique RNA thermosensor has also been proposed to regulate the cold-induced expression of the *E. coli cspA*. *cspA*, like most other cold shock mRNAs, have long 5' UTRs that form RNA secondary structures. It is postulated that cold-induced structural alterations (not melting) within the RNA secondary structure, particularly around the SD sequence, may enhance ribosome accessibility and/or stabilize the transcript at low temperature (Yamanaka *et al.*, 1999). It is also plausible that RNA melting of the *cspA* 5' UTR at high temperatures may destabilize the transcript by enhancing accessibility to ribonucleases. Structural changes and/or melting within RNA secondary structures could therefore act as both a heat and cold-thermosensor.

Though the exact cold sensor is unknown, combinations of the above proposed thermosensors may be required to trigger the two-component signal transduction pathway or may act alone to induce the cold shock response. Cold-specific cellular changes such as membrane fluidity may activate the cold two-component pathway, which then elicits a pleiotrophic downstream response essential for cold acclimation. Thus, thermosensors provide a signal mechanism for the cell to sense change in temperature and in turn allow the cell to communicate and regulate the specific downstream events necessary for cellular adaptation to cold stress.

1.7 DNA-BINDING PROTEINS

1.7.1 Transcriptional Regulators

Not all genes within the genome are expressed constitutively, rather the majority are expressed or repressed depending on the cell's condition, function, and developmental stage. DNA-binding proteins play a central role in regulating gene expression, genome replication, and DNA repair (Pabo and Sauer, 1992). One of the most diverse classes of DNA-binding proteins are the transcription factors (regulators). Transcription factors can regulate transcription by interacting directly with sequence-

specific DNA-binding domains on their target DNA. Transcription factors are involved in the regulation of cell development, differentiation, and cell growth by binding to specific nucleic acid sites, and activating or repressing gene expression (Pabo and Sauer, 1992).

DNA-binding proteins are grouped into classes that use related structural motifs for DNA recognition. Families of DNA-binding proteins include helix-turn-helix, homeodomain, zinc finger, steroid receptor, leucine zipper, helix-loop-helix, and β-sheet motifs (Pabo and Sauer, 1992). The helix-turn-helix motif, the first DNA-recognition motif identified, is found in the majority of prokaryotic DNA-binding proteins including the *E. coli* CAP protein (McKay and Steitz, 1981), the Lac repressor (Kaptein *et al.*, 1985), the Fis protein (Kostrewa *et al.*, 1990) and LexA (Lamerichs *et al.*, 1990). Approximately 95% of all transcription factors described in prokaryotes utilize the helix-turn-helix motif to bind their target DNA (Sauer *et al.*, 1992).

Several basic principles have been identified that demonstrate the mechanisms by which DNA-binding proteins recognize and regulate target gene expression. Site-specific recognition always involves contact with the bases and with the DNA backbone via hydrogen bonding. Most DNA-binding protein families use α-helices to make base contacts within the major groove of the DNA, with multiple DNA-binding domains necessary for site-specific recognition (Pabo and Sauer, 1992). Protein-DNA recognition and interaction is a very detailed process but because of its specificity, specific genes can be activated or repressed depending on their role within the cell.

Promoters, the *cis*-acting signals, are responsive to specific stimuli. Promoter activity is mediated by *trans*-acting regulators (i.e. transcription factors) that interact with the promoter to adjust the transcription of a specific gene. Promoter induction by a regulatory protein is dependent on the environmental stimuli and the physiological state of the cell (Vicente *et al.*, 1999). The final transcript product is also dependent on the role of the transcription factor and the recruitment of the RNA-polymerase complex to the promoter. By exploiting the molecular mechanisms involved in transcription, bacteria have developed unique methods for regulating gene expression.

1.7.1.1 Transcription Activators

Transcription factors can be grouped into two categories based on their regulatory roles on target gene expression; transcriptional activators and transcriptional repressors. Transcriptional activators are proteins that increase the transcription of a specific gene by recognizing specific *cis*-acting enhancer elements (i.e. -10 and -35 sequences) (Blackwood and Kadonago, 1998). Transcriptional activators are widespread throughout bacteria and vary in the mechanisms used to contact RNA polymerase and activate transcription. Eubacterial sigma (σ) factors can also be referred to as transcriptional activators due to their involvement with RNA polymerase, directing the RNA polymerase to the promoter for transcription initiation. Currently 14 different classes of σ-factors have been identified, each recognizing a different consensus sequence within the *cis*-acting region of a promoter (Wosten, 1998). Two major σ-factors are found in eubacteria; σ^{70}, the primary σ-factor present in all eubacteria, required for promoter recognition and DNA strand opening (Ko *et al.*, 1998) and σ^{54}, the nitrogen regulating σ-factor, which is not essential for growth (Merrick, 1993). Several other σ factors co-ordinate the expression of groups of genes in response to specific environmental or developmental signals. For example, Loewen *et al.* (1998) illustrated that σ^{S}, a general stress σ-factor encoded by the *rpoS* gene, acts as a major transcriptional activator in *E. coli* (and other bacteria) to regulate the expression of a large number of genes involved in stress acclimation.

A large majority of σ-factors comprise a regulatory cascade, in which the activity of each σ-factor depends on the action of the preceding σ-factor in the cascade (Stragier and Losick, 1990). For example, during *B. subtilis* endospore formation, programmed gene expression is governed by the sequential appearance of five developmental σ-factors (Piggot, 1996; Stragier and Losick, 1990). Tightly regulated expression of the σ-factors allows for activation of various genes involved in the different stages of endospore formation. The heat shock response also requires a σ factor to transcriptionally activate the heat shock regulon. σ^{32} transiently activates specific heat shock genes during heat stress by recognizing and binding specific heat shock promoters (Segal and Ron, 1998). Unlike the heat shock response, no general sigma factor has been

identified for cold shock gene expression. Although the list of σ-factors is long, their role in gene regulation, cell maintenance, differentiation, and adaptation are essential for cell survival.

1.7.1.2 Transcription Repressors

The importance of transcription repressors was first identified by Jacob and Monod (1961) approximately forty years ago when they were shown to be involved in the negative regulation of the *E. coli lac* operon (Maldonado *et al.,* 1999). A transcriptional repressor blocks the ability of RNA polymerase to initiate transcription from the repressed gene. Transcriptional repressors play a large role in silencing genes by directly interacting with their target DNA through a DNA-binding domain, or indirectly by interacting with other DNA-bound proteins.

Repressor proteins can inhibit transcription through three modes of action; masking of a transcriptional activation domain, blocking interaction of an activator with other components of the transcriptional machinery, or displacing an activator already present on the DNA (Johnson, 1995). For example, some prokaryotic repressors act by recruiting and binding the RNA polymerase too strongly to the promoter, thus inhibiting transcription of the cognate sequence and any steps downstream of the formation of an open complex (Vicente *et al.,* 1999). DNA response elements can also cause allosteric effects on transcriptional factors, exerting dualistic roles on transcriptional repressors by activating transcription of one gene while repressing transcription of another (Lefstin and Yamamoto, 1998).

Transcriptional repressors can be gene-specific or can exhibit a more general effect. A common family of bacteria transcriptional repressors having a general effect on gene expression is the anti-σ family. Anti-σ factors bind to specific σ factors and prevent the assembly of the RNA polymerase holoenzyme thereby inhibiting transcription (Helmann, 1999). Similarly, eukaryotic general repressors block the formation of transcription initiation complexes by targeting specific components of the RNA polymerase II transcriptional machinery. Therefore, control of gene expression depends on gene-specific repressors or the combined actions of gene-specific activators and general negative regulators.

Reactivation of a repressed gene involves the removal, or derepression, of the transcriptional repressor from the promoter. Derepression can occur by a DNA conformational change, protein-protein interaction (i.e. anti anti-σ factors), protein-RNA/DNA interactions (coproteases), autoproteolysis, or post-translational modification (Shinagawa, 1996). In *E. coli*, the well-characterized general repressor LexA is involved in negative transcriptional regulation of the SOS response. LexA binds to the regulatory region of over 20 different SOS genes, and represses their transcription in the absence of DNA damage (Shinagawa, 1996). In the presence of extensive single-stranded DNA, the LexA protein autocleaves, thereby derepressing and allowing transcription of SOS genes to resume. The directive for LexA autoproteolysis is provided by the ssDNA-RecA filament, which binds to multiple copies of LexA and activates the protein to digest neighboring LexA molecules (Stryer, 1995). Therefore, DNA damage represented by ssDNA, serves as a coprotease in the derepression of LexA. Thus, bacteria have developed highly advanced processes to differentially regulate gene expression. Specific DNA-protein interactions have provided a mechanism via transcriptional activators and repressors, for switching gene expression on and off at essential and distinct times.

Transcription termination can also occur in the absence of a transcription factor. Transcriptional attenuation can occur due to alterations in RNA folding of the nascent transcript, under different conditions. The *E. coli trp* was the first operon shown to have a regulated site of transcription termination, found within the leader sequence. In the presence of accumulated charged $tRNA^{Trp}$, a specific hairpin structure forms within the mRNA, terminating transcription. However, when $tRNA^{Trp}$ is deficient, the ribosome will stall at a Trp codon, preventing formation of the hairpin structure (anti-termination) and permitting expression of the *trp* operon (Yanofsky, 2000; Yanofsky *et al.*, 1996). Similarly, transcription can also be terminated by binding of small RNAs to complementary sequences within the nascent transcript and/or the formation of pseudoknots, blocking transcription from that point on. By using of a variety of different mechanisms to regulate gene expression it allows the cell to have specific and coordinated regulation.

1.8 THESIS OBJECTIVES

The objective of this thesis is to identify the regulatory mechanism(s) conveying temperature-dependent expression to the cyanobacterial RNA helicase gene, *crhC*. Previous work done in our lab demonstrated that *crhC* transcript accumulation is limited specifically to cold shock conditions (Chamot *et al.*, 1999). This thesis addresses two potential regulatory mechanisms providing cold-induced *crhC* expression; transcription and post-transcriptional regulation.

Transcriptional regulation was investigated with electrophoretic gel mobility shift assays (EMSA) and DNA affinity chromatography, used to identify a putative transcription factor(s) binding to an AT-rich region of the *crhC* promoter, just upstream of the –10 motif. Preliminary protein phosphorylation studies, performed to provide clues as to the nature of the upstream regulatory pathways, indicated that the DNA-binding protein bound the *crhC* promoter in the phosphorylated form, as binding was only observed in protein extracts obtained from *Anabaena* grown at 30°C. These results suggest that the DNA-binding protein functions as a repressor of *crhC* transcription. Transcriptional analysis using *crhC* promoter-reporter fusion constructs (*lux*) revealed that the *crhC* promoter and/or its motifs contribute minimally to temperature-dependent expression.

Post-transcriptional regulation was investigated by analyzing the role performed by the 5' UTR. The RNA secondary structure of the 5' UTR was predicted using MFOLD and used to construct transcriptional reporter fusions to determine which 5' UTR structure(s) were required to convey temperature-dependent expression to the reporter gene. Together the data indicates that temperature regulation of transcription plays a minor role while the 5' UTR is necessary and sufficient for conveying temperature-regulated expression to a reporter gene, even in heterologous systems. The 5' UTR of *crhC* therefore appears to function as a temperature sensor (i.e. RNA thermosensor), capable of providing extremely rapid responses, at both the molecular and physiological level, to changing environmental conditions.

CHAPTER TWO
MATERIALS AND METHODS

2.1. BACTERIAL STRAINS AND GROWTH CONDITIONS

The bacteria used in this study, their relevant genotypes and their sources are listed in Table 2.1. Throughout the text, bacteria harboring plasmids will be designated with the bacterial strain first followed by the plasmid (p) in parentheses [for example, DH5α (pSIG11) denotes the strain DH5α containing plasmid pSIG11]. *E. coli* DH5α cells were grown in liquid LB media (Luria broth media containing 10 g/L bacto tryptone, 5 g/L yeast extract, 5 g/L NaCl, and buffered with 1mL of 1N NaOH) and maintained on solid media containing 1.2% (w/v) bacto agar. When required, LB medium was supplemented with the appropriate antibiotics at the following concentrations: ampicillin 100 μg/mL, kanamycin 50 μg/mL. All *E. coli* strains were grown at 37°C, with liquid cultures aerated by shaking at 200 rpm. When cold shock treatment was required, liquid cultures were transferred to either 20°C incubators (Coldstream) or a 20°C water bath shaker for the indicated times, with shaking at 200 rpm.

Anabaena sp. strain PCC 7120 was maintained on agar plates composed of BG-11 (Allen, 1968), containing 1% (w/v) Difco grade Bacto-agar, grown in Coldstream incubators at 30°C under constant illumination (Phillips Alto cool, white fluorescent light, 30 μmoles photons/m^2/sec). Liquid cultures were aerated by bubbling with air and shaking at 200 rpm. When cold shock treatment was required, liquid cultures were transferred to a 20°C Coldstream incubator, with bubbling and shaking, for the indicated times.

2.2 ISOLATION AND PURIFICATION OF PLASMID DNA

2.2.1 Small Scale Plasmid Purification from *E. coli*

To isolate and purify small amounts of high copy plasmid DNA from *E. coli*, the TENS mini-prep method (Zhou *et al.*, 1990) was employed. A 1.5 mL aliquot of a saturated overnight culture was harvested by microcentrifuging for 10 seconds at 14,000 rpm. The supernatant was decanted and the pellet resuspended in the remaining ~100 μL

TABLE 2.1: Bacterial Strains

Strain	Relevant Genotype	Reference / Source	Use
Anabaena variabilis UTCC 387 (equivalent to *Anabaena* sp. strain PCC[a] 7120)	Wild Type	University of Toronto Culture Collection (UTCC)	Study Subject
Synechocystis sp. strain PCC[a] 6803	Wild Type	University of Toronto Culture Collection (UTCC)	Control
Synechococcus sp. strain PCC[a] 7942	Wild Type	University of Toronto Culture Collection (UTCC)	Control
Escherichia coli DH5α	*Δ(lacZYA-argF)* $_{U169}$ *(m80 lacZ ΔM15) hsdR17(*$r_K^- m_K^+$*) recA1 F'/endA1 thi-1 relA1 gyrA supE44*	Ausubel *et al*., 1995	Plasmid propagation

[a]Pasteur Culture Collection

media. The cells were lysed by vortexing for 1 - 2 seconds in 300 μL of TENS solution (100mM Tris, pH 8.0, 1 mM EDTA, pH 8.0, 1 NaOH: 0.5% [w/v] SDS). Following lysis, the solution was neutralized by vortexing for 1 - 2 sec in 150 μL of 3 M sodium acetate, pH 5.2. Cellular debris was pelleted by microcentrifugation for 5 minutes and the supernatant transferred to a sterile microfuge tube. The plasmid DNA was precipitated by the addition of 900 μL of ice-cold 100% ethanol and immediately pelleted by microcentrifugation at room temperature for 5 minutes at 14,000 rpm. The pellet was washed with 1 mL of ice-cold 70% [v/v] ethanol and microcentrifuged for 5 minutes at room temperature. The pellet was air dried and resuspended in 50 - 100 μL sterile MilliQ (mQ) dH_2O.

To isolate and purify low copy number plasmids from *E. coli* using the TENS mini-prep protocol, a few alterations were made. A 6 mL aliquot of saturated overnight culture was harvested and the cells were lysed with 450 μL of TENS and 225 μL of 3M NaOAc, pH 5.2. Upon ethanol precipitation, the DNA pellets were resuspended in 30 μL of sterile $mQdH_2O$.

2.2.2 Large Scale Plasmid Purification from *E. coli*

High copy number plasmid DNA was isolated and purified from a 100 mL *E. coli* overnight culture using the QIAGEN plasmid Midi kit according to the manufacturer's protocol. Low copy number plasmid DNA was purified using the QIAGEN manufacturer's protocol suggested for purifying low copy number plasmids, using a 500 mL *E. coli* overnight culture.

2.3 MANIPULATION OF DNA

2.3.1 Quantifying DNA

DNA was quantified by measuring the absorbance of a diluted sample at a wavelength of 260 nm. A 1 μL aliquot of the DNA sample was diluted in 500 μL of Tris-HCl, pH 8.0, and the absorbance of the solution measured at 260 nm. The DNA concentration was determined using the extinction coefficient one absorbance unit is equivalent to 50 μg/mL of double-stranded (ds) DNA (1.0 A_{260nm} = 50 μg / mL dsDNA).

2.3.2 Digestion, Gel Electrophoresis, and Visualization of DNA

DNA was digested with restriction enzymes (RE) from New England Biolabs (NEB), Roche (Boehringer Mannheim), Invitrogen, Amersham, and Promega. In a 20 μL reaction, up to 5 μg of DNA was digested in 1X RE Buffer, as suggested by the manufacturer.

DNA fragments were separated and visualized on 0.7 -1.4 % [w/v] agarose (electrophoresis grade, ICN Biomedicals, Inc.) gels using either 0.5 X TBE (45 mM Tris-borate, 1 mM EDTA) or 1X TAE (40 mM Tris-acetate, 1 mM EDTA) as the buffering system. One-fifth volume of 5X DNA loading buffer (30% [w/v] sucrose, 0.125% [w/v] bromophenol blue, 5 mM EDTA, pH 8.0) was added to each DNA sample prior to loading. Small-scale plasmid preps were also treated with 1 μL of RNase A (10 mg/mL) at 37^0C for 10 minutes, to remove RNA contaminates. DNA agarose gels were electrophoresed at a constant voltage for the appropriate lengths of time, stained with ethidium bromide (10 μg/mL) for 1 minute, and visualized and recorded digitally by observing fluorescence on a UV transilluminator (Syngene Genius Bio Imaging Systems). DNA fragment sizes were estimated by comparing the sample migration distances to known DNA standards (1 kb+ Ladder, Invitrogen), run simultaneously on each gel.

2.3.3 Purification of DNA from Agarose Gels

DNA fragments were purified from 1X TAE, 1% agarose gels using the PEG-trough method (Zhen and Swank, 1993). Upon electrophoretic separation, a large majority of the 1X TAE (40 mM Tris-acetate, 1 mM EDTA) running buffer was removed and a UV hand-held illuminator (UVP Mineralight Lamp UVGL-58) was used to visualize the DNA. Below the DNA fragment of interest, a small cubic portion of the gel was excised with a clean scalpel, creating a trough. The trough was filled with PEG/TAE (18.75 mM PEG, 1X TAE) and a small amount of 1X TAE running buffer was returned to the electrophoresis apparatus, just enough to cover the bottom of the gel. With constant voltage, the DNA fragment of interest was electrophoresed into the PEG/TAE trough. The PEG/TAE containing the "trapped" DNA fragment was removed from the trough and extracted once with an equal volume of phenol: chloroform (1:1) and once

with an equal volume of chloroform: isoamyl alcohol (24:1). The DNA was precipitated with 2.5X ice-cold 100% ethanol and washed with 1 mL of 70% ethanol. The air-dried pellet was resuspended in $mQdH_2O$, quantified (Section 2.3.1), and stored at -20°C.

2.3.4 Polymerase Chain Reaction (PCR)

DNA fragments were amplified using PCR, with reactions comprised of a combination (written as forward primer: reverse primer) of primer pairs (Table 2.2) and the appropriate template DNA. DNA fragments were amplified using the Expand Long Template PCR System (Roche) in either 50 or 100 µL final volumes. Each 50 µL reaction was comprised of 1X PCR Buffer #1 (17.5 mM $MgCl_2$), 350 µM of each dNTP (A, T, G, C), 10 - 20 pmoles of the required forward and reverse primer, 4 units of Expand DNA polymerase enzyme, and up to 20 fmoles of template DNA. After thorough mixing, the reaction was overlaid with an equal volume of mineral oil and amplified in a MiniCycler (MJ Research) using the specified Touchdown program. After the initial denaturation (94°C), the annealing temperature decreases by 10°C, in 0.5°C increments, over 20 cycles. The program cycles 20 more times at the lowest annealing temperature before completing amplification. The annealing temperature of each PCR reaction was determined based on the T_m of the primers as determined by the supplier (Sigma Genosys). A "hot start" was performed for all PCR reactions in which, the thermocycler was allowed to reach the initial denaturation temperature (94°C) before inserting the reaction tubes.

2.3.5 DNA Ligation

Digested DNA fragments, purified from agarose gels, were ligated into digested plasmid vectors with compatible ends. Ligation reactions (20 µL) were performed with 1 unit of T4 DNA ligase (Roche), 1X Ligase buffer (Roche), and various insert to vector ratios. The ligation reaction was incubated at 15°C or 4°C, for 16–20 hours.

When blunt-end cloning PCR products, a fill-in reaction (Ausubel *et al.*, 1995) was performed with Klenow (Roche). Blunt-ended (2 pmoles) and symmetrically digested (50 pmoles) vectors were dephosphorylated with calf alkaline phosphatase (CIP) (Roche). 1 unit of CIP and one-tenth volume of the supplied buffer (Roche) were

TABLE 2.2: Oligonucleotide Primers

Primer	Sequence (5' - 3')	Origin of Sequence	Use
WCM1	TGTCAGTTGCTACT	*crhC* bp 1031 to 1018 (antisense strand)	EMSA non-competitive assays
GWO36	CCATGAGCGCATTCA	*crhC* bp 920 to 933 (sense strand)	EMSA non-competitive assays
GWO43	CGTCCTGATAAGACAGCAG	*crhC* bp 231 to 213 (antisense strand)	Promoter cutback identification / Sequencing
GWO71	TAATACGACTCACTATAGGG	pBluescript KS+	Biotinylated *T7* for DNA affinity chromatography
GWO72	GGGTGTGGGTTTGGTGTA	*crhC* bp 193 to 176 (antisense strand)	End- labeling
JB1	GGCTGGTTGTAGAGATCTTGG	*crhC* bp -391 to -371 (sense strand)	*crhC* promoter transcriptional fusion to the *lux* operon
JB2	GGACAAGCCGAGATCTGAAAAAG	*crhC* bp 142 to 120 (antisense strand)	*crhC* promoter + 5' UTR 1st stem loop transcriptional fusion to *lux*
JB3	GGCCAGTGAGCGCGCGTAATAC	pBluescript KS+	To replace *T7* which formed primer-dimers with *GWO43*
JB4	GGGGAGAGTAAAGCTGGCAG	*crhC* bp 289 to 269 (antisense strand)	To replace *GWO43* which formed primer-dimers with *T7*
JB5	CTCTGTTAGGATCCACCATTG	*crhC* bp -20 to 1 (sense strand)	Cloning of *crhC* 5' UTR and/or ORF behind an *E. coli* constitutive promoter
JB6	GCGCCAGCTAGCAAATCTCGTC	*crhC* bp 249 to 228 (antisense strand)	Cloning of *crhC* 5' UTR and ORF behind an *E. coli* constitutive promoter
JB7	GGACAAGCCGAGATGAG	*crhC* bp 142 to 126 (antisense strand)	Shorten cutbacks for DNA affinity chromatography
JB8	GGGGTGCAATCTTCGC	*crhC* bp -115 to -100 (sense strand)	Shorten cutbacks for DNA affinity chromatography
JB9	CGTCATTTCCAACTATTA	*crhC* bp -78 to -61 (sense strand)	Shorten cutbacks for DNA affinity chromatography
JB10	CCTGTACTCTGTTAAG	*crhC* bp -26 to -11 (sense strand)	Shorten cutbacks for DNA affinity chromatography
JB11	GATAGCGAATACCCCAATG	*crhC* bp 15 to -4 (antisense strand)	Shorten cutbacks for DNA affinity chromatography
JB12	GGTTTGAGGGGCGGGATG	*crhC* bp 51 to 34 (antisense strand)	Shorten cutbacks for DNA affinity chromatography
JB13	CTTAACAGAGTACAGG	*crhC* bp -11 to -26 (antisense strand)	Shorten cutbacks for DNA affinity chromatography
JB14	TTCCAACGATTAAGATTA	*crhC* bp -72 to -55 (sense strand)	Mutate AT-rich element of *crhC* promoter
JB15	CCCCAATGGTAGATCTTAACAG	*crhC* bp 4 to -18 (antisense strand)	*crhC* promoter only transcriptional fusion to the *lux* operon
JB18	CATGAATTCTTTAGGGGCTGGT	*crhC* bp -156 to -135 (sense strand)	*crhC* AT-rich element and -10 region for transcriptional fusion to *lux*
JB19	CCCGAATTCTGAATCTTAACA	*crhC* bp 3 to -17 (antisense strand)	*crhC* AT-rich element and -10 region for transcriptional fusion to *lux*
JB20	5' - GCGAATTCGGATCCAACTATTAATATT AAAGTTTAGAGAAAGGATCCGAATTCGG - 3'	*crhC* bp -31 to 25 (sense strand)	Along with *JB21*, encodes the *crhC* AT-rich element for transcriptional fusion in front of the *lux* operon
JB21	5' - CCGAATTCGGATCCTTTCTCTAAACTT TAATATTAATAGTTGGATCCGAATTCGC - 3'	*crhC* bp 25 to -31 (antisense strand)	Along with *JB20*, encodes for the *crhC* AT-rich element for transcriptional fusion in front of the *lux* operon
JB22	GTTTTCCCAGATCTAGTTTGAG	*crhC* bp 269 to 248 (antisense strand)	Cloning *crhC* 5' UTR stem loop structure(s) b/w a constituitive promoter and *lux*
JB23	CGCCTAAGACGGATCCCGCTAC	*crhC* bp 62 to 83 (sense strand)	Cloning *crhC* 5' UTR 2nd stem loop structure b/w a constituitive promoter and *lux*
*B*JB12*	GGTTTGAGGGGCGGGATG	*crhC* bp 50 to 34 (antisense strand)	Biotinylated *JB12* for DNA affinity chromatography
pNLP10-F	GCTTCCCAACCTTACCAGAG	pNLP 10	Sequencing pNLP10 constructs
pNLP10-R	CACCAAAATTAATGGATTGCAC	pNLP10	Sequencing pNLP10 constructs
JSA12	CGGTAGAGTTGCCCCTACTCCGGTTTTAG	tRNA^{Ser}	Probe for Northern RNA load control

* Restriction sites found within the primer are show in blue (BamH I), red (EcoR I), green (Bgl II), and orange (Nhe I).

incubated with the appropriate concentration of digested vector for 30 minutes at 37°C. A second unit of CIP was added and incubation continued at 45°C for 45 minutes. CIP was inactivated by phenol: chloroform extraction and ethanol precipitation method as above (Section 2.3.3) and the dephosphorylated DNA was resuspended in $mQdH_2O$ at a final concentration of 0.1 μg/μL.

2.3.6 Bacterial Transformation

DH5α cells were made chemically competent by treating with rubidium chloride/calcium chloride solutions under cold conditions (Ausubel *et al.*, 1995). An overnight culture of DH5α was diluted 1:100 into 100 mL of fresh LB and grown to an OD_{600} of 0.6 by shaking (200 rpm) at 37°C for approximately 3 hours. The culture was cooled on ice for 30 minutes and then harvested at 4°C by centrifugation in a Beckman JA-14 rotor at 4000 rpm for 10 minutes. Upon decanting the supernatant, the pellet was gently resuspended in one-half volume of ice-cold Buffer A (10 mM RbCl, 10 mM MOPS, pH 7.0) and incubated on ice for 20 minutes. The cells were harvested as above and the pellet resuspended in one-half volume of ice cold Buffer B (10 mM RbCl, 0.1 M MOPS, pH 6.5, 50 mM $CaCl_2$). The cells were incubated on ice for a minimum of 30 minutes, pelleted, and resuspended in one-tenth volume of ice-cold Buffer B. DMSO was added to a final concentration of 7% and the competent cells were dispensed in 600 μL aliquots. The competent cells were flash frozen in liquid nitrogen and stored at -80°C.

When transforming the chemically competent DH5α cells with foreign DNA, the heat shock method was employed, with a few modifications (Ausubel *et al.*, 1995). Competent cells were thawed on ice and for each transformation, 200 μL of competent DH5α cells were used. The amount of ligated DNA added to the competent cells depended on the plasmid copy number and concentration of DNA used in the ligation reaction. For high copy plasmids and/or DNA concentrations greater than 1 μg, half of the ligation reaction (10 μL) was added. For low copy plasmids and/or DNA concentrations less than 1 μg, the full ligation reaction (20 μL) was mixed with the 200 μL of competent cells. The transformation mixture was placed on ice for 30 minutes, heat shocked at 42°C for 2 minutes, and incubated on ice for 5 minutes. Prewarmed LB

medium (1 mL) was added to each transformation and incubated at 37°C for 1 – 2 hours. For cells transformed with high copy plasmids, 100 µL of the transformation was plated on LB plates containing the appropriate antibiotics and incubated at 37°C overnight. For low copy plasmids, the complete transformation was harvested by microcentrifugation and the supernatant decanted. The pellet was resuspended in the remaining 50-100 µL of medium and plated on selective LB plates. For detection of β-galactosidase activity using blue/white selection, 50 µL of a 5:1 X-gal: IPTG (2% [w/v] X-gal: 100 mM IPTG) mixture was overlaid on the LB plates 30 minutes prior to plating the transformed cells.

2.3.7 Bacterial Electroporation

To increase the efficiency of transformation, electrocompetent DH5α cells were prepared through a series of ice-cold mQdH_2O and glycerol washes (Ausubel *et al.*, 1995). An overnight culture of DH5α cells was diluted 1:100 into 25 mL of fresh LB and grown to an OD_{600} between 0.5-0.7 at 37°C, with shaking at 200 rpm. The cells were chilled for 15 minutes in an ice water bath and harvested by centrifuging at 4200 rpm for 10 minutes at 4°C. The cell pellet was gently washed three times in 25 mL of ice-cold sterile mQdH_2O, and three times in 10% [v/v] ice-cold glycerol, with centrifugation at 4200 rpm for 10 minutes between each wash. The final resuspension was dispensed in 50 µL aliquots, flash frozen in liquid nitrogen, and stored at -80°C. For each electroporation, 50 µL of electrocompetent cells were thawed on ice, mixed with 100 ng of DNA or 1 µL of unknown DNA concentration, and transferred to a chilled, 1 mm gap sterile electroporation cuvette (Molecular BioProducts). The mixture was electroporated in an Eppendorf Electroporator 2510, pulsed with 1800 volts at a time constant less then 5 msec. Immediately after electroporation, 300 µL of LB medium was added and the mixture incubated at 37°C for 1.5 hours without shaking. Appropriate volumes of transformed cells were plated on selective nutrient agar plates, using the same criteria mentioned in Section 2.3.6.

2.3.8 DNA Sequencing

Dideoxy chain termination sequencing was performed using the DYEnamic ET Terminator Cycle Sequencing Kit (Amersham Biosciences). Prior to sequencing, small-scale plasmid preparations were treated with 1 μL of RNase A (10mg/mL) and incubated at 37°C for 15 minutes. RNase A was inactivated by extracting with phenol: chloroform and ethanol precipitation (Section 2.3.3) and the DNA was resuspended in sterile $mQdH_2O$. In a final volume of 20 μL, the sequencing reaction contained 1X sequencing dilution buffer (80 mM Tris, 2 mM $MgCl_2$, pH 9.0), 1X sequencing reagent mix (Thermo sequenase II DNA polymerase, ddNTPs, dNTPs, 80 mM Tris, 2 mM $MgCl_2$, pH 9.0), 5 pmoles of primer, and 500-800 ng of template DNA. The reaction was amplified in a thermocycler (MJ Research) using the following parameters: 95°C denature for 30 sec, 50°C annealing for 15 sec, 60°C elongation for 60 sec, cycled 25 times. Once cycling was complete, the reaction was precipitated with 4 volumes of 95% [v/v] ethanol and one-tenth volume of sodium acetate/EDTA buffer (150 mM sodium acetate, pH 8.0, 225 mM EDTA). The reaction was briefly mixed by vortexing and incubated for 15 minutes at 4°C. The precipitate was pelleted by microcentrifugation at room temperature for 15 minutes at 14,000 rpm. The pellet was washed with 400 μL of 70% [v/v] ethanol, microcentrifuged for 5 minutes, and air-dried. The dried DNA pellet was submitted to the Molecular Biology Service Unit (University of Alberta, Edmonton, Alberta) for automated sequencing using a Genetic Analyzer 3100 (prior to Sept. 2004) or an Applied Bioscience 377 (after Sept. 2004).

2.3.9 Radioactive Labeling of DNA

2.3.9.1 End-labeling DNA

The 5' ends of oligonucleotides or linear dsDNA were radioactively labeled with [γ-^{32}P]dATP (Perkin Elmer) and polynucleotide kinase (PNK)(NEB). Each end-labeling reaction contained 5 pmoles of target DNA, 1X PNK Buffer (NEB), 50 μCi of [γ-^{32}P]-dATP, and 0.01 units of PNK. The 20 μL reaction was incubated in a 37°C water bath for 30 minutes, chilled on ice, and the PNK inactivated by heating for 10 minutes at 75°C and/or by the addition of 8 μL of 3% [w/v] Dextran Blue (Sigma) in TE (10 mM Tris-HCl, pH8, 1 mM EDTA, pH 8). Unincorporated nucleotides were removed by passage

through either a 200 - 400 mesh Biogel-P2 column for oligonucleotides (Bio-Rad) or a Sephadex G-50 column for DNA fragments > 40 bp (Amersham Pharmacia Biotech), prepared in a 1 mL syringe. The probe was eluted with TE buffer and the blue fraction collected into a sterile microfuge tube. The specific activity of the purified probe (1 μL) was determined by Cerenkov counting in a Beckman LS 3801 scintillation counter.

2.3.9.2 Random-primer Labeling of DNA

Linear dsDNA was radioactively labeled using the random primer labeling technique (Feinberg and Vogelstein, 1983). Digested (Section 2.3.2) and gel purified (Section 2.3.3) dsDNA fragments were denatured by boiling for 5 minutes and immediately chilled on ice for 5 minutes. Reagents were added in the following order to synthesize a radioactively labeled complementary strand; 25-100 ng of denatured dsDNA, 75 μM of each dNTP (A, G, and T), 1X hexanucleotide buffer (Roche), 25 μCi of [α-^{32}P]dCTP (Perkin Elmer), and 1 unit of Klenow (Roche), in a 10 μL final volume. The reaction was incubated for 1 hour in a 37°C water bath and quenched by the addition of 3% [w/v] Dextran Blue (Sigma) in TE (10 μL). Unincorporated nucleotides were removed using a Sephadex G-50 column and the specific activity determined by Cerenkov counting (Section 2.3.9.1).

2.3.10 Promoter Nested Deletion Construction

Nested deletion constructs within the *crhC* promoter were created by both Dana Chamot (DC) (unpublished data) and Jordan Ward (JC) (Ward, 2001) using the plasmids pWM753 and pWM75-2, respectively (Figure 2.1, Table 2.3). pWM75-2 contains a 939 bp EcoR V insert containing the complete *crhC* promoter (315 bp), 5' UTR (115 bp) and 510 bp of the 1275 bp *crhC* ORF, cloned into the EcoR V site of pBluescript KS+ (Stragene) (Figure 2.1A). pWM753 contains a 2424 bp Hinc II insert containing the full-length *crhC* gene (promoter, 5' UTR, ORF, and the 257 bp 3'UTR) cloned into pBluescript KS+ (Figure 2.1B).

Exonuclease III (Exo III) digestion was performed on BamH I/Sac I digested pWM75-2 and pWM753 (Table 2.3) using an Erase-a-base kit (Promega). Details of the selected deletions are presented in Table 2.4. 3' to 5' exonuclease activity was stopped at

Figure 2.1. Construction of plasmids pWM75-2 and pWM753. Panel A shows a diagram (not to scale) of pWM75-2, which contains a 939 bp EcoR V cleaved *crhC* insert cloned into the EcoR V multiple cloning site (MCS) of pBluescript II KS+ (pBS). The *crhC* insert was cloned with the 5' end closest to the BamH I site of the pBS MCS. The pWM75-2 *crhC* insert contains the full-length *crhC* promoter, 5' UTR, and 510 bp of the ORF. Panel B shows the diagram of pWM753, which contains a 2424 bp Hinc II cleaved *crhC* insert cloned into the Hinc II site in the MCS of pBS. The *crhC* insert was cloned with the 5' end of the gene closest to the BamH I site within the pBS MCS. The pWM753 *crhC* insert contains the full length *crhC* gene (promoter, 5' UTR, ORF, and 3'UTR) plus ~ 460 bp more of upstream sequence than present in pWM75-2.

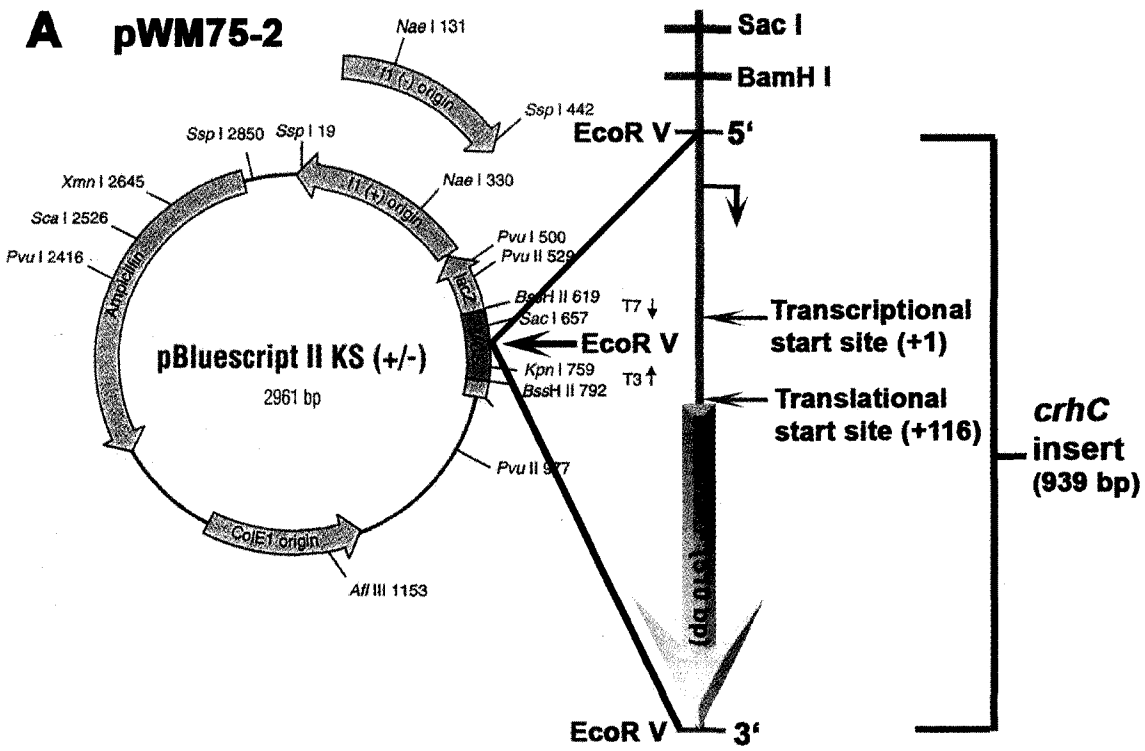

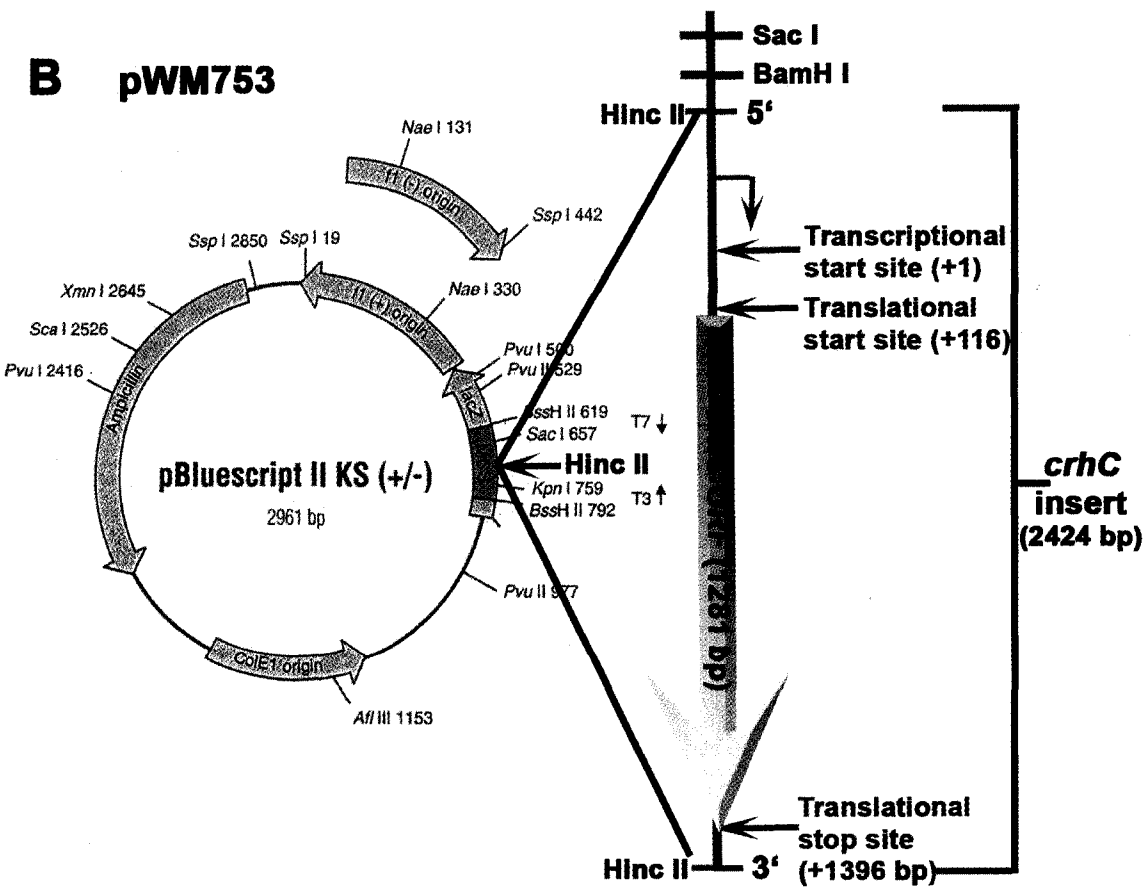

TABLE 2.3: Parent Plasmids

Plasmid	Source	Selective Marker	Importance / Insert Sequence	Use
pBluescript KS+ (pBS)	Stratagene	Ampicillin	Cloning vector	Cloning
pWM753	Magee, 1997	Ampicillin	The complete 2424 bp *crhC* gene (promoter, ORF, 5' and 3' UTR) cloned into the Hinc II site of pBS (Figure 2.1B)	Promoter deletion construction / Cloning / Sequencing / *crhC* expression analysis
pWM75-2	Magee, 1997	Ampicillin	A 939 bp *crhC* insert (promoter, 5' UTR, and portion of ORF) cloned into the EcoR V site of pBS (Figure 2.1A)	Promoter deletion construction/ Cloning Sequencing / EMSA analysis
pCS26	Dr. Mike Surette	Kanamycin	Contains *luxCDABE* operon for transcriptional reporter fusion construct generation	Cloning / *crhC* promoter motif luciferase assays in *E. coli*
pNLP10	Dr. Tracy Raivio	Kanamycin	Contains *luxCDABE* operon for transcriptional reporter fusion construct generation	Cloning / *crhC* promoter and 5' UTR luciferase assays in *E. coli*
pSIG16	Dr. Mike Surette	Kanamycin	pSC26 containing the strong SIG16 constitutive *E. coli* promoter in front of the *lux* operon	Post-transcription studies / 5' UTR luciferase assays in *E. coli*
pSIG11	Dr. Mike Surette	Kanamycin	pCS26 containing the medium strength SIG11 constitutive *E. coli* promoter in front of the *lux* operon	Post-transcription studies / 5' UTR luciferase assays in *E. coli*

TABLE 2.4: *crhC* Promoter Deletion Plasmid Constructs

Plasmid	Parent Plasmid	Insert Size	Cutback Start Site	Motifs Removed
JW2	pWM75-2	892 bp	*crhC* bp -264	none
JW3	pWM75-2	824 bp	*crhC* bp -196	none
JW4	pWM75-2	741 bp	*crhC* bp -113	none
JW5	pWM75-2	664 bp	*crhC* bp -36	AT-rich element
JW6	pWM75-2	649 bp	*crhC* bp -21	AT-rich element
JW7	pWM75-2	608 bp	*crhC* bp +20	Complete *crhC* promoter
JW8	pWM75-2	520 bp	*crhC* bp +108	Complete *crhC* promoter and cold shock box
DC1	pWM753	2227 bp	*crhC* bp -574	none
DC2	pWM753	1864 bp	*crhC* bp -211	none
DC3	pWM753	1845 bp	*crhC* bp -192	none
DC4	pWM753	1729 bp	*crhC* bp -76	none
DC5	pWM753	1696 bp	*crhC* bp -43	AT-rich element
DC6	pWM753	1656 bp	*crhC* bp -3	AT-rich element and -10 region
DC7	pWM753	1484 bp	*crhC* bp +170	Complete *crhC* promoter, 5'UTR, and downstream box
DC8	pWM753	1416 bp	*crhC* bp +238	Complete *crhC* promoter, 5'UTR, and downstream box

one-minute intervals, for a total of ten minutes, and the single-stranded DNA degraded with an S1 nuclease mix (Promega). The samples were heat inactivated at 70°C for 10 minutes, filled in with Klenow (Roche) (Section 2.3.5), blunt-end religated, and transformed into *E.coli* DH5α (Section 2.3.6). The identification of each deletion was confirmed by PCR using the primer pairs *T7:GWO43* or *JB3:JB4* (Table 2.2) and by sequencing (Section 2.3.8).

2.4 PROTEIN MANIPULATION

2.4.1 Protein Isolation

2.4.1.1 Protein Extraction from Cyanobacteria

From a BG-11 plate, a heavy inoculum of cyanobacteria was aseptically inoculated into 50 mL BG-11 and grown at 30°C with shaking until exponential phase (3 days) (Section 2.1). The complete 50 mL culture was transferred to 300 mL BG-11 and grown at 30°C with aeration until exponential phase (4 days). When required, the 300 mL culture was aliquoted into two 150 mL cultures and placed either at 30°C (optimal) or at 20°C (cold shock/stress), for the indicated times. The cells were harvested at the appropriate temperature by centrifugation (Janetzki T5) in 15 mL polypropylene tubes (Corning) at 10,000 g for 10 minutes. The pellet was washed with an equal volume of 50/100 TE (50 mM Tris, 100 mM EDTA) and 1 mM DTT, and recentrifuged. Upon decanting the supernatant, the cell pellet was flash frozen in liquid nitrogen, and either stored at –80°C or thawed immediately for protein extraction.

For cell lysis, the pellet was resuspended in an equal volume of cyanobacterial protein extraction buffer (20 mM Tris-HCl, pH 8, 10 mM NaCl, 1 mM EDTA, pH 8) containing a protease inhibitor cocktail (Complete Mini-Roche) and lysed at a temperature corresponding to the growth temperature. Cell lysis was accomplished by vortexing in the presence of an equal volume of Dyno-Mill Lead free 0.2 - 0.3 mm glass beads (Impandex Inc.) for 8 X 1 minute, with one-minute incubation in an ice-water bath between each vortex. Cellular debris was removed by microcentrifugation for 5 minutes at 14,000 rpm. Proteins were quantified using the Bradford Assay (Bio-Rad), with BSA as the standard. Protein aliquots were stored in 10% [v/v] glycerol at –80°C.

2.4.1.2 Protein Extraction from *E. coli*

An overnight *E. coli* culture was diluted 1:50 into 20 mL of fresh LB and incubated with shaking at 37°C until an OD_{600} of 0.6. For cold-shocked cells, 10 mL of the exponentially grown culture was transferred to a 20°C water bath shaker (Gyrotory Model G76, New Brunswick Scientific) for the indicated times. Cells were harvested by microcentrifuging at 14,000 rpm at the appropriate temperature for 5 minutes, flash froze, and the pellets stored at –80°C. Thawed cells were resuspended in 500 µL of chilled cyanobacterial extraction buffer including a protein inhibitor cocktail (Section 2.4.1.1) and lysed by sonicating 4 X 30 seconds with 1 minute in an ice-water bath, between each sonication. Cellular debris was removed by microcentrifugation and protein concentration quantified by the Bradford assay, as described above (Section 2.4.1.1).

2.4.2 Protein Electrophoresis

2.4.2.1 Non-Denaturing Polyacrylamide Gel Electrophoresis (PAGE)

EMSA reactions (Section 2.5.1) were separated on 8%, 10%, or 12% [w/v] native 1X TBE or 1X TAE gels. Each 12% native gel contained 1875 µL of 40% [w/v] acrylamide:bis (37.5:1) (BioRad), 78.12 µL of 1X TBE (0.1 M Tris, 0.1 M Boric acid, 2 mM EDTA, pH 8) or 1X TAE (40 mM Tris-acetate, 1 mM EDTA, pH 8), 93.75 µL of 100% glycerol, 3184.4 µL of $mQdH_2O$, 312.5 µL of 1.5% [w/v] APS, and 3.125 µL of TEMED. Slab gels (5 mL) were cast in a Bio-Rad Mini-PROTEAN II electrophoresis cell, allowed to polymerize for 30 minutes, and the wells rinsed with running buffer. Prior to loading, the gel was electrophoresed at 150 V for 30 minutes in 1X running buffer corresponding to the buffer used to make the gel. Once the samples were loaded, the gel was electrophoresed at a constant voltage of 150 V for 60 minutes at 37°C. After electrophoresis, the gel was dried at 70°C for 45 minutes (Savant Slab Gel Dryer SGD4050) and placed on X-ray film at –80°C or on the phosphoimager (Molecular Dynamics), for visualization.

2.4.2.2 SDS-Polyacrylamide Gel Electrophoresis (SDS-PAGE)

Protein samples were denatured and separated on a 10% [w/v] SDS-PAGE gel cast in a Bio-Rad Mini-PROTEAN II electrophoresis cell. The resolving gel was

comprised of: 937.5 µL of 40% [w/v] acrylamide:bis (37.5:1)(BioRad), 468.75 µL of 3 M Tris-HCl, pH 8.8, 37.5 µL of 10% [w/v] SDS, 2,120 µL of $mQdH_2O$, 187.5 µL of 1.5% [w/v] APS, and 1.875 µL of TEMED. A 3.75 mL aliquot of resolving gel was poured into the cast and immediately overlaid with isopropanol and allowed to polymerize for 30 minutes. The isopropanol was thoroughly rinsed off with $mQdH_2O$ and dried with 3MM Whatmann paper. The stacking gel was comprised of: 125 µL of 40% [w/v] acrylamide:bis (37.5:1), 315 µL of 0.5 M Tris, pH 6.8, 12.5 µL of 10% [w/v] SDS, 741.25 µL of $mQdH_2O$, 50 µL of 1.5% [w/v] APS, and 1.25 µL of TEMED. A 1.25 mL aliquot of the stacking gel was overlaid on the resolving gel, a 10-well comb inserted, and allowed to polymerize for 30 minutes.

One-third volume of SDS loading buffer (125 mM Tris, pH 6.8, 4% [w/v] SDS, 20% [v/v] glycerol, 10% [v/v] β-mercaptoethanol, and 0.02% bromophenol blue) was added to each protein sample prior to incubation in a boiling water bath for 5 minutes. Samples were electrophoresed in 1X SDS running buffer (25 mM Tris, 0.192 M glycine, 0.1% [w/v] SDS) at a constant voltage of 200 V for 1 - 1.5 hours. Protein sizes were determined by electrophoresing 10 µL of a 1:20 dilution of Low Range (LR) SDS-PAGE standards (Bio-Rad) or 10 µL of the Broad Range (BR) Prestained Protein markers (NEB), alongside the protein samples.

2.4.3 Staining SDS-Polyacrylamide Gels

Following electrophoresis, proteins were fixed in the gel by shaking for 5 minutes in destain solution (30% [v/v] methanol, 10% [v/v] glacial acetic acid). Proteins were visualized by staining with Coomassie Brilliant Blue Stain (14% [v/v] methanol, 10% [v/v] glacial acetic acid, 0.25% [w/v] Coomassie Brilliant Blue R250) for 10 minutes with shaking. Gels were destained until the desired stain intensity and then dried onto 3MM filter paper at 70°C for 45 minutes (Section 2.4.2.2).

PAGE gels containing proteins for protein sequencing were stained with SeeBand Protein Staining Solution (Gene Bio-Application) or Silver Stain Plus (Bio-Rad). SeeBand Protein Staining Solution was used according to the manufacturer's instruction. The Silver staining protocol had a few modifications. Following fixation, the staining solution was mixed in the followed order; 8.75 mL $mQdH_2O$, 1.25 mL of Silver Complex

solution, 1.25 mL of Reduction Moderator solution, and 1.25 mL Image Development reagent, poured over the gel with vigorous shaking. 25 mL of Accelerator solution was quickly added and the gel was stained until the optimal banding intensity. The reaction was stopped and stored in 5% [w/w] acetic acid and when necessary, the desired polypeptide excised from the gel and sent to the Institute for Biomolecular Design (IBD) (University of Alberta, Edmonton, AB, Canada) for protein identification. Automated in-gel tryptic digestion was performed and the tryptic peptides subjected to LC/MS/MS. The generated LC/MS/MS data were used as queries for database searches using Mascot (Matrix Science, UK) and the National Center for Biotechnology Information (NCBI).

2.4.4 Protein Precipitation

Proteins eluted from DNA affinity chromatography columns (Section 2.5.2) were concentrated by TCA precipitation. Protein samples were mixed with one-tenth volume of 100% trichloro-acetic acid (TCA) (Anachemia) and one-tenth volume deoxycholate (10mg/mL) (Sigma) and incubated on ice for 30 minutes. The protein precipitate was pelleted at 14,000 rpm for 15 minutes at 4°C and washed 4 - 5 times with 1 mL of 100% chilled acetone. The protein pellet was resuspended in 20 µL of 0.1 M DTT, 0.1 M Na_2CO_3 and size fractionated by SDS-PAGE gel electrophoresis (Section 2.4.2.2).

2.4.5 Western Analysis

Equivalent concentrations of protein extracts (Section 2.4.1.2), as determined by the Bradford assay (Section 2.4.1.1), were loaded and separated on a 10% [w/v] SDS-PAGE gel (Section 2.4.2.2). Following electrophoresis, the proteins were immobilized to a solid matrix through electroblotting, using the semi-dry transfer method. Proteins from an unstained SDS-PAGE gel were transferred to a 0.45 micron Hybond ECL nitrocellulose membrane (Amersham Pharmacia Biotech) using an Electrophoretic Transfer System ET-10 (Tyler Research Instruments), according to the manufacturer's instructions. Prior to transfer, the membrane and four pieces of 3 MM Whatmann papers were soaked in 1X Tyler transfer buffer (25 mM Tris, 150 mM glycine, pH 8.3, 20% [v/v] methanol) for 30 minutes and the SDS-PAGE gel soaked for 5 minutes. The transfer components were assembled in the following order: 2 pieces of 3 MM

Whatmann paper, SDS-PAGE gel closest to the cathode, membrane, and 2 pieces of 3 MM Whatmann paper. One gel was transferred at room temperature for 60 minutes at a constant 60 mA, whereas two gels were transferred at a constant 80 mA for 60 minutes. Following transfer, the gel was stained with Coomassie Brilliant Blue (Section 2.4.2.3) to determine the efficiency of protein transfer.

Western blot analysis was performed as described by Lane and Harlow (1982). The nitrocellulose membrane was blocked by incubating at room temperature in fresh 1X BLOTTO (1X TBS (150 mM NaCl, 10 mM Tris-HCl, pH 8.0), 5% [w/v] skim milk powder (Carnation), 0.02% [v/v] sodium azide) for 30 minutes, with gentle agitation. To fresh 1X BLOTTO, anti-*crhC* serum (1:5000) (Chamot *et al.*, 1999; Yu, 1999) was added and incubated at room temperature for 16 - 24 hours. Three consecutive 10 mL washes were performed for 10 minutes with 1X TBS, 1X TBST (0.05% [v/v] Tween in 1X TBS), and 1X TBS, to reduce background. The membrane was incubated for 30 minutes in 20 mL 1X TBS containing goat anti-rabbit IgG antibody conjugated to horse-radish peroxidase (HRP) (1:20,000) (Sigma). The membrane was consecutively washed for 10 minutes with 10 mL of 1X TBS, 1X TBST, and 1X TBS and wrapped in saran warp. CrhC was visualized using the ECL Western Blotting Detection kit (Amersham Biosciences), according to the manufacture's instructions. Chemilluminescence was detected with autoradiography.

2.5 PROTEIN - DNA INTERACTIONS

2.5.1 Electrophoretic Gel Mobility Shift Assays (EMSA)

Promoter target DNA fragments were generated by PCR (Table 2.2) (Section 2.3.4) and/or by RE digestion of the appropriate vector (Table 2.3 & 2.5). All DNA targets were gel purified as described above (Section 2.3.3), radioactively labeled by end-labeling (Section 2.3.9.1), and the specific activity determined by Cerenkov counting. For EMSA analysis, the probe was diluted in $mQdH_2O$ to a specific activity of 2000 - 5000 cpm/μL. Protein - DNA interactions were carried out in 20 μL reactions comprised of, 2000 - 5000 cpm of target DNA, 1X EMSA buffer (10 mM Tris, pH 7.5, 50 mM NaCl, 1mM EDTA, 5% [v/v] glycerol, 1 mM DTT, 10 mM $MgCl_2$), 1 μg of poly dI/dC (Roche), and the indicated amounts of *Anabaena* protein extract (Section 2.4.1.1). The

reaction was incubated at the indicated temperature (4°C, 20°C, 37°C) for 30 minutes prior to loading on a 8%, 10%, or 12% native 1X TAE or 1X TBE polyacrylamide gel (Section 2.4.2.1). Alongside the samples, 5 μL of 5X DNA loading buffer (Section 2.3.2) was also loaded to track the approximate migration distance of the DNA, as no loading dye was added directly to the samples. The gels were electrophoresed at 150 V for 60 minutes, dried, and visualized by autoradiography at -80°C.

2.5.1.1 Competition Assays

EMSA competition assays were performed using the standard EMSA conditions (Section 2.5.1) with the addition of either competitive or non-competitive DNA. Unlabeled target DNA was used as competitor DNA and an unrelated and unlabeled fragment of DNA of equivalent size was used as the non-competitor DNA. The non-competitor DNA was amplified from within the *crhC* ORF, using the primers *GWO36:WCM1* (Table 2.2) to produce a 113 bp product.

2.5.1.2 Dephosphorylation Studies

Dephosphorylation studies were performed using calf intestinal alkaline phosphatase (CIP) (Roche), as described by Ausubel *et al.* (1995). *Anabaena* protein extract (10 μg) was dephosphorylated prior to the addition of target DNA to the EMSA binding reaction. In a 20 μL final volume, 30 μg of protein extract was incubated with 1X EMSA buffer (Section 2.5.1), 1 μg of poly dI/dC (Roche), at 30°C for 10 minutes. CIP (2.5 U) and 1mM $ZnSO_4$ were added to the mixture and incubation continued at 30°C for 15 minutes. The enzymatic reaction was terminated by the addition of sodium pyrophosphate (10 mM). The dephosphorylated protein sample was used directly in the EMSA reaction, as described above (Section 2.5.1).

2.5.2 DNA-Binding Protein Purification

DNA affinity chromatography was performed using a μMACS Streptavidin kit (Miltenyi Biotec) and MACS separation columns (Miltenyi Biotec) to isolate and purify proteins that interact with specific DNA targets. Using a biotinylated primer (Table 2.2), target DNA fragments were PCR amplified (Section 2.3.4) to carry a single biotin tag at

the 5' end, which are specifically bound by target protein(s) via incubation with a total protein lysate. The protein bound biotinylated target DNA is then magnetically labeled by complexing the biotin tag to streptavidin ligands, which are conjugated to paramagnetic Microbeads. This molecular complex is immobilized on μ columns placed in a strong magnetic field generated by a μMAC separator. Following magnetic separation, the bound proteins can be eluted with increasing salt concentration.

In a final volume of 3 ml, protein - DNA interactions were allowed to occur by incubating 10 - 15 mg of *Anabaena* protein lysate (Section 2.4.1.1), 1X JB_{50} buffer ((1X JB buffer = 10 mM HEPES, pH 8, 1 mM EDTA, 5% [v/v] glycerol, 1 mM DTT, 10 mM $MgCl_2$) 1X JB_{50} buffer = JB buffer + 50 mM KCl), 50 μg of poly dI/dC (Roche), and 20 - 50 μg of biotinylated target DNA, at 4°C for 2 hours with shaking. Following incubation, 100 μL of μMACS Microbeads conjugated to streptavidin (Miltenyi Biotec) were added and incubated at 4°C for 30 minutes, to allow for streptavidin-biotin complexes to form. At 4°C, the MACS μ columns (Miltenyi Biotec) were placed in the magnetic field of the μMACS separator (Miltenyi Biotec) and equilibrated by washing sequentially with 300 μL of Protein Application Equilibration Buffer (Miltenyi Biotec) and 300 μL of 1X JB_{50} buffer. The 3 mL binding reaction was added to the column in 500 μL aliquots and the flow-through collected. The column was stringently washed five times with 250 μL of 1X JB_{50} (W1), three times with 250 μL of 1X JB_{100} (W2) (1X JB buffer + 100 mM KCl), three times with 250 μL of 1X JB_{250} (W3) (1X JB buffer + 250 mM KCl), three times with 250 μL 1X JB_{1000} washes (W4) (1X JB buffer + 1 M KCl), and three times with 250 μL of 1X JB_{2000} (W5) (1X JB buffer + 2 M KCl). The column was completely cleaned of proteins by rinsing twice with 250 μL of 1X JB_{2000}, with the column removed from the magnet. The eluted fractions (W1-W5) were TCA precipitated (Section 2.4.3), separated on a 10% SDS-PAGE gel (Section 2.4.2.2), and polypeptides of interest excised from the gel and provided to IBD for protein sequencing (Section 2.4.2.3).

2.6 RNA MANIPULATION

2.6.1 RNA Extraction from *E. coli*

An overnight culture was diluted 1:25 into 25 mL of fresh LB (including appropriate antibiotics) and incubated at 37°C until an OD_{600} of 0.6. Half of the culture was removed into 50 mL sterile flasks and cold-shocked at 20°C with shaking at 200 rpm for the indicated times. Optimally grown samples remained at 37°C where they were harvested by centrifugation (Janetzki T5) at 10,000 rpm in 15 mL polypropylene tubes. At 37°C or 20°C and under nuclease free conditions, the cell pellet was resuspended in 650 µL of 65°C RNA extraction buffer (1% [w/v] SDS, 10 mM sodium acetate, pH 4.5, 150 mM sucrose) and transferred to a clean microfuge tube. 650 µL of hot (65°C) phenol was then added and the mixture extracted at 65°C for 15 minutes. After microcentrifugation at 7000 rpm for 5 minutes, proteins were extracted with equal volume organic phases; once with phenol, twice with phenol: chloroform (1:1), and once with chloroform:isoamyl alcohol (24:1), with a 5 minute microcentrifugation at 7000 rpm, between each extraction. The RNA was precipitated by adding an equal volume of 4 M LiCl to the extracted aqueous phase, mixing well and incubating at -20°C overnight. Precipitated material was pelleted at 14,000 rpm for 30 minutes at 4°C, resuspended in 300 µL of nuclease-free TE (10 mM Tris-HCl, pH 8, 1 mM EDTA, pH 8), and precipitated by the addition of one-tenth volume 3M sodium acetate, pH 5.2 and 2.5X volume of 100% ethanol and stored at -80°C. When the RNA was needed, the sample was microcentrifuged at 14,000 rpm for 15 minutes at 4°C and washed with of 80% [v/v] ethanol (1 mL). The air-dried pellet was resuspended in RNase-free sterile $mQdH_2O$ (30-50 µL) and quantified spectrophotometrically at a wavelength of 260 nm. The RNA concentration was determined spectrophotometrically similar to that of DNA (Section 2.3.1) using an extinction coefficient of 40 µg/mL (1.0 A_{260nm} = 40 µg/mL dsRNA).

2.6.2 Northern Analysis

Northern analysis was carried out as described by Ausubel *et al.* (1995). In a nuclease-free environment, 10 - 20 µg of RNA (Section 2.6.1) was denatured and electrophoresed on a ~100 mL formaldehyde gel (1.2% [w/v] agarose, 97 mL of 1X MOPS Buffer, 5.1 mL of formaldehyde). Prior to electrophoresis, RNA samples were

denatured by heating at 65°C for 15 minutes in 1X RNA formaldehyde loading buffer (50% [v/v] formamide, 17% [v/v] formaldehyde, 7% [v/v] glycerol, 0.2% [w/v] bromophenol blue in 1X MOPS), briefly chilled on ice, and ethidium bromide (1 µl of 0.5%) added. RNA samples were separated on a 5.1% formaldehyde, 1.2% agarose gel in 1X MOPS running buffer (20 mM MOPS, 5 mM sodium acetate, 1 mM EDTA, pH 7), at 125 V for 2-3 hours, with gel rotation every 30 minutes. Monitoring of RNA degradation and loading consistency were visualized using a Syngene Genius Bio Imaging System.

RNA was transferred from the agarose gel to a positively charged Hybond-XL nylon membrane (Amersham Pharmacia Biotech) using capillary action and 20X SSC (3 M NaCl, 0.3 M Na_3citrate, pH 7). The high salt upward capillary transfer was performed according to standard procedures (Ausubel *et al.*, 1995), with transfer occurring over 16 - 24 hours. Following dismantling of the transfer apparatus, the ribosomal RNA was distinctly marked and the RNA was immobilized by UV-crosslinking at 120 mJ/cm^2 in a SpectroLinker XL-1000 UV Crosslinker (Spectronics Corporation). Excess salts were removed by washing at 65°C for 60 minutes in a Post-bake wash buffer (1X SSC, 0.1% [w/v] SDS) and transferred to a seal-a-meal bag (Rival). To reduce background, the membrane was blocked by prehybridization at 65°C in 1 mL/cm^2 of membrane in Aqueous Hybond solution (50% [v/v] formamide, 5X Denhardts, 0.2% [w/v] SDS, 5X SSPE, and 50 µg/mL of boiled salmon sperm ssDNA) for 4 - 24 hours. 1 X 10^6 cpm/mL of random-primed DNA probe (Section 2.3.9.2) was added to fresh Aqueous Hybond (1 mL/cm^2) solution and incubation continued at 65°C for 16 - 24 hours. Following hybridization, the membrane was washed once at 65°C with a low stringency wash (1X SSPE [180 mM NaCl, 10 mM NaH_2PO_4, 1 mM EDTA, pH 8], 0.1 % [w/v] SDS) and once at 65°C with a high stringency wash (0.1X SSPE, 0.1% [w/v] SDS). The membrane was wrapped in saran wrap and the bound probe was detected by autoradiography at -80°C for 24 - 48 hours. Prior to storage, the membrane was stripped of probe by immersion in 500 mL of boiling 0.1% [w/v] SDS and slow cooling to room temperature with mild agitation.

2.6.3 Riboprobe Generation

A 268 bp *crhC* 5' UTR riboprobe was generated using a Riboprobe System kit (Promega) as instructed by the manufacturer. Under RNase-free conditions, promoter deletion construct DC6 (Table 2.4) was linearized with Nhe I (Section 2.3.2), phenol: chloroform extracted and ethanol precipitated (Section 2.3.3), and used as the DNA target for transcription by RNA polymerase. A 107 nucleotide (nt) ssRNA control was also generated by performing a Hae III digestion of the vector pGEM3CS and transcribed with SP6 RNA polymerase for riboprobe generation. The following reagents were added to a 20 µL riboprobe reaction: 1X Transcription Optimized Buffer (Promega), 10 mM DTT, 20 units of Recombinant Rnasin Ribonuclease Inhibitor, 500 µM of each rATP, rCTP, rGTP, 12 µM rUTP, 1 µg of linearized Nhe I DC6 or Hae III pGEM3CS, 50 µCi of [α^{32}P] rUTP, and 20 units of T7 RNA polymerase for the DC6 reaction or SP6 in the case of the pGEM3CS template. The reaction was incubated at 37°C for 60 minutes. Prior to electrophoresis, 10 µL of 3X SDS loading buffer was added to the sample. The riboprobes were isolated by electrophoreses on an 8 M urea, 10% denaturing polyacrylamide gel (PAGE) (1.7 mL of 30% [w/v] acrylamide, 8 M urea, 500 µL of 10X TBE, 2.75 mL mQdH_2O, 25 µL of 10% [w/v] APS, 3 µL of TEMED). The gel was electrophoresed at 200 V for 30 minutes, visualized by autoradiography after exposure for 1 minute. The radioactive region was excised from the gel and eluted overnight in RNA elution buffer (500 µL) (0.5 M ammonium acetate, 1 mM EDTA, 0.1% [w/v] SDS). The elution product was extracted with phenol: chloroform (Section 2.3.3) and ethanol precipitated at –80°C. For safe-keeping, one tube remained stored at –80°C and the other tube was resuspended in 50 µL of RNase-free mQdH_2O and Cerenkov counted (Section 2.3.9.1).

2.6.4 Ribozyme Reaction

To determine if the *crhC* 5' UTR is a ribozyme (Winkler *et al.*, 2002), a 20 µL self-cleavage reaction was performed. 100 - 200 fmoles (5000 cpm) of the 5' UTR *crhC* riboprobe (Section 2.6.3) was incubated in 1X Ribozyme Reaction buffer (50 mM Tris-HCl, pH 8.5, 100 mM KCl and 20 mM $MgCl_2$). Three identical reactions were incubated

at 37°C, 30°C, or 20°C for 17 - 40 hours with shaking. Reaction products were separated on an 8 M urea, 10% [w/v] denaturing polyacrylamide gel (Section 2.6.3). The gel was dried (Section 2.4.2.1) and the cleavage products visualized by autoradiography at –80°C for 24 - 48 hours under an intensifying screen.

2.7 TRANSCRIPTIONAL REPORTER FUSIONS

The majority of transcriptional *lux* reporter fusion constructs (Table 2.5) were constructed by amplifying the indicated insert regions using PCR (Table 2.2) (Section 2.3.4), digesting the PCR ends with the appropriate restriction enzyme(s) (Section 2.3.2), gel purifying the insert (Section 2.3.3), and ligating (Section 2.3.5) the insert into a compatible, linearized vector containing the *lux* operon (Table 2.3). Due to the lack of restriction sites present within the multiple cloning sites (MCS) of pNLP10, pSIG11, and pSIG16, alternate cloning strategies were performed to allow for proper insertion of the desired DNA sequence. pJBm1 and pJBm2 (Table 2.5) were constructed by performing a triple ligation into BamH I cleaved pSIG16(lux$^-$) and pSIG11(lux$^-$) respectively. A 269 bp upstream region containing the *crhC* 5' UTR was amplified using primers *JB5:JB6* and cleaved with BamH I/Nhe I. Downstream sequence containing the *crhC* ORF and 3'UTR was isolated by a BamH I/Nhe I digestion of pWM753R. The BamH I/Nhe I upstream and downstream sequences were ligated together to produce a *crhC* insert lacking the *crhC* promoter. Alternate cloning strategies were also employed to construct pJBm5 and pJBm6 (Table 2.5). The *crhC* gene lacking the 3'UTR was isolated by a Hinc II/SnaB I digestion of pWM753, producing a 2170 bp insert. Due to incompatible restriction sites present within the MCS of pNLP10, several of the *crhC* inserts were first cloned into pBluescript (pBS) KS+, cleaved out of KS+ with BamH I/Xho I, and then cloned into BamH I/Xho I cleaved pNLP10.

For promoter studies, the *crhC* promoter regions were cloned upstream of the *lux* operon in pNLP10 whereas for mRNA stability studies the *crhC* 5' UTR regions were cloned between a constitutive *E. coli* promoter (pSIG11) and the *lux* operon (Table 2.3 and Table 2.5). Positive clones were identified by restriction digestion (Section 2.3.2) and sequencing (Section 2.3.8), and stored as 10% [v/v] glycerol stocks at -80°C.

TABLE 2.5: Plasmid Constructions

Plasmid	Parent Plasmid	Selective Marker	Insert Size	Region of *crhC* Inserted	Cloning Strategy (vector digest / insert digest)	Molecular Use
pWM753R	pWM753	Ampicillin	2424 bp	Reverse orientation of full length *crhC* gene from pWM753	Hinc II digest and religation of pWM753	Construction of pJBm1 and pJBm2
pJBp1	pCS26	Kanamycin	39 bp	AT-rich element of the *crhC* promoter	BamH I/BamH I with annealed complementary primers (*JB20:JB21*) (Section 2.7)	Luciferase Assays / Promoter studies
pJBp2	pNLP10	Kanamycin	154 bp	AT-rich element and -10 regions of the *crhC* promoter	EcoR I/EcoR I with *JB18:JB19* PCR product (Section 2.7)	Luciferase Assays / Promoter studies
pJBp3	pNLP10	Kanamycin	371 bp	*crhC* promoter lacking the transcriptional start site	BamH I/Bgl II with *JB1:JB15* PCR product (Section 2.7)	Luciferase Assays / Promoter studies
pJBp4	pNLP10	Kanamycin	511 bp	full-length *crhC* promoter and the 1st stem loop structure of the 5' UTR (11 bp into ORF)	BamH I/Bgl II with *JB1:JB2* PCR product (Section 2.7)	Luciferase Assays / Promoter studies
pSIG16(lux$^-$)	pSIG16	Kanamycin	N/A	N/A	Not I digestion to remove the *lux* operon	Construction of pJBm1
pSIG11(lux$^-$)	pSIG11	Kanamycin	N/A	N/A	Not I digestion to remove the *lux* operon	Construction of pJBm2
pJBm1	pSIG16(lux$^-$)	Kanamycin	1664 bp	full-length *crhC* 5' UTR (both stem loop structures), ORF and 3' UTR	BamH I/BamH I triple ligation with PCR (*JB5:JB6*), pWM753R, and pSIG16(lux$^-$) (Section 2.7)	Post-transcription studies
pJBm2	pSIG11(lux$^-$)	Kanamycin	1664 bp	full-length *crhC* 5' UTR (both stem loop structures), ORF and 3' UTR	BamH I/BamH I triple ligation with PCR (*JB5:JB6*), pWM73R, and pSIG11(lux$^-$) (Section 2.7)	Post-transcription studies
pJBm3	pSIG11	Kanamycin	274 bp	both stem loop structures of the *crhC* 5' UTR	BamH I/Bgl II with *JB5: JB22* PCR product	Luciferase Assays / mRNA stability studies
pJBm4	pSIG11	Kanamycin	191 bp	2nd stem loop structure only of the *crhC* 5' UTR	BamH I/Bgl II with *JB23: JB22* PCR product	Luciferase Assays / mRNA stability studies
pJBm5	pNLP10	Kanamycin	2426 bp	full-length *crhC* gene from pWM753	Xho I/BamH I of pWM753R into Xho I/BamH I pNLP10 (Section 2.7)	mRNA stability control
pJBm6	pNLP10	Kanamycin	2168 bp	*crhC* gene lacking the 3' UTR	Hinc II/SnaB I pWM753 into pBS, Xho I/BamH I pBS into Xho I/BamH I pNLP10 (Section 2.7)	3'UTR's role in mRNA stability

* Primers used for PCR amplification are shown in italics in the order of forward primer : reverse primer.

2.7.1 Luciferase Assays

Overnight cultures were diluted 1:25 into LB_{Kan} (50 μg/mL) and incubated at 37°C until an OD_{600} of 0.4 - 0.6. In replicates of five, a 250 μL aliquot of the culture was transferred to one well of a 96-well clear bottom assay plate (Corning Incorporated 3610) in a 37°C incubator. The luciferase activity (cpm) and the number of cells (OD_{600}) of the optimally grown transcriptional fusion constructs were immediately determined using a Wallac Victor 2 1420 Multilabel Counter (Perkin Elmer Life Science). The remaining culture was transferred to a 20°C water bath shaker where it was cold-shocked for the indicated times. At the specified times, 250 μL aliquots were removed (in quintuplicate) and the luciferase activity and OD_{600} were determined as mentioned above. An LB medium control was also treated identically to the test samples and used to determine background emissions from the medium alone. For comparative analysis, the corrected luciferase activity (cpm/OD_{600}) was determined, taking into account the LB medium background: Corrected luciferase activity = (cpm (construct) – cpm (LB)) / (OD_{600} (construct) – OD_{600} (LB)). The results were plotted graphically as histograms using Microsoft Excel.

CHAPTER THREE
RESULTS

3.1 TRANSCRIPTIONAL REGULATION of *crhC*

3.1.1 Generation of *crhC* Promoter Deletion Constructs

CrhC expression, at both the transcript and protein level in *Anabaena*, was shown to be tightly regulated by a temperature downshift from 30°C to 20°C (Chamot and Owttrim, 2000; Chamot *et al.*, 1999). The primary objective of this section of the thesis was to understand the role of the *crhC* promoter in providing temperature-regulated gene expression, at the level of transcription. Putative *crhC* promoter motifs were identified by sequence comparison to conserved motifs found within the promoter regions of well-studied *E. coli* cold shock (CS) genes (*cspA*, *cspB*, and *csdA*) (Yu, 1999). The conserved motifs previously identified to regulate CS gene transcription in other systems and found within the *crhC* promoter include, a transcription enhancing AT-rich element (-65 to -53 bp) and a –10 region (-14 to -9 bp) required for RNA polymerase binding (Figure 3.1A). Downstream of the *crhC* promoter is a long (115 bp) 5' untranslated region (5' UTR) possessing an 11-base conserved cold shock box (+87 to +97 bp) potentially involved in transcriptional attenuation, and a putative Shine-Dalgarno sequence (+106 to +113 bp) required for ribosome loading during translation initiation. A downstream box (+137 to +151 bp), reported to be required for translation initiation in other CS genes, was identified downstream of the translational start site (+116 bp).

To investigate regions of the *crhC* promoter that are important for temperature-dependent expression, a series of nested deletions were made within the *crhC* promoter (Section 2.3.10). pWM75-2, containing a 939 bp EcoR V fragment coding for the promoter, 5' UTR, and 510 bp of the *crhC* ORF, was used as the source of the JW series of deletions (Figure 2.1A, Table 2.4) (Magee, 1997). pWM75-2 was digested with Exo III over one-minute intervals, generating a series of seven promoter deletion constructs (JW2 - JW8) that varied in *crhC* promoter length (Figure 3.1B) (Ward, 2001). A second set of promoter deletion constructs named the DC series was also generated to create a wider array of nested deletions lacking different regulatory regions required for temperature-dependent expression (Dana Chamot, unpublished data). pWM753 was used

Figure 3.1. Upstream sequence of the *crhC* gene used to generate the JW nested deletions series from pWM75-2. Panel A shows the conserved motifs found within the upstream sequence of the *crhC* gene. The transcriptional start site (+1) is shown in red and indicated with an asterisk, the AT-rich element is in blue, the –10 region in green, and the cold shock box shown in yellow. The translational start site (ATG) is italicized in red, the Shine-Dalgarno sequence is underlined in black, and the downstream box shown in purple. The numbering above the sequence indicates where the various JW promoter deletions are located in relationship to the EcoR V fragment cloned into pWM75-2. Panel B shows a scaled diagram of the *crhC* promoter deletion in relation to the conserved motifs. BamH I/Sac I cleaved pWM75-2 (939 bp) was digested with Exo III for one-minute intervals and the single stranded ends removed with S1 nuclease. The resulting overhangs were filled in and blunt-end ligated. The religated plasmids were transformed into *E. coli* and enriched for positive deletions. Promoter deletions were confirmed by restriction enzyme digestion, PCR, and sequencing (Ward, 2001). Numbering of the JW series of deletions and regulatory motifs are in relation to the distance from the transcription start site (+1).

A

pWM75-2

-365 ATCGCTGGTT TGTTGCAAGG CTACGTTTCT GGACAAGCTA TCAACGGGAT TGATATCATC TCCCTGCTTA -296

#2

-295 CCTATACTTT AGGCTTCGGT TTAACTCAGT ATGCAATCGC CACTAGCACC AGACGACTAG TTAGCGATAG -226

#3

-225 TCTATCCACC ATTGTTCGTT TTGTAGGTTT TGCTTTTATA GCGATCGGTT TTGTATTTTG CGGTAACTTC -156

#4

-155 ATCAATTTTT TAGGGGCTGG TAATTTTTAA CATATCTCAC GGGGTGCAAT CTTCGCGCCC CTACTAGTCC -86

#5 #6

-85 ATCGAATCGT CATTTCCAAC TATTAATATT AAAGTTTAGA GAAATTGGAT TATATGTAAC CTGTACTCTG -16

* #7

-15 TTAAGATTCA CCATTGGGGT ATTCGCTATC AGTCTTGGCG CTACTGCCCA TCCCGCCCCT CAAACCTTTG +55

#8

+56 TCCGTCCGCC TAAGACTGAT ACCGCTACTG GTGACAGCCC GATGTTATAT CTGGAGTTCT *ATG*TCTTTTT +125

+126 CTCATCTCGG CTTGTCCAAT GAAATTATCA ATGCTGTTAC TGAGTTGGGG TACACCAAAC CCACACCCAT +195

B

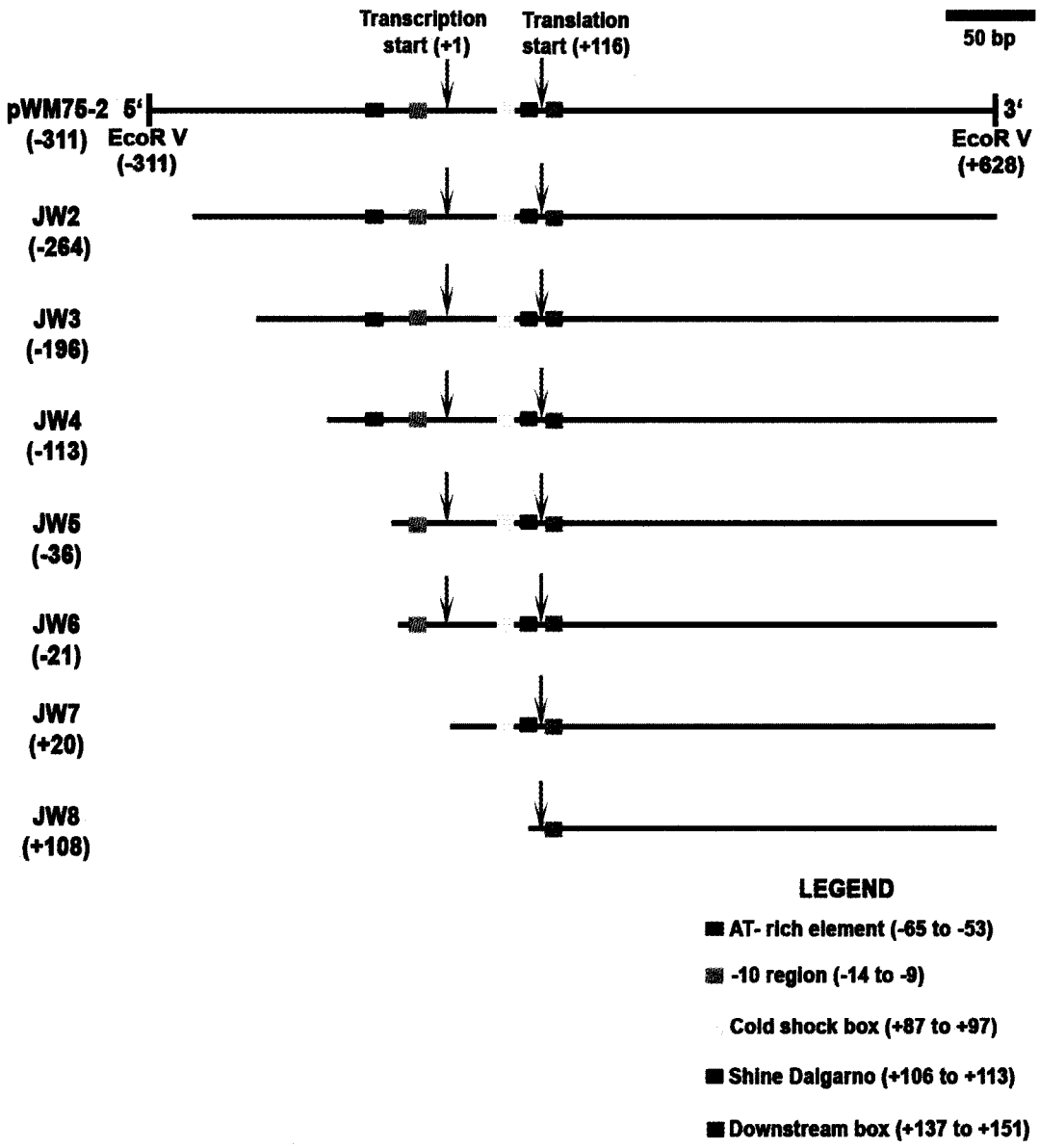

as the second source for exonuclease digestion, containing a 2424 bp Hinc II fragment coding for the full-length *crhC* gene (promoter, 5' UTR, ORF, and 3'UTR) (Figure 2.1B, Table 2.3) (Magee, 1997). Exo III-digested pWM753 generated eight more deletion constructs (DC1 - DC8) varying in length from the 5' end (Figure 3.2).

Shown in Figure 3.1B, promoter deletions JW2 - JW4 contain all of the conserved motifs within the *crhC* promoter and therefore should be regulated by temperature, similar to the full-length *crhC* gene (pWM753). Deletion constructs JW5 and JW6 lack the AT-rich element, JW7 lacks the complete promoter including the transcriptional start site, and JW8 lacks the full promoter and the majority of the 5' UTR. As shown in Figure 3.2, DC1 - DC4 contain the complete *crhC* promoter, DC5 lacks the AT-rich element, DC6 lacks both the AT-rich region and –10 regions, and DC7 and DC8 both lack the full promoter, 5' UTR, and a small portion of the ORF (including the downstream box). Correlation between the removal of a specific promoter motif and changes in *crhC* temperature-dependent expression is expected to provide insight into which promoter region is required for temperature regulation.

3.1.2 Optimization of Electrophoretic Gel Mobility Shift Assays (EMSA)

Transcriptional regulation was investigated using electrophoretic gel mobility shift assays (EMSA) to determine if a DNA-binding protein(s) was interacting with the *crhC* promoter during growth at either 30°C (optimal growth) or 20°C (cold stress). It is important to note, that different sized *crhC* promoter DNA targets were used in the EMSA reactions performed throughout this thesis, dependent on the time-line of when the experiments were executed. For example, the first EMSA reactions were performed with the full-length *crhC* promoter however, following identification of the minimal binding sequence, smaller sized *crhC* promoter fragments were used as the EMSA target DNA.

Using deletion construct JW3 as the template, the full-length *crhC* promoter was PCR amplified using the external T7 forward primer and the internal GWO43 reverse primer (Table 2.2, Section 2.3.4). The amplified promoter region was end-labelled (Section 2.3.9.1), incubated with *Anabaena* soluble protein lysate grown at 30°C or 20°C, and separated on a 8%, 10%, or 12% native gel. Protein-DNA interactions are expected

Figure 3.2. Nested deletion series within the *crhC* promoter generated from pWM753. A scaled diagram of the *crhC* promoter deletions shown in relation to the upstream conserved motifs. The DC series of promoter deletions were created from BamH I/Sac I cleaved pWM753 (2424 bp) as described in Figure 3.1B. Promoter deletions were confirmed by restriction enzyme digestion, PCR and sequencing (Chamot, unpublished data). Numbering of the DC promoter deletions and of the conserved regulatory motifs are in relation to the distance from the transcriptional start site (+1).

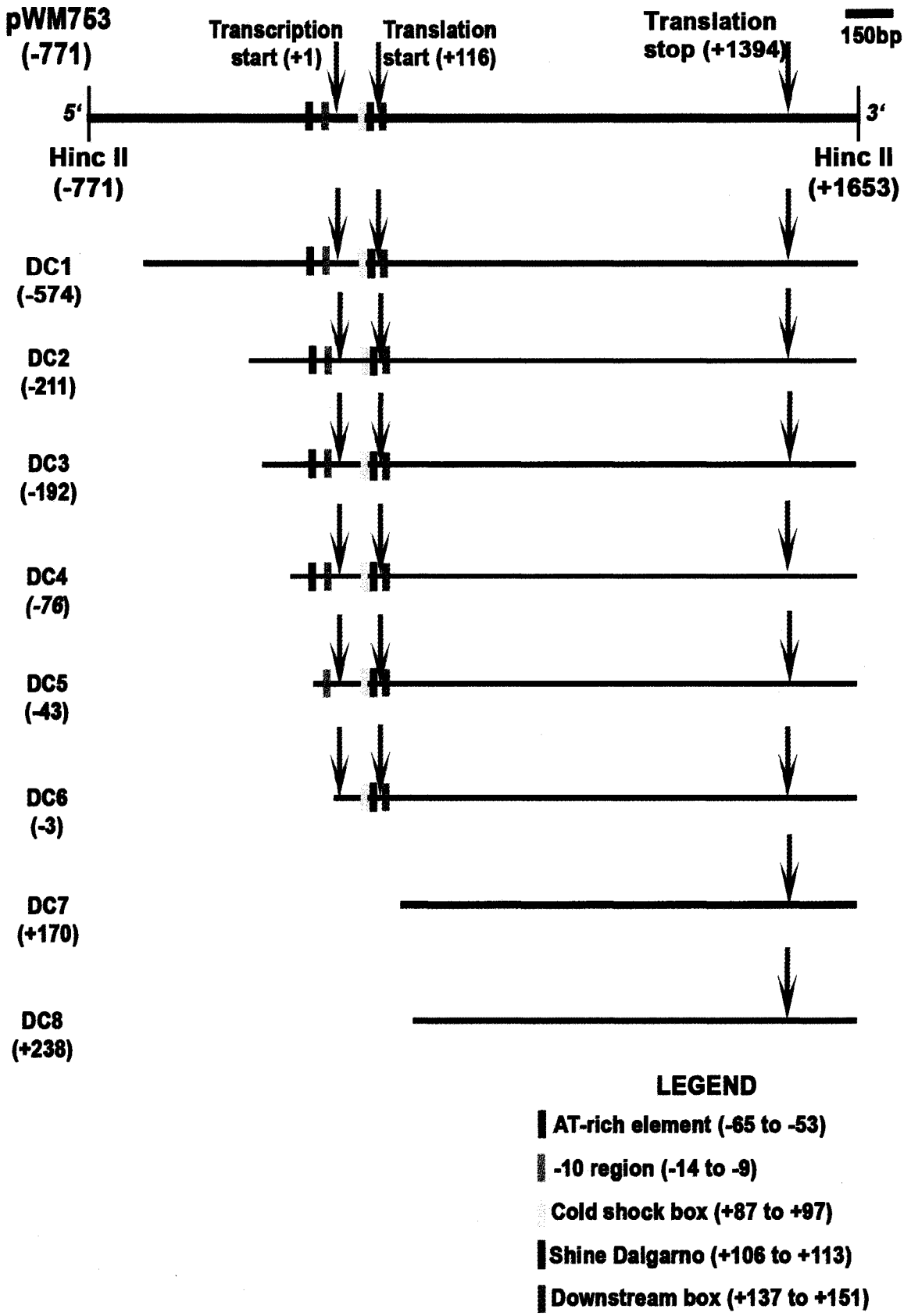

to be recognized by retardation in DNA probe migration, indicative that a protein has bound the probe, slowing its migration through the gel.

Several EMSA attempts were made without success, suggesting that the binding affinity of the putative regulatory protein(s) for the *crhC* promoter may be very specific, short lived, or require other cofactors to bind. To optimize the binding reaction, alterations were made in gel composition, electrophoresis temperature, magnesium concentration, and pH. As shown in Figure 3.3A, no retardation was seen in probe migration throughout the TBE gel, regardless of the growth temperature or protein concentration. This indicated that a regulatory protein was not able to interact with the *crhC* promoter when borate was used as the buffering system. However, when the identical DNA-protein interactions were separated on a TAE gel, retardation in probe migration was evident when the *crhC* promoter was incubated with *Anabaena* protein lysates (Figure 3.3B). These results indicate that the regulatory protein(s) binds optimally when acetate is used as the buffering system. Interestingly, a mobility shift was only observed with protein extracts obtained from *Anabaena* cells grown at 30°C (Figure 3.3B, lane 4) and not with extracts from cells grown at 20°C (Figure 3.3B, lanes 5 – 7).

Magnesium concentration and pH were also altered to enhance protein binding to the *crhC* promoter. As shown in Figure 3.4A, zero to low levels of magnesium (0 – 10 mM) enhanced DNA-protein complex formation compared to the higher magnesium concentrations (15 – 50 mM), as suggested by the intensity of the shifts. Variations in pH however (Figure 3.4B), had little effect on the binding reaction, illustrated by similar shift intensities at a pH range from 7 to 8.5. Based on these results, all EMSA binding reactions were performed at a pH of 7.5 and magnesium concentration of 10 mM, and separated on 1X TAE, 8%, 10%, or 12% native gels (Section 2.4.2.1).

3.1.3 Identification of DNA-Binding Protein(s) that Interacts with *crhC* Promoter

In order to determine the action of the putative regulatory protein, EMSA reactions were employed to identify the presence of a temperature-dependent transcriptional repressor or activating factor. EMSA reactions were performed with protein lysate extracted from *Anabaena* cells growth either at 30°C (optimal) or 20°C

Figure 3.3 A DNA-binding protein(s) interacts with the *crhC* promoter when the binding reaction is optimized in TAE buffer. EMSA reactions were performed by incubating 2000 cpm of end-labeled, full-length *crhC* promoter (458 bp) (deletion construct JW3 PCR amplified with *T7:GWO43*) with the indicated concentrations (μg) of optimally grown (30°C) or cold stressed (20°C) *Anabaena* protein lysate and separated on 8% native gels. Panel A shows the migration of the DNA-protein complexes when separated on a 1X TBE gel, compared to the full-length *crhC* promoter in the absence (-) of *Anabaena* protein extract (lane 1). Lanes 2 – 4 and 5 – 7 show the probe migration patterns in the presence of increasing protein concentration from cells grown at 30°C (optimal) and 20°C (cold), respectively. Panel B shows the migration distances of the identical DNA-protein binding reactions from panel A, when separated on a 1X TAE gel. The formation of DNA-protein complexes are labeled as bound.

A

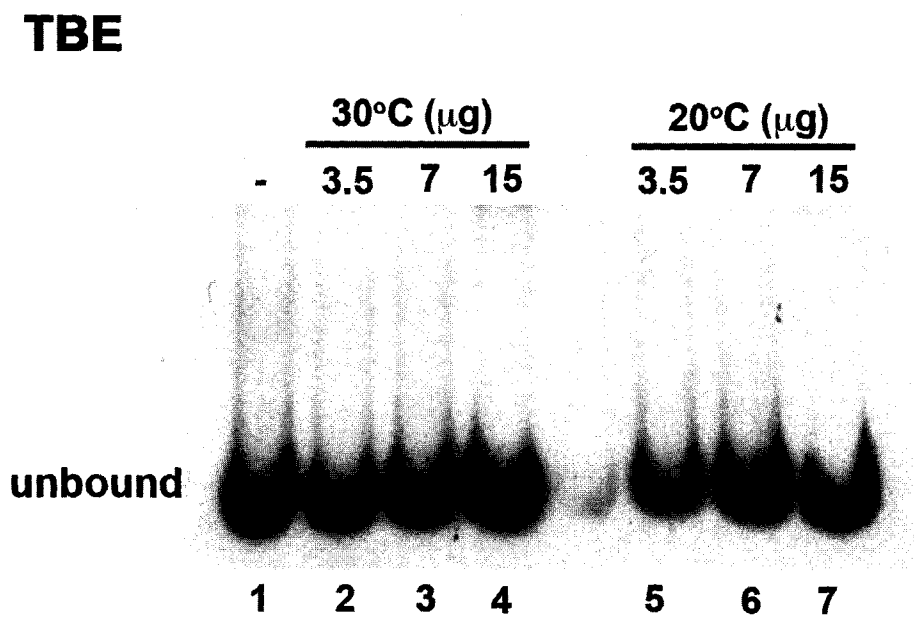

B

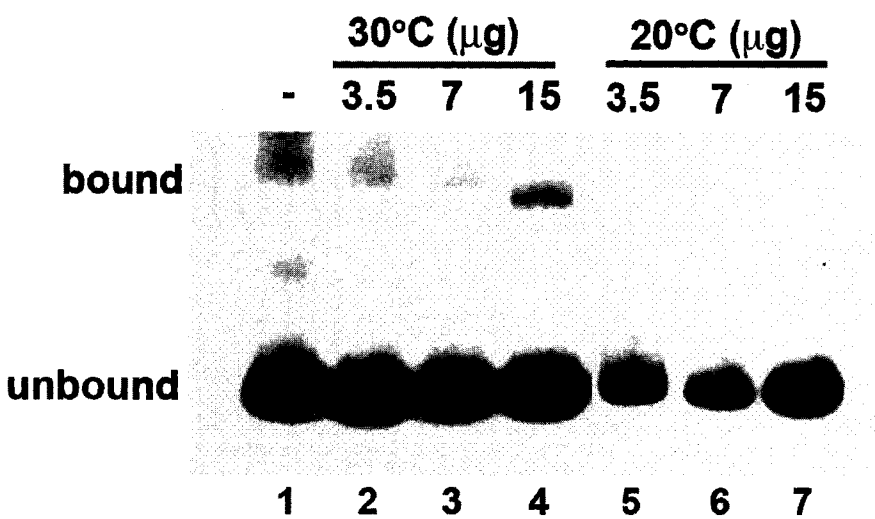

Figure 3.4. [Mg^{+2}] and pH are important for optimizing DNA-protein complex formation during an EMSA reaction. EMSA reactions were carried out by incubating an end-labeled portion (5000 cpm) of the *crhC* promoter (*JB9:JB12*, 129 bp) with 30 μg of optimally grown (30°C) *Anabaena* protein lysate and separated on a 1X TAE, 10% native gel. Panel A shows the EMSA binding reactions in the presence of increasing magnesium concentration (0 – 50 mM). Panel B shows the EMSA binding reactions performed over the pH range of 7 - 8.5.

A

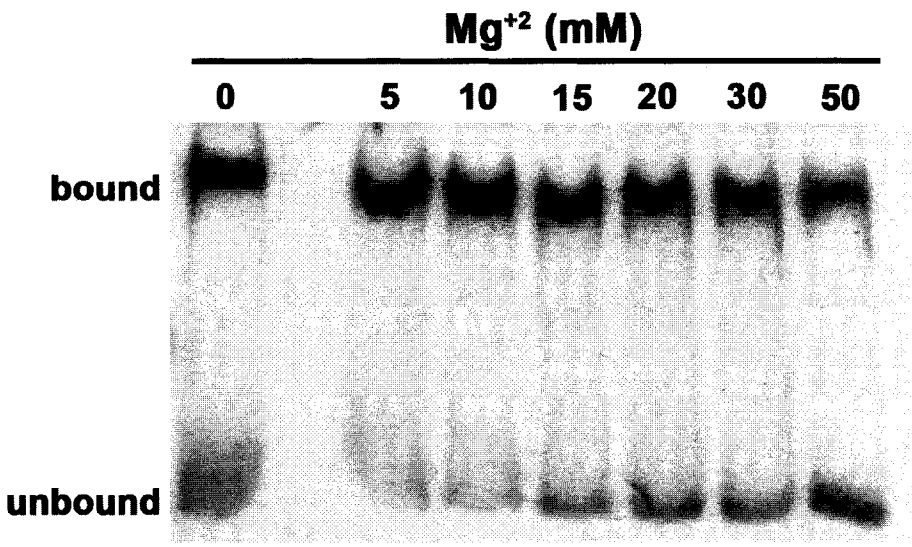

B

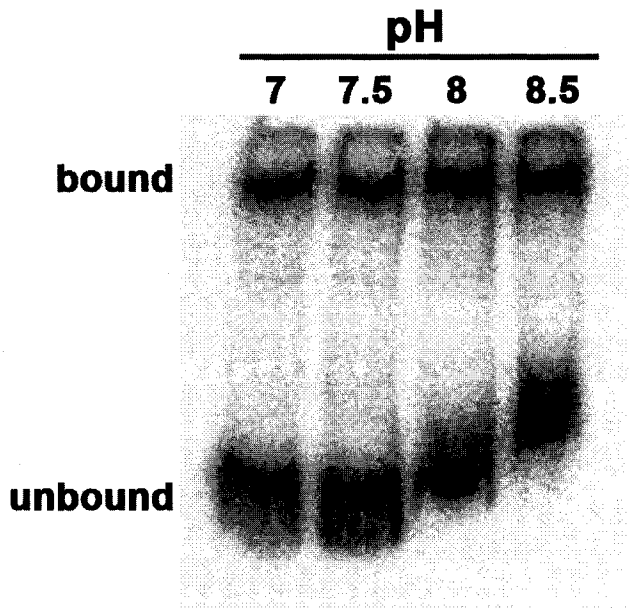

(cold stress) and incubated with *crhC* promoter target DNA. Illustrated in Figure 3.5, the presence of shifted probe (lane 3) confirmed that a regulatory protein bound to the full-length *crhC* promoter under optimal growth conditions (30°C), which is absent at reduced growth temperatures (20°C) (lane 2). Since DNA-protein interactions are only observed in extracts from cells grown at 30°C combined with the absence of *crhC* transcript accumulation at 30°C (Chamot *et al.*, 1999), suggests that the regulatory protein binding to the *crhC* promoter acts as a transcriptional repressor, inhibiting *crhC* transcription at 30°C. The presence of this potential repressor suggests that *crhC* is transcriptionally regulated by a classic DNA-protein interaction that is temperature-dependent.

3.1.4 Protein-DNA Binding Specificity

A series of EMSA reactions were performed to study the specificity of repressor binding to the *crhC* promoter. The effect of protein concentration was tested by adding increasing amounts of optimally grown (30°C) or cold stressed (20°C) *Anabaena* protein lysate to the EMSA reactions (Figure 3.6). A linear relationship was found between the concentration of optimally grown (30°C) protein extract and the bound probe intensity, indicating that the repressor binds the *crhC* promoter in a concentration-dependent manner (Figure 3.6A). As expected, a DNA-protein complex (shift) was not detected when the *crhC* promoter was incubated with protein lysate isolated from cells grown at 20°C, regardless of protein concentration (Figure 3.6B). This confirmed the inability of the repressor protein to bind to the *crhC* promoter under cold stress conditions, even at high protein concentrations.

Competition assays were also performed to determine if repressor binding to the *crhC* promoter was sequence-specific. Theoretically, if a DNA-binding protein is sequence-specific, it will bind both P^{32}-labeled target DNA and unlabeled target DNA (competitive) equally, but will not bind other strands of DNA, similar in length but not in sequence (non-competitive). EMSA reactions were performed under standard conditions (Section 2.5.1) using a 129 bp, *JB9:JB12* PCR amplified portion of the *crhC* promoter (Table 2.2) as P^{32}-labeled target DNA. The competition assay was performed using increasing amounts of unlabeled *crhC* promoter (*JB9:JB12*) as competitive DNA and a 113 bp DNA fragment amplified (*GWO36:WCM1*) from within the *crhC* ORF, as non-

Figure 3.5. A putative repressor binds to the *crhC* promoter during growth at optimal temperatures (30°C). EMSA reactions were performed by incubating 10 μg of optimally grown (30°C) or cold stressed (20°C) *Anabaena* protein extract with 2000 cpm of end-labeled, full-length *crhC* promoter DNA (458 bp) (deletion construct JW3 PCR amplified with *T7:GWO43*) and separated on a 1X TAE, 8% native gel. A DNA-protein interaction is represented by a decrease in probe migration (lane 3, labeled bound) compared to the no protein (-) control (lane 1).

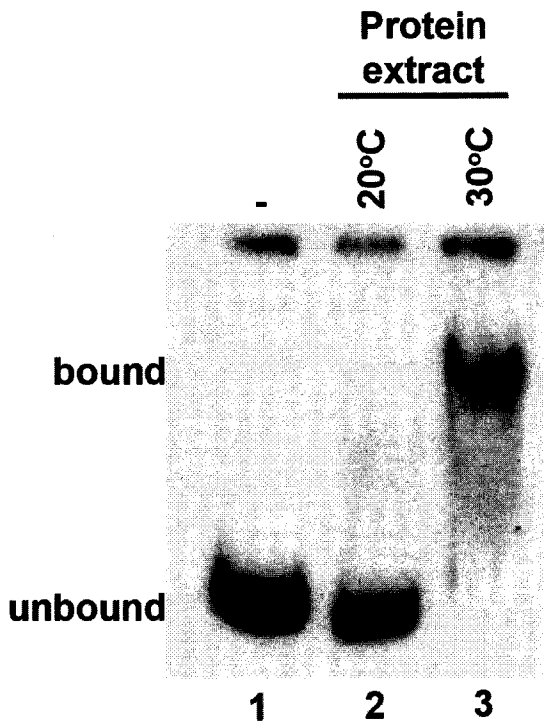

Figure 3.6. A putative repressor binds to the *crhC* promoter in a concentration-dependent manner. EMSA reactions were performed by incubating an end-labeled portion (5000 cpm (A) and 2000 cpm (B)) of the *crhC* promoter (*JB9:JB11*, 93 bp) with increasing concentrations of *Anabaena* protein lysate. Panel A shows the EMSA reaction when incubated with increasing concentrations of protein extract for *Anabaena* cells grown at an optimal temperature (30°C). Panel B shows the EMSA reaction when incubated with increasing concentrations of cold stressed (20°C) *Anabaena* protein extract. Protein- DNA interactions are labeled as bound, compared to the no protein control (–).

A

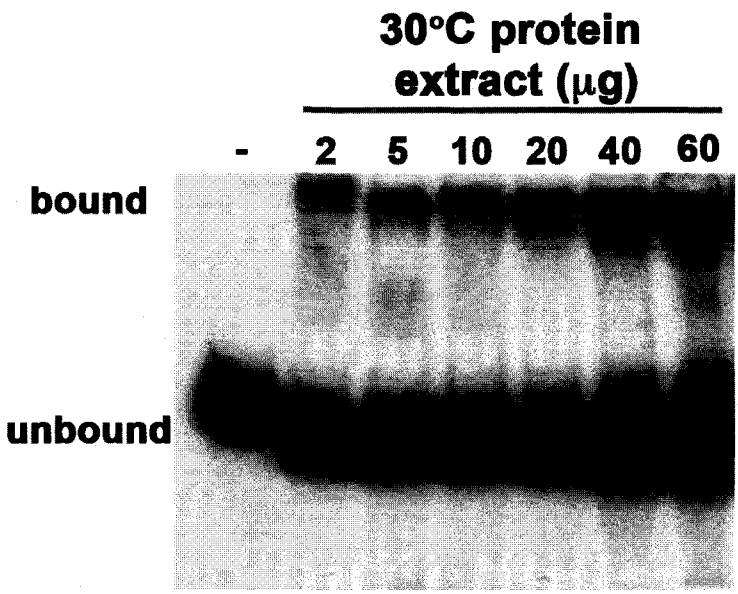

B

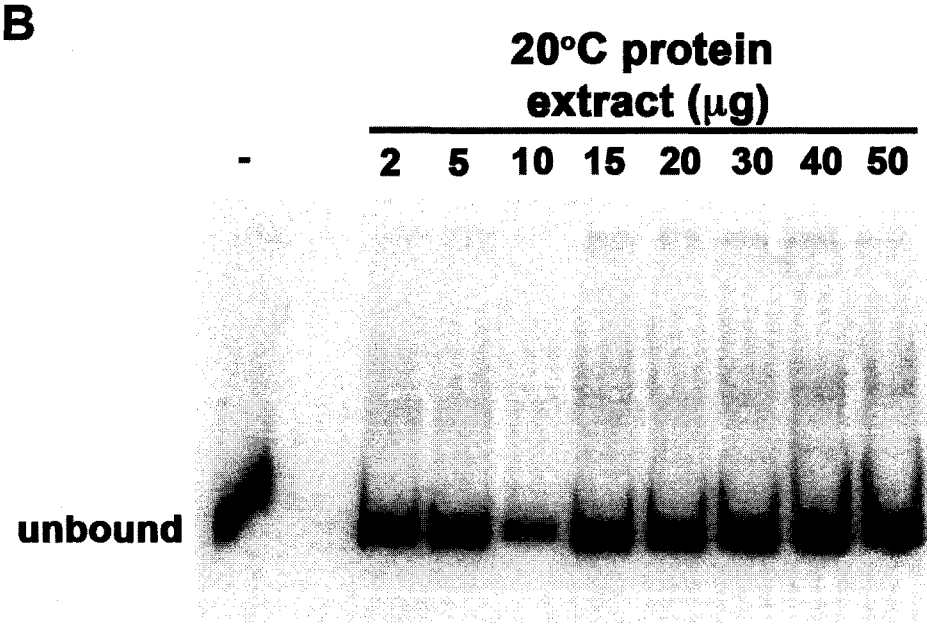

competitive DNA. As shown in Figure 3.7, specificity of the repressor for the *crhC* promoter was detected by a decrease in bound probe intensity with an increase in concentration of unlabeled competitive DNA (Figure 3.7, lanes 3 – 6). Repressor specificity for the *crhC* promoter is also supported by the observation that the addition of non-competitive DNA does not result in a change in bound probe intensity (lanes 7 - 10), even at concentrations 1000X fold greater than original end-labelled *JB9:JB12* target DNA. These results indicate that the repressor protein recognizes and binds a specific sequence within the *crhC* promoter.

3.1.5 Repressor Protein Conservation

To determine if the repressor recognition sequence or its DNA binding domain is conserved among cyanobacterial species, EMSA reactions were employed using soluble protein extracts isolated from several cyanobacterial species grown at 30°C (Figure 3.8). Optimally grown (37°C) *E. coli* protein extracted served as a control (Figure 3.8, lanes 7-8). EMSA analysis detected tight and intense shifts for all of the cyanobacterial protein lysates tested, when incubated with the 281 bp *crhC* promoter fragment amplified from the deletion construct JW6 (*JB3:JB4*) (Figure 3.8, lanes 2 – 6). Comparably, a weaker shift was obtained when *E. coli* protein lysate was incubated with the *crhC* promoter (lanes 7 - 8). These results are indicative that the *crhC* promoter may contain a putative global binding sequence for similar DNA-binding proteins (i.e. similar DNA-binding domains), prominently conserved within cyanobacterial species. From these results it is plausible that there may be *crhC*-like promoter sequences regulating other cold shock genes in *Synechocystis* and *Synechococcus*. These *crhC*-like promoters are capable of interacting with DNA-binding proteins found in *Synechocystis* and *Synechococcus* however their involvement in providing temperature-dependent transcriptional regulation is not known. The presence of a weak shift with *E. coli* protein lysate suggests that *E. coli* may lack a DNA-binding protein similar to the repressor protein found in *Anabaena*, or if present, it may recognize a different/altered binding sequence.

Interestingly, variations in probe migration were also evident among the cyanobacterial protein lysates tested. These results suggest that the various cyanobacterial DNA-binding proteins are not identical in size and/or may have a different

Figure 3.7. Repressor binding to the *crhC* promoter is sequence specific. EMSA reactions were performed by incubating an end-labeled (5000 cpm) portion of the *crhC* promoter (*JB9:JB12*, 129 bp) with 20 μg of *Anabaena* protein lysate grown at 30°C (optimal). Unlabeled target DNA (*JB9:JB12*, 129 bp) was added to the EMSA binding reaction as competitor DNA (lanes 3 - 6). A similar sized DNA strand amplified from the *crhC* ORF (*GWO36: WCM1*, 113 bp) was added to the binding reaction as non-competitor DNA (lanes 7 – 10). Protein-DNA interactions are labeled as bound, compared to the no protein (-) control (lane 1, unbound).

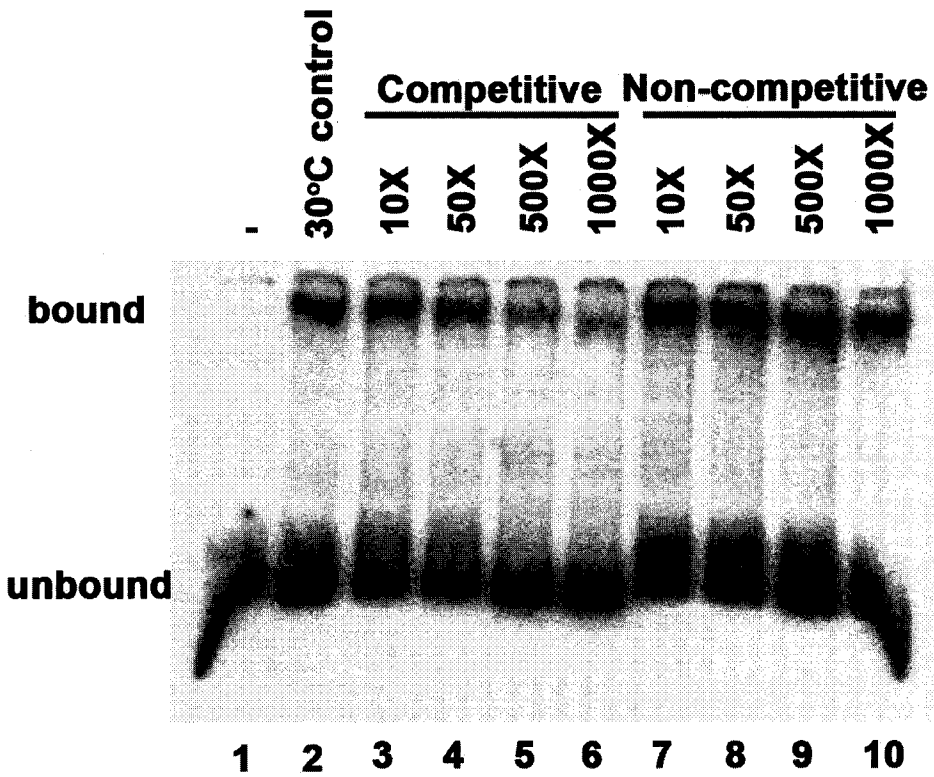

Figure 3.8. The *Anabaena* repressor DNA-binding domain may be conserved amongst cyanobacterial species. EMSA reactions were performed using various protein lysates grown under optimal conditions (30°C for cyanobacteria and 37°C for *E. coli*). Protein extract was isolated from the indicated cyanobacterial species (*Anabaena* sp. strain PCC 7120, *Synechococcus* sp. strain PCC 7942, and *Synechocystis* sp. strain PCC 6803) (lanes 2 – 6) and *E. coli* DH5α (lanes 7 – 8). 5 μg and 20 μg (indicated in brackets) of optimally grown protein extract were incubated with an end-labeled (3000 cpm) portion of the *crhC* promoter (281 bp) (deletion construct JW6 PCR amplified with *JB3:JB4*) and separated on a 1X TAE, 8% native gel. Protein bound *crhC* probe is labeled as bound, compared to the unbound, no protein (-) control (lane 1).

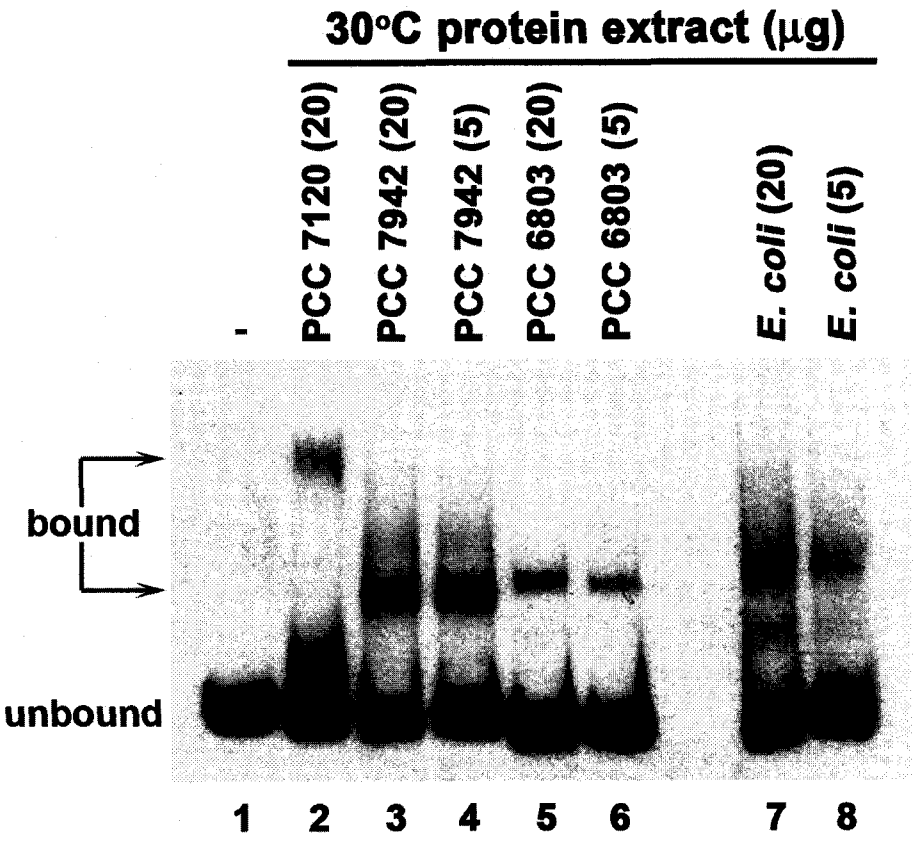

number of sites for protein binding. They are similar in the fact that these organisms contain a DNA-binding protein capable of binding to a related DNA recognition sequence within the *crhC* promoter.

3.1.6 Preliminary Size Determination of the Repressor Protein

To determine the approximate size of the repressor protein interacting with the *crhC* promoter, EMSA reactions were performed using optimally grown (30°C) *Anabaena* protein lysate, size fractionated through molecular weight exclusion columns (Millipore). Based on the molecular weight exclusion of each column, proteins were isolated based on size ranging from less than 10 kDa to greater than 100 kDa. As shown in Figure 3.9, bound probe was not visible when the *crhC* promoter was incubated with proteins smaller than 30 kDa (Figure 3.9, lanes 2 and 4), indicative that the repressor protein must be larger than 30 kDa. Intense shifts were observed when the *crhC* promoter was incubated with proteins >10 kDa, >30 kDa, and >100 kDa in size (Figure 3.9, lanes 3, 5, and 8), with the most intense DNA-protein complex formation occurring with the >100 kDa protein fraction. These results suggest that the repressor protein is large, possibly >100 kDa in size. In contrast, a weaker shift was visible in the <100 kDa protein fraction indicating that the cellulose columns may have been overload, reaching maximum protein binding capacity. In support, when the cellulose column was washed to remove proteins that should have originally been excluded in the <100 kDa fraction, a shift was noted (Figure 3.9, lane 7). This result suggests that the cellulose columns were overloaded with total protein extract making exclusion of the higher molecular weight proteins difficult. The presence of DNA-protein complexes in both the >100 kDa and <100 kDa protein fractions could also be explained by protein-protein interactions, protein aggregation, and/or the formation of multiple higher order complexes. It is possible that the repressor can interact with the *crhC* promoter in both a monomeric and dimeric form. In its monomeric form it is <100 kDa in size whereas as a dimer, its size is doubled (>100 kDa). Further evidence is needed to confirm this hypothesis.

Figure 3.9. DNA-binding protein size determination. EMSA reactions were performed using optimally (30°C) grown *Anabaena* protein extract that was size fractionated by centrifugation through cellulose columns (Millipore) with molecular weight exclusions of 10, 30 and 100 kDa. After transferring the excluded higher molecular protein fraction to a higher molecular weight cellulose column, the original column was washed with $mQdH_2O$ to determine if the columns were overloaded (lane 7). 30 μg of the fractionated protein isolates (lanes 2 – 6, and 8) and their washes (lane 7) were incubated with an end-labeled (5000 cpm) portion of the *crhC* promoter (281 bp) (deletion JW6 PCR amplified with *JB3:JB4*) and separated on a 1X TAE, 12% native gel. Protein-DNA interactions are labeled as bound, compared to the unbound, no protein(-) control (lane 1).

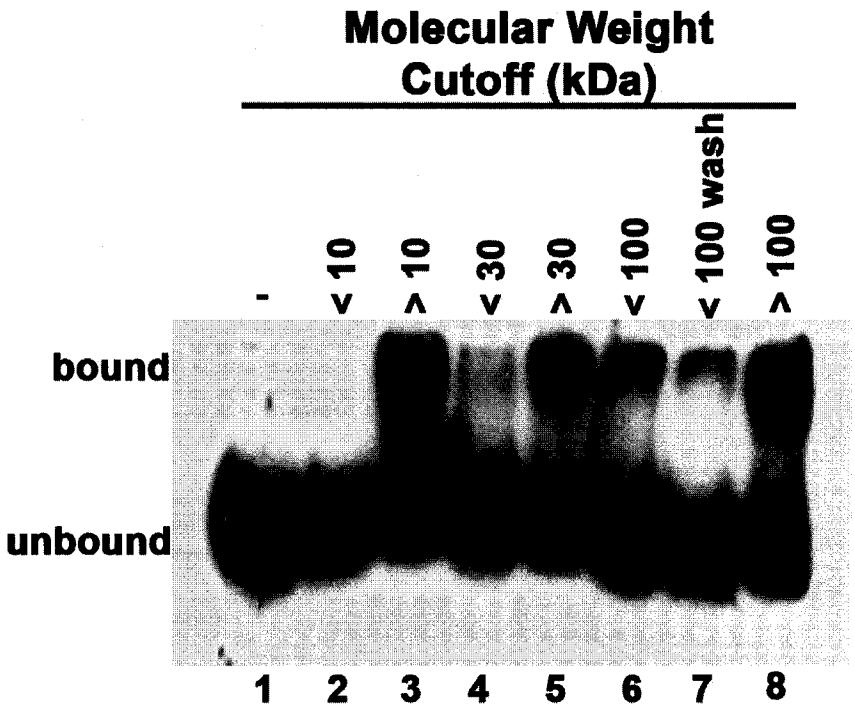

3.1.7 Dephosphorylation Studies

Bacterial transcription factors are frequently intermediates within a signal transduction pathway, in which protein activity is regulated by changes in its phosphorylation state (Appleby *et al.*, 1996). To analyze if phosphorylation was involved in regulating the repressor's ability to interact with the *crhC* promoter, EMSA reactions were performed with protein lysates dephosphorylated with calf intestinal alkaline phosphatase (CIP) prior to the binding reaction (Figure 3.10). Theoretically, if phosphorylation state was important for DNA-binding, dephosphorylation of the repressor would alter its interaction with the *crhC* promoter.

As expected, control reactions showed that 30°C protein extracts resulted in a target DNA shift (Figure 3.10A, lane 3), which was not observed in extracts from *Anabaena* cells grown at 20°C (Figure 3.10A, lane 2). Phosphorylated alterations in repressor activity were first investigated by determining if there was a difference in the repressor's phosphorylation state when grown at 30°C, compared to 20°C. More specifically, could the presence of protein lysates grown at 20°C, induce a change in the phosphorylation state of protein lysates grown at the 30°C (or vice versa), due to temperature-dependent phosphate acting enzymes (kinases or phosphatases). To investigate this, EMSA reaction were performed using *Anabaena* protein lysate containing a mixture of both optimally grown (30°C) and cold-shocked (20°C) protein extracts (Figure 3.10A, lane 4). Compared to the 30°C control (Figure 3.10A, lane 3), a decrease in shift intensity and migration was noted when both 30°C and 20°C protein extracts were present. The results suggest that cold-induced factors (e.g. phosphatase) present in the mixed lysate, may inhibit repressor binding activity.

Dephosphorylation studies using CIP also confirmed that temperature-dependent modifications in the repressor's phosphorylation state, regulates DNA binding. Shown in lane 6 (Figure 3.10A), dephosphorylation of the repressor protein by CIP completely eliminated the presence of bound probe at 30°C. Removal of a phosphate group(s) (decreasing the phosphorylation state) from the repressor inhibited its ability to bind to the *crhC* promoter, therefore preventing a retardation in probe migration. To ensure that the CIP enzyme wasn't removing the 5'-P^{32}-phosphate group from the end-labelled probe, the same EMSA experiment was performed using *Synechocystis* sp. strain PCC

Figure 3.10. The putative repressor binds to the *crhC* promoter in a phosphorylation-dependent manner. EMSA reactions were performed with an end-labeled portion of the *crhC* promoter (281 bp) (deletion construct JW6 PCR amplified with *JB3:JB4*) incubated with 30 μg of *Anabaena* protein extract, and separated on a 1X TAE, 8% native gel. *Anabaena* protein extracts added to the binding reactions were grown either at 30°C (optimal), 20°C (cold stressed), or contained a mixture of both temperature lysates (mixed) (controls, lanes 2 – 4). Where indicated, protein extracts were dephosphorylated using CIP (Section 2.5.1.1), and the CIP inactivated with sodium pyrophosphate (10 mM) prior to the protein's addition to the EMSA binding reaction. Panel A shows the autoradiogram of CIP-treated *Anabaena* protein extracts (lanes 5 – 7). Panel B shows the autoradiogram of CIP-treated *Synechocystis* sp. strain PCC 6803 protein lysates (lanes 5 – 7). DNA-protein complex formations are labeled as bound, compared to the unbound, no protein (-) control (lane 1).

A

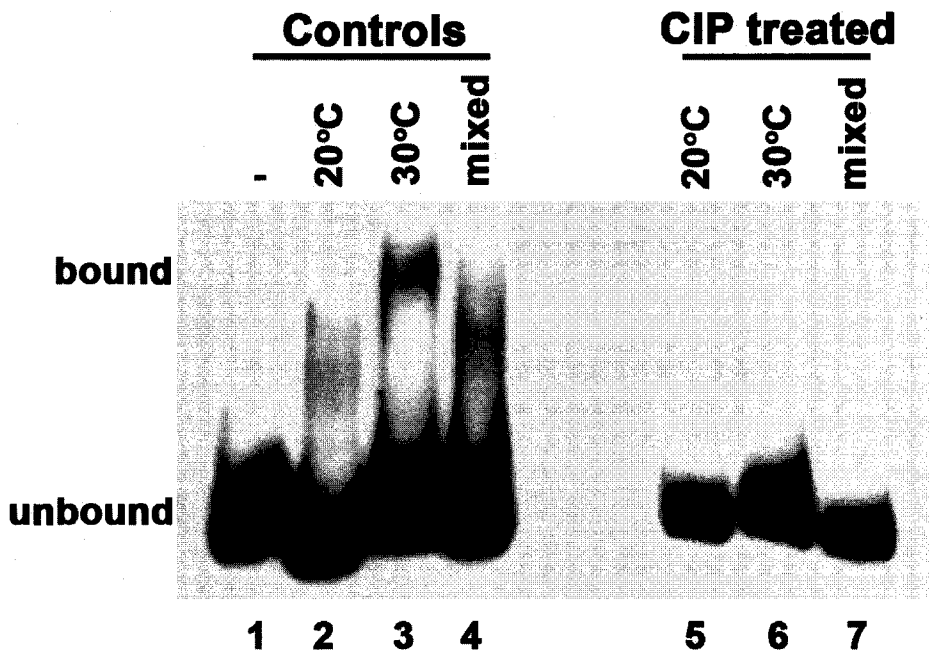

B

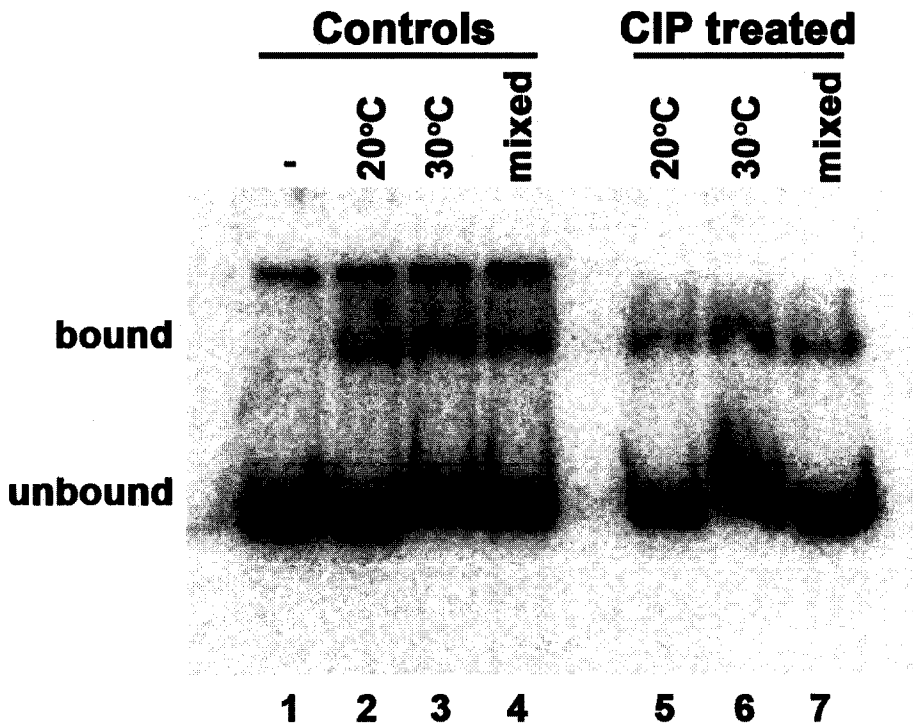

6803 total protein lysate (Figure 3.10B), previously shown to interact with the *crhC* promoter (Figure 3.8). Compared to the control lanes (Figure 3.10B, lanes 1 - 4), no change in shift migration was evident when *Synechocystis* protein extract was treated with CIP (lanes 5 – 7). These results indicate that the P^{32} label was not removed and suggest that the absence of shift seen with CIP-treated *Anabaena* 30°C protein extract (Figure 3.10A) was due to the lack of a protein-DNA interaction and not the absence of radioactively labelled probe. The results also suggest that a similar protein is binding to this DNA fragment in both cyanobacterial species however, they are regulated by different mechanisms. The presence of bound probe with both 20°C and 30°C *Synechocystis* protein extract (Figure 3.10B, lanes 2 and 3) suggests that the *Synechocystis* DNA-binding protein is not involved in transcriptionally regulating temperature-dependent processes. Also, the *Synechocystis* DNA-binding protein does not appear to be regulated in phosphorylation-dependent manner as no change was seen between the control and CIP-treated protein extracts (Figure 3.10B). In summary, these results suggest that phosphorylated activation of the repressor allows for binding to the *crhC* promoter at 30°C but not 20°C however, further analysis of the repressor protein needs to be done to confirm these results.

3.1.8 Promoter Binding Site Identification

To more precisely delineate what region of the *crhC* promoter the repressor was binding, EMSA analysis was performed using the JW promoter deletion constructs (Figure 3.1). Target DNA was generated by amplifying (*JB3*:*JB4*) the promoter region of the deletion constructs, producing promoter fragments that varied in length at the 5' end. EMSA results showed the presence of bound probe when optimally grown (30°C) *Anabaena* protein extract was incubated with target DNA amplified from the promoter deletion constructs JW2 – JW6 (Figure 3.11). Target DNA amplified from deletion construct JW8 however, showed no shift whereas JW7 produced a faint shift. These results demonstrated that the repressor can bind to portions of the *crhC* promoter in the vicinity of the -10 region but binding is tightest when the full-length promoter (and its motifs) is present.

Figure 3.11. The putative repressor binds to the *crhC* promoter region encompassing the AT-rich element and –10 regions. EMSA reactions were performed using 5000 cpm of end-labeled target DNA amplified (*JB3:JB4*) from the JW promoter deletion series (Table 2.4, Figure 3.1). The target DNA was incubated with 30 μg of protein lysate isolated for *Anabaena* cells grown at optimal (30°C) or cold stress (20°C) temperatures and separated on a 1X TAE, 8% native gel.

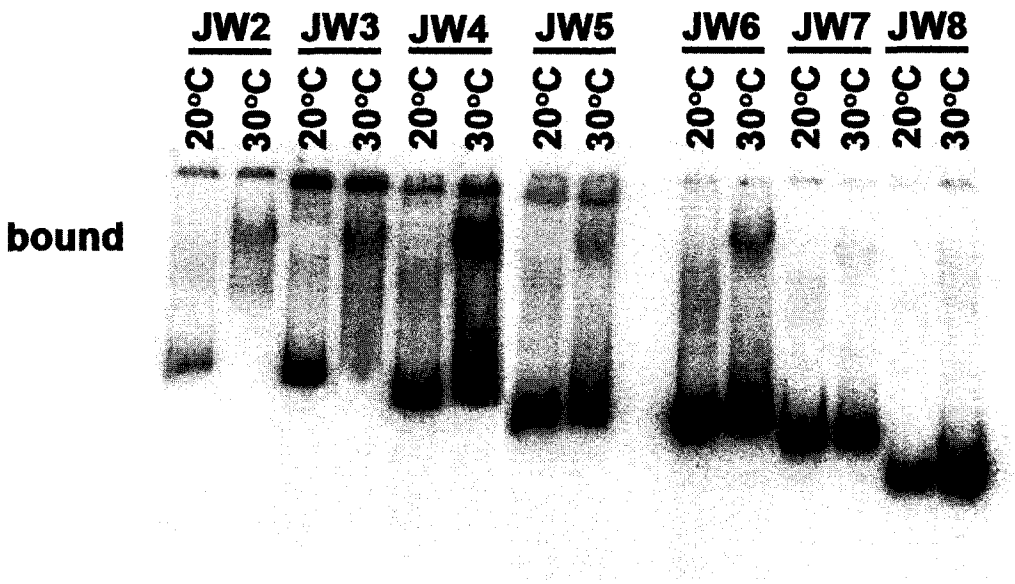

In relationship to the promoter motifs, a substantial decrease in shift intensity is noted between deletion constructs JW4 and JW5. Sequence analysis reveals that the primary difference between JW4 and JW5 is the presence (JW4) or absence (JW5) of the AT- rich element. These results provide preliminary evidence that sequence within the proximity of the AT-rich and -10 elements of the *crhC* promoter may be important for repressor binding and may therefore contain the binding recognition sequence.

Although the shift intensity decreased when JW5 and JW6 were used as target DNA, a distinct shift is still noticeable even though the DNA targets lack the AT-rich element. These results indicate that the repressor binding sequence includes both the AT-rich element and the –10 region of the *crhC* promoter. Therefore, the promoter sequence surrounding both the AT-rich element and the –10 region is required for repressor binding. The reduction in shift intensity following the removal of the AT-rich element (JW4 to JW5) can also be explained by the possible presence of a protein dimer. As previously mentioned (Section 3.1.2), the repressor-DNA interaction appears to be very short lived or may require cofactors to bind. Also, EMSA results using protein extracts from the cellulose spin columns (Figure 3.9) showed a strong shift with proteins larger than 100 kDa (Section 3.1.6). Taken together, these results support the possibility of repressor dimerization required for optimal DNA binding. If repressor dimerization is required for promoter recognition and binding, removal of specific promoter motifs could affect its ability to bind. For example, if the *crhC* promoter lacked the AT-rich element but contained the –10 region (JW5 and JW6), the dimerized repressor only has a portion of the DNA recognition sequence of which it can bind. With only half of the site available, the protein-DNA interaction might not be as tight, producing a weaker, less distinct shift on the EMSA gels.

3.1.9 *crhC* DNA-Binding Protein Isolation by DNA Affinity Chromatography

In order to characterize the repressor, attempts were made to isolate the protein using biotin-streptavidin DNA affinity columns (Miltenyi Biotec). The premise of the columns applies the affinity of biotin for streptavidin. The streptavidin ligand is conjugated to paramagnetic beads, which can be immobilized on a separation column, in the presence of a strong magnetic field. A biotinylated DNA target and any associated

proteins can therefore be reversibly bound to the column and the DNA-binding proteins eluted with increasing salt concentration.

As the shortest *crhC* promoter region to interact with repressor protein (Figure 3.11), promoter deletion construct JW6 was chosen as the target DNA and was biotinylated at the 5' end by PCR amplification with primers *GWO71:GWO43* (311 bp). EMSA reactions demonstrated that the optimal buffer for improved protein binding to the biotinylated target DNA was buffer JB_{50} (Section 2.5.2), indicated by slight alterations in bound probe migration, compared to the 30°C control (Figure 3.12). Therefore, all streptavidin-biotin binding reactions were performed using JB_{50} buffer rather than the normal 1X EMSA buffer, the primary difference being the buffering and salt solutions (HEPES, pH 8 vs. Tris, pH 7.5 and KCl vs. NaCl).

Initial attempts at DNA-binding protein isolation demonstrated that several proteins within the optimally grown (30°C) *Anabaena* protein lysate bound and eluted from the affinity column with 1M KCl (Figure 3.13A, lane W4). Amongst the array of proteins found within the 1M KCl elution fraction, a protein doublet (indicated by the arrows) was reproducibly seen. To confirm that the eluted proteins were not artifacts, several control columns were performed including replacing optimally grown (30°C) *Anabaena* protein extract with cold-shocked (20°C) protein extract, columns run in the absence of target DNA, and using optimally grown (30°C) *Synechococcus* sp. strain PCC 7942 protein extract, previously shown to interact with the *crhC* promoter (Figure 3.8, lanes 3 and 4). The latter control experiment is shown in Figure 3.13B, demonstrating that a different protein pattern eluted from the column in the 1 M KCl fraction (lane W4) than that observed with *Anabaena* 30°C protein extract. These results suggested that the protein doublet isolated from *Anabaena* 30°C total protein extract was not an artifact and therefore may represent putative DNA-binding proteins involved in regulating *crhC* expression. The protein doublet, approximately 60 kDa and 65 kDa in size, were separately excised from the gel and sent for mass spectroscopy sequence analysis (Section 2.4.2.3). Due to unknown circumstances the proteins could not be sequenced, therefore requiring further investigation.

To limit the number of proteins binding to the *crhC* promoter, efforts were made to determine the minimal promoter length in which a strong protein-DNA interaction was

Figure 3.12. An optimized binding buffer is used for DNA affinity chromatography. EMSA reactions were performed using an end-labeled (5000 cpm) and biotinylated portion of the *crhC* promoter which was PCR amplified (*GWO71:GWO43*) from the promoter deletion construct JW6 (311 bp). Biotinylated target DNA was incubated with 20 μg optimally grown (30°C) *Anabaena* protein lysate, in the presence of either 1X EMSA buffer (10 mM Tris-HCl, pH 7.5, 50 mM NaCl, 1mM EDTA, 5% [v/v]) glycerol, 1 mM DTT, 10 mM $MgCl_2$) (lane 3), 1X JB_{50} buffer (10 mM HEPES, pH 8, 1 mM EDTA, 5% [v/v] glycerol, 1 mM DTT, 10 mM $MgCl_2$, 50 mM KCl) (lane 4), or 1X EMSA buffer without $MgCl_2$ (30°C control, lane 2). The binding reactions were separated on a 1X TAE, 12% native gel with retardation in gel migration indicative of protein-DNA interactions (labeled bound), compared to the unbound, no protein (-) control (lane 1).

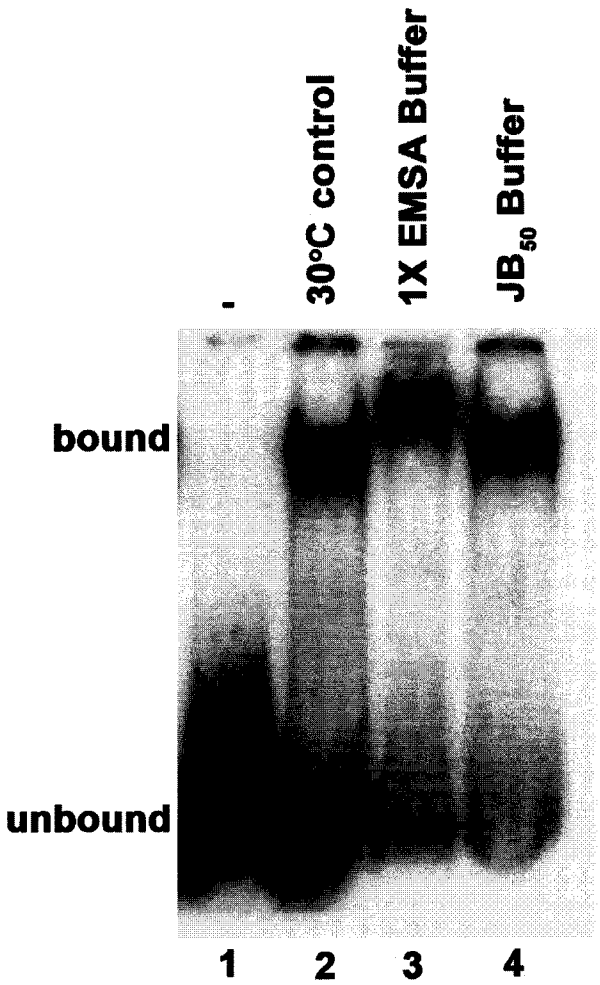

Figure 3.13. Two DNA-binding proteins are reproducibly isolated by DNA affinity chromatography. Streptavidin-biotin binding reactions were performed using 10 mg of optimally grown (30°C) protein lysate incubated with 30 μg of biotinylated *crhC* promoter DNA (311 bp) (deletion construct JW6 PCR amplified with *GWO71:GWO43*). The binding reaction was applied and magnetically separated on μMACS columns, immobilized in a strong magnetic field (Miltenyi Biotec). Non-specific proteins were stringently washed and the target DNA-binding proteins eluted with high salt (KCl) concentration. Panel A shows the silver stained, polyacrylamide gel (10%) of the TCA precipitated proteins eluted from the streptavidin-biotin column when optimally grown (30°C) *Anabaena* sp. strain PCC 7120 total protein extract was used. Two reproducible DNA-binding proteins of interest are indicated by arrows. Panel B shows the silver stained, polyacrylamide gel (10%) of the TCA precipitated protein products eluted from the streptavidin-biotin column when optimally grown (30°C) *Synechococcus* sp. strain PCC 7942 total protein extract was used. A single DNA-binding protein (indicated by the arrow) was isolated, having a different migration distance from the two DNA-binding proteins isolated in panel A. Migration distances of the molecular weight markers are indicated in kDa. Abbreviations: BR = Bio-Rad broad range molecular weight marker, LR = Bio-Rad low range molecular weight marker, FT = flow-through, W1 = 50mM KCl (JB_{50}), W2 = 100 mM KCl (JB_{100}), W3 = 250 mM KCl (JB_{250}), W4 = 1M KCl (JB_{1000}), W5 = 2M KCl (JB_{2000}) (Section 2.5.2).

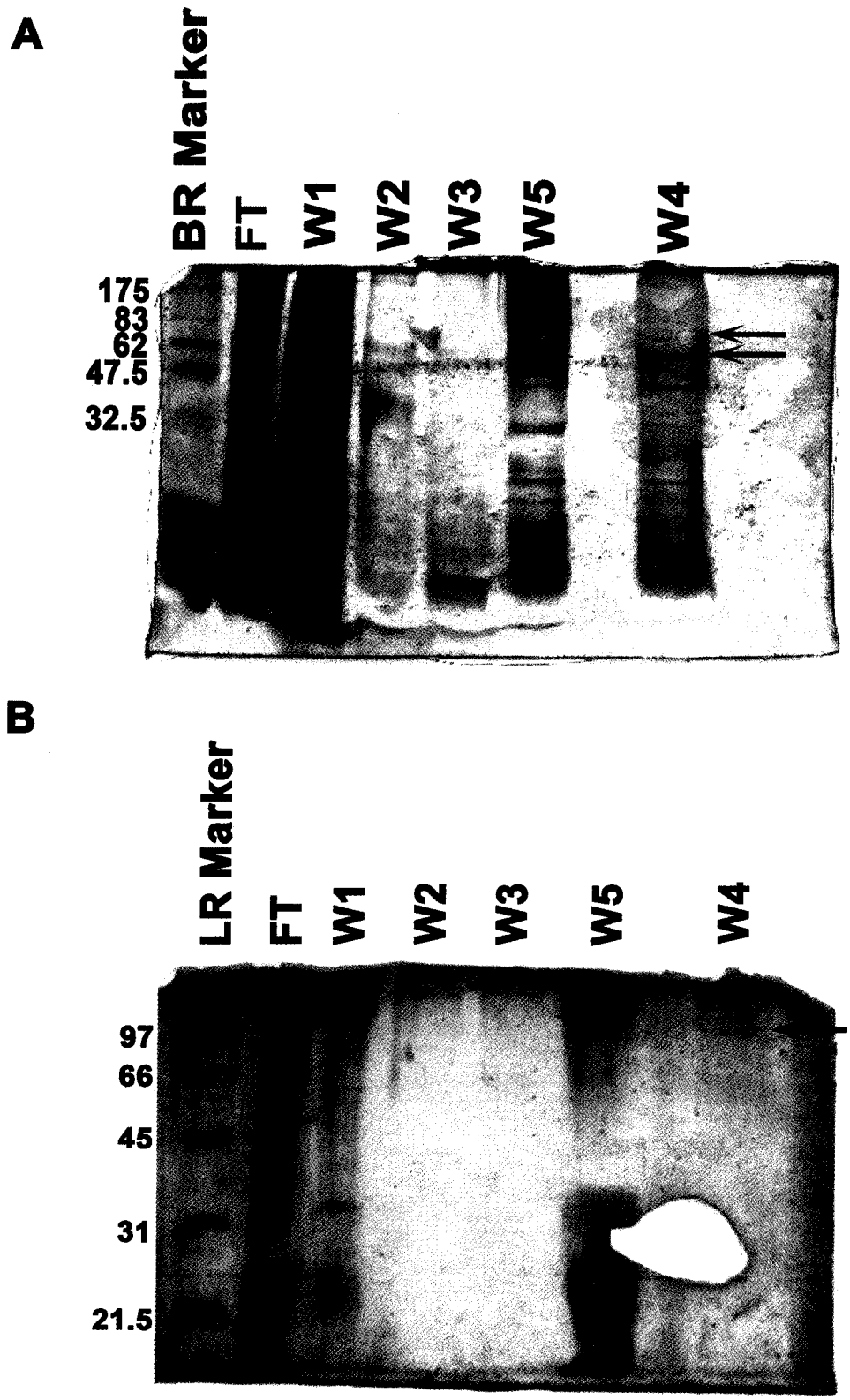

observed. Previous results indicated that deletion construct JW4 bound the repressor protein very tightly whereas JW5 did not (Figure 3.11), the primary difference being the absence/presence of the AT-rich element (Figure 3.1). Focusing on the AT-rich region, EMSA reactions were performed using shortened target DNA fragments generated by PCR amplification with the forward primers *JB8*, *JB9,* or *JB10* and the reverse primers *JB11* or *JB12* (Figure 3.14A) (Table 2.2). Illustrated by the presence of shift in the EMSA reactions shown in Figure 3.14B and C, promoter fragments *JB8*:*JB11* (130 bp), *JB9*:*JB11* (93 bp), *JB8*:*JB12* (166 bp), and *JB9*:*JB12* (129 bp) all contain the recognition sequence required for repressor binding. Strong EMSA shifts were not observed with promoter fragments *JB10*:*JB11* (41 bp) and *JB10*:*JB12* (77 bp), which therefore do not contain the repressor binding sequence. The differential sequence between *JB9*:*JB11* (presence of a shift) and *JB10*:*JB11* (absence of a shift) suggested that the repressor binding sequence is located in a 52 bp region including the AT-rich element.

DNA affinity chromatography was repeated using the 129 bp biotinylated *JB9*:*JB12* promoter fragment as the target DNA. On a SeeBand stained, 10% SDS-PAGE gel (Figure 3.15A) an overall decrease in the number of proteins was observed, as only two DNA-binding proteins (indicated by the arrows), approximately 60 kDa and 65 kDa in size, eluted with 1M KCl. Interestingly, these two DNA-binding proteins were similar in size to the protein doublet found in Figure 3.13A, lane W4. The two putative regulatory proteins underwent mass spectroscopy sequencing on a number of occasions, and again no protein sequence was generated.

3.1.10 Temperature-regulated *crhC* Expression in *E. coli*, from the Promoter Deletion Constructs

It has been reported that *crhC* transcript accumulation in *E. coli* is regulated in the same temperature-dependent fashion as that observed in *Anabaena* (Chamot and Owttrim, unpublished). In order to study the regulatory regions of the *crhC* promoter required for temperature-dependent expression in *E. coli*, cold-induced *crhC* transcript and protein levels were analyzed from the DC1 – DC8 promoter nested deletion series (Figure 3.2, Table 2.4). Western blot analysis using a polyclonal anti-CrhC antibody was performed on both optimally grown (37°C) and cold stressed (20°C) *E. coli* protein

Figure 3.14. A 52 bp region containing the AT-rich element of the *crhC* promoter is sufficient for repressor binding. Panel A shows a schematic of the primers used to amplify shorter *crhC* promoter fragments used as target DNA in EMSA reactions and DNA affinity chromatography. The PCR product lengths are: *JB8:JB11* = 130 bp, *JB9:JB11* = 93 bp, *JB10:JB11* = 41 bp, *JB8:JB12* = 166 bp, *JB9:JB12* = 129 bp, *JB10:JB12* = 77 bp. Panel B illustrates the EMSA results using the shortened target DNA fragments (5000 cpm) amplified with the *JB11* reverse primer, in the absence (-) or presence (+) of 20 μg of protein lysate isolated from *Anabaena* cells grown at optimal temperature (30°C). Panel C shows the EMSA reaction using the shortened target DNA fragments amplified with the *JB12* reverse primer, in the absence (-) or presence (+) of 20 μg of optimally grown (30°C) *Anabaena* protein lysate. DNA-protein interactions are labeled as bound, compared to the no protein controls (labeled as unbound).

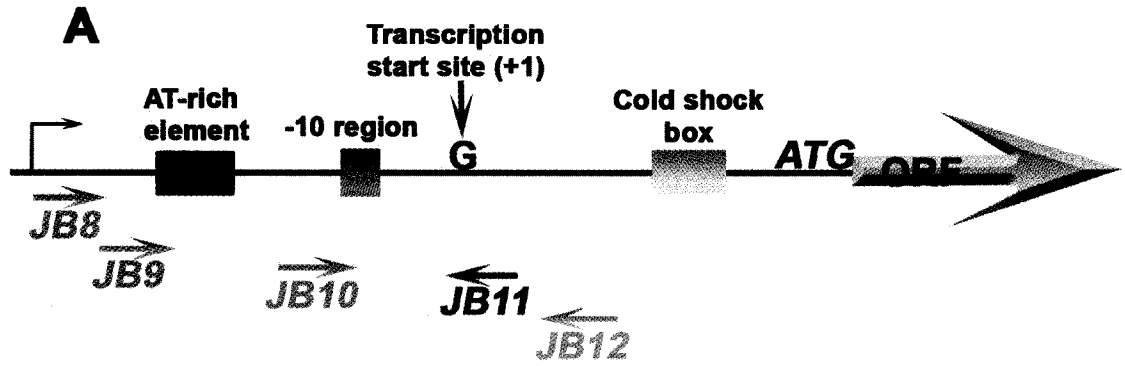

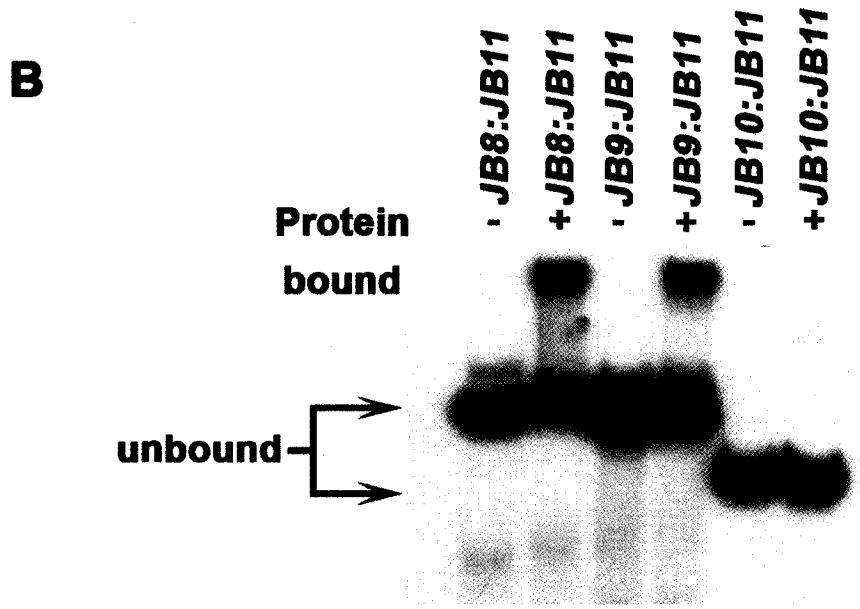

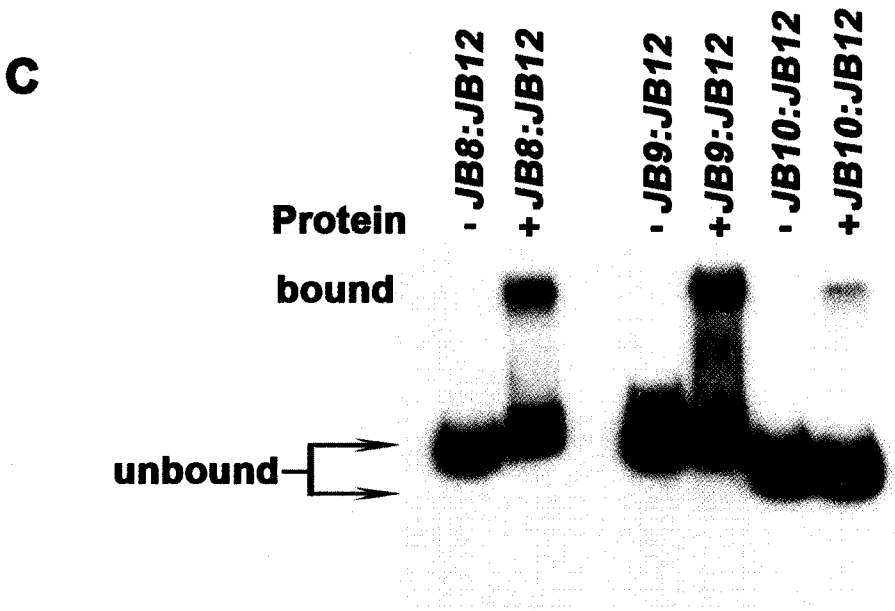

Figure 3.15. DNA affinity chromatography isolated 60 kDa and 65 kDa DNA-binding proteins. The SeeBand stained, polyacrylamide gel (10%) shows the TCA precipitated proteins eluted from the streptavidin-biotin column when optimally grown (30°C) *Anabaena* protein extract was used in the binding reaction. The streptavidin-biotin binding reaction was performed using 15 mg of optimally grown (30°C) *Anabaena* protein lysate incubated with 30 μg of biotinylated *JB9:JB12* (129 bp) *crhC* promoter DNA. The binding reaction was applied and separated on μMACS columns in the presence of a strong magnetic field (Miltenyi Biotec). Non-specific proteins were stringently washed from the column and the target proteins bound to the target DNA were eluted with high salt (KCl) concentration. The isolated 60 kDa and 65 kDa DNA-binding proteins (W4), sent for mass spectrometry sequencing, are indicated by arrows. Migration distances of the molecular weight markers are indicated in kDa. Abbreviations: LR = Bio-Rad low range molecular weight marker, FT = flow-through, W1 = 50mM KCl (JB_{50}), W2 = 100 mM KCl (JB_{100}), W3 = 250 mM KCl (JB_{250}), W4 = 1M KCl (JB_{1000}), W5 = 2M KCl (JB_{2000}) (Section 2.5.2).

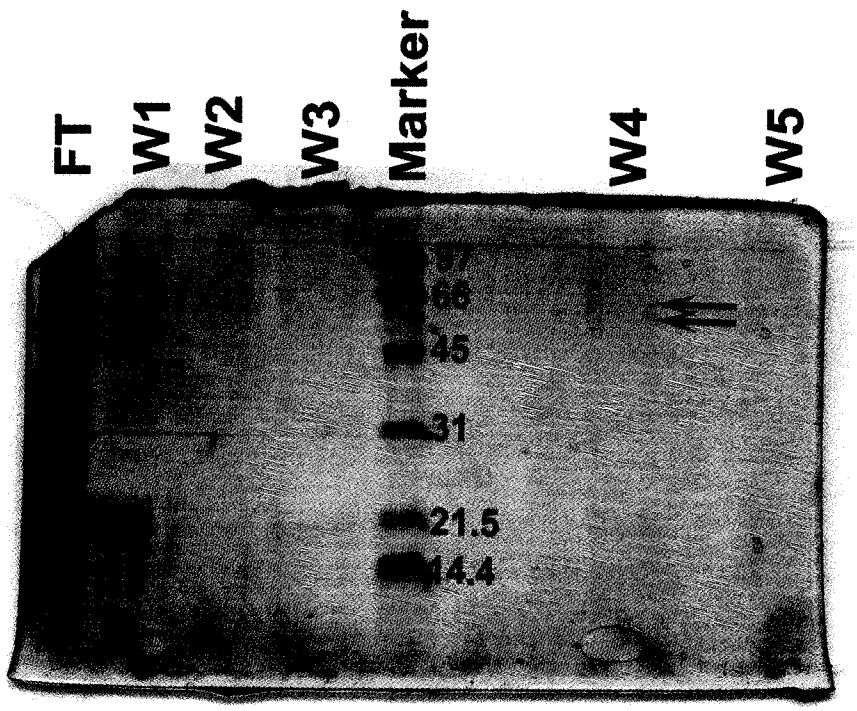

lysates (Figure 3.16A). CrhC expression was dramatically increased at 20°C compared to 37°C for deletions DC1 - DC4 (Figure 3.16A, lanes 1 - 4) whereas, little to no CrhC expression was observed for deletions DC5 - D8, regardless of growth temperature. The borderline of cold-induced CrhC expression lies within a 33 bp region between promoter deletion constructs DC4 and DC5 (Figure 3.2). In relation to the *crhC* promoter motifs, temperature-dependent expression of CrhC was found if the promoter deletion construct contained the AT-rich element however, if the AT-rich element was removed, CrhC expression was dramatically reduced (Figure 3.16). Note, that the -10 region was present in both the DC4 and DC5 deletion constructs suggesting that the -10 region may be required for repressor binding (Section 3.1.8) however, it may not required for temperature-dependent CrhC expression. Conversely, the AT-rich element appears to be involved in both repressor binding and temperature-regulated CrhC expression.

Northern analysis was performed on several of the DC promoter deletion constructs (DC1, DC2 and DC5) for two reasons: to confirm the importance of the AT-rich element in transcription regulation of *crhC*, and to determine if the transcript levels correlated to the protein levels observed in the Western results. Supporting the previous report by Chamot and Owttrim (unpublished), Figure 3.16B shows that both DC1 and DC2 show temperature-dependent transcript accumulation in *E. coli,* similar to that observed in *Anabaena.* Also in correlation to the Western results, increased transcript accumulation was seen for deletion constructs DC1 and DC2 at 20°C (cold) compared to 37°C (optimal), both containing the AT-rich element (Figure 3.16). Comparably, a dramatic decrease but not a complete abolishment of transcript accumulation was seen for deletion construct DC5 at 20°C, which lacked the AT-rich element. The decrease in transcript accumulation when the AT-rich element is absent from the promoter supports, that either the AT-rich region is important for temperature-dependent *crhC* transcript and protein accumulation in *E. coli* or, that the AT-rich element is necessary for general promoter function. In correlation to previous results (Figure 3.11), it appears that the AT-rich element is required for both general transcription initiation (promoter activity) and for repression of transcription via repressor binding to the AT-rich element and –10 region.

Figure 3.16. *crhC* transcript and protein expression in *E. coli*, from the DC promoter deletion series. The indicated DC promoter deletion constructs (Figure 3.2) were grown to log phase at 37°C (optimal) and cold stressed by transferring to a 20°C incubator for 3 hours. Panel A shows the Western blot analysis on 30 μg of *E. coli* protein extract separated on a 10% SDS-PAGE gel, transferred, and detected with anti-CrhC antibody (1:5000). Panel B shows the Northern blot analysis on 30 μg of total RNA isolated from the same DC deletion cultures used in panel A. RNA was separated on a 10% formaldehyde gel, transferred, and probed with a random primed (Section 2.3.9.2) *crhC* DNA probe (Nhe I/EcoR V cleaved pWM753, 390 bp).

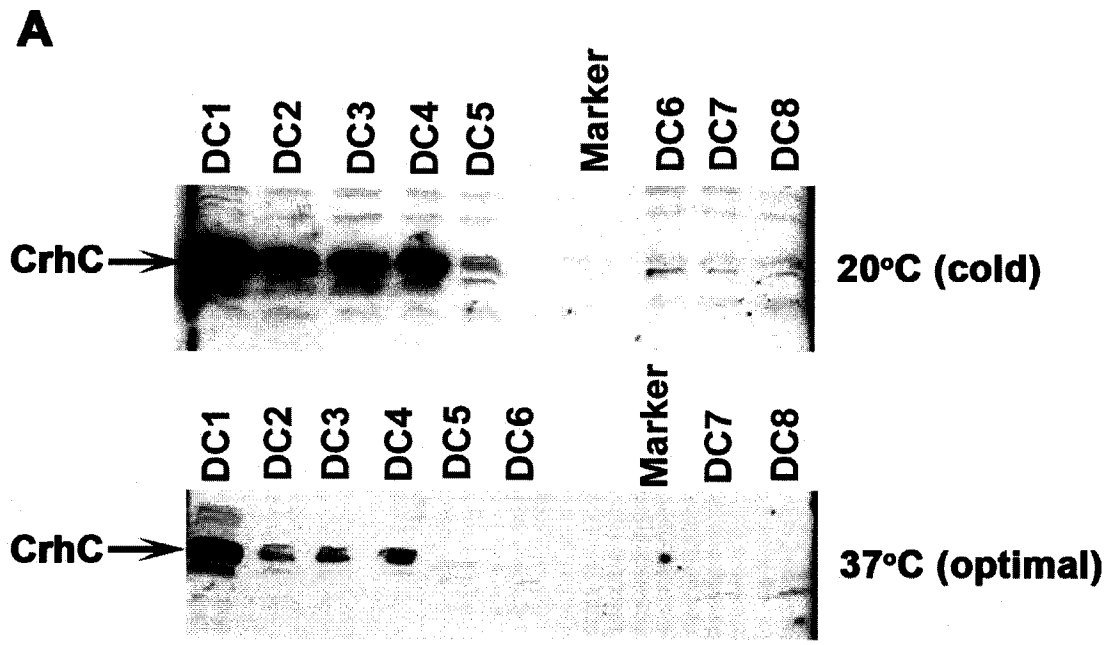

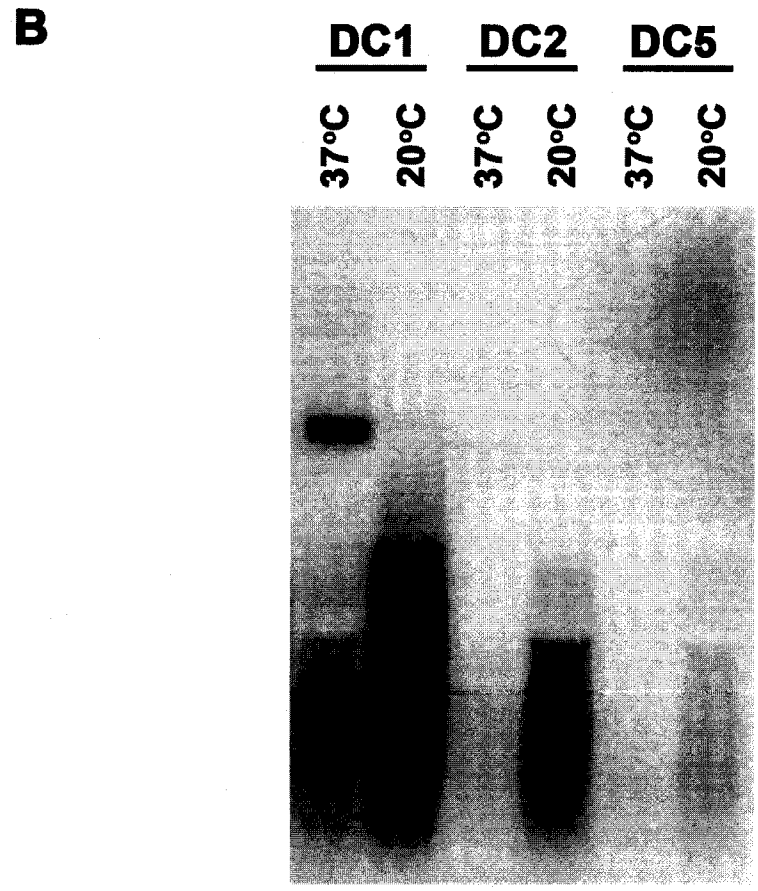

Transcript and protein analysis of the DC1 promoter deletion construct showed a difference in transcript and protein accumulation levels during the temperature downshift, compared to promoter deletion constructs DC2 – DC4. This was surprising because deletions DC1 – DC4 all contain the full-length *crhC* promoter. Although DC1 expression is still temperature-dependent, there is an increase in the overall transcript and protein levels observed at both 20°C and 37°C (Figure 3.16A and B). Promoter deletion construct DC1 contains the full-length *crhC* gene including 363 bp of upstream sequence, which is not present in DC2. This 363 bp upstream sequence may contain an enhancer element or it is possible that the upstream *hupE* gene has a polar effect on *crhC* expression, explaining why an overall increase in *crhC* expression is observed at both 37°C and 20°C. Although interesting, this observation was not pursued.

3.1.11 Promoter Luciferase Assays

In order to determine if temperature-dependent regulation of *crhC* was conveyed solely by the *crhC* promoter, transcriptional reporter fusions were constructed to determine if the *crhC* promoter and/or individual motifs could convey differential expression to the *lux* reporter gene. To clone individual portions of the *crhC* promoter, an array of primers were designed with various restriction sites inserted at the 5' end, to assist in cloning (Table 2.2). Following PCR amplification and digestion with the appropriate restriction enzymes, the promoter fragments were cloned into the pNLP10 vector, upstream of the *luxCDABE* genes (Figure 3.17A). Based on the results observed in Section 3.1.8, two *crhC* promoter motif regions were cloned; the sequence containing both the AT-rich element and -10 region (154 bp) (Figure 3.17C) and the sequence containing only the AT-rich element (39 bp) (Figure 3.17B), creating constructs pJBp2 and pJBp1 respectively (Table 2.5). To analyze sequence upstream and downstream of the promoter and to determine the strength of the *crhC* promoter, pJBp3 and pJBp4 were also constructed. pJBp3 contains the majority of the *crhC* promoter (lacking 8 bp upstream of the +1 transcription start site) including ~313 bp of upstream sequence (371 bp) (Figure 3.18B), inserted upstream of the pNLP10 *lux* operon (Figure 3.18A). pJBp4 contains the full-length *crhC* promoter (plus upstream sequence), 5' UTR, and 11 bp into the ORF (lacks the 3' stem-loop structure of the 5' UTR (Section 3.2)) (511 bp) (Figure

Figure 3.17. Strategy to transcriptionally fuse *crhC* promoter motifs upstream of the *lux* reporter gene. Panel A shows the pNLP10 cloning vector used to make *crhC* promoter transcriptional fusions to the *lux* operon. Panel B illustrates the 39 bp sequence of the AT-rich element (*JB20:JB21*) cloned into the BamH I site of pNLP10, creating pJBp1. Panel C shows the 154 bp sequence containing both the AT-rich element and the -10 region (*JB18:JB19*) of the *crhC* promoter, cloned into the EcoR I site of pNLP10, creating pJBp2. The 5' and 3' restriction sites used for cloning are underlined in orange with the mutated/ additional basepairs shown in orange letters. The AT-rich element is shown in blue and the -10 region shown in green. The sequence was numbered according to its location with respect to the transcription start site (+1).

A

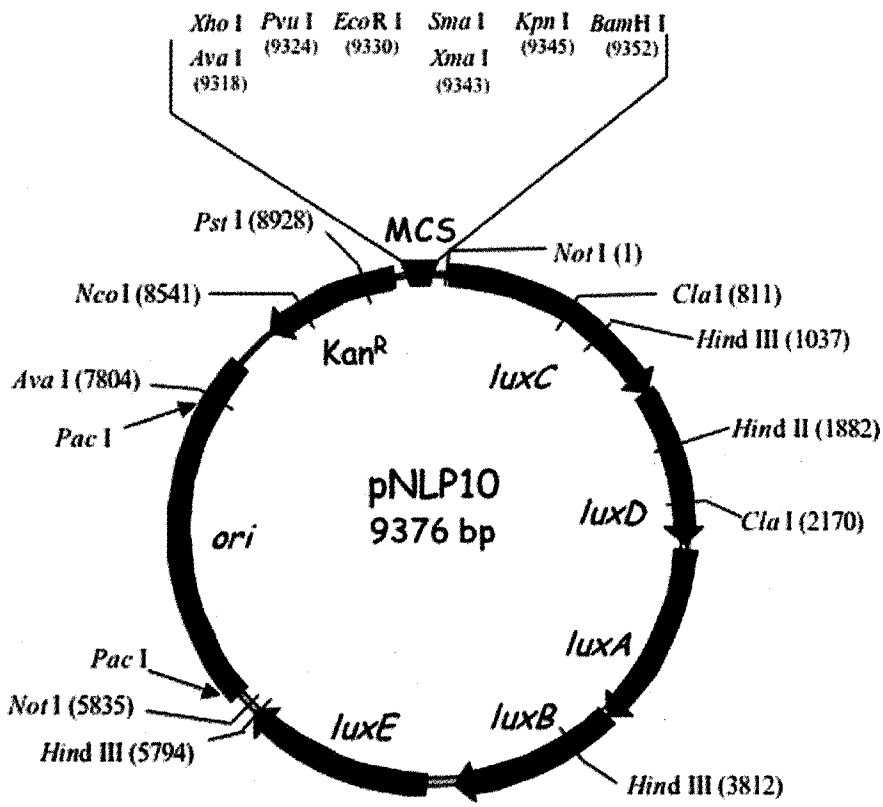

B AT-rich element (*JB20:JB21*) (pJBp1)

-71 GGATCCAACT ATTAATATTA AAGTTTAGAG AAAGGATCC -42
BamHI BamHI

C

AT-rich element and -10 region (*JB18:JB19*) (pJBp2)

EcoRI
-153 GAATTCTTTA GGGGCTGGTA ATTTTTAACA TATCTCACGG GGTGCAATCT -104

-103 TCGCGCCCCT ACTAGTCCAT CGAATCGTCA TTTCCAACTA TTAATATTAA -54

-53 AGTTTAGAGA AATTGGATTA TATGTAACCT GTACTCTGTT AAGATTCAGA -4

-3 ATTC +1
EcoRI

Figure 3.18. Generation of promoter transcriptional fusion constructs containing the *crhC* promoter or the *crhC* promoter including a portion of the 5' UTR, fused to the *lux* reporter gene. Panel A shows a schematic diagram of the regions of the *crhC* promoter and/or 5' UTR cloned into the pNLP10 vector, upstream of the *lux* operon. Panel B illustrates the 371 bp sequence of the *crhC* promoter (*JB1:JB15*) lacking the transcriptional start site, cloned into the BamH I site of pNLP10, creating pJBp3. The 5' and 3' restriction sites used for cloning are underlined in orange with the mutated basepairs shown in orange letters. The AT-rich element is shown in blue and the -10 region shown in green. Panel C illustrates the 511 bp sequence of the full-length *crhC* promoter, 5' UTR and 11 bp of the ORF (lacks 3' stem-loop structure of 5' UTR) (*JB1:JB2*) cloned into the BamH I site of pNLP10, creating pJBp4. As shown in panel A, the 5' and 3' restriction sites are underlined in orange with the mutated basepairs shown in orange letters. The AT-rich element is shown in blue, the -10 region in green, and the cold shock box in yellow. The transcription start site (+1) is shown in red with a red asterisk, the Shine-Dalgarno sequence is underlined in black, and the translation start site (ATG) shown in red italics. For both panel A and B, the sequence was numbered according to its location with respect to the transcription start site (+1).

A

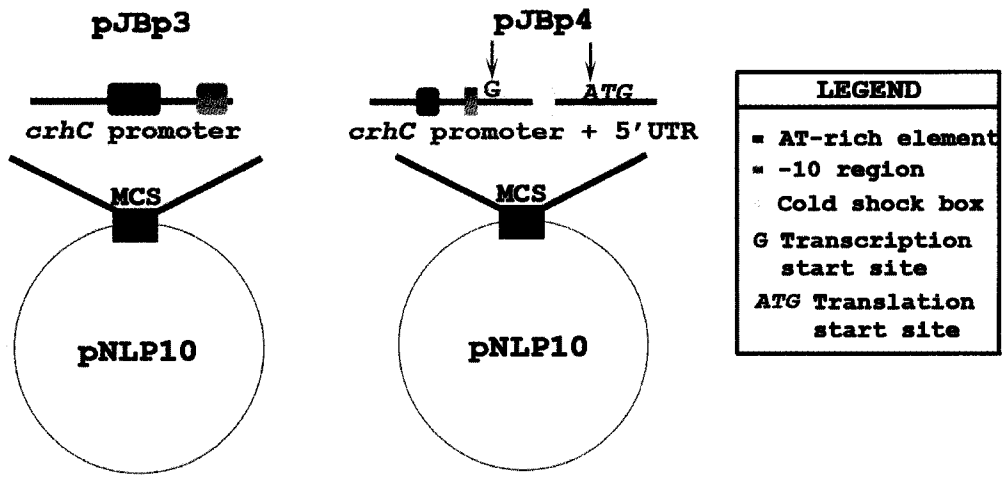

B *crhC* promoter (*JB1:JB15*) (pJBp3)

Bgl II

-379 AGATCTTGGG AGCGATCGCT GGTTTGTTGC AAGGCTACGT TTCTGGACAA GCTATCAACG -320

-319 GGATTGATAT CATCTCCCTG CTTACCTATA CTTTAGGCTT CGGTTTAACT CAGTATGCAA -260

-259 TCGCCACTAG CACCAGACGA CTAGTTAGCG ATAGTCTATC CACCATTGTT CGTTTTGTAG -200

-199 GTTTTGCTTT TATAGCGATC GGTTTTGTAT TTTGCGGTAA CTTCATCAAT TTTTTAGGGG -140

-139 CTGGTAATTT TTAACATATC TCACGGGGTG CAATCTTCGC GCCCCTACTA GTCCATCGAA -80

-79 TCGTCATTTC CAACTATTAA TATTAAAGTT TAGAGAAATT GGATTATATG TAACCTGTAC -20

-19 TCTGTTAAGA TCT -9

Bgl II

C *crhC* promoter, 5'UTR and 11 bp into ORF (*JB1:JB2*) (pJBp4)

Bgl II

-379 AGATCTTGGG AGCGATCGCT GGTTTGTTGC AAGGCTACGT TTCTGGACAA GCTATCAACG -320

-319 GGATTGATAT CATCTCCCTG CTTACCTATA CTTTAGGCTT CGGTTTAACT CAGTATGCAA -260

-259 TCGCCACTAG CACCAGACGA CTAGTTAGCG ATAGTCTATC CACCATTGTT CGTTTTGTAG -200

-199 GTTTTGCTTT TATAGCGATC GGTTTTGTAT TTTGCGGTAA CTTCATCAAT TTTTTAGGGG -140

-139 CTGGTAATTT TTAACATATC TCACGGGGTG CAATCTTCGC GCCCCTACTA GTCCATCGAA -80

-79 TCGTCATTTC CAACTATTAA TATTAAAGTT TAGAGAAATT GGATTATATG TAACCTGTAC -20

-19 TCTGTTAAGA TTCACCATTG GGGTATTCGC TATCAGTCTT GGCGCTACTG CCCATCCCGC +40

+41 CCCTCAAACC TTTGTCCGTC CGCCTAAGAC TGATACCGCT ACTGG[illegible]TGTT +100

+101 ATATCTGGAG TTCTATGTCT TTTTCAGATC T +131

Bgl II

3.18C) also cloned into pNLP10, upstream of the *lux* operon (Figure 3.18A). The promoter transcriptional fusion constructs were transformed into *E. coli* DH5α and verified by DNA sequencing. Luciferase activity was then determined in quintuplet over a cold stress (20°C) time course (Section 2.7.1).

Preliminary data gathered from the luciferase assays was difficult to interpret due to a large degree of variability between constructs, temperature, sample times, days, and replicas. When interpreting the generated bar graphs, a large degree of variability arose due to the temperature parameters being tested. One critical parameter when trying to convey temperature-dependent expression to a reporter gene is that temperature downshifts are the variable within the experiment, producing uncontrollable changes in cellular metabolism, growth rate, and enzymatic activity (Phadtare *et al.*, 1999). These cellular changes make it difficult to attribute changes in luciferase activity due solely to conveyance by the DNA fragment being tested and not due to metabolic and enzymatic changes within the cell. For example, upon a temperature downshift in *E. coli* from 37°C (optimal) to 20°C (cold stress), all of the transcriptional fusion constructs and vector controls tested showed a rapid decrease in luciferase activity upon transfer to the cold. This dramatic reduction in luciferase activity after only a few minutes (5- 15 minutes) of cold shock suggests a cold-induced reduction in enzyme kinetics thereby reducing the overall enzymatic activity within the cell. Ideally, when attempting to convey cold-induced temperature dependence to *lux*, you would predict to observe an increase in luciferase activity upon cold treatment. However, due to an overall decrease in enzymatic and metabolic processes caused by reduced temperature, general cellular processes, including the expression of *lux,* are reduced. Therefore, for the purpose of this experiment, conveyance of temperature-dependent expression was evaluated by performing all assays on the same day in quintuplicate, and monitoring the overall luciferase activity pattern throughout a cold stress time course, in comparison to the 37°C optimal temperature control (0 minutes).

Luciferase assay variability may have also arisen due to plasmid copy number. Although low copy plasmids (pNLP10, pSIG16(lux$^-$)) were used (~ 3 copies/cell) for the generation of the transcriptional fusion constructs, they were not integrated into the

chromosome. The differences in plasmid copy number may have a multi-copy effect on the luciferase results, which may not directly reflect what is happening *in vivo*.

To determine what increase in luciferase activity could be considered as indicative of differential expression, the full-length *crhC* gene (promoter, 5' UTR, ORF, and 3'UTR) was transcriptionally fused upstream of the *luxCDABE* operon, into Xho I/BamH I cleaved pNLP10 (Figure 3.17A), creating pJBm5 (Table 2.5). As shown in Figure 3.19, a 56% (2.3X fold) decrease in luciferase activity was observed for pJBm5 after the initial 10 minutes of cold stress at 20°C. After prolonged exposure to 20°C, a gradual increase in luciferase activity was observed, where after 180 minutes the luciferase levels were 1.2X greater than that observed at 37°C (0 minutes). The maximum cold induction of *lux* was observed after 360 minutes at 20°C, reaching activity levels 2.8X greater than observed at 37°C (0 minutes). Based on these results, cold-induced, temperature-dependent expression was considered conveyed to the *lux* reporter gene when the luciferase levels were greater then 2.8X of that observed at optimal growth temperatures (37°C). As a control, the pNLP10 vector was also assayed to detect background levels of luciferase activity (Figure 3.19).

The bar graph displayed in Figure 3.20B, shows the corrected luciferase activity (Section 2.7.1) when only the AT-rich element of the *crhC* promoter (pJBp1) was transcriptionally regulating *lux*. When compared to the pNLP10 vector control (Figure 3.20A), a similar pattern of luciferase activity was observed but the luciferase levels at 37°C (0 minutes) increased approximately 22X when the AT-rich element sequence was inserted. These results suggest that the AT-rich element processes weak promoter activity but more importantly, the overall luciferase pattern of pJBp1 mirrors the pNLP10 vector pattern. As demonstrated in Figure 3.20B, a 67% (3X fold) reduction in luciferase activity occurred following initial induction (15 minutes) of pJBp1 into the cold. After 210 minutes of exposure to 20°C, luciferase levels increased to 57% of that observed at 37°C (0 minutes), but never become equal to or greater than the 37°C (optimal temperature) levels. These results are indicative that the AT-rich element alone cannot convey temperature-dependent expression to *lux*.

The bar graph in Figure 3.20C shows the corrected luciferase activity versus cold stress exposure time for the transcriptional fusion construct pJBp2, containing the AT-

Figure 3.19. The full-length *crhC* gene conveys temperature-dependent expression to the *lux* reporter gene after prolonged exposure to low temperatures (20°C). Luciferase assays (Section 2.7.1) were performed on the pNLP10 vector (purple) (Figure 3.18) and the transcriptional fusion construct pJBm5 (blue), which contains the full-length *crhC* gene (pWM753R, 2424 bp) inserted upstream of the *lux* operon. The two constructs were grown at 37°C (0 minutes) till log phase and then cold shocked by transferring to a 20°C incubator for the times indicated. The generated luciferase activity data was used to plot a bar graph containing the corrected luciferase activity (cpm (construct) – cpm (LB medium)) / (OD_{600} (construct) – OD_{600} (LB medium)) versus the incubation time at 20°C. The standard deviation of each time point was determined from measurements performed in quintuplicate. The x-axis is not to scale.

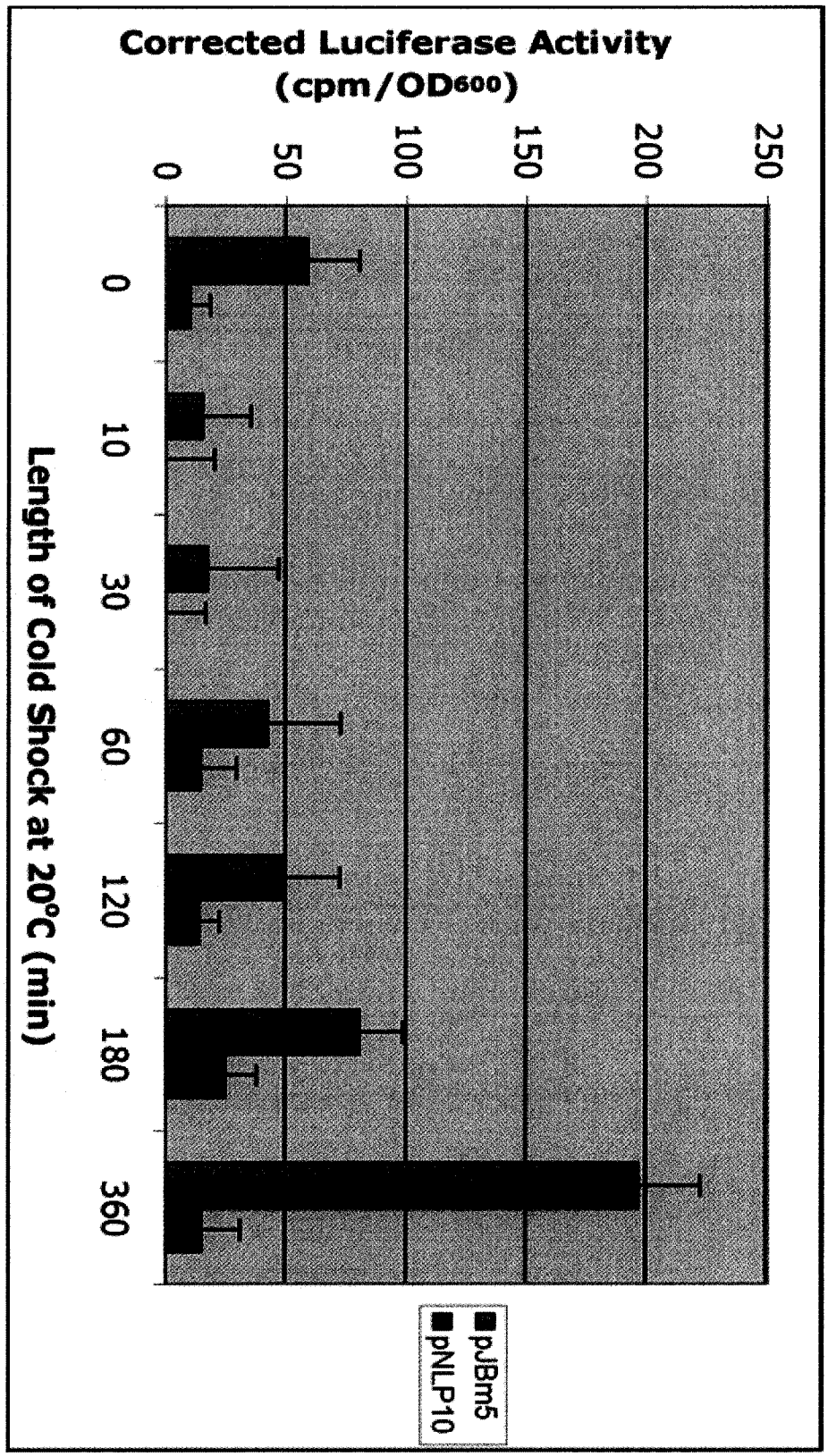

Figure 3.20. Motifs of the *crhC* promoter alone do not convey temperature-dependent expression to *lux*, in *E. coli*. Luciferase assays were performed as described in Section 2.7.1. The bar graphs show the corrected luciferase activity (cpm (construct) – cpm (LB medium)) / (OD_{600} (construct) – OD_{600} (LB medium)) of the vector control (pNLP10) and the various promoter motif transcriptional fusion constructs (pJBp1 and pJBp2) (Figure 3.18) versus the length of time (min) cold shocked at 20°C. The standard deviation of each time point was determined from measurements performed in quintuplicate. Panel A, pNLP10 vector control; Panel B, pJBp1, which contains the AT-rich element of the *crhC* promoter (39 bp); Panel C, pJBp2, which contains the sequence harboring the AT-rich element and the –10 region of the *crhC* promoter (154 bp). Note differences in the y-axis scale. The x-axis is not to scale.

A

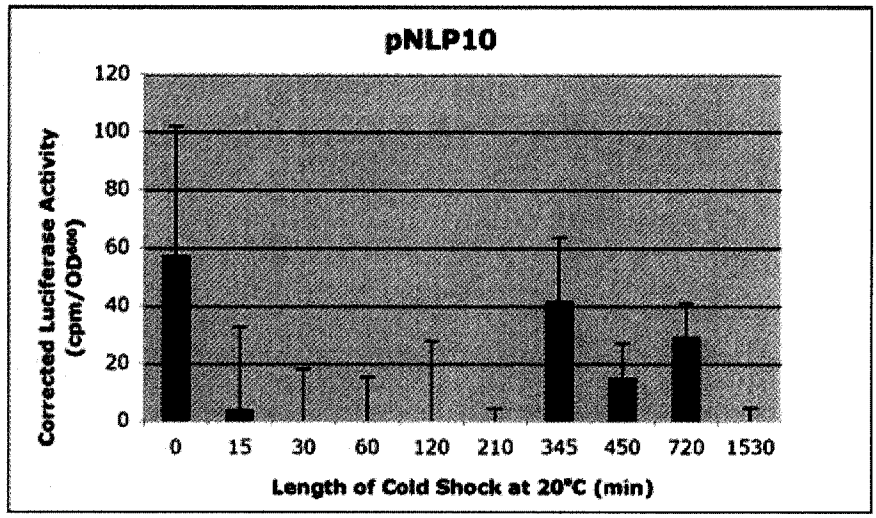

B

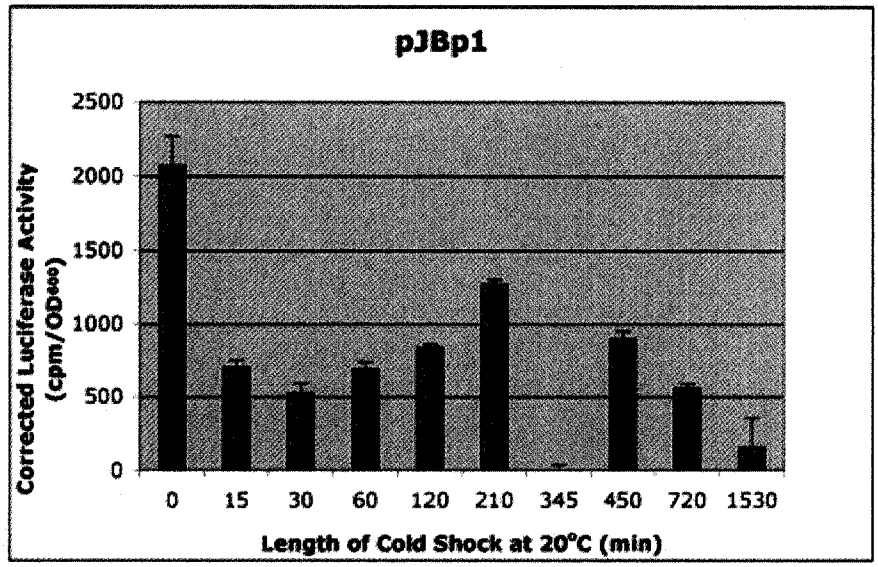

C

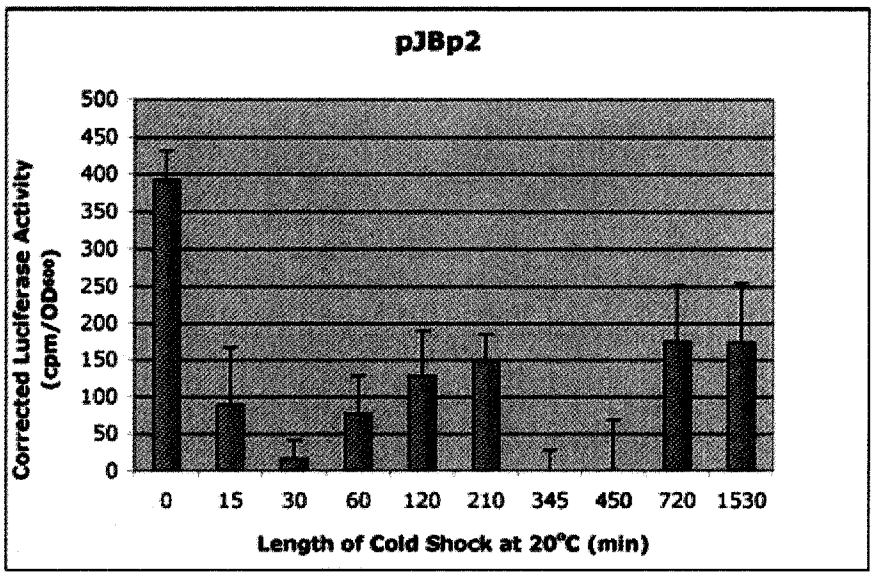

rich element and -10 region of the *crhC* promoter cloned into pNLP10. Compared to pJBp1 (Figure 3.20B) and pNLP10 (Figure 3.20A) levels, there is an approximate 5X fold decrease and 4X fold increase respectively, in the overall levels of luciferase activity at 37°C. These results suggest that the promoter sequence downstream of the AT-rich element (i.e. –10 region) decreases the strength of the promoter. From Figure 3.20C, it was also observed that following 15 minutes of cold stress there is a 62% (2.6X fold) decrease in luciferase activity, with levels remaining at least 41% less than those observed at 37°C (0 minutes). The AT-element and -10 motifs therefore, do not alone convey temperature-dependent expression to *lux* as no increase in luciferase activity above the 37°C levels was observed after prolonged exposure to the cold. In conclusion, although these promoter elements conveyed a basal level of promoter activity to the *lux* reporter gene, temperature-dependent promoter activity was not observed.

To determine if further upstream promoter sequence was required to convey temperature-dependent expression to *lux*, a 371 bp *crhC* promoter fragment (lacking 8 bp from the transcription start site) including 313 bp of upstream sequence from the AT-rich element (Figure 3.18B), was cloned into BamH I cleaved pNLP10, creating pJBp3 (Figure 3.18A). As illustrated in Figure 3.21B, a 66% decrease in luciferase activity occurred after cold shocking for 15 minutes and the activity levels remained relatively constant at this level for the remainder of the cold stress time course. Importantly, for the subsequent understanding of the regulatory process, a similar luciferase activity pattern was observed when the *crhC* promoter sequence was lengthened 138 bp downstream to include the transcriptional start site, 5' UTR, and 11 bp into the *crhC* ORF (contains only the 5' stem-loop structure of the 5' UTR) (Figure 3.18C), creating pJBp4 (Figure 3.18A). Again, cold stress decreased the luciferase activity of pJBp4 84% (6.3X fold) compared to the 37°C control (0 minutes) (Figure 3.21C). Luciferase activity levels remained relatively constant throughout the cold stress time course, with levels never exceeding 25% (210 minutes) of what was observed at the optimal growth temperature.

Comparing the luciferase levels of pJBp3 and pJBp4 to pNLP10 (Figure 3.21A) also demonstrated that the *crhC* promoter could convey promoter activity 11.4X or 10.6X greater than the promoterless *lux* operon in pNLP10. However, it appears that the *crhC*

Figure 3.21. The *crhC* promoter and/or the 5' stem-loop of the 5' UTR do not convey temperature-dependent expression to *lux*, in *E. coli*. The bar graphs show the corrected luciferase activity (cpm (construct) – cpm (LB medium)) / (OD_{600} (construct) – OD_{600} (LB medium)) of the vector control (pNLP10) and the various promoter transcriptional fusion constructs (pJBp3 and pJBp4) (Figure 3.19) versus the length of time (min) cold shocked at 20°C. The vertical lines indicate the standard deviation of each time point, performed in quintuplicate. Panel A, pNLP10 vector control; Panel B, pJBp3, which contains 371 bp of upstream sequence including the majority of the *crhC* promoter, lacking 8 bp adjacent to the transcription start site; Panel C, pJBp4, which contains the full-length *crhC* promoter, 5' UTR and 11 bp into the *crhC* ORF (511 bp). Due to the length into the ORF, pJBp4 only contains the 5' stem-loop structure of the 5' UTR (Section 3.2). Note differences in the y-axis scale. The x-axis is not to scale.

A

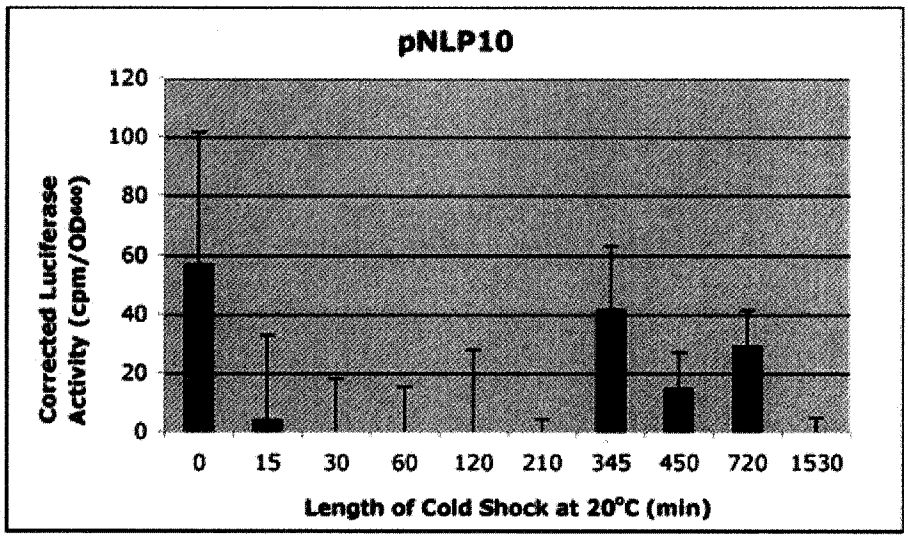

B

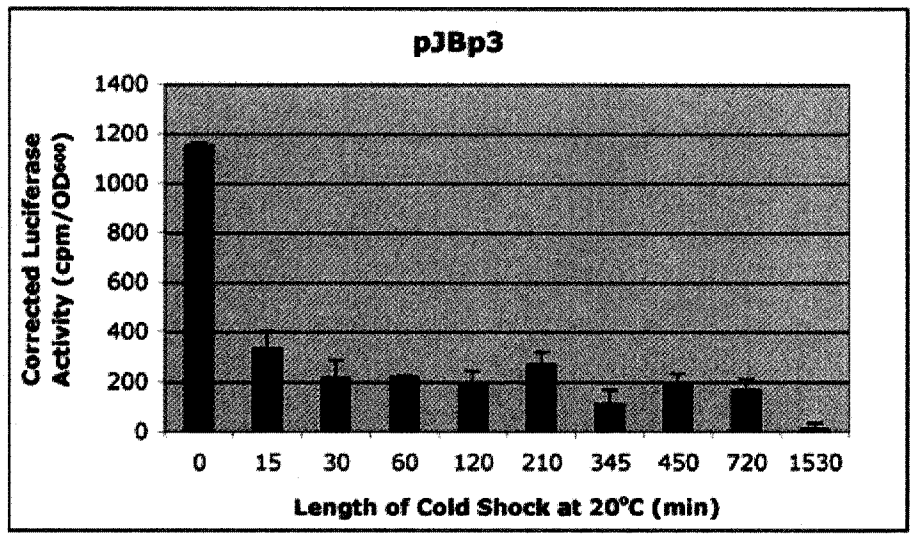

C

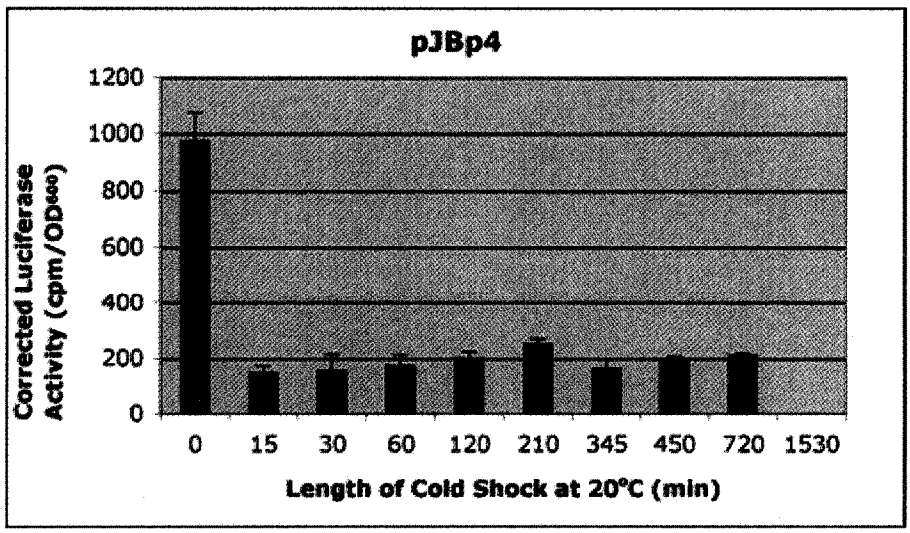

promoter is fairly weak in comparison to the strength of other known *E. coli* promoters (for example, pSIG11) (Figure 3.22)

Overall, it was concluded that the *crhC* promoter, including both upstream and downstream sequence to 11 bp into the ORF (only included the 5' stem-loop structure of the 5' UTR), could not convey temperature-regulated expression to the *lux* reporter gene. Surprisingly, the promoter transcriptional fusion results indicated that the *crhC* promoter was not the major regulatory element providing temperature-dependent transcriptional regulation of *crhC* or *lux* in response to temperature, suggesting the involvement of a hierarchy of regulatory mechanisms.

3.2 POST-TRANSCRIPTIONAL REGULATION of *crhC*

The inability of the *crhC* promoter motifs or the full-length *crhC* promoter to convey temperature-dependent expression to *lux* suggested that *crhC* expression is regulated at multiple levels. Previous work in our lab demonstrated that the transcript half-life of *crhC* increased significantly during growth of *Anabaena* at reduced temperature (20°C) suggesting, that the *crhC* transcript is stabilized in the cold (Chamot and Owttrim, 2000). In support, mRNA stability has also been shown to be a key regulator in the temperature-dependent expression of CspA, the major cold shock protein in *E. coli* (Yamanaka *et al.*, 1999; Goldenberg *et al.*, 1996). Sequence analysis of CspA and most other cold shock genes identified unusually long (between 100 - 250 bp) 5' untranslated regions (UTR), believed to convey mRNA stability during cold stress. Examination of *crhC* identified a long, 115 bp 5' UTR which prompted further investigation into the role of mRNA stability in the temperature-dependent differential expression of *crhC* (Chamot and Owttrim, 2000; Chamot *et al.*, 1999).

The involvement of post-transcriptional regulation via the 5' UTR providing temperature-regulated *crhC* expression was first examined by construction of the plasmids pJBm1 and pJBm2 (Table 2.5) from the pSIG16 and pSIG11 vector backbones, respectively (Figure 3.22A). By removing the *lux* operon to create pSIG16(lux$^-$) and pSIG11(lux$^-$) (Table 2.5), the vectors' strong and medium strength *E. coli* constitutive promoters were exploited to provide constitutive transcriptional regulation to the *crhC* gene, in the absence of its own promoter. Using PCR amplification (*JB5*:*JB6*) (Table

Figure 3.22. *crhC* 5' UTR and ORF under the transcriptional control of a strong constitutive promoter in *E. coli*. Panel A shows the vector map of pSIG16, which contains a strong, constitutive *E. coli* promoter in front of the *lux* operon. The pSIG16(lux$^-$) vector was constructed by a Not I digestion of pSIG16, to remove the *lux* operon. A 1664 bp *crhC* gene fragment (5' UTR, ORF, and 3'UTR), lacking its own promoter, was cloned into the pSIG16(lux$^-$) BamH I site, downstream of the constitutive promoter, creating pJBm1. Panel B illustrates the portion of the *crhC* gene including the 5' UTR and the 3' sequence of the *crhC* ORF and 3'UTR, cloned into the pSIG16(lux$^-$) vector. The 5' and 3' restriction sites used for cloning are underlined in orange with the mutated basepairs shown in orange letters. The transcription start site (+1) is shown in red with a red asterisk, the translation start site is indicated in red italics (ATG) and the translation stop site (TAA) is boxed in red. The cold shock box is shown in yellow, the downstream box in purple, and the Shine-Dalgarno sequence is underlined once in black. The Rho-independent terminator is indicated by inverted arrows and the cloned pBluescript KS+ sequence is underlined twice in black. The sequence between the two blue arrows illustrates the 5' UTR MFOLD query sequence used to predict the two stem-loop structures within the *crhC* 5' UTR. The sequence was numbered according to its location relative to the transcription start site (+1).

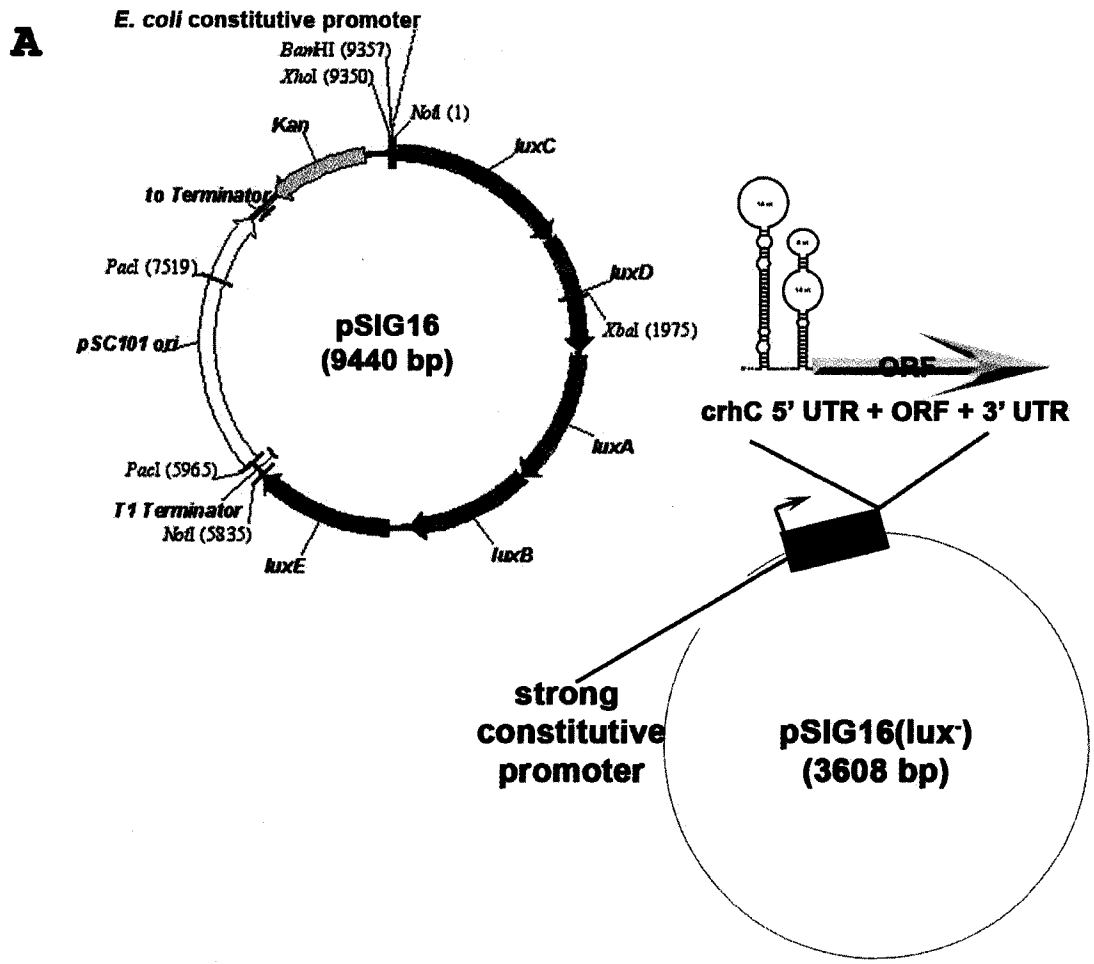

B *crhC* 5'UTR, ORF and 3'UTR (pJBm1)

BamHI

-12 GGATCCACCA TTGGGGTATT CGCTATCAGT CTTGGCGCTA CTGCCCATCC CGCCCCTGAA +48

+49 ACCTTTGTCC GTCCGCCTAA GACTGATACC GCTACTGG[illegible]T GTTATATCTG +108

+109 GAGTTCTATG TCTTTTTCTC ATCTCGGCTT GTCCAATGAA ATTATCAATG ..... +158

.....

+1387 AAAAAGGTAA TACGTACAAA AGAAAGTATG AAAAACTCTA CCCACAAGGG GGTAGAGTTT +1446

+1447 TCGGTAATGG GTAATGGGTA ATTTATGAGA GCCAAGATTA CTCAATCGTT AGTATGAGCG +1506

+1507 ATCGCTTTAG AAGGCTCCGA CTCTAGCGAC GATAACGTAA ATTGTTTACC CATCAGTAGG +1566

+1567 AGGTCGTATA GAGGATGCCG ATTATTTGAT ATTGCAAATG TAAATCTACT ATCTGTTCAA +1626

+1626 AGTTTTCACA TGAGAGCGTC CGTTGACGGT ATCGATAAGC TGATATCGAT TTCCTGCAGC +1653

CCGGGGGATC C

BamHI

2.2) and restriction enzyme digestion, the complete 1664 bp 5' UTR, ORF and 3'UTR (lacking its own promoter) (Figure 3.22B) of *crhC* was cloned into BamH I cleaved pSIG16(lux$^-$) (pJBm1) and pSIG11(lux$^-$) (pJBm2), downstream of the respective *E. coli* constitutive promoters (Figure 3.22A). Theoretically, if post-transcriptional regulation via the 5' UTR was not involved in the temperature-dependent expression of *crhC*, constitutive expression of *crhC,* regardless of the growth temperature, would be observed.

Western and Northern blot analysis of pJBm1 (Figure 3.23) and pJBm2 (data not shown) in *E. coli* demonstrated cold-induced temperature-dependent expression of *crhC* at both the transcript and protein level. Western blot analysis of pJBm1 *E. coli* protein lysates probed with anti-CrhC antibody, did not detect CrhC when grown at 37°C (Figure 3.23A, lane 2), compared to the promoter deletion construct DC1 cold stress control (Figure 3.23A, lane 1). Upon cold shocking at 20°C, a significant accumulation of CrhC was detected after 15 minutes (Figure 3.23A, lane 3); with protein levels continuing to increase with lengthened exposure to cold temperatures (Figure 3.23A, lanes 4 – 7). A similar cold-induced accumulation pattern was also found for *crhC* transcript levels. Northern analysis on pJBm1 RNA showed a dramatic increase in *crhC* transcript accumulation upon a temperature downshift from 37°C to 20°C (Figure 3.23B, lanes 1 and 2). The *crhC* transcript accumulated after only 5 minutes of exposure to cold stress temperatures (Figure 3.23B, lane 2), with the transcript levels remaining relatively constant as the exposure time increased (Figure 3.23B, lanes 3 – 8). The presence of a RNA smear, indicative of *crhC* transcript accumulation, is attributed to transcriptional run-on through the pSIG16(lux$^-$) plasmid, producing transcript and degradation products varying in length. In conclusion, these results demonstrated that even under the transcriptional control of a strong *E. coli* constitutive promoter, temperature-dependent expression of *crhC* still occurred. Overall, the results suggest the involvement of multiple levels of regulation, which primarily include post-transcriptional regulation perhaps mediated by the *crhC* 5' UTR.

To investigate if RNA secondary structure was providing transcript stability during cold stress, efforts were focused on the *crhC* 5' UTR region. The RNA secondary structure of the 5' UTR was predicted using the computer program MFOLD

Figure 3.23. Post-transcriptional regulation is involved in temperature-dependent *crhC* expression, in *E. coli*. Panel A shows the Western results for the constitutively expressed *crhC* gene (pJBm1) (Figure 3.22) after being cold shocked at 20°C for the times indicated (lanes 3 –7) or grown at 37°C (0 min, lane 2). 20 μg of *E. coli* (DH5α(pJBm1)) protein lysate was separated on a 10% SDS gel, transferred to a nitrocellulose membrane, and detected with polyclonal anti-CrhC antibody (1:5000). Cold shocked (20°C) promoter deletion construct DC1 (lane 1), which contains the full-length *crhC* gene (Figure 3.2), was used as a positive control for CrhC detection. Panel B shows the Northern results of total RNA (10 μg) isolated from the constitutively expressed *crhC* construct (DH5α(pJBm1)), cold shocked at 20°C for the times indicated (lanes 2 –8) or grown at 37°C (0 min, lane 1). RNA was separated on a 10% formaldehyde gel, transferred to a nylon membrane, and probed with a random primed *crhC* DNA probe (Nhe I/EcoR V cleaved pWM753, 390 bp) (Section 2.3.9.2).

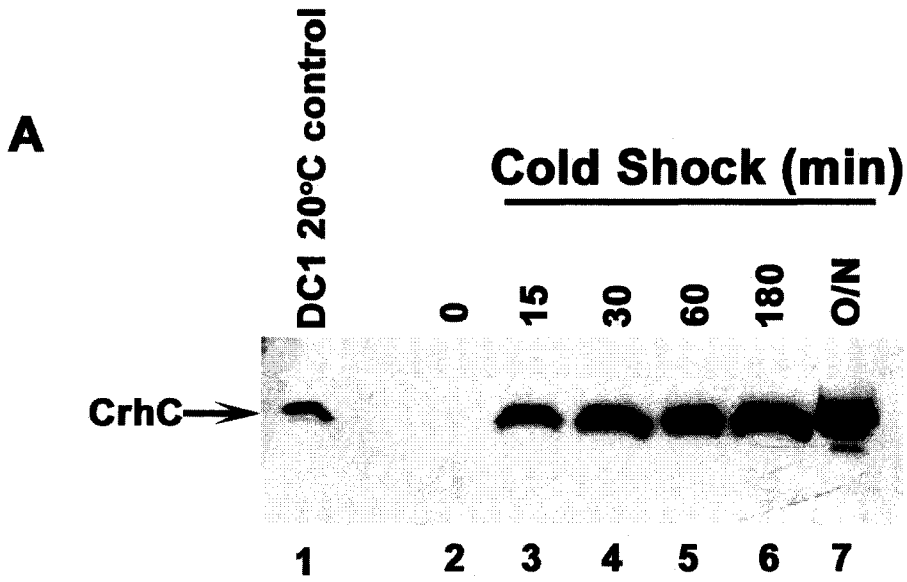

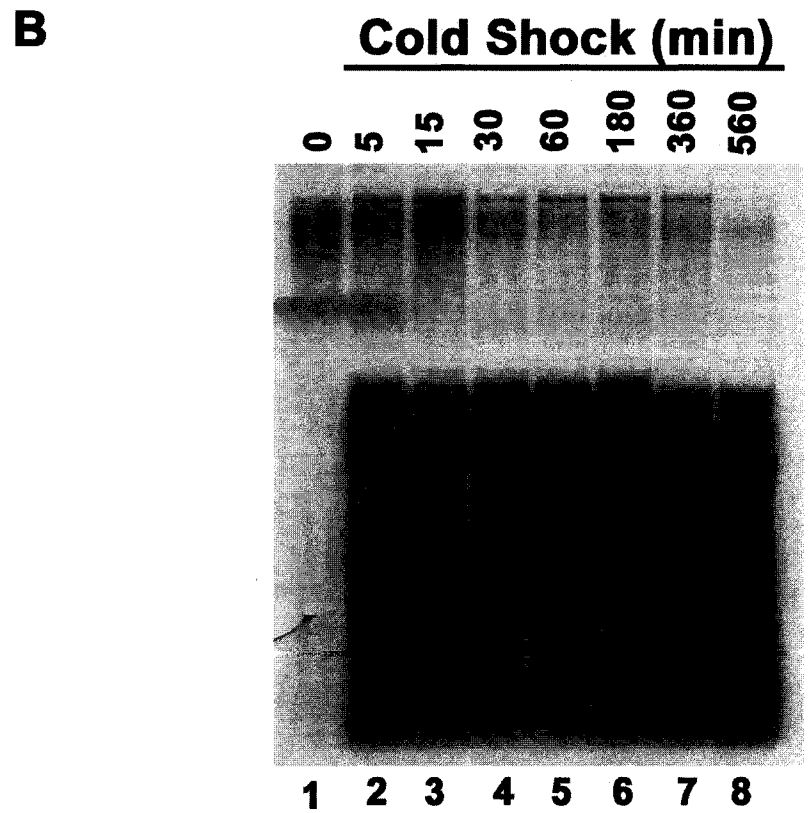

(http://bioweb.pasteur.fr/seqanal/interfaces/mfold-simple.html). A 141 bp 5' UTR sequence, starting from the transcriptional start site (+1) and ending 26 bp into the ORF, was used as the query sequence to identify two 5' UTR stem-loop structures with a ΔG of -42.9 kcal/mL and –49.1 kcal/mL, predicted to form at 30°C (optimal) and 20°C (cold stress) respectively (Figure 3.24 and Figure 3.25). It should be clearly noted, that it was necessary for the 5' UTR query sequence to contain at least 26 bp into the *crhC* ORF for both stem-loop structures to be observed in MFOLD. For example, if the query sequence was shortened to contain only 11 bp into the ORF, as utilized in the promoter-*lux* transcriptional fusion pJBp4, only the 5' stem-loop structure was observed (data not shown).

By altering the temperature parameters within MFOLD it was possible to visualize alternations in the 5' UTR stem-loop structures based solely on thermodynamics. At 30°C, the 5' stem-loop structure consisted of a 25 bp duplex stem with four small (2 – 4 nucleotide (nt)) internal loops and an 18 nt hairpin loop (Figure 3.24 and Figure 3.26A), with a ΔG of –22.6 kcal/mL. The 3' stem-loop consisted of a smaller 15 bp duplex stem with two internal loops, 2 nt and 14 nt in size, and an 8 nt hairpin loop, with a ΔG of -18.7 kcal/mol. The 5' stem has a 56% G - C content and displayed 24 Watson-Crick bonds and 1 wobble base pair (G-U). The 3' stem-loop contains all of the regulatory elements (indicated by colored boxes), with the stem having a 67% G – C content and displaying 12 Watson-Crick bonds and 3 wobble base pairings (G-U). Upon a temperature downshift, alterations in the 5' UTR secondary structure arose at temperatures ≤ 24°C, which is within the *Anabaena* cold shock range (Chamot *et al.*, 1999). The major changes in secondary structure predicted by MFOLD arose within the loop of the 5' stem-loop structure (Figure 3.25 and Figure 3.26B, indicated by the orange box). Between 25°C and 24°C, the 5' loop becomes constricted with a ΔG of –26.4 kcal/mL. The 5' hairpin loop present at 30°C (and 25°C) becomes a 7 nt junction loop with two smaller hairpin loops, 7 nt and 4 nt in size. The 5' duplex stem also shortens from 25 bp to 22 bp with only 3 small internal loops. No alterations were predicted within the 3' stem-loop structure where the majority of the regulatory motifs are located however, the ΔG increased to –21.1 kcal/mL. These results suggest that cold-induced alterations within the 5' UTR secondary structure may provide a regulatory

Figure 3.24. MFOLD predicted secondary structure within the 5' UTR of *crhC*, at 30°C. *crhC* sequence from the transcription start site (+1), through the 5' UTR and 26 bp into the ORF (141 bp total) was used to determine the RNA secondary structure of the 5' UTR, as predicted by MFOLD at 30°C. Important regulatory motifs are boxed in specific colors; the transcription start site (G) is in light blue, and the translation start site (ATG) is in red. The cold shock box is in yellow, the Shine-Dalgarno sequence in black, and the partial downstream box in purple.

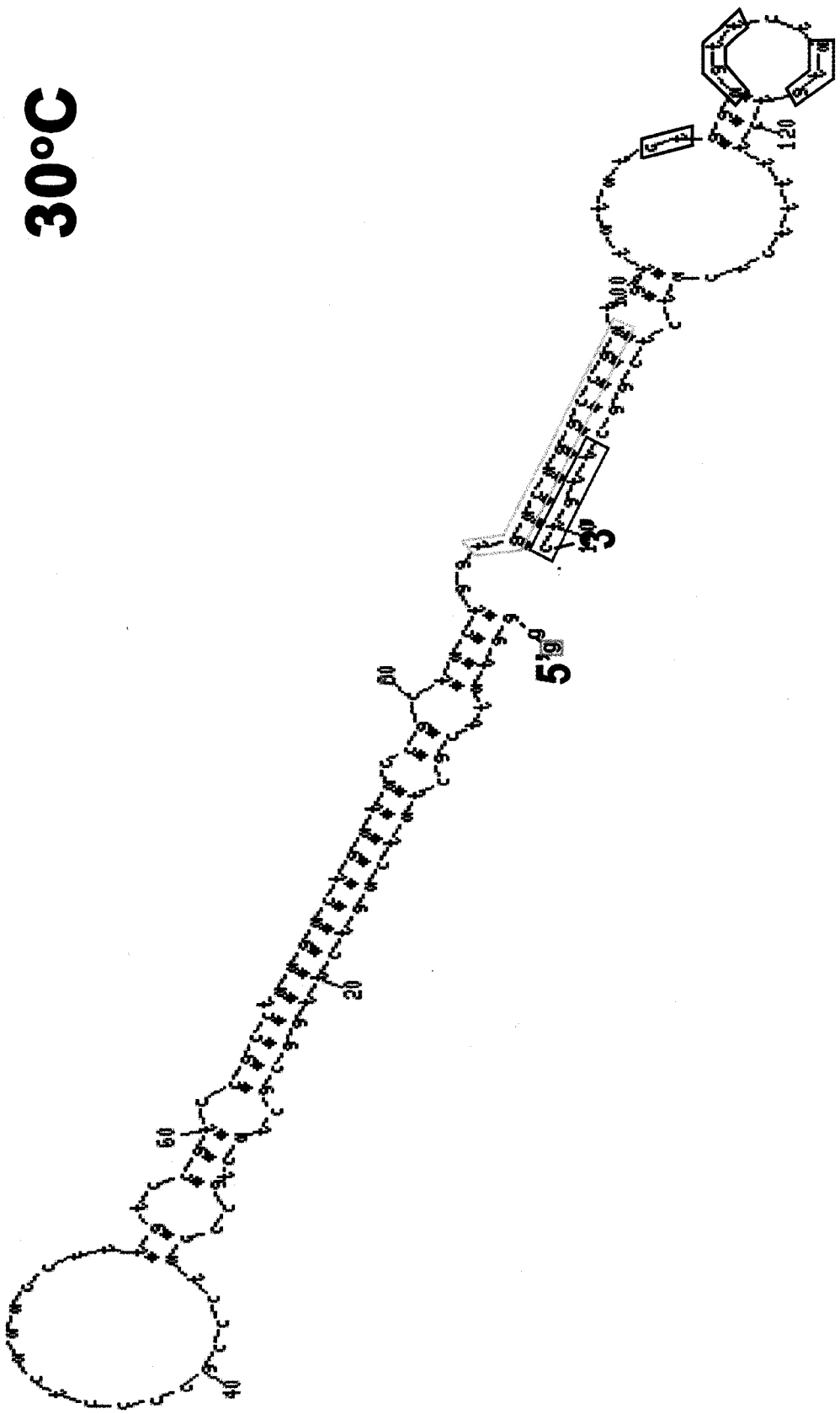

Figure 3.25. MFOLD predicted alterations in the *crhC* 5' UTR stem-loop structure during cold stress (≤ 24°C). *crhC* sequence from the transcription start site (+1), through the 5' UTR and 26 bp into the ORF (141 bp total) was used to determine the RNA secondary structure of the 5' UTR, as predicted by MFOLD at ≤ 24°C. Important regulatory motifs are boxed in specific colors; the transcription start site (G) is shown in light blue and the translation start site in red. The cold shock box is in yellow, the Shine-Dalgarno sequence in black, and the partial downstream box in purple. Alterations in the loop of the 5' stem-loop structure due to a temperature downshift is boxed in orange.

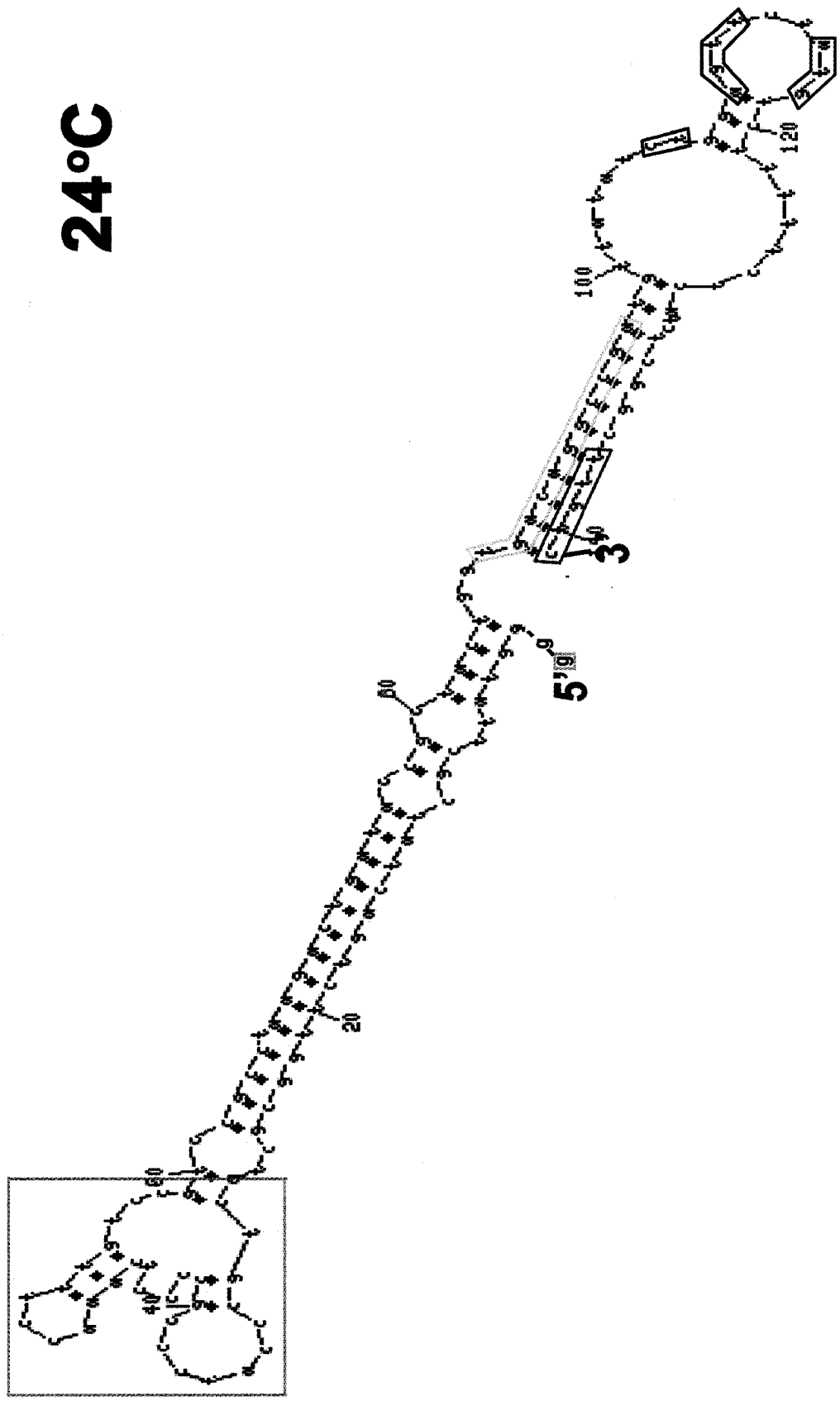

Figure 3.26. A schematic diagram of the *crhC* 5' UTR secondary structure as predicted by MFOLD, illustrates alterations within the loop of the 5' stem-loop structure upon a temperature shift from 30°C to 24°C. Panel A shows the *crhC* 5' UTR secondary structure at 30°C. The 5' stem-loop consists of a 25 bp stem and an 18 nt loop. The 3' stem-loop consists of a 15 bp stem and two loops, 14 nt and 8 nt in size. Panel B shows the 5' UTR secondary structure at ≤24°C (cold stress). Compared to panel A, the loop of the 5' stem-loop is constricted to 7 nt, with two protruding hairpin structures, 7 nt and 4 nt in size. The approximate regions of the regulatory motifs are indicated with colored boxes; the transcription start site (+1) is shown in light blue and translation start site is boxed in red. The cold shock box is boxed in yellow, the Shine-Dalgarno sequence in black, and the partial downstream box in purple. Temperature-induced alterations in the 5' UTR RNA secondary structure are indicated by the orange box.

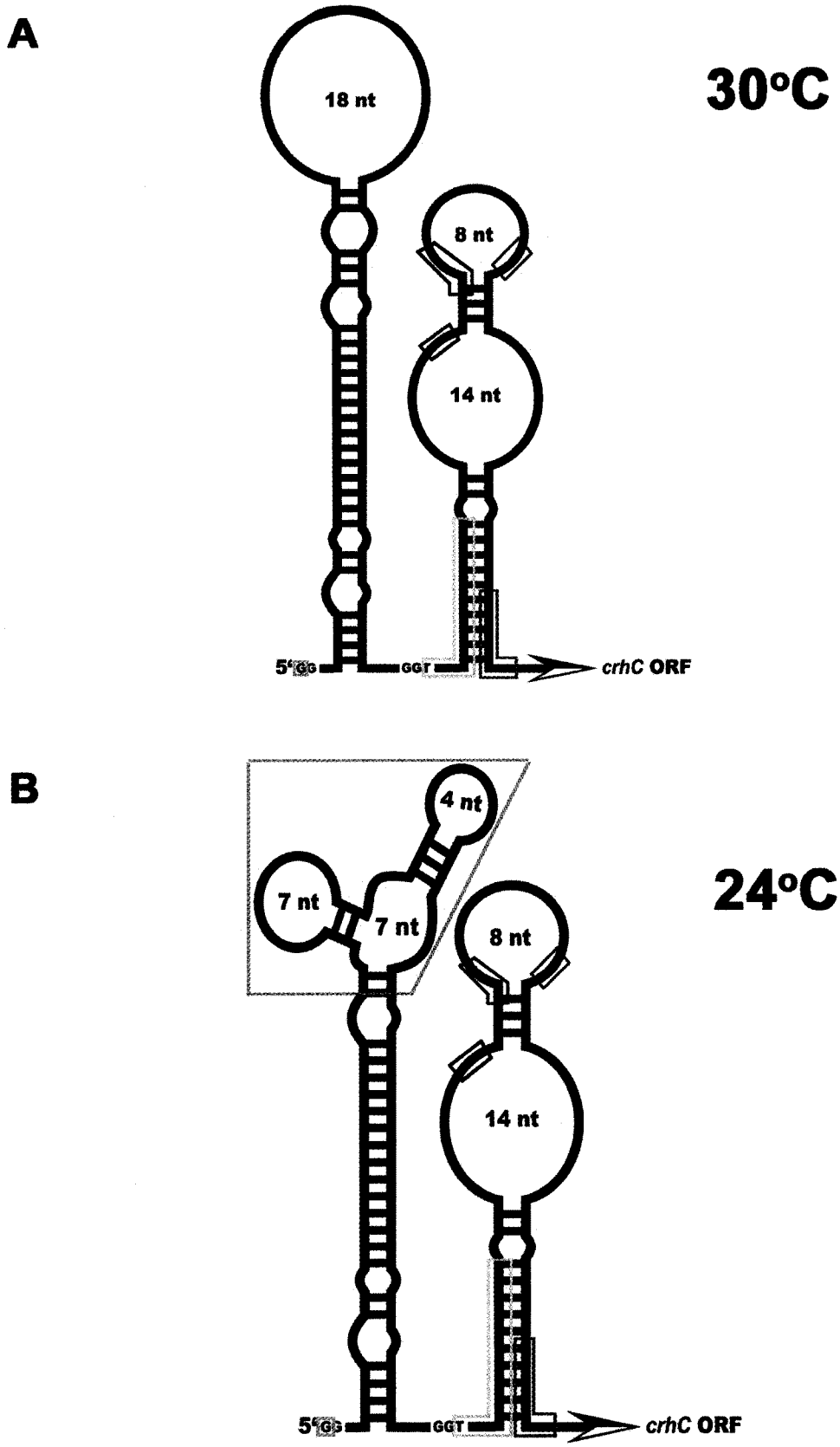

mechanism for differential expression of *crhC*, by conveying mRNA stability at cold stress temperatures and by destabilizing the transcript at optimal growth temperature.

3.2.1 5' UTR Luciferase Assays

In order to determine if temperature-dependent expression of *crhC* is regulated post-transcriptionally via mRNA stability conveyed by the 5' UTR, transcriptional reporter fusions were constructed to determine if the 5' UTR stem-loop structures could convey temperature-dependent expression to *lux*. Plasmids pJBm3 and pJBm4 (Table 2.5) were constructed by cloning both of the 5' UTR stem-loop structures (*JB5:JB22*) (Figure 3.27B) or only the 3' stem-loop structure (*JB23:JB22*) (Figure 3.27C) respectively, into pSIG11. The 5' UTR stem-loop structures were cloned between a medium strength *E. coli* constitutive promoter and the *lux* operon (Figure 3.27A). The constitutive promoters (pSIG11 and pSIG16) were made using the native *E. coli* sigma (σ) 70 sequence and random primers to generate a degenerate σ^{70} sequences, which varied in promoter strength from the wildtype (Mike Surette, unpublished). If the 5' UTR was involved in post-transcriptional regulation, an increase in luciferase activity upon cold stress would be expected as a result of stabilization of the *lux* transcript by the *crhC* 5' UTR.

The 5' UTR-*lux* transcriptional fusion constructs were grown to exponential phase (37°C) and subjected to identical cold stress conditions as those performed in the promoter luciferase assays (Section 3.1.11). As illustrated in Figure 3.28, a dramatic decrease in luciferase activity was observed for pSIG11, pJBm3, and pJBm4, following transfer to reduced temperature (20°C). These results are similar to those observed for luciferase activity patterns produced by the promoter transcriptional fusion constructs shown in Figure 3.20 and 3.21. Although the exact reason(s) for high levels of luciferase activity at 37°C is not know, these results may indicate that the *lux* portion of the mRNA may stabilize the transcript at high temperatures, as a similar result was found with a *cspA-lacZ* fusion (Goldenberg *et al.*, 1996). The drastic decrease in luciferase activity following cold-induction may again be due to an overall drop in cellular enzymatic and metabolic processes (Section 3.1.11). Therefore, to interpret the ability of the 5' UTR to convey temperature dependence to *lux*, it is important to analyze the overall pattern of

Figure 3.27. Generation of 5' UTR transcriptional reporter fusion constructs by cloning various *crhC* 5' UTR stem-loop structures into pSIG11. Panel A demonstrates where the 5' UTR stem-loop structures were cloned into pSIG11, between the medium-strength *E. coli* constitutive promoter and the *lux* operon. Panel B shows the amplified sequence (*JB5:JB22,* 274 bp) used to clone both (5' and 3') 5' UTR stem-loop structures into BamH I cleaved pSIG11, creating pJBm3. Panel C shows the amplified sequence (*JB23:JB22*, 191 bp) used to clone only the 3' stem-loop structure of the 5' UTR into BamH I cleaved pSIG11, creating pJBm4. The 5' and 3' restriction sites used for cloning are underlined in orange with the mutated basepairs shown in orange letters. The transcription start site (+1) is indicated in red with a red asterisk and the translation start site (ATG) is italicized in red. The cold shock box is shown in yellow, the Shine-Dalgarno sequence underlined in black, and the downstream box shown in purple. An important internal Nhe I restriction site, used for riboprobe generation is boxed in black.

A

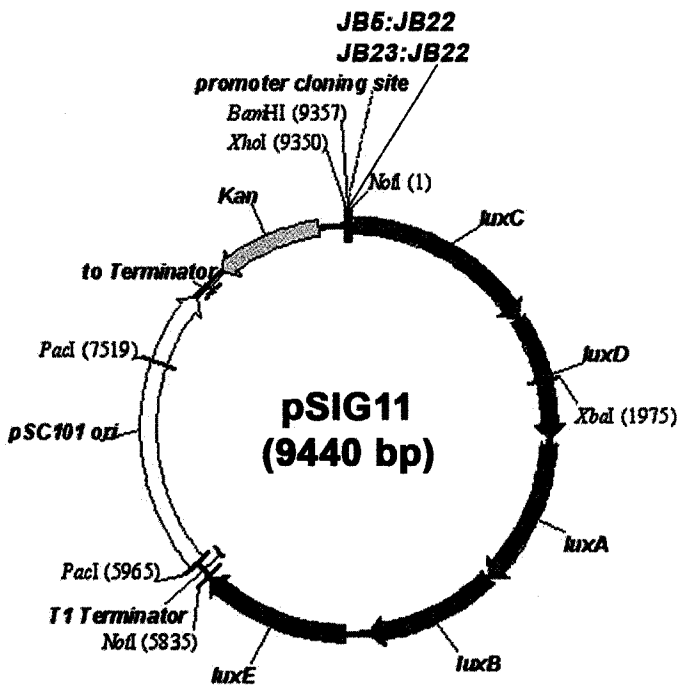

B both 5′UTR stem loop structures (*JB5:JB22*) (pJBm3)

BamHI

-12 GGATCCACCA TTGGGGTATT CGCTATCAGT CTTGGCGCTA CTGCCCATCC +38

+39 CGCCCCTCAA ACCTTTGTCC GTCCGCCTAA GACTGATACC GCTACTGGCG +88

+89 ACAGGCCGAT GTTATATCTG GAGTTCTATG TCTTTTTCTC ATCTCGGCTT +138

+139 GTCCAATGAA ATTATCAATG CTGTTACTGA GTTGGGGTAC ACCAAACCCA +188

+189 CACCCATCCA GATGCAGTCT ATTCCTGCTG TCTTATCAGG ACGAGATTTG +238

+239 CTAGCTGGCG CTCAAACTAG ATCT +262

NheI Bgl II

C 3′ stem loop structure only (*JB23:JB22*) (pJBm4)

BamHI

+72 GGATCCCGCT ACTGGTGACA GGCCGATGTT ATATCTGGAG TTCTATGTCT +121

+122 TTTTCTCATC TCGGCTTGTC CAATGAAATT ATCAATGCTG TTACTGAGTT +171

+172 GGGGTACACC AAACCCACAC CCATCCAGAT GCAGTCTATT CCTGCTGTCT +221

+222 TATCAGGACG AGATTTGCTA GCTGGCGCTC AAACTAGATC T +262

NheI Bgl II

Figure 3.28. Both the 5' and 3' stem loop structures of the *crhC* 5' UTR are required to convey temperature-dependent expression to *lux*, in *E. coli*. Luciferase assays were performed as described in Section 2.7.1 and the corrected luciferase activity (cpm (construct) – cpm (LB medium)) / (OD_{600} (construct) – OD_{600} (LB medium)) was plotted versus length of time at 20°C (cold stress), shown as a bar graph. Panel A, pSIG11 vector control; Panel B, pJBm4, which contains the 3' stem-loop structure only (*JB23:JB22*) of the *crhC* 5' UTR (Figure 3.27C); Panel C, pJBm3, which contains both the 5' and 3' stem-loop structures of the *crhC* 5' UTR (*JB5:JB22*) (Figure 3.27B). The vertical lines indicate the standard deviation of each time point, performed in quintuplicate. Note the differences in the y-axis scale. The x-axis is not to scale.

A

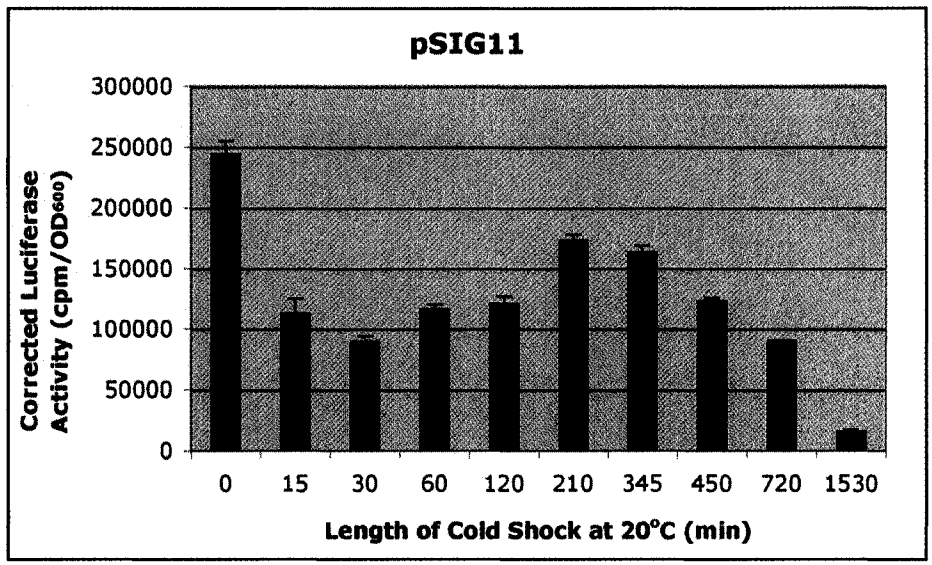

B

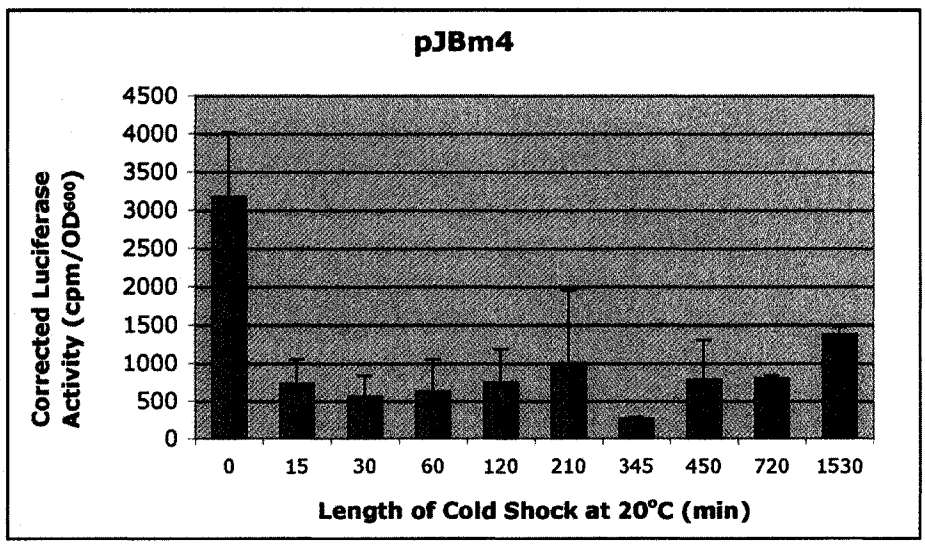

C

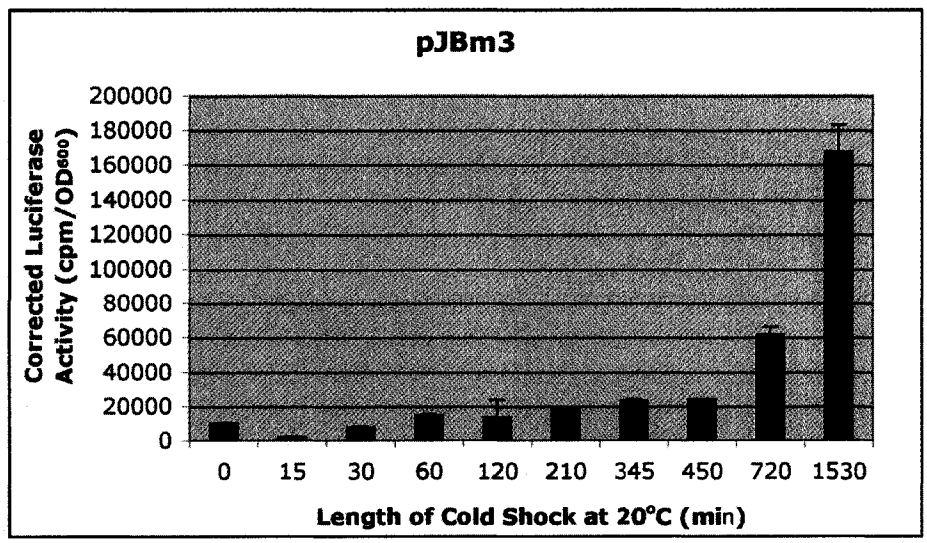

luciferase activity throughout the cold stress time course, in relation to the 37°C control (0 minutes).

The luciferase activity levels shown in Figure 3.28A are indicative of the strength of the *E. coli* constitutive promoter found in pSIG11. Compared to the *crhC* promoter (Figure 3.21C), the pSIG11 constitutive promoter is 237X stronger, supporting that the *crhC* promoter activity is relatively weak. Following cold treatment, the pSIG11 luciferase activity levels drop to 51% of that observed at 37°C (0 minutes), and remained constantly below the 37°C activity throughout cold stress. As illustrated in Figure 3.28B, when only the 3' stem-loop structure of the *crhC* 5' UTR (Figure 3.27C) was cloned between the pSIG11 constitutive promoter and the *lux* operon (pJBm4), no overall change in the luciferase activity pattern was noted throughout the cold stress time course (15 minutes – 1530 minutes) however, the luciferase levels were much lower. As expected, upon the initial cold stress induction (15 minutes), pJBp4 luciferase activity decreased 74% (3.8X fold) and remained between 51% - 93% (2.1X - 14.4X) less than the 37°C control (0 minutes). These results indicate that the 3' stem-loop structure of the *crhC* 5' UTR is unable to convey temperature-dependent expression to *lux*.

When both stem-loop structures of the *crhC* 5' UTR (Figure 3.27B) were cloned between the constitutive pSIG11 promoter and the *lux* operon (pJBm3), a dramatic change in the luciferase activity pattern was noted (Figure 3.28C). After 15 minutes of cold stress, a 78% (4.5X fold) decrease in luciferase activity was observed. Importantly, this was followed by an increase in luciferase activity with prolonged exposure to 20°C. The presence of both 5' UTR stem-loop structures produced a luciferase activity pattern that exceeded the 37°C control by 1.5X, after 60 minutes of cold stress. Luciferase activity continued to increase up to 18X greater than the 37°C control, after 1530 minutes at 20°C. In comparison, when the full-length *crhC* gene was transcriptionally fused to the *lux* operon only a 2.8X fold increase in luciferase activity was observed after an overnight exposure to 20°C (Figure 3.19). The cold-induced increase in pJBm3 luciferase activity suggests that the *crhC* 5' UTR does convey temperature-dependent expression to *lux* and that both stem-loop structures are required for *lux* transcript stability at 20°C. In addition, the contribution of mRNA stability conveyed by the 5'

UTR was significantly more important than transcriptional regulation by the *crhC* promoter, for temperature-regulated expression.

When the actual levels of luciferase activity were monitored (rather then the pattern) between the 5' UTR transcriptional fusion constructs and the pSIG11 vector control, vast changes in activity were observed. When comparing luciferase levels between pJBm3 and pJBm4, a 2.5X fold increase in luciferase activity was observed when both 5' UTR stem-loop structures were present (Figure 3.28B and C). This increase in luciferase activity suggests that the presence of both *crhC* 5' UTR stem-loop structures stabilizes the *lux* transcript, thereby increasing Lux protein levels. Interestingly, when comparing the luciferase activity of both pJBm3 and pJBm4 to the pSIG11 vector control, a decrease was noted when either of the 5' UTR stem loop structures were inserted. The luciferase activity level of the pSIG11 vector 37°C control (0 minutes) (Figure 3.28A) was 25X and 63X greater then when both of the 5' UTR stem-loop structures or only the second stem-loop structure were inserted, respectively. Although the exact reason is not know, the decrease in luciferase activity at 37°C when the 5' UTR sequences are inserted suggests that the presence of the stem-loop structures may destabilize the *lux* transcript at 37°C or, the 5'UTR inserts may decrease the strength of the constitutive *E. coli* promoter by increasing the secondary structure of the intergenic sequences, altering the transcription rate. It is also plausible that the presence of the *crhC* 5' UTR may also decrease translation thereby limiting the number of Lux products. Therefore, the next logical experiment would be to translationally fuse the 5' UTR in-frame with the *lux* operon to determine if the *crhC* 5' UTR has an effect on transcription and/or translation rates.

When comparing the corrected luciferase activity levels of pSIG11 to pJBm4 following overnight exposure to the cold, pSIG11 was observed to be 11.6X greater than pJBm4. However, when pSIG11 was compared to pJBm3 following an overnight exposure to the cold, pSIG11 activity was 10.7X less than the luciferase activity levels observed with pJBm3. The overall magnitude of luciferase activity observed at the various temperatures tested indicates: pSIG11warm (1.4X) > pJBm3 cold (10.7X) >> pSIG11 cold (1.7X) > pJBm3 warm (2.5X) > pJBm4 warm (2.7X) > pJBm4 cold. In conclusion, the 5' UTR insertion sequences may destabilize the *lux* transcript in the warm

therefore decreasing the overall luciferase levels at 37°C, compared to the pSIG11 vector control. However, following cold treatment the *lux* transcript is stabilized only when both 5' UTR stem-loops structures are present, increasing the overall luciferase activity at 20°C.

3.2.2 Potential Intrinsic Ribozyme Activity of the *crhC* 5' UTR

Recent literature has identified a post-transcriptional regulatory mechanism in which mRNA transcripts possess self-cleavage properties in the presence of an inducer molecule (Brantl, 2004). Winkler *et al.* (2004) identified the 5' UTR of the *glmS* transcript as a ribozyme, such that in the presence of the inducer metabolite GlcN6P, the *glmS* transcript auto-cleaves, acting as its own genetic switch. To determine if temperature could induce the *crhC* 5' UTR to self-cleave, preliminary ribozyme reactions were performed on the *crhC* 5' UTR (268 bp) at various temperatures (Section 2.6.4). Shown in Figure 3.29, ribozyme reactions were performed at 37°C, 30°C, and 20°C (cold stress), with natural self-cleavage being recognized by the presence of a distinct cleavage product(s). A no-reaction (NR) control (Figure 3.29, lane 5) was performed without any incubation, to represent uncleaved transcript. A 107 nt ssRNA control transcribed from pGEM3CS, was treated identically to the *crhC* 5' UTR, to monitor for contaminating RNase activity. As illustrated in Figure 3.29, lanes 1 to 4, the control RNA fragments are degraded completely, presumably due to variation in contaminating ribonuclease activity at the temperatures tested. For all the temperatures tested (Figure 3.29, lanes 2 - 4) a faint smear of small RNA fragments are observed compared to the ssRNA NR control (Figure 3.29, lane 1). These results suggest that the contaminating ribonucleases are completely and randomly cleaving some of the ssRNA, producing small RNA fragments, which are separated off of the gel. Compared to the ssRNA control, variations in the *crhC* 5' UTR cleavage patterns and kinetics were observed. As shown in Figure 3.29, lanes 6 to 8, distinct smears were observed at various temperatures, indicative of varying degrees of RNA degradation. The NR 5' UTR control (Figure 3.29, lane 5) contained essentially intact 5' UTR transcript due to the absence of a smear. Following incubation at 20°C (Figure 3.29, lane 6), little degradation of the 5' UTR was observed, indicated by the intensity of the intact transcript in the upper portion of the gel. These results suggest that

Figure 3.29. Preliminary evidence suggests that the *crhC* 5' UTR may have intrinsic ribozyme activity. The *crhC* riboprobe (268 bp) was transcribed from within the *crhC* 5' UTR and the ssRNA riboprobe control (107 nt) was transcribed from within the pGEM3CS vector (Section 2.6.3). The *crhC* riboprobe (lanes 6 – 8) and the 107 nt ssRNA control (lanes 2 – 4) were incubated in 1X Ribozyme Reaction buffer (Section 2.6.4) at 37°C and 30°C for 17 hours, and 20°C for 40 hours. A no-reaction (NR) control was also performed, in which no incubation period was allotted (lanes 1 and 5). The resulting reaction products were separated on a 10% denaturing PAGE gel, dried, and visualized by autoradiography.

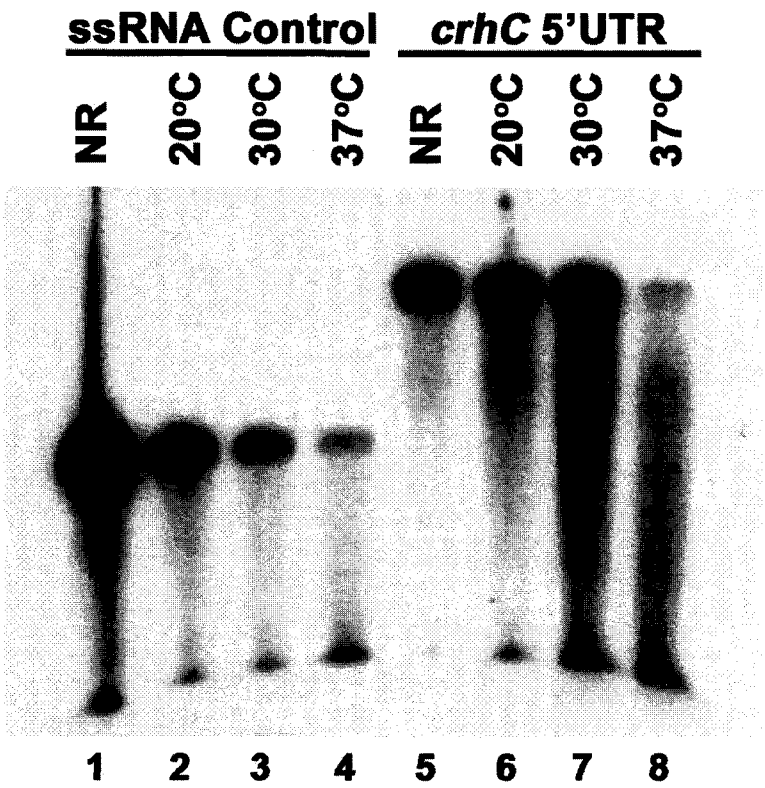

at 20°C, the *crhC* 5' UTR is significantly more stable and not specifically or randomly degraded as compared to 30°C (Figure 3.29, lane 7) or the ssRNA control. Incubation of the 5' UTR at 30°C (Figure 3.29, lane 7), showed cleavage products arrayed in size however, hints of specific degradation are present within the dark smear. These results suggest that partial degradation or specific cleavage of the 5' UTR may have occurred at 30°C, producing intermediate sized RNA fragments. Subsequent random cleavage by contaminating RNases would then produce the observed smear. Finally, the 5' UTR transcripts incubated at 37°C (Figure 3.29, lane 8) had the highest rate of degradation indicated by the presence of a smear. Although these results are preliminary, the initial results suggest that the *crhC* 5' UTR may have self-cleaving properties. The presence of intact 5' UTR at 20°C compared to the non-random degradation observed at 30°C potentially indicates that the *crhC* 5' UTR may be a ribozyme, initiating self-cleavage of the transcript at 30°C. Variations in the degradation rate observed at 30°C and 37°C is most likely due to the difference in contaminating RNase activity at the two temperatures. In conclusion, although distinct cleavage products were not observed, preliminary results suggest that the *crhC* 5' UTR may possess intrinsic ribozyme activity however further research is needed to confirm this exciting result.

CHAPTER FOUR
DISCUSSION

Bacterial growth at reduced temperatures results in major cellular constraints that are adjusted by the expression of a specific set of genes, the cold shock (CS) genes. The cold shock response in the cyanobacterium *Anabaena,* the model organism for this thesis, is induced following a temperature downshift of greater than 5°C, from its optimal growth temperature (30°C) (Chamot *et al.*, 1999; Yu and Owttrim, 2000). Although the majority of cold shock research has focused on the CS genes (*des*) involved in altering cell membrane fluidity, our lab has focused on a CS gene potentially involved in removing the block in translation initiation (Section 1.4.1.2). CrhC, a cold-induced RNA helicase from *Anabaena*, was proposed to alleviate inhibitions in translation initiation by unwinding stable RNA secondary structures formed at low temperature (Chamot and Owttrim, 2000; Yu and Owttrim, 2000).

To provide a better understanding of how cyanobacteria sense and respond to cold stress, the mechanisms by which temperature regulates *crhC* expression at the transcriptional and post-transcriptional level were investigated. Studies of CS gene regulation in *E. coli* and *B. subtilis* has identified several different regulatory mechanisms including transcription, mRNA stability, and/or translational control, required for temperature-dependent CS gene expression (Nickel *et al.*, 2004; Beckering *et al.*, 2002; Weber and Marahiel, 2002; Ramos *et al.*, 2001, Phadtare *et al.*, 2000; Fang *et al.*, 1998; Yamanaka *et al.*, 1998; Mitta *et al.*, 1997). Previous research in the Owttrim lab has also provided evidence for similar multi-level regulatory mechanisms (Chamot and Owttrim, 2000). Specifically, with respect to this thesis, temperature-induced regulation of transcription and mRNA stability of *crhC* at low temperature was observed, however the mechanism(s) by which these processes are regulated at the molecular level are not established.

Sequence analysis of the *crhC* gene upstream of the translation initiation region revealed several sequences related to known regulatory *cis*-elements found within *E. coli* CS genes. In *E. coli*, the AT-rich element and the cold shock box are known *cis*-acting elements involved in transcriptional regulation whereas translational regulation involves

the downstream box. In *E. coli*, the AT-rich element was shown to be a transcriptional enhancer whereas the cold shock box, a transcriptional attenuator (Fang *et al.*, 1998; Mitta *et al.* 1997). The downstream box was proposed to enhance translation initiation via interactions with the 16S rRNA (Mitta *et al.*, 1997). Previous sequence analysis detected related sequences in *crhC* (Chamot *et al.*, 1999). A putative AT-rich element was identified upstream of the -10 region and a putative cold shock box was found within the long 5' UTR of *crhC* (Chamot *et al.*, 1999). A putative downstream box was also located within the *crhC* coding region, containing complementary sequence to the 3' end of the *Anabaena* 16S rRNA (Chamot and Owttrim, 2000; Chamot *et al.*, 1999). The downstream box is postulated to enhance CrhC translation by increasing the formation of a more stable translation initiation complex between the 16S rRNA and the ribosome.

Like most *E. coli* cold shock mRNAs, *crhC* also has a long (115 bp) 5' UTR which may be involved in post-transcriptional regulation with respect to the observed enhancement of *crhC* transcript stability at low temperature (Chamot and Owttrim, 2000). Similar enhancement of mRNA stability by the 5' UTR of *cspA* has also been demonstrated (Yamanaka *et al.*, 1999; Goldenberg *et al.*, 1996). The presence of sequences within the *crhC* leader sequence known to regulate cold shock genes in *E. coli* prompted further investigation into whether these regions within the *crhC* promoter are involved in temperature-dependent gene expression.

4.1 Transcriptional Regulation of *crhC*

Native gel shift assays identified that a DNA-binding protein bound to the *crhC* promoter when incubated with protein extracts isolated from *Anabaena* cells grown at 30°C (optimal growth temperature). The absence of a DNA-binding protein in cells grown at 20°C (cold stress) together with the expression of CrhC during cold stress, suggests that the DNA-binding protein isolated at 30°C acts as a repressor of *crhC* transcription at optimal growth temperatures. These observations provide the potential for a *crhC* regulatory mechanism via a transcriptional repressor. At optimal growth temperature (30°C), repressor binding prevents the RNA holoenzyme from interacting with the transcriptional start site, and consequently inhibiting *crhC* transcription and expression. At reduced temperatures (20°C), the repressor may be modified and/or

down-regulated, preventing binding to the *crhC* promoter and thereby allowing *crhC* transcription to resume in response to cold stress. Modification appears to be the more likely scenario due to the rapidity with which *crhC* transcript accumulates in response to a temperature downshift and evidence presented in thesis indicating that cold-induced modification of the repressor occurs via phosphotransfer.

Several parameters appear to affect the DNA-protein complex formation in the EMSA binding reactions. The duration of complex formation appeared to be very short-lived and required adjustments in temperature (37°C), binding buffer composition (10 mM Mg^{+2}), gel concentration (8%, 10%, or 12%), and gel composition (TAE). Due to the sensitivity and rapid induction of CrhC upon cold stress, several precautions were taken to ensure a true 30°C (optimal) reaction. The interaction between the repressor protein and the *crhC* promoter was dependent on minimal to no exposure of the optimally (30°C) grown *Anabaena* cells to reduced temperature (which includes transferring to room-temperature). For this reason, all EMSA binding reactions were performed at the corresponding growth temperature of the culture of interest (20°C vs. 30°C). The native gels were also electrophoresed at 37°C to prevent cold-induced protein modifications (i.e. dephosphorylation) that may inhibit DNA binding (see below). The EMSA binding reactions were also optimized in 1X binding buffer containing a minimal amount (0 – 10 mM) of magnesium. High magnesium concentrations (> 15 mM) appeared to slightly decrease complex formation between the *crhC* promoter and the repressor protein. Similar results were observed by Tagashira *et al.* (2002), demonstrating that low levels of magnesium can enhance DNA-protein complexes by inhibiting magnesium-dependent base pairing between the overhangs of the target DNA. Base pairing of nucleotide overhangs could mask potential protein recognition sites thereby decreasing the capacity of complex formation. However, the ability of a weaker *crhC*-repressor complex to form in the presence of >15 mM of magnesium can be explained by the binding requirements for each DNA-binding protein. For example, the formation of the cAMP response element (CRE)-CERB complex requires 10 mM magnesium for stability and sequence-specificity (Moll *et al.*, 2002). It has also been previously shown that several nucleic acid binding proteins require magnesium ions for activity. The ability of the repressor protein to complex with the *crhC* promoter in the absence of magnesium ions suggests that

magnesium is not needed for DNA-protein interaction however, small amounts of magnesium were added for optimal binding.

Ionic strength, conducted by the native gel running buffer, also had a large affect on the repressor's ability to remain complexed with the *crhC* promoter. The inability of the DNA-protein complex to remain in the presence of 1X TBE running buffer suggests that the ionic strength of the TBE buffer may disrupt essential ionic bonds, destabilizing the *crhC*-repressor complex as observed for other DNA-protein complexes (Roder and Schweizer, 2001). The absence of a protein-bound shift in the presence of 1X TGE buffer (a high ionic buffer) also supports ionic-destabilization of the *crhC*-repressor complex (results not shown). It is also plausible that the repressor may assume two functionally different conformations as a result of the ionic environment. It has been demonstrated that borate ions have a potential to interact with proteins, which could induce a conformational change (Coss, 1966; Parker and Bearn, 1963). For example, Urh *et al.* (1995) demonstrated that some proteins could bind DNA independently in a TBE buffered system while exhibiting a high degree of cooperativity in TAE buffered system. Although the exact reason is not known, the ability of the repressor to bind to the *crhC* promoter only in the presence of 1X TAE suggests that the repressor may bind in a cooperative fashion. In the presence of borate ions (TBE), the repressor may undergo a conformational change inhibiting DNA interaction. Cooperative binding of the repressor to the *crhC* promoter may also be supported by the EMSA results indicating that repressor binding is concentration dependent. By way of positive cooperativity, the affinity of the repressor for the *crhC* promoter may increase depending on the amount of repressor protein already bound.

EMSA reactions were also undertaken to determine if the repressor bound specifically to the *crhC* promoter *in vitro*. Competition assays demonstrated that in the presence of unlabeled competitor DNA (cold *crhC* promoter), the repressor was titrated from the probe (hot *crhC* promoter). However, the inability of non-competitor DNA (cold *crhC* ORF sequence) to titrate the repressor protein from the probe indicates that repressor binding is specific for the *crhC* promoter sequence. EMSA reactions performed using protein extracts from several different optimally (30°C) grown cyanobacterial species (*Synechocystis*, *Synechococcus*, and *Anabaena*) also suggests that

the *crhC* promoter may have a common sequence that is recognized by similar cyanobacterial DNA-binding proteins. The various cyanobacterial DNA-binding proteins may have a common DNA binding domain with different relative affinities for the *crhC* promoter sequence. The ability of the *E. coli* crude lysate to form only a weak complex with the *crhC* promoter suggests that the DNA recognition sequence may be specific to cyanobacterial species and/or the *E. coli* DNA-binding protein may recognize an altered/different DNA binding sequence.

Overall, the above observations suggest that the *Anabaena* repressor protein binds specifically to the *crhC* promoter. The repressor protein does not appear to be unique to *Anabaena*, as potentially similar regulatory proteins appear to be common throughout the different cyanobacterial species. The presence of similar putative regulatory factors interacting with the same promoter sequence is intriguing from both a global and evolutionary perspective, suggesting a conserved and important role for both the repressor-like regulatory proteins and *crhC*-like regulatory genes during cold stress. Since a cold stress sigma (σ) factor has not been identified, it is plausible that the repressor interacting with the *crhC* promoter may regulate a family of cold shock promoters. Thus, cold shock gene transcription may be regulated by a repressor, with a general σ factor directing the RNA polymerase to the promoter in the absence of the repressor (20^{o}C).

The repressor DNA binding sequence was investigated using a series of nested deletions within the *crhC* promoter. EMSA reactions using *crhC* DNA targets varying in promoter length, delineated that the repressor bound upstream of the transcriptional start site. The degree of protein affinity for the promoter deletion sequences was dependent on the absence or presence of certain promoter regulatory elements. The presence of a 52 bp region surrounding the AT-rich element was required for maximum *crhC* promoter-repressor complex formation however, in its absence, a minimal amount of repressor binding still occurred as long as the -10 region of the promoter remained. Possible reasons for this are discussed below.

Evidence that the sequence surrounding the AT-rich element is important for repressor binding was also supported by the DNA-affinity chromatography results. Two DNA-binding proteins, 60 kDa and 65 kDa in size, were specifically and routinely

isolated using a DNA target encompassing the AT-rich and -10 elements of the *crhC* promoter. The repressor DNA recognition sequence is therefore found within this 52 bp region surrounding the AT-rich element, suggesting that the AT-rich element and -10 region may have an direct role in transcriptionally regulating *crhC* however, further evidence is needed to confirm this. Characterization of the two DNA-binding proteins would provide insight into upstream events regulating *crhC* and would also clarify exactly where and how the repressor(s) is binding to transcriptionally regulate *crhC*. Unfortunately, due to the inability to sequence the isolated proteins, these explanations are only speculative.

In vivo analysis of the *crhC* promoter deletion constructs' transcript and protein levels performed in a heterologous system, also provided insight into whether or not the AT-rich element was important for temperature-dependent transcriptional regulation of *crhC*. *E. coli* was chosen as the heterologous system to study *crhC* expression as it was previously demonstrated that cold-induced *crhC* transcript and protein accumulation was similar to that observed in *Anabaena* (Chamot and Owttrim, unpublished). The dramatic reduction of *crhC* transcript accumulation and protein levels following removal of the AT-rich element suggests that this element is important for *crhC* transcription; its presence is required either for promoter strength through interactions with the RNA polymerase (enhancer element) and/or provides temperature-dependent *crhC* expression, possibly through repressor binding.

Luciferase assays used to elucidate if the AT-rich element could convey temperature-dependent expression to the *lux* reporter gene demonstrated, that neither the full-length *crhC* promoter and/or the individual regulatory elements (i.e. AT-rich element) could convey temperature-regulated expression to *lux* in *E. coli*. These results demonstrate that the AT-rich element is not required for temperature-dependent expression of *crhC* but is required for transcription initiation. The AT-rich element possibly enhances transcription initiation similar to the *E. coli* AT-rich UP element, increasing the affinity of the C-terminal domain of the α-subunit for the promoter (Ozoline *et al.*, 2001). Promoter studies on the *E. coli cspA* gene also demonstrated similar results. The AT-rich element was not required for temperature-dependent *cspA* expression rather, it played an important role in efficient transcription initiation during

cold stress (Fang *et al.*, 1997; Goldenberg *et al.*, 1997; Mitta *et al.*, 1997). The presence of a repressor protein binding to the AT-rich element of the *crhC* promoter therefore provides a regulatory mechanism for efficient transcriptional control but is potentially only involved in fine-tuning the differential expression of *crhC* during cold stress.

When using a heterologous system (*E. coli*) to study gene regulation, questions arise with regards to differences in cellular components and/or regulatory mechanisms providing similar *crhC* expression profiles. EMSA results using *E. coli* protein extract demonstrated that the *E. coli* DNA-binding protein(s) did not complex as tightly to the *crhC* promoter as observed with the putative repressor found in *Anabaena*. The absence of an *E. coli* protein binding tightly to the *crhC* promoter suggests that temperature-dependent *crhC* transcription may not occur, or may occur differently in *E. coli*. Therefore, the mechanism(s) providing temperature-dependent *crhC* expression in *E. coli* may therefore occur post-transcriptionally.

In an effort to explain why two DNA-binding proteins were isolated using DNA-affinity chromatography and the ability of the repressor to bind in the absence of the complete *crhC* promoter (contains -10 region), we speculated that repressor activity is dependent on protein dimerization. This idea is not far fetched as some CSPs have been reported to form dimers *in vitro* (Yamanaka *et al.*, 2001; Mayr *et al.*, 1996; Makhatadze and Marahiel, 1994). It was hypothesized that at optimal growth temperature (30°C) and in the presence of the complete *crhC* promoter, the repressor binds as a protein dimer, interacting with the complete DNA binding sequence (surrounding the AT-rich element). In the absence of the complete *crhC* promoter, the repressor is still capable of binding to the minimal amount of promoter sequence however, only a portion of the repressor dimer can bind forming a weak DNA-protein complex. The small migration distance of the EMSA shifts, indicative of a large DNA-protein complex (i.e. dimer), supports this hypothesis. The isolation of two slightly different sized DNA-binding proteins capable of interacting with the *crhC* promoter may also indicate that other protein co-factors may be required for repressor binding, or that the DNA-binding protein is differentially modified (i.e. phosphorylation).

Better evidence for dimerized repressor binding was obtained from EMSA results using size-fractioned, optimally grown (30°C) *Anabaena* protein extracts. In correlation

with the DNA affinity chromatography results, if the repressor bound solely as a 60 kDa or 65 kDa monomer we would expect protein bound complexes to form only in the protein fractions between 30 – 100 kDa. Although this is true, the strongest shift was evident with proteins greater than 100 kDa, much larger then the monomeric proteins themselves. If homodimerization or heterodimerization was occurring we would expect a 120 kDa, 130 kDa, or a 125 kDa protein complex respectively, which would fractionate into the >100 kDa sample. Protein dimer DNA recognition also requires a small inverted palindrome sequence for binding (Baichoo and Helmann, 2002; Giraldo *et al.*, 1998; Lamb and McKnight, 1991). Sequence analysis of the *crhC* promoter region identified a 6 bp direct repeat (TATTAA) and 5 bp indirect repeat (TTAATATTAA), found within the AT-rich element, which may act as a putative binding site for the dimerized repressor however further evidence is need to confirm this. These results are not surprising as transcription factor dimerization is commonly found throughout prokaryotic and eukaryotic systems, playing a key role in gene regulation. Protein dimerization increases the cell's regulatory options by allowing small proteins to recognize large DNA sequences, creating dual functions, creating novel binding specificities, or by increasing DNA binding affinity (Lamb and McKnight, 1991). If the above hypothesis is true, questions still need to be addressed regarding the exact binding sequence of the repressor, the regulatory capabilities of the repressor when bound as a dimer or monomer, and how temperature affects dimerization.

In vitro protein modification by phosphorylation was investigated using CIP to determine if the repressor phosphorylation state had an affect on DNA-binding. EMSA reactions performed with CIP dephosphorylated proteins suggested that the repressor is active at 30°C due to a higher phosphorylation state. These results propose that a temperature-induced phosphotransfer mechanism may be in place to regulate repressor activity. Regulation of repressor activity via phosphorylation has been shown in the CpxA/CpxR two-component signal transduction pathway involved in regulating *E. coli* adhesion processes (Jubelin *et al.*, 2005; Dorel *et al.*, 1999). Induction of CpxA by high osmolarity, phosphorylates CspR which in turn negatively affects curli gene (*csgD*) expression (Jubelin *et al.*, 2005). Some other examples of two-component regulatory systems phosphoactivating a transcriptional repressor (RR) include CovR/S of

Streptococcus pyogenes (Dalton and Scott, 2004), ArcB/A of *E. coli* (Lee *et al.*, 2001), DegS/U of *B. subtilis* (Amati *et al.*, 2004), and RocS1/R of *Pseudomonas aeruginosa* (Kulasekara *et al.*, 2005).

The presence of a putative phosphorelay system suggests that transcriptional repression (or derepression) of *crhC* may involve a signal transduction pathway, mediated by temperature. The repressor protein may therefore be present within the cell at all times and alterations in the level of phosphorylation (i.e. phosphatase or kinase) determine its ability to bind to the *crhC* promoter thereby enhancing the rapidity with which the cell can respond to temperature change. Proposed models for repression or depression of *crhC* include; at an optimal growth temperature (30°C) the repressor protein is phosphorylated via phosphotransfer from an upstream protein (i.e. histidine kinase, response regulator), altering the confirmation of the repressor and allowing it to bind to the *crhC* promoter thereby repressing transcription. Conversely, reverse phosphorylation may occur at low temperatures. At an ambient temperature of 30°C the repressor is phosphorylated however, in response to cold stress the repressor is dephosphorylated actively by a phosphatase possibly in combination with inhibition of kinase activity. A decrease in phosphorylation state will alter the repressor's confirmation, inhibiting promoter binding and allowing *crhC* transcription to occur. In terms of application for these models it is interesting to note, that in a laboratory setting the repressor would be continuously phospho-activated at its ambient temperature (30°C). However, in terms of natural habitat we must remember that *Anabaena* lives outdoors, in fresh water, at temperatures well below 30°C. Therefore, in context to its natural environment, the laboratory cold stress temperatures (20°C) would be considered ambient. The data presented in this thesis favors the latter model.

Both of the above models involve the transfer of a phosphate group(s), which requires a signal transduction cascade involving a membrane-bound histidine kinase(s) (HK), capable of receiving external stimuli (temperature) and mounting the appropriate genetic and cellular defense reactions. Extensive efforts have been made to identify a global "cold sensor" in the cyanobacterium *Synechocystis* sp. strain PCC 6803. Forty-one putative HK were identified of which, only one knockout, Hik33, was proposed to be a cold sensor for the desaturase genes, specifically *desB* (Sakamoto and Murata, 2002;

Suzuki *et al.*, 2000). DNA microarray analysis with ΔHik33 significantly diminished the extent of cold-induction for one CS gene, *desB* (Sakamoto and Murata, 2002; Suzuki *et al.*, 2001; Kaneko *et al.*, 1996). Similar results were observed in *B. subtilis* upon mutational analysis of the DesK/R two-component system. Mutation of DesKR proved essential for the cold-induction of the desaturase gene (*des*) however did not play a global role in cold signal perception and transduction (Beckering *et al.*, 2002). The presence 211 putative *Anabaena* genes involved in two-component systems along with the presence of Hik33 homologs in *Anabaena* sp. strain PCC 7120, suggests that a similar sensor kinase may phosphorylate downstream proteins such as the *crhC* repressor. However this is only speculative, as no global "cold sensor" has been identified in any bacteria to date (Wang *et al.*, 2002; Kaneko *et al.*, 2001).

On the basis of the above observations, it is very tempting to speculate that the transcriptional regulation of *crhC* involves a signal transduction cascade which activates or represses *crhC* promoter activity. Although no sole key transcription factor involved bacterial cold-sensing is known, cold-induced activation of specific promoters has been implicated in several *E. coli* CS genes. For example, both the *hns* and *gryA* CS genes are transcriptionally activated by CspA during cold stress (Jones *et al.*, 1992; La Teana *et al.*, 1991). Illustrated in Figure 4.1, a similar regulatory model could also be applied for transcriptional regulation of *crhC* in *Anabaena*. At optimal growth temperatures (30°C), an activated (i.e. directly or indirectly via thermosensors) histidine sensor kinase (HK) (and response regulator) mediates the transfer of a phosphate group(s) to the repressor protein. Alterations in the phosphorylation state change the confirmation of the repressor, allowing it to dimerize and/or interact with binding cofactors. The temperature-dependent structural alterations allow the repressor to recognize and bind in the proximity of the AT-rich element of the *crhC* promoter, blocking access of the RNA polymerase to the promoter thereby inhibiting *crhC* transcription at 30°C (Figure 4.1A). Following exposure to reduced temperature (20°C), the histidine kinase (HK) is inactivated, permitting dephosphorylation of the repressor by a constitutive phosphatase. The phosphatase is always present within the cell however only in the absence of HK kinase activity can it alter the phosphoryl flow. Dephosphorylation of the repressor alters the repressor structure so that it can no longer dimerize, associated with co-factors, or

Figure 4.1. Proposed model for transcriptional regulation of *crhC*. Panel A illustrates a mechanism by which *crhC* is transcriptionally repressed at 30°C. At optimal growth temperature (30°C) a putative repressor is activated via phosphorelay from an upstream histidine kinase (HK) or response regulator (RR). An increase in the repressor phosphorylation state changes the protein's confirmation allowing binding to the region of the *crhC* promoter around the AT-rich element, inhibiting *crhC* transcription. Panel B shows how *crhC* transcription is derepressed at 20°C. In the absence of the activated signal transduction pathway, a constitutive phosphatase can dephosphorylate the repressor, changing its conformation so that it can no longer bind to the *crhC* promoter. The removal of the repressor allows the RNA polymerase to transcribe *crhC* during cold stress.

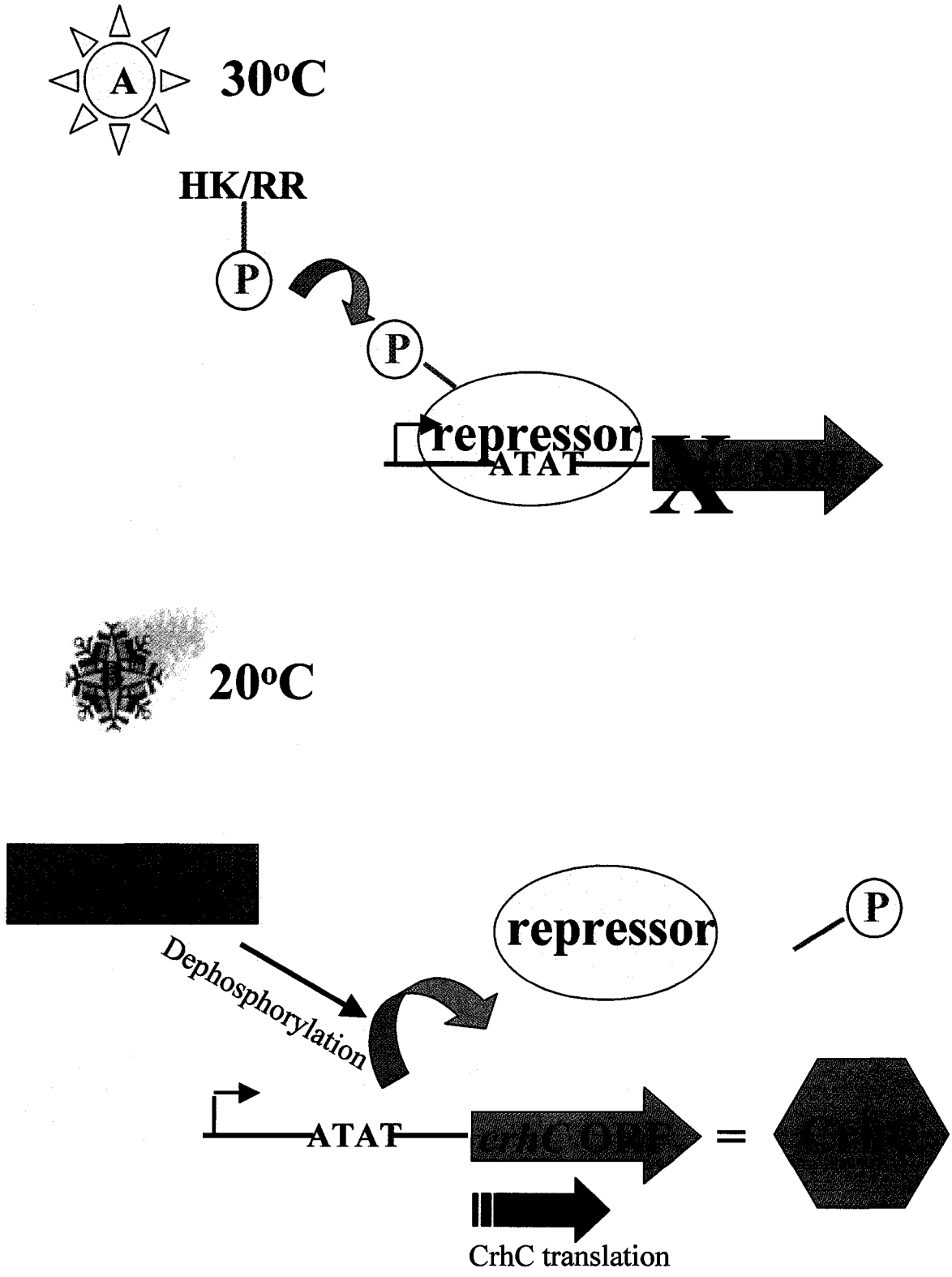

bind to the *crhC* promoter, allowing *crhC* transcription to resume (Figure 4.1B). It is interesting to note, that the above models are opposite to what has been proposed for cold shock gene regulation via signal transduction pathways in *Synechocystis* (Hik33/Rer1) and *B. subtilis* (DesK/R). Hik33 and DesK are both activated by cold stress where as the histidine kinase responsible for repressor phosphorylation is activated at optimal growth temperatures (30°C). Also, both of the cold-activated response regulators (RerI and DesR) are transcriptional activators of cold shock genes whereas our putative response regulatory is a transcriptional repressor of *crhC*. There are obviously distinct differences in the two-component systems regulating *crhC* in *Anabaena* and the *des* genes in *B. subtilis* and *Synechocystis* however, the presence of a cold-activated signal transduction pathway involved in regulating cold shock gene expression in *Anabaena* can not be ruled out.

Although the presence of a repressor molecule can provide a simplistic link between the external environment and gene expression, our luciferase assay results indicated that the temperature-dependent regulation of *crhC* is much more complex. The inability to convey temperature-dependent expression to a chimeric gene when transcriptionally regulated by the *crhC* promoter and/or its individual motifs suggests that the activity of the promoter is not dependent on temperature. Regulation of transcription initiation therefore provides *Anabaena* with secondary regulatory options to adjust *crhC* expression, indicating that promoter-independent, cold-induced *crhC* regulation must occur post-transcriptionally.

4.2 Post-Transcriptional Regulation of *crhC*

Recent studies on CS gene regulation indicate that bacteria use a variety of post-transcriptional regulatory mechanisms to coordinate gene expression. Chamot and colleagues (2000) demonstrated with half-life studies that the *crhC* transcript was stabilized (6X) at reduced temperatures (20°C), providing evidence that mRNA stability is important for temperature-regulated *crhC* expression. Northern and Western analysis presented here indicate a small amount of transcript and protein accumulate at 30°C in *E. coli*. The presence of CrhC at 30°C indicates that translation can occur at 30°C and therefore, the limiting factor is the availability of functional transcript. Although the

mechanism(s) providing RNA stabilization is not know, a large number of CS mRNAs (e.g. *rbpA1, des, cspA*) are regulated via temperature-induced RNA stabilization (Sato and Nakamura, 1998; Los *et al.*, 1997; Sakamoto and Bryant, 1997; Brandi *et al.*, 1996; Goldenberg *et al*, 1996). The discovery that most CS genes including *crhC*, have long 5' UTRs prompted investigation into the presence of *cis*-acting regulatory RNAs conveying temperature-dependent mRNA stability to the *crhC* transcript. The role of the 5' UTR in temperature-dependent *crhC* expression was first investigated in *E. coli*, where the *crhC* gene (lacking its own promoter) was placed under the transcriptional control of a constitutive *E. coli* promoter (pSIG16). The observation that transcript and protein accumulation was cold-induced and not constitutive indicated that post-transcriptional events are regulating *crhC* expression. These results confirmed that transcriptional regulation was not required for temperature-dependent expression rather, *crhC* is differentially regulated by transcript stabilization at reduced temperatures, possibly via the 5' UTR.

Based on the minimal free energy (ΔG), MFOLD predicted that the *crhC* 5' UTR contained two *cis*-acting stem loops that exist in different secondary structures at 30°C and 24°C (http://bioweb.pasteur.fr/seqanal/interfaces/mfold-simple.html; Zuker and Stiegler, 1981). MFOLD predicted that at temperatures ≥ 25°C the 5' UTR would fold in one RNA secondary formation whereas at temperatures ≤ 24°C an altered RNA secondary structure would form. Surprisingly, a difference of 1°C (25°C to 24°C) as predicted by MFOLD, was capable of thermodynamically altering the *crhC* 5' UTR. In support, previous work performed by Chamot and Owttrim (2000) demonstrated the threshold temperature for *crhC* transcript accumulation was in the vicinity of 25°C, which correlates with the MFOLD predicted temperature where altered RNA secondary structure occurs. Following a downshift in temperature, extensive secondary structure was predicted within the 5' stem loop structure of the *crhC* 5' UTR whereas no temperature-induced alterations were observed in the 3' stem loop structure. *cspA* , the major cold shock gene in *E. coli*, has also been shown to exist in two different mRNA secondary structures at 37°C and 15°C (Yamanaka *et al.*, 1999; Goldenberg *et al.*, 1996). Mutational analysis of the *cspA* 5' UTR identified an important upstream box (UB), found just upstream of the Shine-Dalgarno (SD) sequence which is required for CspA

cold-induction. The authors proposed that at low temperature, the UB, SD, and downstream box secondary structure permits ribosomal entry thereby allowing translation of *cspA* during cold stress (Yamanaka *et al.*, 1999).

From these results we can speculate that low temperature-induced alterations in the *crhC* 5' UTR stabilize the transcript, permitting ribosomal loading and translation of *crhC* at 20°C. In relationship to the *crhC* translational regulatory elements, the SD sequence and DB (no UB consensus sequence was found) are all located within the 3' stem loop structure suggesting that structural inhibition of ribosome access for translation initiation is not a regulatory factor. Indeed, no temperature-induced structural changes were predicted by MFOLD. Therefore, the 3' stem loop structure alone is not enough to differentiate between 20°C and 30°C as no thermodynamic structural changes were predicted to allow for differential ribosome access to the SD and DB. Based on the above observations, CrhC's differential regulation does not appear to originate from temperature-induced alterations in ribosomal loading capacities. That being said, a translational bias for the 3' stem loop structure and its regulatory elements during cold stress may still arise due to temperature effects on the ribosome (i.e. cold-adapted) and/or translational machinery; an increase in *trans*-acting factors such as translation initiation factors (Section 1.4.1.2), changes in the conformation of ribosomal RNA or protein (VanBogelen and Neidhardt, 1990), or altered translation kinetics (Hurme and Rhen, 1998) may allow for selective translation of *crhC* during cold stress.

Cold-induced stabilization of the *crhC* transcript is likely triggered by local changes within the secondary structure of the 5' loop, reducing its targeted degradation. In contrast, it is postulated that the 5' UTR secondary structure at temperatures above 24°C inactivates the *crhC* mRNA either through interactions with cellular factors (i.e. RNases) which either cleave or bind the RNA, or by self-cleavage via intrinsic ribozyme activity. With changes in mRNA secondary structure the cell can alter the rate of mRNA degradation, having a dramatic effect on gene expression (Rauhut and Klugg, 1999).

Proposed models illustrating temperature-induced stabilizing/destabilizing of the *crhC* 5' UTR, in relationship to the MFOLD results, are shown in Figure 4.2. Figure 4.2A illustrates that at optimal growth temperatures (30°C), base pairing of the *crhC* 5' loop is "melted" creating a 18 nt unpaired region potentially accessible for degradation

Figure 4.2. Proposed model(s) permitting translation of the *crhC* transcript at reduced temperature, as determined by the mRNA stability of the *crhC* 5' UTR. Panel A illustrates how temperature-induced structural changes within the *crhC* 5' UTR permits binding of accessory factors to the mRNA, altering stability. At 30°C, changes in the 5' UTR structure permits access of an RNase(s) (indicated by the green pac-man) to a specific target site, causing rapid mRNA degradation and transcript destabilization. Following a temperature downshift (20°C), temperature-induced changes within the 5' UTR secondary structure mask the putative ribonuclease target site (indicated by a red X), preventing transcript degradation and allowing translation of CrhC during cold stress. Changes in the 5' UTR structure at 20°C may also allow RNA binding proteins (indicated by the light blue triangle) to bind to the 5' UTR, facilitating stabilization of the transcript at low temperatures. Panel B illustrates how temperature-induced changes within the *crhC* 5' UTR can initiate primary cleavage via intrinsic ribozyme activity. At 30°C, changes within the secondary structure of the 5' UTR liberate the 5' UTR core domain (boxed as a light red background) as a ribozyme, inducing self-cleavage (indicated by a blue lighting bolt) of the *crhC* mRNA, and destabilizing the transcript. At 20°C, cold-induced structural changes within the 5' UTR secondary structure do not favor ribozyme activity thereby preventing self-cleavage and allowing translation of CrhC during cold stress.

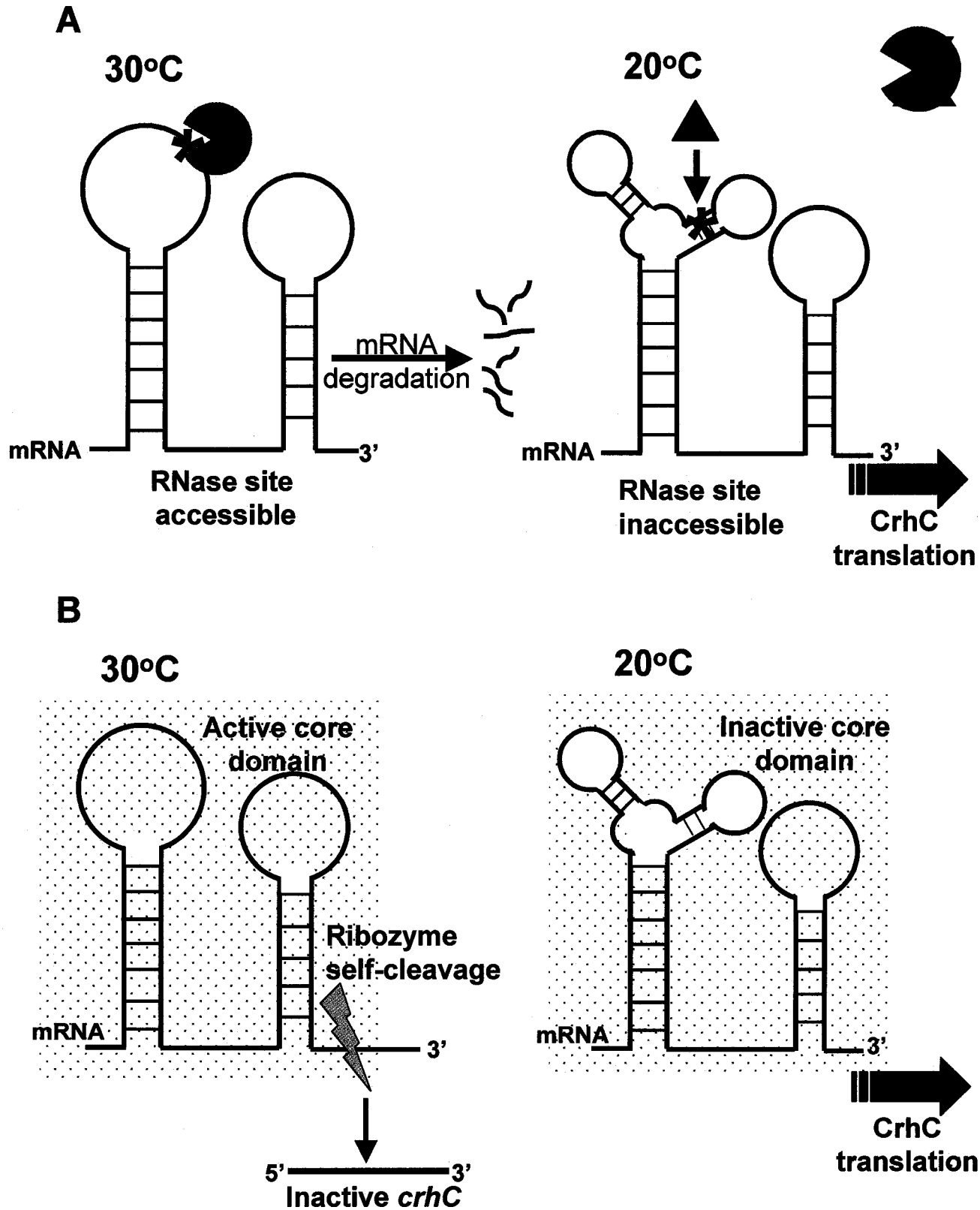

by ribonucleases (RNases), first by endonucleases such as RNase E, followed by exonuclease digestion (e.g. RNase R, PNPase, RNase II) (Cairrao *et al.*, 2003). Constriction of the *crhC* 5' loop at reduced temperature ($\leq 24^{\circ}C$) could stabilize the transcript by masking endoribonuclease target site(s) and inhibiting RNA degradation. A similar example was observed in the *E. coli ompA* gene, where mRNA levels were regulated by RNase E cleavage within the 5' UTR (Afonyushkin *et al.*, 2003). At elevated temperatures ($37^{\circ}C$) structural changes within the 5' UTR resulted in more efficient cleavage by RNase E, which in turn decreased *ompA* transcript accumulation (Afonyushkin *et al.*, 2003; Rosenbaum *et al.* 1993). The inability of specific ribonucleases or the RNA degradosome to initiate *crhC* mRNA degradation due to increased 5' UTR secondary structure and/or the notion that some mRNA degradation machinery is temporally inactivated at low temperature (Goldenberg *et al.*, 1996) may also contribute to providing mRNA stability to *crhC* during cold stress.

mRNA stability of CS genes can also be altered by interacting with specific nucleic acid binding proteins (Figure 4.2A). Potentially, the thermodynamic alterations predicted within the *crhC* 5' UTR could provide access to, or mask, a recognition site(s) for RNA binding proteins, stabilizing or destabilizing the transcript. For example, during cold stress the altered (constricted) secondary structure of the 5' loop could create a protein recognition site, allowing an RNA binding protein to bind and stabilize the transcript, and/or potentially facilitate translation initiation. In this context, it is interesting to note that cyanobacteria encode a family of RNA binding proteins, the Rbp gene family, whose expression is temperature-regulated (Graumann and Marahiel, 1996). These proteins have been proposed to functionally replace the *csp* gene family and it is tempting to speculate that they may be involved in stabilization of cold shock mRNAs in cyanobacteria.

Although the results presented in this thesis provide a general outline of how *crhC* mRNA is stabilized at low temperature, a major problem remains to be answered, the mechanism by which the *crhC* transcript is destabilized at $30^{\circ}C$. As mentioned above, transcript stabilization at $20^{\circ}C$ can be generated through the temperature-induced change in RNA secondary structure possibly combined with an RNA binding protein, which protects *crhC* RNA from degradation. Understanding *crhC* transcript destabilization at

30°C appears to be more complex. The ability of the *crhC* promoter to activate temperature-induced transcription at 30°C suggests that *crhC* transcription is constitutive and independent of temperature. Thus, the absence of *crhC* transcript at 30°C indicates that the *crhC* transcript is being actively degraded. Inhibition of translation by RNA secondary structure also does not appear to play a role here, as it does in other systems (Chang *et al.*, 1995; Hartz et al., 1991; Christensen *et al.*, 1984) as limited protein accumulation is observed at 30°C when *crhC* was cloned on a high copy plasmid, thus implying that *crhC* mRNA is translationally active at all temperatures. *crhC* mRNA must therefore be actively degraded at temperatures above 24°C. The mechanism(s) destabilizing *crhC* presumably involves recognition of the temperature-induced secondary structure formed at 30°C and is initiated by primary cleavage by two possible mechanisms (Figure 4.2): 1) an endogenous RNase recognizes the secondary structure at 30°C but not 20°C AND is conserved between cyanobacteria and *E. coli* (our heterologous system), or 2) the RNA secondary structure of the 5'UTR which spontaneously forms at 30°C possesses intrinsic RNA cleavage activity (i.e. ribozyme activity). The presence of a ribozyme is more conducive for our results as it does not require protein conservation between species.

Preliminary evidence presented in this thesis suggested that the *crhC* 5' UTR may possess intrinsic ribozyme activity, activated by temperature cues. The results were somewhat inconclusive due to the absence of distinct, stable degradation intermediates however, a significant difference was noted between the *crhC* 5' UTR and control RNA degradation patterns. Although further research is need, initial results showed that at 30°C the *crhC* 5' UTR degradation appeared somewhat non-random, possibly via intrinsic ribozyme activity. Ribozymes have been identified within both prokaryotes and eukaryotes with over 1500 ribozyme sequences known (Lilley *et al.*, 2005; Mandal *et al.*, 2003). Indeed, as proposed above, a limited number of prokaryotic mRNAs have recently been shown to possess intrinsic ribozyme activity which provides a mechanism by which their expression is regulated (Barrick *et al.*, 2004; Winkler *et al.*, 2003; Winkler *et al.*, 2002; Apirion and Miczak, 1993). In these examples, ribozyme activity and thus gene expression is controlled by the presence or absence of a metabolic effector molecule. Control elements found within the mRNA directly bind to a metabolite related

to the function of the gene product, promoting specific folding of the RNA, which in turn induces ribozyme cleavage of the mRNA thereby modulating gene expression (Lilley, 2005; Brandl *et al.*, 2004; Winkler *et al.*, 2004; Winkler and Breaker, 2003). In *B. subtilis*, the upstream sequence of *glmS* mRNA forms two stem-loop structures proposed to be a ribozyme, undergoing natural self cleavage in the presence of glucosamine-6-phosphate (GlcN6P) (Barrick *et al.*, 2004; Winkler *et al.*, 2004). This intimate connection between mRNA secondary structure and mRNA destabilization may regulate *crhC* destabilization at 30°C.

In support of *crhC* destabilization via ribozyme activity, preliminary analysis of temperature-regulated CrhC protein accumulation in *E. coli* RNase mutants, including Δ*rnc*, Δ*pnp*, and Δ*rne*, does not identify altered CrhC expression. If one of these RNases was required for the initial cleavage, constitutive CrhC expression would be detected. These results suggest that these RNases are not involved in the initial cleavage of the *crhC* transcript at 30°C. RNase E is considered to be the primary activity required for the initial cleavage of prokaryotic RNAs (Kushner, 2002; Regnier and Arraiano, 2000). Although the RNase E recognition and cleavage site is not specific, it cleaves within an A-U rich ss-region between two stem-loop structures (McDowall *et al.*, 1994; Mackie and Genereaux, 1993). The *crhC* 5' UTR is not predicted to contain sequences which comprise a potential RNase E cleavage site. In summary, all of these results suggest that the *crhC* 5' UTR may function as a ribozyme whose secondary structure produces an active RNA enzyme at 30°C and not 20°C, however further analysis needs to be performed to conclude this. If further analysis indicates that indeed the *crhC* 5' UTR is a ribozyme, it would be unique as it does not involve an effector molecule to alter secondary structure. Rather, temperature-induce structural changes within the 5' UTR would regulate ribozyme activity.

Although mRNA stability (via the 5' UTR) appears to play a major role in cold-regulated *crhC* expression, other post-transcriptional regulatory mechanisms can not be ruled out. Ideally, temperature-induced alterations within the *crhC* 5' UTR may also be involved in transcriptional attenuation mechanisms such as transcription termination or antitermination. At 30°C, the secondary structure of the *crhC* 5' UTR may permit transcription attenuation by the 5' "melted" loop structure providing access to nucleic

acid binding protein recognition sites. Protein binding to the *crhC* 5' UTR would terminate transcription thereby inhibiting *crhC* expression at 30°C. Conversely, constriction of the 5' loop at ≤ 24°C may also create a different recognition site(s) for RNA binding proteins to facilitate antitermination mechanisms. In B. *subtilis*, transcription attenuation occurs by binding of the *trp* RNA binding attenuation protein (TRAP) to the RNA leader region of the *trp* operon under high tryptophan concentrations, promoting transcription termination (Gollnick and Babitzke, 2001).

Luciferase assays performed with various regions of the *crhC* 5' UTR demonstrated that both the 5' and 3' stem loops structures (the entire 5' UTR) were required for conveying temperature-dependent expression to the *lux* reporter gene. Similar results were observed when the 3'-deleted *rbpA1* sequence was fused to the *lacZ* reporter gene. Sato and Nakamura (1998) found that the entire 5' UTR was required to convey cold-induced expression to the *lacZ* gene. These results suggest that *crhC*'s temperature sensitive regulation may occur due to defined interaction(s) between the 5' and 3' stem loop structures. For example, the 5' stem loop structure may have a "zipper" function (or vice versa), promoting proper folding of the 3' stem loops structure during RNA synthesis (Chowdhury *et al.*, 2003). Improper folding of the 3' stem loop by the 5' structure would inhibit selective translation at reduced temperature due to unrecognizable secondary structure by the translational machinery. RNA-mediated control could also be explained by the possible formation of a pseudoknot(s) between the two 5' UTR loop structures however preliminary sequence analysis does not indicate so. The inability of the individual stem loops to convey temperature-dependent expression to *lux* indicates that both stem loops are very important, and possibly interact together, in stabilizing the transcript at reduced temperatures. However, the exact mechanism of how this is occurring is not known. Site-directed mutagenesis of both of the 5' and 3' stem loops structures will provide a better understanding of what regions of the 5' UTR provide temperature-dependent mRNA stability and how (if at all) the two stem loop structures interact.

The presence of temperature responsive *cis*-elements within the *crhC* 5' UTR suggests that the 5' untranslated region of *crhC* may act as a "cellular thermometer", as was recently proposed for *cspA* and *rpoH* (Morita *et al.*, 1999; Yamanaka *et al.*, 1999)

Thermosensing mechanisms have been identified at both the transcriptional and translation level and can involve several different events; changes in DNA supercoiling, membrane fluidity, mRNA confirmation, and protein confirmation (Winkler, 2005; Inaba *et al.*, 2003; Hurme and Rhen, 1998). From this study, it appears that *crhC*'s thermoregulation occurs primarily due to thermosensitive structural alterations within the 5' UTR.

Translational control of heat shock (HS) and virulence genes are both regulated by thermoresponsive structures in the 5'-untranslated region. For example, the translation efficiency of the *E .coli* heat shock transcription factor RpoH (σ^{32}) is greatly reduced at low temperatures due to extensive secondary structure that forms within two *cis*-acting regions of the 5' mRNA coding sequence. At high temperatures (>35°C), the secondary structure partially melts providing ribosomal access to the cold-sequestered SD sequence and allowing translation to occur during heat stress (Morita *et al.*, 1999). Similar thermosensing mechanisms have also been shown to regulate the expression of virulence genes in *Listeria monocytogenes* (*prfA*) (Johansson *et al.*, 2002) and *Yersinia pestis* (*lcrF*) (Hoe and Goguen, 1993) required for host infection, and several heat shock genes in *Bradyrhizobium japonicum* (Chowdhury *et al.*, 2003; Narberhaus, 1998). *crhC* appears to be regulated by a different mechanism, as the *crhC* transcript is destabilized at the higher temperatures (≥ 25°C) and stabilized in the cold. Temperature-induced alterations of the 5' UTR destabilize the transcript by "melting" the 5' UTR secondary structure, providing RNA degradation. Similarly however, both methods provide a thermosensing mechanism for sensory RNA to perceive difference in temperature and alter gene expression accordingly.

Although cold regulated expression of *crhC* potentially occurs due to cold-induced structural alterations of the 5' UTR conveying stabilty, temperature sensing may also originate at the level of transcription. Even though it does not appear that the *crhC* promoter responds to temperature, temperature-mediated conformational changes in the repressor protein should not be ruled out as a secondary putative thermosensor. TlpA, an autoregulatory repressor protein in *Salmonella*, was identified as a proteinaceous "thermometer" due to its ability to regulate DNA-binding based on its folding equilibrium (Reini and Hurmer, 1998; Hurme *et al.*, 1997). At reduced temperatures,

TlpA is found as folded oligomers (coiled coils) capable of binding to the *tlpA* promoter and repressing transcription. However at elevated temperatures, TlpA's confirmation changes to a monomeric form, incapable of DNA-binding, thereby providing derepression of *tlpA*. Although further research is need, it is plausible that the repressor protein interacting with the *crhC* promoter may also be a thermosensor, found as a DNA-binding dimer at 30°C and a monomer at 20°C. If this is true, it would support the results observed during our transcriptional analysis (Section 4.1). The presence of two thermosensors regulating *crhC* would allow the cell to quickly express CrhC for efficient cold adaptation.

In summary, expression of the cold-induced RNA helicase, CrhC, from *Anabaena* sp. strain PCC7120 was shown to be regulated at both the transcriptional and post-transcriptional level. *In vitro*, it was demonstrated that *crhC* was regulated at the transcriptional level by a putative repressor that recognized a 52 bp portion of the *crhC* promoter surrounding an AT-rich element. The involvement of the AT-rich element and the remainder of the *crhC* promoter were shown not to be required for temperature-dependent *crhC* expression however, the AT-rich element was shown to be required for *crhC* promoter strength. Phosphorylation studies demonstrated that the repressor binds DNA in the phosphorylated state, suggesting an involvement of a temperature sensing signal transduction pathway.

Investigation into the *crhC* 5' UTR demonstrated that the 5' UTR is involved in post-transcriptionally regulating *crhC* expression. Transcriptional reporter fusions constructs demonstrated that the 5' UTR was sufficient to convey temperature-dependent expression as long as both stem loops structures were present. Using MFOLD predictions combined with *in vivo* expression patterns in *E. coli*, it was hypothesized that temperature-induced structural changes within the *crhC* 5' UTR stabilized the transcript at 20°C whereas the 5'UTR structure at 30°C destabilized the transcript via intrinsic ribozyme activity or endogenous RNase activity. Temperature-induced structural alterations of the mRNA suggest that the *crhC* 5' UTR likely acts as a thermosensor, regulating mRNA stabilty/destability. The presence of overlapping regulatory mechanisms acting as a potential molecular thermometer to regulate *crhC* temperature-

dependent expression provides unique insights into both *crhC* regulation and the mechanisms by which cyanobacteria sense and respond to temperature.

BIBLIOGRAPHY

Abramson, R.D., Dever, T.E., Lawson, T.G., Ray, B.K., Thach, R.E., and Merrick, W.C. 1987. The ATP-dependent interaction of eukaryotic initiation factors with mRNA. *J. Biol. Chem.* **262**:3826-3832.

Afonyushkin, T., Moll, I., Blasi, U., and Kaberdin, V.R. 2003. Temperature-dependent stability and translation of *Escherichia coli ompA* mRNA. *Biochem. Biophys. Res. Commun.* **311**:604-609.

Aguilar, P.S., Hernandez-Arriaga, A.M., Cybulski, L.S., Erazo, A.C., and de Mendoza, D. 2001. Molecular basis of thermosensing: a two-component signal transduction thermometer in *Bacillus subtilis*. *EMBO J.* **20**:1681-1691.

Aguilar, P.S., Cronan, J.E.J., and de Mendoza, D. 1998. A *Bacillus subtilis* gene induced by cold shock encodes a membrane phospholipid desaturase. *J. Bacteriol.* **180**:2194–2200.

Allen, M.M. 1968. Simple conditions for growth of unicellular blue-green algae on plates. *J. Phycol.* **4**:1-4.

Amati, G., Bisicchia, P., and Galizzi, A. 2004. DegU-P represses expression of the motility *fla-che* operon in *Bacillus subtilis*. *J. Bacteriol.* **186**:6003-6014.

Apirion, D. and Miczak, A. 1993. RNA processing in prokaryotic cells. *Bioessays.* **15**:113-120.

Appleby, J.L., Perkinson, J.S., and Bourret, R.B. 1996. Signal transduction via the multi-step phosphorelay: not necessarily and road less traveled. *Cell.* **86**:845-848.

Araki, T. 1991. Changes in rates of synthesis of individual proteins in a psychrophilic bacterium after a shift in temperature. *Can. J. Microbiol.* **37**:840-847.

Arenas, J.E., and Abelson, J.N. 1997. Prp43: An RNA helicase-lie factor involved in spliceosome disassembly. *Proc. Natl. Acad. Sci. USA.* **94**:11798-11802.

Aubourg, P., Kreis, M., and Lecharny, A. 1999. The DEAD box RNA helicase family in *Arabidopsis thaliana*. *Nucleic Acids Research.* **27**:628-636.

Ausubel, F.M., Brent, R., Kingston, R.E., Moore, D.D., Seidman, J.G., Smith, J.A., and Struhl, K. 1995. Current protocols in molecular biology. John Wiley & Sons, Inc., U.S.A.

Bae, W., Xia, B., Inouye, M., and Severinov, K. 2000. *Escherichia coli* CspA-family RNA chaperons are transcription antiterminators. *Proc. Natl. Acad. Sci. USA.* **97**:7784–7789.

Bae, W., Jones, P.G., and Inouye, M. 1997. CspA, the major cold shock protein of *E. coli*, negatively regulates its own gene expression. *J. Bacteriol.* **179**:7081-7088.

Baichoo N, Helmann JD. 2002. Recognition of DNA by Fur: a reinterpretation of the Fur box consensus sequence. *J. Bacteriol.* **184**:5826-5832.

Bancroft, I., Wolk, C.P., and Oren. E.V. 1989. Physical and genetic maps of the genome of the heterocyst-forming cyanobacterium *Anabaena* sp. Strain PCC 7120. *J. Bacteriol.* **171**:5940-5948.

Barrick, J.E., Corbino, K.A., Winkler, W.C., Nahvi, A., Mandal, M., Collins, J., Lee, M., Roth, A., Sudarsan, N., Jona, I., Wickiser, J.K., and Breaker, R.R. 2004. New RNA motifs suggest an expanded scope for riboswitches in bacterial genetic control. *Proc. Natl. Acad. Sci. USA.* **101**:6421-6426.

Bauer, C.C. and Haselkorn, R. 1995. Vectors for determining the differential expression of genes in heterocysts and vegetative cells of *Anabaena* sp. strain PCC 7120. *J. Bacteriol.* **177**:3332-3336.

Beckering, C.L., Steil, L., Weber, M.H., Volker, U., and Marahiel, M.A. 2002. Genome wide transcriptional analysis of the cold shock response in *Bacillus subtilis*. *J Bacteriol.* **184**:6395-6402.

Beran, R.K. and Simons, R.W. 2001. Cold-temperature induction of *Escherichia coli* polynucleotide phosphorylase occurs by reversal of its autoregulation. *Mol. Microbiol.* **39**:112–125.

Blackwood, E.M. and Kadonaga, J.T. 1998. Going the distance; a current view of enhancer action. *Science.* **281**:60-63.

Boddeker, N., Stade, K., and Franceshi, F. 1997. Characterization of DbpA, an *Escherichia coli* DEAD box protein with ATP independent RNA unwinding activity. *Nucleic Acids Res.* **25**:537-544.

Brandi, A., Pietroni, P., Gualerzi, C.O., and Pon, C.L. 1996. Post-transcriptional regulation of CspA expression in *Escherichia coli*. *Mol. Microbiol.* **19**:231-240.

Brantl, S. 2004. Bacterial gene regulation: from transcription attenuation to riboswitch and ribozyme. *Trends Microbiol.* **11**:473-475.

Cai, Y. and Wolk, C.P. 1990. Use of a conditionally lethal gene in *Anabaena* sp. strain PCC 7120 to select for double recombinants and to entrap insertion sequences. *J. Bacteriol.* **172**:3138-3145.

Cairroa, F., Cruz, A., Mori, H., and Arraiano, C.M. 2003. Cold shock induction of RNase R and its role in the maturation of the quality control mediator SsrA/tmRNA. *Mol. Microbiol.* **50**:1349-1360.

Carmichael, W.W., Azevedo, S.M., An, J.S., Molica, R.J., Jochimsen, E.M., Lau, S., Rinehart, K.L., Shaw, G.R., and Eaglesham, G.K. 2001. Human fatalities from cyanobacteria: chemical and biological evidence for cyanotoxins. *Environ. Health Perspect.* **109**:663-668.

Carty, S.M., Sreekumar, R.K.R., and Raetz, C.R.H. 1999. Effect of cold shock on lipid A biosynthesis in *Escherichia coli. J. Bio. Chem.* **274**:9677-9685.

Caruthers, J.M., Johnson, E.R., and McKay, D.B. 2001. Crystal structure of yeast initiation factor 4A, DEAD-box RNA helicase. *Proc. Natl. Acad. Sci. USA.* **97**:13080-13085.

Chamot, D., Colvin, K.R., Kujat-Choy, S.L., and Owttrim, G.W. 2005. RNA structural rearrangement via unwinding and annealing by the cyanobacterial RNA helicase, CrhR. *J. Biol. Chem.* **280**:2036-2044.

Chamot, D. and Owttrim, G.W. 2000. Regulation of cold shock-induced RNA helicase gene expression in the cyanobacterium *Anabaena* sp. strain PCC 7120. *J. Bacteriol.* **182**:1251-1256.

Chamot, D., Magee, W., Yu, E., and Owttrim, G.W. 1999. A cold shock-induced cyanobacterial RNA helicase. *J. Bacteriol.* **181**:1728-1738.

Chang, J.T., Green, C.B., and Wolf, R.E. 1995. Inhibition of translation initiation on *Escherichia coli gnd* mRNA by formation of a long-range secondary structure involving the ribosome binding site and the internal complementary sequence. *J. Bacteriol.* **177**:6560-6567.

Charollais, J., Dreyfus, M., and Iost, I. 2004. CsdA, a cold shock RNA helicase from *Escherichia coli*, is involved in the biogenesis of 50S ribosomal subunit. *Nucleic Acids Res.* **32**:2751-2759.

Charollais, J., Pflieger, D., Vinh, J., Dreyfus, M., and Iost, I. 2003. The DEAD-box RNA helicase SrmB is involved in the assembly of 50S ribosomal subunits in *Escherichia coli. Mol. Microbiol.* **48**:1253-1265.

Chen, J.Y., Stands, L., Staley, J.P., Jackups, R.R., Latus. L.J., and Chang, T.H. 2001. Specific alterations of U1-C protein or U1 small nuclear RNA can eliminate the requirement of Prp28p, an essential DEAD box splicing factor. *Mol. Cell.* 7:227-232.

Cho, H., Ha, N., Kang, L., Chung, K.M., Back, S.H., Jang, S.K., and Oh, B. 1998. Crystal structure of an RNA helicase from genotype 1b hepatitis C virus. A feasible mechanism of unwinding duplex RNA. *J. Biol. Chem.* **273**:15045-15052.

Chowdhury, S., Ragaz, C., Kreuger, E., and Narberhaus, F. 2003. Temperature-controlled structural alterations of an RNA thermometer. *J. Biol. Chem.* **278**:47915-47921.

Coss, J.R. 1966. Multiple electrophoretic zones arising from protein-buffer interaction. *Biochemistry.* **5**:1108-1112.

Christensen, T., Johnsen, M., Fiil, N.P., and Friesen, J.D. 1984. RNA secondary structure and translation inhibition: analysis of mutants in the *rplJ* leader. *EMBO J.* **3**:1609-1612.

Cybulski, L.E., del Solar, G., Craig, P.O., Espinosa, M., and de Mendoza, D. 2004. *Bacillus subtilis* DesR functions as a phosphorylation-activated switch to control membrane lipid fluidity. *J. Biol. Chem.* **279**:39340-39347.

Dalton, T.L. and Scott, J.R. 2004. CovS inactivates CovR and is required for growth under conditions of general stress in *Streptococcus pyogenes*. *J. Bacteriol.* **186**:3928-3937.

Dam, E., Pleij, K., and Draper, D. 1992. Structural and functional aspects of RNA pseudoknots. *Biochemistry.* **31**:11665-11676.

Danyluk J, Rassart, E., and Sarhan, F. 1991. Gene expression during cold and heat shock in wheat. *Biochem. Cell Biol.* **69**:383-391.

de la Cruz, E.M., Kressler, J.D., and Linder, P. 1999. Unwinding RNA in *Saccharomyces cerevisiae*: DEAD-box proteins and related families. *TIBS.* **24**:192-198.

Diges, C.M. and Uhlenbeck, O.C. 2001. *Escherichia coli* DbpA is an RNA helicase that requires hairpin 92 of 23S rRNA. *EMBO J.* **20**:5503-5512.

Dmitry. A.L. and Murata, N. 1999. Responses to cold shock in cyanobacteria. *J. Mol. Microbiol. Biotechnol.* **2**:221-230.

Dmitry, A.L., Malay, K.R., and Murata, N. 1997. Differences in the control of the temperature-dependent expression of four genes for desaturases in *Synechocystis* sp. PCC 6803. *Mol. Microbiol.* **25**:1167-1175.

Dorel, C., Vidal, O., Prigent-Combaret, C., Vallet, I., and Lejeune, P. 1999. Involvement of the Cpx signal transduction pathway of *E. coli* in biofilm formation. *FEMS Microbiol. Lett.* **178**:169-175.

Egelman, E.H. 1998. Bacterial helicases. *J. Struct. Biol.* **124**:123-128.

El-Fahmawi, B. and Owttrim, G.W. 2003. Polar-biased localization of the cold stress-induced RNA helicase, CrhC, in the cyanobacterium *Anabaena* sp. strain PCC 7120. *Mol. Microbiol.* **50**:1439-1448.

Elhai, J. and Wolk, C.P. Conjugal transfer of DNA to cyanobacteria. *Methods. Enzymol.* **167**:747-754.

Etchegaray, J.P. and Inouye, M. 1999. A sequence downstream of the initiation codon is essential for cold shock induction of *cspB* in *Escherichia coli. J. Bacteriol.* **181**:5852-5854.

Etchegaray, J.P. and Inouye, M. 1999. CspA, CspB and CspG, major cold shock proteins in *Escherichia coli*, are induced at low temperature under conditions that completely block protein synthesis. *J. Bacteriol.* **181**:1827-1830.

Fang, L., Hou, Y., and Inouye, M. 1998. Role of the cold-box region in the 5' untranslated region of the *cspA* mRNA in its transient expression at low temperature in *Escherichia coli. J. Bacteriol.* **180**:90-95.

Fang, L., Jiang, W., Bae, W., and Inouye, M. 1997. Promoter-independent cold shock induction of *cspA* and its derepression at 37°C by mRNA stabilization. *Mol. Microbiol.* **23**:355-364.

Fay P. 1983. The blue-greens. Edward Arnold. Baltimore, MD. p.88

Feinberg, A.P., and Vogelstein, B. 1983. A technique for radiolabelling DNA restriction endonuclease fragments to high specific activity. *Anal. Biochem.* **132:**6-13.

Flores-Rozas, H. and Hurwitz, J. 1993. Characterization of a new RNA helicase from nuclear extracts of HeLa cells which translocates in the 5' to 3' direction. *J Biol.Chem.* **268**:21372-21383.

Fuller-Pace, F.V. 1994. RNA helicases: modulators of RNA structure. *Trends Cell Biol.* **4:**271-274.

Fuller-Pace, F.V., Nicol, S.M., Reid, A.D., and Lane, D.P. 1993. DbpA; a DEAD box protein specifically activated by 23S rRNA. *EMBO J.* **12**:3619-3626.

Gallinari, P., Brennan, D., Nardi, C., Brunetti, M., Tomei, L., Steikuhler, C., De Francesco, R. 1998. Multiple enzymatic activities associated with recombinant NS3 protein hepatitis C virus. *J. Virol.* **72**:6758-6769.

Giraldo, R., Andreu, J.M., and Diaz-Orejas, R. 1998. Protein domains and conformational changes in the activation of RepA, a DNA replication initiator. *EMBO J.* **17**:4511-4526.

Giuliodori, A.M., Brandi, A., Gualerzi, C.O., and Pon, C.L. 2004. Preferential translation of cold shock mRNAs during cold adaptation. *RNA.* **10**:265-276.

Golden, S.S. 1988. Mutagenesis of cyanobacteria by classical and gene-transfer-based methods. *Methods Enzymol.* **167**:714-727.

Goldenberg, D., Azar, I., Oppenheim, A.B., Brandi, A., Pon, C.L., and Gualerzi, C.O. 1997. Role of *Escherichia coli cspA* promoter sequences and adaptation of translational apparatus in the cold shock response. *Mol. Gen. Genet.* **256**:282-290.

Goldenberg, D., Azar, I., and Oppenheim, A.B. 1996. Differential mRNA stability of the *cspA* gene in the cold shock response of *Escherichia coli. Mol. Microbiol.* **19**:241-248.

Goldstein, J., Pollitt, N.S., and Inouye, M. 1990. Major cold shock protein of *Escherichia coli. Proc. Natl. Acad. Sci. USA.* **27**:283-287.

Gollnick, P. and Babitzke, P. 2001. Posttranscription initiation control of tryptophan metabolism in *Bacillus subtilis* by the *trp* RNA-binding attenuation protein (TRAP), anti-TRAP, and RNA structure. *J. Bacteriol.* **183:**5795–5802.

Gorbalenya, A.E. and Koonin, E.V. 1993. Helicases: amino acid sequence comparisons and structure-function relationships. *Curr. Opin. Struct. Biol.* **3**:419-429.

Gorbalenya, A.E., Koonin, E.V., Donchenko, A.P., and Blinov, V.M. 1988. A conserved NTP-motif in putative helicases. *Nature.* **333**:22.

Grau R., Gardiol, D., Glikin, G.C., and de Mendoza, D. 1994. DNA supercoiling and thermal regulation of unsaturated fatty acid synthesis in *Bacillus subtilis. Mol. Microbiol.* **11**:933-941.

Graumann, P.L, and Marahiel, M.A. 1999. Cold shock proteins CspB and CspC are major stationary-phase-induced proteins in *Bacillus subtilis. Arch. Microbiol.* **171**:135-138.

Graumann, P., Wendrich, T.M., Weber, M.H.W., Schroder, K., and Marahiel, M.A. 1997. A family of cold shock proteins in *Bacillus subtilis* is essential for cellular growth and for efficient protein synthesis at optimal and low temperatures. *Mol. Microbiol.* **25**:741-756.

Graumann, P. and Marahiel, M.A. 1996. Some like it cold: response of microorganisms to cold shock. *Arch. Microbiol.* **166**:293-300.

Graumann, P., Schroder, K., Schmid, R., and Marahiel, M.A. 1996. Identification of cold shock stress induced proteins in *Bacillus subtilis*. *J. Bacteriol.* **178**:4611-4619.

Gray, M.W. and Doolittle, W.F. 1982. Has the endosymbiont hypothesis been proven? *Microbiol. Rev.* **46**:1-42.

Grebe, T.A. and Stock, J.B. 1999. The histidine protein kinase superfamily. *Adv. Microb. Physiol.* **41**:139-227.

Grifo, J.A., Abramson, R.D., Satler, C.A., and Merrick, W.C. 1984. RNA-stimulated ATPase activity of eukaryotic initiation factors. *J. Biol. Chem.* **259**:8648-8654.

Gross, C.H. and Shuman, S. 1998. The nucleoside triphosphatase and helicase activities of vaccinia virus NPH-II are essential for virus replication. *J. Virol.* **72**:4729-4736.

Gualerzi, C.O., Giuliodori, A.M., and Pon, C.L. 2003. Transcriptional and post-transcriptional control of cold shock genes. *J. Mol. Biol.* **331**:527-539.

Gururajan, R. and Weeks, D.L. 1997. An3 protein encoded by a localized maternal mRNA in *Xenopus laevis* is an ATPase with substrate-specific RNA helicase activity. *Biochim. Biophys. Acta.* **1350**:169-182.

Hartz, D., McPheeters, D.S., and Gold, L. 1991. Influence of mRNA determinants on translation initiation in *Escherichia coli*. *J. Mol. Biol.* **218**:83-97.

Haselkorn, R. 1991. Genetic systems in cyanobacteria. *Methods Enzymol.* **204**:418-430.

Helmann, J.D. 1999. Anti-sigma factors. *Curr. Opin. Microbiol.* **2**:135-141.

Herdman, M., Janvier, M., Rippka, R., and Stanier, R.Y. 1979. Genome size of cyanobacteria. *J. Gen. Microbiol.* **111**:73-85.

Herschlag, D. 1995. RNA chaperones and the RNA folding problem. *J. Biol. Chem.* **270**:20871-20874.

Herendeen, S.L., VanBogelen, R.A., and Neidhardts, F.C. 1979. Levels of major proteins of *Escherichia coli* during growth at different temperatures. *J. Bacteriol.* **139**:185-194.

Hirling, H., Schemffner, M., Restel, T., and Stahl, H. 1989. RNA helicase activity associated with the human p68 protein. *Nature.* **339**:562-564.

Hodgman, T.C. 1988. A new superfamily of replication proteins. *Nature.* **333**:22-23.

Hoe, N.P. and Goguen, J.D. 1993. Temperature sensing in *Yersinia pestis*: translation of the LcrF activator protein is thermally regulated. *J. Bacteriol.* **175**:7901-7909.

Howe, J.G. and Hershey, J.W. 1983. Initiation factor and ribosome levels are coordinately controlled in *Escherichia coli* growing at different rates. *J. Biol. Chem.* **258**:1954-1959.

Hurme, R. and Rhen, M. 1998. Temperature sensing in bacterial gene regulation – what it all boils down to. *Mol. Microbiol.* **30**:1-6.

Hurme, R., Berndt, K.D., Normark, S.J., and Rhen, M. 1997. A proteinaceous gene regulatory thermometer in *Salmonella*. *Cell.* **90**:55-64.

Iggo, R., Picksley, S., Southgate, J., McPheat, J., and Lane, D.P. 1990. Identification of a putative RNA helicase in *E. coli*. *Nuc. Acid Res.* **18**:5413-5417.

Inaba, M., Suzuki, I., Szalontai, B., Kanesaki, Y., Los, D.A., Hayashi, H., and Murata, N. 2003. Gene-engineered rigidification of membrane lipids enhances the cold inducibility of gene expression in *Synechocystis*. *J. Biol. Chem.* **278**:12191-12198.

Iost, I., Dreyfus, M., and Linder, P. 1999. Ded1p, a DEAD-box protein required for translation initiation in *Saccharomyces cerevisiae*, is an RNA helicase. *J. Biol. Chem.* **274**:17677-17683.

Jacob, C., and Shapiro, L. 1999. Bacterial cell division: a moveable feast. *Proc. Natl. Acad. Sci. USA.* **96**:5891-5893.

Jacob, F. and Monod, J. 1961. Genetic regulatory mechanisms in the synthesis of proteins. *J. Mol. Biol.* **3**:318-356.

Jager, S., Evguenieva-Hackenberg, E., and Klug, G. 2004. Temperature-dependent processing of the *cspA* mRNA in *Rhodobacter capsulatus*. *Microbiology.* **150**:687-695.

Jankowsky, E., Gross, C.H., Shuman, S., and Pyle, A.M. 2001. Active disruption of an RNA-protein interaction by a DexH/D RNA helicase. *Science.* **291**:121-125.

Jiang, W., Fang, L., and Inouye, M. 1996. The role of the 5'-end untranslated region of the mRNA for CspA, the major cold shock protein of *Escherichia coli*, in cold shock adaptation. *J. Bacteriol.* **178**:4919-4925.

Jiang, W., Jones, P., and Inouye, M. 1993. Chloramphenicol induces the transcription of the major cold shock protein of *Escherichia coli*, CspA. *J. Bacteriol.* **175**:5824-5828.

Johansson, J., Mandin, P., Renzoni, A., Chiaruttini, C., Springer, M., and Cossart, P. 2002. An RNA thermosensor controls expression of virulence genes in *Listeria monocytogenes*. *Cell.* **110**:551-561.

Johnson, A.D. 1995. The price of repression. *Cell.* **81**:655-658.

Johnson, E.R. and McKay, D.B. 1999. Crystallographic structure of the amino terminal domain of yeast initiation factor 4A, a representative DEAD-box RNA helicase. *RNA.* **5**:1526-1534.

Jones, P.G. and Inouye, M. 1996. RbfA, a 30S ribosomal binding factor, is a cold shock protein whose absence triggers the cold shock response. *Mol. Microbiol.* **21**:1207-1218.

Jones, P.G. and Inouye, M. 1994. The cold shock response – a hot topic. *Mol. Microbiol.* **11**:811-818.

Jones, P.G., Cashel, M., Glaser, G., and Neidhardt, F.C. 1992a. Function of a relaxed-like state following temperature downshifts in *Esherichia coli. J. Bacteriol.* **174**:3903-3914.

Jones, P.G., Krah, R., Tafuri, S.R., and Wolffe, A.P. 1992b. DNA gyrase, CS7.4, and the cold shock response in *Escherichia coli. J. Bacteriol.* **174**:5798–5802.

Jones, P.G., VanBogelen, R.A., Neidhardt, E.C. 1987. Induction of proteins in response to low temperature in *Escherichia coli. J. Bacteriol.* **27**:2092–2095.

Jubelin, G., Vianney, A., Beloin, C., Ghigo, J.M., Lazzaroni, J.C., Lejeune, P., and Dorel, C. 2005. CpxR/OmpR interplay regulates curli gene expression in response to osmolarity in *Escherichia coli. J. Bacteriol.* **187**:2038-2049.

Kaneko, T., Nakamura, Y., Wolk, C.P., Kuritz, T., Sasamoto, S., Watanabe, A., Iriguchi, M., Ishikawa, A., Kawashima, K., Kimura, T., Kishida, Y., Kohara, M., Matsumoto, M., Matsuno, A., Muraki, A., Nakazaki, N., Shimpo, S., Sugimoto, M., Takazawa, M., Yamada, M., Yasuda, M., and Tabata, S. 2001. Complete genomic sequence of the filamentous nitrogen-fixing cyanobacterium *Anabaena* sp. strain PCC 7120. *DNA Res.* **5**:205-253.

Kaneko, T., Sato, S., Kotani, H., Tanaka, A., Asamizu, E., Makamura, Y., Miyajima, N., Hirosawa, M., Sugiura, M., Sasamoto, S. 1996. Sequence analysis of the genome of the unicellular cyanobacterium *Synechocystis* sp. strain PCC 6803. II. Sequence determinations of the entire genomes and assignment of potential protein-coding regions. *DNA Res.* **3**:109–136.

Kankaanpaa, H.T., Holliday, J., Schroder, H., Goddard, T.J., von Fister, R., and Carmichael, W.W. 2005. Cyanobacteria and prawn farming in northern New South Wales, Australia-a case study on cyanobacteria diversity and hepatotoxin bioaccumulation. *Toxicol. Appl. Pharmacol.* **203**:243-256.

Kaptein, R., Zuiderwieg, E.R.P., Sheek, R.M., Boelens, R., and van Gunsteren, W.F. 1985. A protein structure from nuclear magnetic resonance data *lac* repressor headpiece. *J. Mol. Biol.* **182**:179-182.

Kenan, D.J., Query, C.C., and Keene, J.D. 1991. RNA recognition: towards identifying determinants of specificity. *Trends Biochem. Sci.* **16**:214-220.
Khemici V, Toesca I, Poljak L, Vanzo NF, Carpousis AJ. 2004. The RNas e E of *Escherichia coli* has at least two binding sites for DEAD-box RNA helicases: functional replacement of RhlB by RhlE. *Mol. Microbiol.* **54**:1422-1430.

Kim, S.H., Lin, R.J. 1996. Spliceosome activation by PRP2 ATPase prior to the first transesterification reaction of pre-mRNA splicing. *Mol. Cell Biol.* **16**:6810-6819.

Kim, S.H., Smith, J., Claude, A., Lin, R.J. 1992. The purified yeast pre-mRNA splicing factor PRP2 is an RNA-dependent NTPase. *EMBO J.* **11**:2319-2326.

Ko, D.C., Marr, M.T., Guo, J., and Roberts, J.W. 1998. A surface of *Escherichia coli* σ^{70} required for promoter function and antitermination by phage λ Q protein. *Genes Dev.* **12**:3276-3285.

Koo, J.T., Choe, J., Moseley, S.L. 2004. HrpA, a DEAH-box RNA helicase, is involved in mRNA processing of a fimbrial operon in *Escherichia coli. Mol. Microbiol.* **52**:1813-1826.

Kostrewa, D., Granzin, J., Koch, C., Choe, H.W., Raghunathan, S., Wolf, W., Labahn, J., Kahmann, R., and Saenger. W. 1991. Three-dimensional structure of the *E. coli* DNA-binding protein FIS. *Nature.* **349**:178-180.

Kressler, D., de la Cruz, J., Rojo, M., and Linder, P. 1997. Fal1p is and essential DEAD-box protein involved in 40S-ribosomal-subunit biogenesis in *Saccharomyces cerevisiae. Mol. Cell. Biol.* **17**:7283-7294.

Kruppa, M., Krom, B.P., Chauhan, N., Bambach, A.V., Cihlar, R.L., and Calderone, R.A. 2004. The two-component signal transduction protein Chk1p regulates quorum sensing in *Candida albicans. Eukaryot. Cell.* **3**:1062-1065.

Kujat, S.L. and Owttrim, G.W. 2000. Redox-regulated RNA helicase expression. *Plant Physiol.* **124**:703-714.

Kulasekara, H.D., Ventre, I., Kulasekara, B.R., Lazdunski, A., Filloux, A., and Lory, S. 2005. A novel two-component system controls the expression of *Pseudomonas aeruginosa* fimbrial cup genes. *Mol. Microbiol.* **55**:368-380.

Kushner, S.R. 2002. mRNA decay in *Escherichia coli* come of age. *J. Bacteriol.* **184**:4658-4665.

La Teana, A., Brandi, A., O'Conner, M., Freddi, S., and Pon, C.L. 2000. Translation during cold adaptation does not involve mRNA - rRNA base pairing through the downstream box. *RNA.* **6**:1393-1402.

La Teana, A., Brandi, A., Falconi, M., Spurio, R., Pon, C.L., and Gualerzi, C.O. 1991. Identification of a cold shock transcriptional enhancer of the *Escherichia coli* gene encoding nucleoid protein H-NS. *Proc. Natl. Acad. Sci. USA.* **88**:10907-10911.

Ladomery, M., Wade. E., and Sommerville, J. 1997. Xp54, the Xenopus homologue of human RNA helicase p54, is an integral component of stored mRNP particles in oocytes. *Nucleic Acids Res.* **25**:965-973.

Lamb, P. and McKnight, S.L. 1991. Diversity and specificity in transcriptional regulation: the benefits of heterotypic dimerization. *Trends Biochem. Sci.* **16**:417-422.

Lamerichs, R.M., Padilla, A., Boelens, R., Kaptein, R., Ottleben, G., Ruterjans, H., Granger-Schnarr, M., Oertel, P., and Schnarr, M. 1989. The amino-terminal domain of LexA repressor is alpha-helical but differs from canonical helix-turn-helix proteins: a two-dimensional 1H NMR study. *Proc. Natl. Acad. Sci USA.* **86**:6863-6867.

Lane, D. and Harlow, E. 1982. Two different viral transforming proteins bind the same host tumor antigen. *Nature.* **298**:517.

Lang, E.A. and Marques, M.V. 2004. Identification and transcriptional control of Caulobacter crescentus genes encoding proteins containing a cold shock domain. *J. Bacteriol.* **186**:5603-5613.

Lee, Y.S., Han, J.S., Jeon, Y., and Hwang, D.S. 2001. The arc two-component signal transduction system inhibits *in vitro Escherichia coli* chromosomal initiation. *J. Biol. Chem.* **276**:9917-9923.

Lee, C.G and Hurwitz. J. 1992. A new RNA helicase isolated from HeLa cells that catalytically translocates in the 3' to 5' direction. *J. Biol. Chem.* **267**:4398-4407.

Lefstin, J.A. and Yamamoto, K.R. 1998. Allosteric effects of DNA on transcriptional regulators. *Nature.* **392**:885-888.

Lewis, P.J., Thaker, S.D., and Errington, J. 2000. Compartmentalization of transcription and translation in *Bacillus subtilis*. *EMBO J.* **19**:710-718.

Li, S., Ault, A., Malone, C.L., Raitt, D., Dean, S., Johnston, L.H., Deschenes, R.J., and Fassler, J.S. 1998. The yeast histidine protein kinase, Sln1p, mediates phosphotransfer to two response regulators, Ssk1p and Skn7p. *EMBO J.* **17**:6952-6962.

Liang, L., Diehl-Jones, W., and Lasko, P. 1994. Localization of vasa protein to the *Drosophila* pole plasm is independent of its RNA-binding and helicase activities. *Development.* **120**:1201-1211.

Lilley, D.M.J. 2005. Structure, folding and mechanisms of ribozymes. *Curr. Opin. Struct. Biol.* **15**:1-11.

Linder, P., Tanner, N.K., and Banroques, J. 2001. From, RNA helicases to RNPases. *Trends Biochem. Sci.* **26**:339-341.

Linder, P., Lasko, P.F., Ashburner, M., Leroy, P., Nielen, P.J., Nishi, K., Schnier, J., and Slonimsk, P. 1989. Birth of the D-E-A-D box. *Nature.* **337**:121-122.

Liou, G.G., Jane, W.N., Cohen, S.N., Lin, N.S., and Lin-Chao, S. 2001. RNA degradosomes exist *in vivo*. *Escherichia coli* as multicomponent complexes associated with the cytoplasmic membrane via the N-terminal region of ribonuclease E. *Proc. Natl. Acad. Sci. USA* **98**:63–68.

Loewen PC, Hu, B., Strutinsky, J., and Sparling, R. 1998. Regulation in the *rpoS* regulon of *Escherichia coli*. *Can. J. Microbiol.* **44**:707-717.

Los, D.A. 2004. The effect of low-temperature-induced DNA supercoiling on the expression of the desaturase genes in *Synechocystis*. *Cell Mol. Biol.* **50**:605-612.

Los, D.A., Ray, M.K., and Murata, N. 1997. Differences in the control of the temperature-dependent expression of four genes for desaturases in *Synechocystis* sp. PCC 6803. *Mol. Micrbiol.* **25**:1167-1175.

Mackie, G.A. and Genereaux, J.L. 1993. The role of RNA structure in determining RNase E-dependent cleavage sites in the mRNA for ribosomal protein S20 in vitro. *J. Mol. Biol.* **234**:998-1012.

Magee, W. 1997. Characterizing a cyanobacterial RNA helicase. M.Sc. Thesis. University of Alberta, Edmonton, Canada.

Makhatadze, G.I. and Marahiel, M.A. 1994. Effect of pH and phosphate ions on self-association properties of the major cold shock protein from *Bacillus subtilis*. *Protein Sci.* **3**:2144-2147.

Makino, S., Kiba, T., Imamura, A., Hanaki, N., Nakamura, A., Suzuki, T., Taniguchi, M., Ueguchi, C., Sugiyama, T., and Mizuno, T. 2000. Genes encoding pseudo response regulators: insight into his-to-Asp phosphorelay and circadian rhythm in *Arabidopsis thaliana*. *Plant Cell Physiol.* **41**:791-803.

Maldonado, E., Hampsey, M., and Reinberg, D. 1999. Repression: targeting the heart of the matter. *Cell.* **99**:455-458.

Mandal, M., Boese, B., Barrick, J.E., Winkler, W.C., and Breaker. R.R. 2003. Riboswitches control fundamental biochemical pathways in *Bacillus subtilis* and other bacteria. *Cell.* **113**:577-586.

Maniak M. and Nellen, W. 1988. A developmentally regulated membrane protein gene in *Dictyostelium discoideum* is also induced by heat shock and cold shock. *Mol. Cell Biol.* **8**:153-159.

Mansilla, M.C. and de Mendoza, D. 2005. The *Bacillus subtilis* desaturase: a model to understand phospholipid modification and temperature sensing. *Arch. Microbiol.* **183**:229-235.

Matsumoto, K., Tanaka, K.J., and Tsujimoto, M. 2005. An acidic protein, YBAP1, mediates the release of YB-1 from mRNA and relieves the translational repression activity of YB-1. *Mol. Cell Biol.* **5**:1779-1792.

Mayr, B., Kaplan, T., Lechner, S., and Scherer, S. 1996. Identification and purification of a family of dimeric major cold shock protein homologs from the psychrotrophic *Bacillus cereus. J. Bacteriol.* **178**:2916-2929.

McDowall, K.J., Lin-Chao, S., and Cohen, S.N. 1994. A+U content rather than a particular nucleotide determines the specificity of RNase E cleavage. *J. Biol. Chem.* **269**:10790-10796.

McKay, D.B. and Steitz, T.A. 1981. Structure of catabolite gene activator protein at 2.9Å resolution suggests binding to left-handed B-DNA. *Nature.* **290**:744-749.

Merrick, M.J. 1993. In a class of its own – the RNA polymerase sigma factor σ^{54} (σ^{N}). *Mol. Microbiol.* **10**:903-909.

Miczak, A., Kaberdin, V.R. Wei, C., and Lin-Chao, S. 1996. Proteins associated with Rnase E in a multicomponent ribonucleolytic complex. *Proc. Natl. Acad. Sci. USA* **93**:3865-3869.

Mitta, M., Fang, L., and Inouye, M. 1997. Deletion analysis of cspA of *Escherichia coli*: requirement of the AT-rich UP element for *cspA* transcription and the downstream box in the coding region for its cold shock induction. *Mol. Microbiol.* **26**:321-335.

Mizuno, T. 1997. Compilation of all genes encoding two-component phosphotransfer signal transducers in the genome of *Escherichia coli. DNA Res.* **4**:161-168.

Mizuno T. 1996. Compilation of all genes encoding bacterial two-component signal transducers in the genome of the cyanobacterium, *Synechocystis* sp. Strain PCC 6803. *DNA Res.* **3**:407-414.

Mizyshima, T., Kataoka, K., Ogata, Y., Inoue, R., and Sekimizu, K. 1997. Increase in negative supercoiling of plasmid DNA in *Escherichia coli* exposed to cold shock. *Mol. Microbiol.* **23**:381-386.

Moll, J.R., Acharya, A., Gal, J., Mir, A.A., and Vinson, C. 2002. Magnesium is required for specific DNA binding of the CREB B-ZIP domain. *Nucleic Acids Res.* **30**:1240-1246.

Morita, M., Kanemori, M., Yanagi, H., and Yura, T. 1999. Heat-induced synthesis of σ^{32} in *Escherichia coli*: Structural and functional dissection of *rpoH* mRNA secondary structure. *J. Bacteriol.* **181:** 401-410.

Motoyama, T., Kadokura, K., Ohira, T., Ichiishi, A., Fujimura, M., Yamaguchi, I., and Kudo, T. 2005. A two-component histidine kinase of the rice blast fungus is involved in osmotic stress response and fungicide action. *Fungal Genet. Biol.* **42**:200-212.

Mulligan, M.E. and Haselkorn, R. 1989. Nitrogen fixation *(nif)* genes of the cyanobacterium *Anabaena* species strain PCC 7120: the *nifB-fdxN-nifS-nifU* operon. *J. Biol. Chem.* **264**:19200-19207.

Murata, N. and Wada, H. 1995. Acyl-lipid desaturases and their importance in the tolerance and acclimatization to cold of cyanobacteria. *Biochem. J.* **308**:1-8.

Murata, N. 1989. Low-temperature effects on cyanobacterial membranes. *J. Bioenerg. Biomembr.* **21**:61-75.

Mustardy, L., Dmitry, L., Gombos, A., and Murata, N. 1996. Immunocytochemical localization of acyl-lipid desaturases in cyanobacterial cells: evidence that both thylakoid membranes and cytoplasmic membranes are sties for lipid desaturation. *Proc. Natl. Acad. Sci. USA.* **93**:10524-10527.

Nagai, K., Oubridge, C., Ito, N., Avis, J., and Evans, P. 1995. The RNP domain: a sequence-specific RNA-binding involved in processing and transport of RNA. *Trends Biochem. Sci.* **20**:235-240.

Narberhaus, F., Kaser, R., Nocker, A., Hennecke, H. 1998. A novel DNA element that controls bacterial heat shock gene expression. *Mol. Microbiol.* **28**:315-323.

Nickel, M., Homuth, G., Bohnisch, C., Mader, U., and Schweder, T. 2004. Cold induction of the *Bacillus subtilis bkd* operon is mediated by increased mRNA stability. *Mol. Genet. Genomics.* **272**:98-107.

Nicol, S.M. and Fuller-Pace. F.V.. 1995. The "DEAD box" protein DbpA interacts specifically with the peptidyltransferase center in 23S rRNA. *Proc. Natl. Acad. Sci. USA.* **92**:11681-11685.

Nishi, S.M., Morel-Deville, F., Hershey, J.W.B., Leighton, T., and Schnier, J. 1988. An eIF-4A-like protein is a suppressor of an *Escherichia coli* mutant defective in 50S ribosomal subunit assembly. *Nature.* **336**:496-498.

Nocker, A., Hausherr, T., Balsiger, S., Krstulovic, N.P., Hennecke, H., and Narberhaus, F. 2001. A mRNA-based thermosensor controls expression of rhizobial heat shock genes. *Nucleic Acids Res.* **29**:4800-4807.

O'Conner, M., Asai, T., Squires, C.L., and Dahlberg, A.E. 1999. Enhancement of translation by the downstream box does not involve base pairing of mRNA with the penultimate stem sequence of 16 S rRNA. *Proc. Natl. Acad. Sci. USA.* **96**:8973-8978.

Ohmori, H. 1994. Structural analysis of the *rhlE* gene of *Escherichia coli. Jpn. J. Genet.* **69**:1-12.

Okanami M, Meshi T, Iwabuchi M. 1998. Characterization of a DEAD box ATPase/RNA helicase protein of Arabidopsis thaliana. *Nucleic Acids Res.* **26**:2638-2643.

Ozoline, O.N., Fujita, N., and Ishihama, A. 2001. Mode of DNA–protein interaction between the C-terminal domain of *Escherichia coli* RNA polymerase α-subunit and T7*D* promoter UP element. *Nucleic Acids Res.* **29**:4909-4919.

Pabo, C.O. and Sauer, R.T. 1992. Transcription factors: structural families and principles of DNA recognition. *Annu. Rev. Biochem.* **61**:1053-1095.

Parker, W.C. and Bearn, A.G. 1963. Boric acid-induced heterogeneity of conalbumin by starch-gel electrophoresis. *Nature.* **199**:1884-1886.

Patocka, J. 2001. The toxins of Cyanobacteria. *Acta. Medica.* **44**:69-75.

Pause, A. and Sonenberg, N. 1993. Helicases and RNA unwinding in translation. *Curr. Opin. Struct. Biol.* **3**:953-959.

Pause, A., Methot, N., and Sonenberg, N. 1993. The HRIGRXXR region of the DEAD box RNA helicase eukaryotic translation initiation factor 4A is required for RNA binding and ATP hydrolysis. *Mol. Cell Biol.* **13**:6789-6798.

Pause, A. and Sonenberg, N. 1992. Mutational analysis of a DEAD box RNA helicase: the mammalian translation initiation factor eIF-4A. *EMBO J.* **11**:2643-2654.

Perraud, A.L., Weiss, V., and Gross, R. 1999. Signaling pathways in two-component phosphorelay systems. *Trends Microbiol.* **7**:115-120.

Phadtare, S. 2004. Recent developments in bacterial cold shock response. *Curr. Issues Mol. Biol.* **6**:125-136.

Phadtare, S., Inouye, M., and Severinov, K. 2004. The mechanism of nucleic acid melting by a CspA family protein. *J. Mol. Biol.* **337**:147-155.

Phadtare, S. and Inouye, M. 2004. Genome-wide transcriptional analysis of the cold shock response in wild-type and cold-sensitive, quadruple-csp-deletion strains of Escherichia coli. *J. Bacteriol.* **186**:7007-7014.

Phadtare, S., Hwang, J., Severinov, K., and Inouye, M. 2003. CspB and CspL, thermostable cold shock proteins from *Thermotoga maritima. Genes Cells.* **8**:801-810.

Phadtare, S., Yamanaka, K., and Inouye, M. 2000. The cold shock response: in bacterial stress responses. Washington, DC: American Society for Microbiology Press, p. 33-45.

Phadtare, S., Alsina, J., and Inouye, M. 1999. Cold shock response and cold shock proteins. *Curr. Opin. Microbiol.* **2**:175-180.

Piggot, P.G. 1996. Spore development in *Bacillus subtilis. Curr. Opin. Genet. Dev.* **6**:531-537.

Plumpton M., McGarvey, M., and Beggs, J.D. 1994. A dominant negative mutation in the conserved RNA helicase motif 'SAT' causes splicing factor PRP2 to stall in spliceosomes. *EMBO J.* **13**:879-887.

Porankiewicz, J. and Clarke. A.K. 1997. Induction of a heat shock protein ClpB affects cold acclimation in the cyanobacterium *Synechocccus* sp. strain PCC 7942. *J. Bacteriol.* **179**:5111-5117.

Psenner, R. and Sattler, B. 1998. Life at the freezing point. *Science.* **250**:2073-2074.

Pugh, G.E., Nicol, S.M., and Fuller-Pace, F.V. 1999. Interaction of the *Escherichia coli* DEAD box protein DbpA with 23 S ribosomal RNA. *J. Mol. Biol.* **292**:771-778.

Py, B., Higgins, C.F., Krisch, H.M., and Carpousis, A.J. 1996. A DEAD-box RNA helicase in the *Escherichia coli* RNA degradosome. *Nature.* **381**:169-172.

Ramos, J.L., Callegos, M.T., Marques, S., Ramose-Gonzalex, M.I., Espinosa-Urgel, M., and Segura, A. 2001. Responses of Gram-negative bacteria to certain environmental stressors. *Curr. Opin. Microbiol.* **4**:166-171.

Rapala, J., Sivonen, K., Luukkainen, R., and Niemelä. S.I. 1993. Anatoxin-a concentration in *Anabaena* and *Aphanizomenon* at different environmental conditions and comparison of growth by toxic and non-toxic *Anabaena* strains - a laboratory study. *J. Appl. Phycology.* **5**:581-591.

Rauhut, R. and Klug, G. 1999. mRNA degradation in bacteria. *FEMS Microbiol Rev.* **23**:353-370.

Ray, B.K., Lawson, T.G., Kramer, J.C., Cladaras, M.H., Grifo, J.A., Abramson, Merrick, W.C. and Thach, R.E. 1985. ATP-dependent unwinding of messenger RNA structure by eukaryotic initiation factors. *J. Biol. Chem.* **260**:7651-7658.

Regnier, P. and Arraiano, C.M. 2000. Degradation of mRNA in bacteria: emergence of ubiquitous features. *Bioessays.* **22**:235-244.

Rippka, R., Deruelles, J., Waterbury, J.B., Herdman, M., and Stanier, R.Y. 1979. Generic assignments, strain histories and properties of pure cultures of cyanobacteria. *J. Gen. Microbiol.* **111**:1-61.

Rocak, S. and Linder, P. 2004. DEAD-box proteins: the driving forces behind RNA metabolism. *Nat. Rev. Mol. Cell Biol.* **3**:232-241.

Rocha, E.P., Danchin, A., and Viaria, A. 2000. The DB case: pattern matching evidence is not significant. *Mol. Microbiol.* **37**:216-221.

Roder, K, and Schweizer, M. 2001. Running-buffer composition influences DNA-protein and protein-protein complexes detected by electrophoretic mobility-shift assay (EMSA). *Biotechnol. Appl. Biochem.* **33**:209-214.

Rogers, G.W., Komar, A.A., and Merrick, W.C. 2002. eIF4A: the godfather of the DEAD box helicases. *Prog. Nucleic Acid Res. Mol. Biol.* **72**:307-331.

Rosenbaum, V., Klahn, T., Lundberg, U., Holmgren, E., von Gabain, A., Riesner, D. 1993. Co-existing structures of an mRNA stability determinant. The 5' region of the *Escherichia coli* and *Serratia marcescens ompA* mRNA. *J. Mol. Biol.* **229**:656-670.

Ross, W., Gosink, K.K., Salomon, J., Igarashi, K., Zou, C., Ishihama, K., Severinov, K., and Gourse, R.L. 1993. A third recognition element in bacterial promoters: DNA binding by the subunit of RNA polymerase. *Science.* **262**:1407:1413.

Rössler, O.G., Straka, A., and Stahl, H. 2001. Rearrangement of structured RNA via branch migration structures catalysed by the highly related DEAD-box proteins p68 and p72. *Nucleic Acids Res.* **29**:2088-2096.

Rozen, F., Edery, I., Meerovitch, K., Dever, T.E., Merrick, W.C., and Sonenberg, N. 1990. Bidirectional RNA helicase activity of eucaryotic translation initiation factors 4A and 4F. *Mol. Cell. Biol.* **10**:1134-1344.

Rozen, F., Pelletier, J., Trachsel, H., and Sonenberg, N. 1989. A lysine substitution in ATP-binding site of eukaryotic initiation factor 4A abrogates nucleotide-binding activity. *Mol. Cell. Biol.* **9**:4061-4063.

Sakamoto, T. and Murata, N. 2002. Regulation of the desaturation of fatty acids and its role in tolerance to cold and salt stress. *Curr Opin Microbiol.* **5**:208-210.

Sakamoto, T. and Bryant, D.A. 1997. Temperature-regulated mRNA accumulation and stabilization for fatty acid desaturase genes in the cyanobacterium *Synechococcus* sp. strain PCC 7002. *Mol. Microbiol.* **23**:1281-1292.

Sakamoto, T., Higashi, S., Wada, H., Murata, N., and Bryant, D.A. 1997. Low-temperature-induced desaturation of fatty acids and expression of desaturase genes in the cyanobacterium *Synechococcus* sp. PCC 7002. *FEMS Microbiol. Lett.* **152**:313-320.

Sambrook, J., Fritsch, E.F., and Maniatis, T. 1989. Molecular Cloning: a laboratory manual, 2nd ed. Cold Spring Harbor Laboratory Press, Cold Spring Harbor Press, N.Y.

Sato, N., and Nakamura. A. 1998. Involvement of the 5'-untranslated region in cold-regulated expression of the *rbpA1* gene in the cyanobacterium *Anabaena variabilis* M3. *Nucleic Acids Res.* **26**:2192-2199.

Sato, N., Tachikawa, T., Wada, A., and Tanaka, A. 1997. Temperature-dependent regulation of the ribosomal small-subunit protein S21 in the cyanobacterium *Anabaena variabilis* M3. *J. Bacteriol.* **179**:7063-7071.

Sato, N. 1995. A family of cold-regulated RNA-binding protein genes in the cyanobacterium *Anabaena variabilis* M3. *Nucleic Acids Res.* **23**:2161-2167.

Sato, N. 1992. Cloning of a low-temperature-induced gene *lti2* from the cyanobacterium *Anabaena variabilis* M3 that is homologous to alpha-amylases. *Plant Mol. Biol.* **1**:165-170.

Sauer, R.R., Yocum, R.R., Doolittle, R.F., Lewis, M., and Pabo, C.O. 1992. Homology among DNA-binding proteins suggests use of a conserved super-secondary structure. *Nature.* **298**:447-451.

Schmid, S.R., and Linder, P. 1992. D-E-A-D protein family of putative RNA helicases. *Mol. Cell. Biol.* **11**:3463-3471.

Schmid, S.R. and Linder, P. 1991. Translation initiation factor 4A from *Saccharomyces cerevisiae*: analysis of residues conserved in the D-E-A-D family of RNA helicases. *Mol. Cell. Biol.* **11**:3463-3471.

Schneider, S., and Schwer, B. 2001. Functional domains of the yeast splicing factor Prp22p. *J. Biol. Chem.* **276**:21184-21191.

Schopf, J.W., Barghoorn, E.S., Maser, M.D., and Gordon, R.O. 1965. Electron microscopy of fossil bacteria two billion years old. *Science.* **149**:1365-1367.

Schwer, B. 2001. A new twist on RNA helicases: DexH/D box proteins as RNPases. *Nature Struc. Biol.* **8**:113-116.

Schwer, B. and Guthrie, C. 1991. PRP16 is an RNA-dependent ATPase that interacts transiently with the spliceosome. *Nature.* **349**:494-499.

Segal, G. and Ron, E.Z. 1998. Regulation of heat shock response in bacteria. *Ann. N.Y. Acad. Sci.* **851**:147-151.

Serror, P., Dervyn, R., Ehrlich, S.D., and Maguin, E. 2003. *csp*-like genes of *Lactobacillus delbrueckii* ssp. bulgaricus and their response to cold shock. *FEMS Microbiol. Lett.* **226**:323-330.

Sheeler, N.L., MacMillan, S.V., and Nodwell, J.R. 2005. Biochemical activities of the *absA* two-component system of *Streptomyces coelicolor*. *J. Bacteriol.* **187**:687-696.

Shinagawa, H. 1996. SOS response of as an adaptive response to DNA damage in prokaryotes. *EXS.* 77:221-238.

Shpanchenko, O.V., Zvereva, M.I., Ivanov, P.V., Bugaeva, E.Y., Rozov, A.S., Bogdanov, A.A., Kalkum, M., Isaksson, L.A., Nierhaus, K.H., and Dontsova, O.A. 2005. Stepping tmRNA through the ribosome. *J. Biol. Chem.* **280**:18368-18374.

Shuman, S. 1992. Vaccinia virus RNA helicase: an essential enzyme related to the DE-H family of RNA-dependent NTPases. *Proc. Natl. Acad. Sci. USA.* **89**:10935-10939.

Singleton, M.R. and Wigley, D.B. 2002. Modularity and Specialization in Superfamily 1 and 2 Helicases. *J. Bacteriol.* **184**:1819-1826.

Stafleu, F.A. 1971. Lamarck: The birth of biology. *Taxon.* **20**:397-442.

Stanier, R.Y. and Cohen-Bazire, G. 1977. Phototrophic prokaryotes; the cyanobacteria. *Ann. Rev. Microbiol.* **31**:225-274.

Stragier, P. and Losick, R. 1990. Cascades of sigma factors revisited. *Mol. Microbiol.* **4**:1801-1806.

Stryer, L. 1995. Biochemistry. W.H. Freeman and Co., New York, USA. 825-825.

Stulke, J. 2002. Control of transcription termination in bacteria by RNA-binding proteins that modulate RNA structures. *Arch. Microbiol.* **177**:433-440.

Styhler, S., Nakamura, A., and Lasko, P. 2002. VASA localization requires the SPRY-domain and SOCS-box containing protein, GUSTAVUS. *Dev. Cell.* **3**:865-876.

Suzuki, I., Kanesaki, Y., Mikami, K., Kanehisa, M., and Murata, N. 2001. Cold-regulated genes under control of the cold sensor Hik33 in *Synechocystis*. *Mol. Microbiol.* **40**:235-244.

Suzuki, I., Dmitry, A.L., Kanesaki, Y., Mikami, K., and Murata, N. 2000. The pathway for perception and transduction of low-temperature signals in *Synechocystis*. *EMBO J.* **19**:1327-1334.

Szymanski, M. and Barciszewski, J. 2003. Regulation by RNA. *Int. Rev. Cytol.* **231**:197-258.

Tagashira, H., Morita, M., and Ohyama, T. 2002. Multimerization of restriction fragments by magnesium-mediated stable base pairing between overhangs: a cause of electrophoretic mobility shift. *Biochemistry.* **41**:12217-12223.

Tai, C.L., Pan, W.C., Liaw, S.H., Yang, U.C., Hwang, L.H., and Chen, D.S. 2001. Structure-based mutational analysis of the hepatitis C virus NS3 helicase. *J. Virol.* **75**:8289-8297.

Thiel, T. 1994. The molecular biology of cyanobacteria. Kluwer Academic Publishers. Dordrecht, Netherlands. p.581-611.

Thiel, T. and Poo. H. 1989. Transformation of a filamentous cyanobacterium by electroporation. *J. Bacteriol.* **171**:5743-5746.

Thieringer, H.A., Jones, P.G., and Inouye, M. 1998. Cold shock and adaptation. *Bioessays.* **20**:49-57.

Toone, W.M., Rudd, K.E., and Friesen, J.D. 1991. *deaD*, a new *Escherichia coli* gene encoding a presumed ATP-dependent RNA helicase, can suppress a mutation in *rpsB*, the gene encoding ribosomal protein S2. *J. Bacteriol.* **173**:3291-3302.

Tseng, S., Weaver, P.L., Liu, Y., Hitomi, M., Tartakoff, A.M., and Chang, T.H. 1998. Dbp5p, a cytosolic RNA helicase, is required for poly(A)+RnA export. *EMBO J.* **17**:2651-2662.

Tuteja, N. and Tuteja, R. 2004. Unraveling DNA helicases. *Eur. J. Biochem.* **271**:1849:1863.

Ulrich, L.E., Koonin, E.V., and Zhulin, I.B. 2005. One-component systems dominate signal transduction in prokaryotes. *Trends Microbiol.* **13**:52-56.

Urh, M., York, D., and Filutowicz, M. 1995. Buffer composition mediates a switch between cooperative and independent binding of an initiator protein to DNA. *Gene.* **164**:1-7.

Valdez B.C., Perlaky, L., and Henning, D. 2002. Expression, cellular localization, and enzymatic activities of RNA helicase II/Gu (beta). *Exp. Cell Res.* **10**:249-263.

Valgardsdottir, R., and Prydz, H.P. 2003. Transport signals and transcription dependent nuclear localization of the putative DEAD-box helicase MDDX28. *J. Biol. Chem.* **278**:21146-21154.

Valgardsdottir, R., Brede, G., Eide, L.G., Frengen, E., and Prydz, H. 2001. Cloning and characterization of MDDX28, a putative dead-box helicase with mitochondrial and nuclear localization. *J. Biol. Chem.* **276**:32056-32063.

VanBogelen, R.A., and Neidhard, F.C. 1990. Ribosomes as sensors of heat and cold shock in *Escherichia cold. Proc. Natl. Acad. Sci. USA.* **87**:5589-5593.

Valdez, B.C., Henning, D., Perumal, K., and Busch, H. 1997. RNA-unwinding and RNA-folding activities of RNA helicase II/Gu--two activities in separate domains of the same protein. *Eur. J. Biochem.* **250:** 800–807.

Vasseur, C., Baverel, L., Hebraud, M., and Labadie, J. 1999. Effect of osmotic, alkaline, acid or thermal stresses on the growth and inhibition of *Listeria monocytogenes*. *J. Appl. Mircobiol.* **86**:469-476.

Vigh, L., Maresca, B., and Harwood, J.L. 1998. Does the membrane's physical state control the expression of heat shock and other genes? *Trends Biochem. Sci.* **23**:369-374.

Vigh, L., Los, F.A., Horvath, I., and Murata, N. 1993. The primary signal in the biological perception of temperature: Pd-catalyzed hydrogenation of membrane lipids stimulated the expression of the *desA* gene in *Synechocystis* PCC6803. *Proc. Natl. Acad. Sci. USA.* **90**:9090-9094.

Vicente, M., Chater, K.R., and de Lorenzo, V. 1999. Bacterial transcription factors involved in global regulation. *Mol. Microbiol.* **33**:8-17.

Walker, J.E., Saraste, M., Runswick, M.J., and Gay, N.J. 1982. Distantly related sequences in the α- and β-subunits of ATP synthase, myosin, kinases and other ATP-requiring enzymes and a common nucleotide binding fold. *EMBO J.* **1**:945-951.

Wang, N., Yamanaka, K., and Inouye, M. 1999. CspI, the ninth member of the CspA family of *Escherichia coli*, is induced upon cold shock. *J. Bacteriol.* **181:**1603–1609.

Wang, L., Sun, Y.P., Chen, W.L., Li, J.H., and Zhang, C.C. 2002. Genomic analysis of protein kinases, protein phosphatases and two-component regulatory systems of the cyanobacterium *Anabaena* sp. strain PCC 7120. *FEMS Microbiol. Lett.* **217**:155-165.

Wang, Y., Wagner J.D.O., and Guthrie, C. 1998. The DEAD-box splicing factor Prp16 unwinds RNA duplexes in vitro. *Curr. Biol.* **8**:441-451.

Wang, J.Y. and Syvanen, M. 1992. DNA twist as a transcriptional sensor for environmental changes. *Mol. Microbiol.* **6**:1861-1866.

Ward, J. 2001. Identification of DNA sequences required for the temperature regulation of *crhC* transcription in *E. coli*. BSc. 499. University of Alberta. Edmonton, Canada.

Ward, D.M., Ferris, M.J., Nold, S.C., and Bateson, M.M. 1998. A natural view of microbial biodiversity within hot spring cyanobacterial mat communities. *Microbiol. Mol. Biol. Rev.* **62**:1353-1370.

Waterbury J.B. and Stanier, R.Y. 1978. Patterns of growth and development in pleurocapsalean cyanobacteria. *Microbiol. Rev.* **42**:2-44.

Weber, M.H. and Marahiel, M.A. 2003. Bacterial cold shock responses. *Sci. Prog.* **86**:9-75.

Weber, M.H. and Marahiel, M.A. 2002. Coping with the cold: the cold shock response in the Gram-positive soil bacterium *Bacillus subtilis*. *Philos. Trans. R. Soc. Lond. B. Biol. Sci.* **357**:895-907.

West, A.H. and Stock, A.M. 2001. Histidine kinases and response regulator proteins in two-component signaling systems. *Trend Biochem. Sci.* **26**:369-376.

Whitton, B.A. and Potts, M. 1982. The biology of cyanobacteria. Blackwell Scientific Publications, Oxford, USA. p. 515-542.

Wick, L.M. and Egli, T. 2004. Molecular components of physiological stress responses in *Escherichia coli*. *Adv. Biochem. Eng. Biotechnol.* **89**:1-45.

Willimsky G, Bang, H.,Fischer, G., and Marahiel, M.A. 1992. Characterization of *cspB*, a *Bacillus subtilis* inducible cold shock gene affecting cell viability at low temperatures. *J. Bacteriol.* **174**:6326-6335.

Winkler, W.C. 2005. Metabolic monitoring by bacterial mRNAs. *Arch. Microbiol.* **183**:151-159.

Winkler, W.C., Nahvi, A., Roth A., Collins, J.A., and Breaker, R.R. 2004. Control of gene expression by a natural metabolite-responsive ribozyme. *Nature.* **428**:281-286.

Winkler, W.C. and Breaker, R.R. 2003. Genetic control by metabolite-binding riboswitches. *Chembiochem.* **4**:1024-1032.

Winkler, W.C., Nahvi, A., Sudarsan, N., Barrick, J.E., and Breaker, R.R. 2003. An mRNA structure that controls gene expression by binding S-adenosylmethionine. *Nat. Struct. Biol.* **10**:701-707.

Winkler, W.C., Nahvi, A., and Breaker, R.R. 2002. Thiamine derivatives bind messenger RNAs directly to regulate bacterial gene expression. *Nature.* **419**:952-956.

Withey, J.H. and Friedman, D.I. 2003. A salvage pathway for protein structures: tmRNA and trans-translation. *Annu. Rev. Microbiol.* **57**:101-123.

Wosten, M.M. 1998. Eubaterial sigma-factors. *FEMS Micrbiol. Rev.* **22**:127-150.

Xia, B., Ke, H., and Inouye, M. 2001. Acquirement of cold sensitivity by quadruple deletion of the *cspA* family and its suppression by PNPase S1 domain in *Escherichia coli. Mol. Microbiol.* **40:**179-188.

Xu, H. and Hoover, T.R. 2001. Transcriptional regulation at a distance in bacteria. *Curr. Opin. Microbiol.* **4:**138-144.

Yamanaka, K., Zheng, W., Crooke, E., Wang, Y.H., and Inouye, M. 2001. CspD, a novel DNA replication inhibitor induced during the stationary phase in *Escherichia coli. Mol. Microbiol.* **39**:1572-1584.

Yamanaka, K., Mitta, M., and Inouye, M. 1999. Mutation analysis of the 5' untranslated region of the cold shock *cspA* mRNA of *Escherichia coli. J. Bacteriol.* **181**:6284-6291.

Yamanaka, K., Fang, L., and Inouye, M. 1998. The CspA family in Escherichia coli: multiple gene duplication for stress adaptation. *Mol. Microbiol.* **2**:247-55.

Yamanaka, K., Ogura, T., Koonin, E.V., Niki, H., and Hiraga, S. 1994. Multicopy suppressors, *mssA* and *mssB*, of an *smbA* mutation of *Escherichia coli. Mol. Gen. Genet.* **243**:9-16.

Yanofsky, C. 2000. Transcription attenuation: once viewed as a novel tegulatory strategy. *J. Bacteriol.* **182**: 1–8.

Yanofsky, C., Konan, K.V., and Sarsero, J.P. 1996. Some novel transcription attenuation mechanisms used by bacteria. *Biochimie.* **78**:1017-1024.

Yu, E., and Owtrrim, G.W. 2000. Characterization of the cold stress-induced cyanobacterial DEAD-box protein CrhC as an RNA helicase. *Nuc. Acid Res.* **28**:3926-3934.

Yu, E. 1999. Characterizing a cold induced RNA helicase. M.Sc. Thesis. University of Alberta, Edmonton, Canada.

Zakowicz, H., Yang, H.S., Stark, C., Wlodawer, A., Laronde-Leblanc, N., and Colburn, N.H. 2005. Mutational analysis of the DEAD-box RNA helicase eIF4AII

characterizes its interaction with transformation suppressor Pdcd4 and eIF4GI. *RNA.* **3**:261-74.

Zhen, L., and Swank, RT. 1993. A simple and high yield method for recovering DNA from agarose gels. *Biofeedback.* **14**:894-898.

Zhou. C., Yang, Y. and Jong, A.Y. 1990. Mini-prep in ten minutes. *Biotechniques* **8**:172-173.

Zuker, M. and Stiegler, P. 1981. Optimal computer folding of large RNA sequences using thermodynamics and auxiliary information. *Nucleic Acids Res.* **9**:133-148.

Websites

http://bioweb.pasteur.fr/seqanal/interfaces/mfold-simple.html, Accessed June 2004 – March 2005
http://ntp-server.niehs.nih.gov/, Accessed April 2003
http://www.kazusa.or.jp/cyano/Anabaena, Accessed 2002 -2005
http://www.kazusa.or.jp/cyano/cyano.html, Accessed 2002-2005
http://ntp-server.niehs.nih.gov/, Accessed 2003-2005